MmpL proteins in Mycobacterium abscessus : Contribution in glycopeptidolipid transport and in drug resistance

Ana Victoria Gutiérrez

AIX-MARSEILLE UNIVERSITÉ

FACULTÉ DE MÉDECINE DE MARSEILLE

ÉCOLE DOCTORALE DES SCIENCES DE LA VIE ET DE LA SANTÉ

THÈSE DE DOCTORAT

Présentée et publiquement soutenue devant

L'IHU MÉDITERRANÉE INFECTION

Le 22 Novembre 2019

Par Mme Ana Victoria GUTIERREZ

Née le 29 Mars 1990 à Valencia, VENEZUELA

MmpL proteins in *Mycobacterium abscessus*: Contribution in glycopeptidolipid transport and in drug resistance

Pour obtenir le grade de DOCTEUR d'AIX-MARSEILLE UNIVERSITÉ

SPÉCIALITÉ : Pathologies Humaines - Maladies Infectieuses

Membres du Jury de la Thèse :

Président du Jury	Pr. Florence FENOLLAR	Marseille
Rapportrice	Dr. Caroline DEMANGEL	Paris
Rapporteur	Pr. Jean-Phillippe LAVIGNE	Nîmes
Directeur de Thèse	Pr. Michel DRANCOURT	Marseille
Co-directeur de Thèse	Dr. Laurent KREMER	Montpellier

Unité de Recherche sur les Maladies Infectieuses et Tropicales Émergentes (URMITE)
Directeur : Professeur Didier RAOULT

2019

AVANT PROPOS

Le format de présentation de cette thèse correspond à une recommandation de la spécialité Maladies Infectieuses et Microbiologie, à l'intérieur du Master des Sciences de la Vie et de la Santé qui dépend de l'École Doctorale des Sciences de la Vie de Marseille.

Le candidat est amené à respecter des règles qui lui sont imposées et qui comportent un format de thèse utilisé dans le Nord de l'Europe et qui permet un meilleur rangement que les thèses traditionnelles. Par ailleurs, la partie introduction et bibliographie est remplacée par une revue publiée dans un journal scientifique afin de permettre une évaluation extérieure de la qualité de la revue et de permettre à l'étudiant de commencer le plus tôt possible une bibliographie exhaustive sur le domaine de cette thèse. Par ailleurs, la thèse est présentée sur article publié, accepté ou soumis associé d'un bref commentaire donnant le sens général du travail. Cette forme de présentation a paru plus en adéquation avec les exigences de la compétition internationale et permet de se concentrer sur des travaux qui bénéficieront d'une diffusion internationale.

Pr. Didier Raoult

CONTENT

CONTENT

1. Résumé

Mycobacterium abscessus est une espèce mycobactérienne particulièrement réfractaire à l'antibiothérapie classique et peut causer des infections pulmonaires sévères, notamment chez les patients atteints de mucoviscidose. Les mycobactéries contiennent de nombreux gènes codant des protéines de la famille des MmpL (Mycobacterial Membrane Protein Large), agissant comme transporteurs de lipides. Le complexe MmpS4-MmpL4a-MmpL4b intervient notamment dans le transport des glycopeptidolipides (GPL) à travers la membrane plasmique. *M. abscessus* peut présenter deux morphotypes bien distincts : lisse (S) en présence de GPL à la surface de la bactérie ou rugueux (R) en l'absence de GPL. En plus du transport des lipides, les protéines MmpL peuvent également assurer le transport d'une grande variété de substrats, y compris des antibiotiques, et peuvent également participer dans la virulence chez les mycobactéries pathogènes. Par conséquent, ils peuvent être considérées comme une cible thérapeutique prometteuse à exploiter.

Les travaux de cette thèse ont principalement porté sur la contribution des MmpL dans la transition d'un morphotype S vers un morphotype R ainsi que dans les mécanismes de résistance à certains antibiotiques chez *M. abscessus*. Nous nous sommes concentrés également sur le développement de nouveaux outils génétiques permettant une manipulation facilitée au niveau du génome de *M. abscessus*, notamment pour la création de mutants grâce à des événements de recombinaison homologue simple et double. Le système développé est basé sur la présence d'un marqueur de fluorescence rouge (*tdTomato*) qui permet une sélection des clones positifs ayant subi la recombinaison homologue. Les gènes *mmpSL4ab* ont été utilisé pour valider ces techniques, du fait de leur participation dans transport des GPL. Notre méthode nous a permis d'inactiver *mmpL4a* dans le variant S, ce qui coïncide avec un changement vers un morphotype R et à la perte des GPL. Cette transition phénotypique ayant lieu chez l'hôte infecté, nous avons décrit l'hétérogénéité S/R de plusieurs isolats cliniques issus de deux patients atteints de mucoviscidose et co-infectés par les deux variants. Le

séquençage complet des génomes de ces souches a permis l'identification de nouvelles mutations dans le locus *GPL* qui pourraient être impliqués dans la conversion de S en R.

Des travaux antérieurs ont montré la contribution de la pompe à efflux MmpS5/MmpL5 de *M. abscessus* dans la résistance aux analogues du thiacétazone. Nous avons ensuite élucidé les mécanismes de résistance qui impliquent le régulateur de transcription TetR (MAB_4384) dans l'expression MmpS5/MmpL5.

En raison de l'extrême difficulté à traiter *M. abscessus*, de nouvelles alternatives thérapeutiques ont récemment été proposées, incluant notamment la clofazimine et la bedaquiline. Nos études ont consisté à décrire les mécanismes de résistance à ces antibiotiques chez *M. abscessus* et d'identifier les mutations et leur impact au niveau d'un autre régulateur transcriptionnel de la famille TetR (MAB_2299c). Nos données génétiques et biochimiques

démontrent que les mutations affectant MAB_2299c sont associées à une surexpression accrue de deux pompes à efflux distinctes : MAB_2300-2301 et MAB_1135c-1134c, qui toutes deux contribuent dans la résistance intrinsèque de *M. abscessus* à la clofazimine et à la bédaquiline. MAB_2299c pourrait donc représenter un nouveau marqueur de résistance à ces deux antibiotiques dans les isolats cliniques.

La technique d'inactivation génique que nous avons développée représente un outil performant pour générer très facilement et efficacement des mutants non marqués, avec la possibilité de déléter plusieurs gènes dans la même souche. Ainsi, cette approche pourrait permettre de valider de nouvelles cibles médicamenteuses et/ou facteur de virulence non seulement *M. abscessus* mais également chez d'autres mycobactéries non tuberculeuses.

Mots clés : *Mycobacterium abscessus*, mucoviscidose, glycopeptidolipides, outils génétiques, résistance aux antibiotiques, pompe à efflux, MmpL, TetR, régulation.

2. Abstract

Mycobacterium abscessus has recently emerged as one of the most difficult-to-manage Non-Tuberculous mycobacteria (NTM), causing severe pulmonary infections, especially in cystic fibrosis patients. Mycobacteria contain several genes encoding proteins belonging to the mycobacterial membrane protein large (MmpL) family, acting as lipid transporters and proposed to work as efflux pumps. The MmpS4-MmpL4a-MmpL4b complex mediates the biosynthesis/transport of glycopeptidolipids (GPL) across the plasma membrane. *M. abscessus* exhibits either a smooth (S) morphotype when GPL are associated at the bacterial surface or a rough (R) morphotype when GPL are lacking. In addition to lipid transport, MmpL proteins can mediate the transport of a wide panel of substrates, including drugs, and can also be considered as important virulence factors in pathogenic mycobacteria. Therefore, they can be viewed as a promising drug targets to be further exploited against *M. abscessus*.

The research conducted during this thesis focused mainly in the contribution of MmpL in the S-to-R transition and in drug resistance mechanisms. We focused also on the development of genetic tools that allow to easily manipulate the *M. abscessus* genome, particularly to generate mutants, based on a single and double homologous recombination events. The system comprises a red fluorescence marker (*tdTomato*) that simplifies the selection of the positive clones that have undergone gene disruption. The *mmpSL4ab* gene cluster was used to validate these techniques due to their participation in production/transport of GPL. Using this method, inactivation of *mmpL4a* in the S variant was associated with a switch to the R morphotype and absence of GPL production. Since the S-to-R transition has been proposed to occur within the host, we next described the heterogeneity of isolates from two cystic fibrosis patients pulmonary co-infected with both morphotypes using whole genome sequencing. This allowed to identified new single nucleotide polymorphism in the *GPL* locus which may be involved in the S-to-R conversion.

Previous work reported the contribution of the *M. abscessus* MmpS5/MmpL5 efflux pump system in resistance to thiacetazone analogues. Herein, we further elucidated the mechanism of resistances involving the TetR transcriptional regulator (MAB_4384) in the regulation of this efflux pump.

Due to the extreme difficulty encountered in the treatment of *M. abscessus*, alternative therapeutic options have recently been proposed, including for instance the use clofazimine and bedaquiline in current treatments. Our work was aimed at describing the mechanisms of resistance to these drugs and identified mutations in a putative TetR transcriptional regulator (MAB_2299c). Genetic and biochemical approaches demonstrated that mutations in this regulator were associated with increased expression of two efflux pump systems, MAB_2300-2301 and MAB_1135c-1134c, both contributing to the intrinsic resistance level of *M. abscessus* to clofazimine and bedaquiline. Therefore, *MAB_2299c* may represent a useful marker of clofazimine and bedaquiline resistance in clinical isolates.

The double crossing-over gene inactivation technique developed during these studies represent a powerful tool to easily and efficiently generate unmarked mutants and offers the possibility of delete multiple genes in the same strain. It opens the way to future studies aimed at validating novel drug targets and/or virulence genes not only in *M. abscessus* but perhaps also in other NTM.

Key words: *Mycobacterium abscessus*, cystic fibrosis, glycopeptidolipids, genetic tools, drug resistance, efflux pump, MmpL, TetR, regulation.

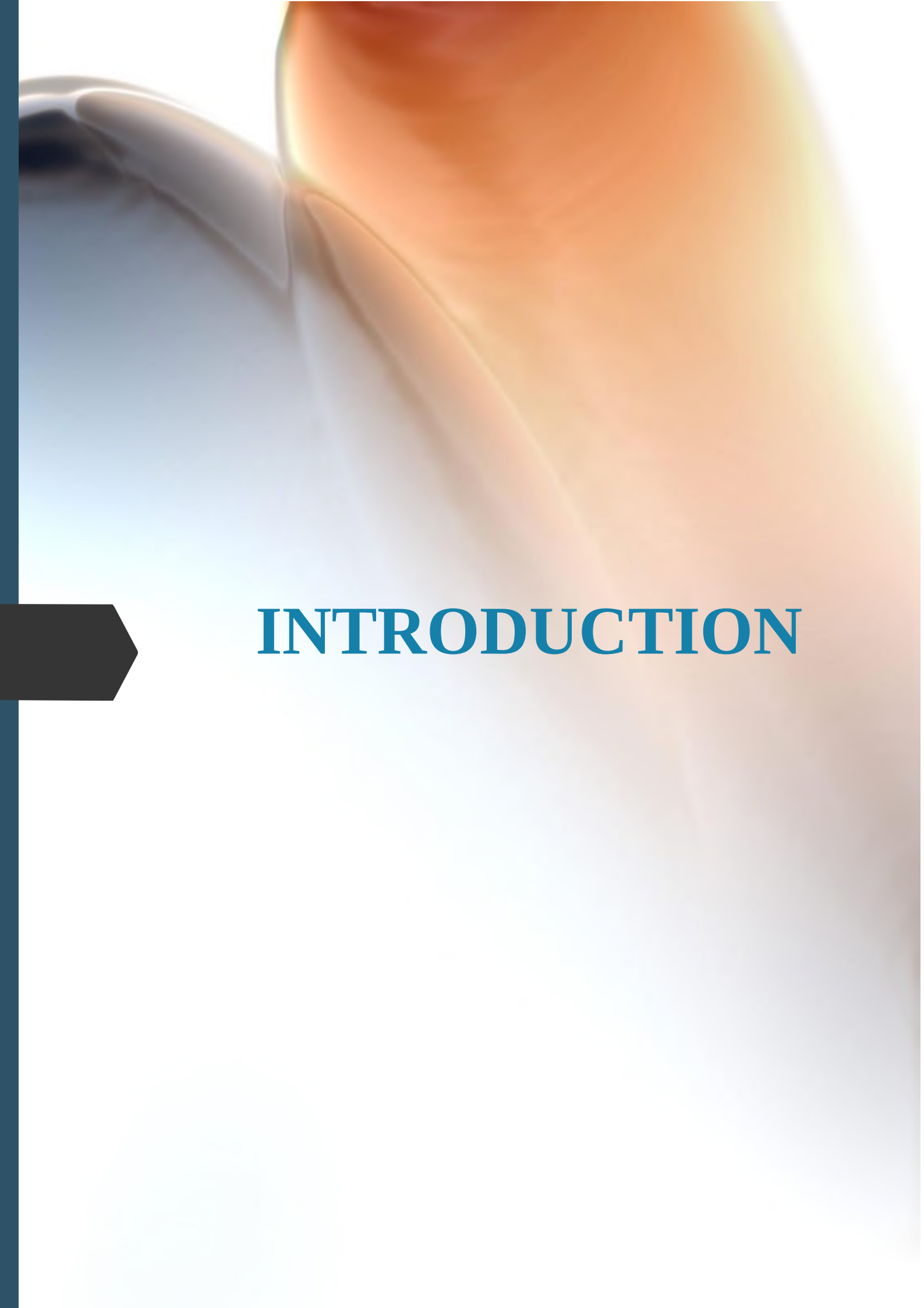

INTRODUCTION

3. Introduction

3.1 Epidemiological generalities of *M. abscessus* infections

Although tuberculosis (TB) remains a major health problem worldwide, the incidence of the disease is being surpassed in several developed countries by mycobacterial species of environmental origin, known as Non-Tuberculous Mycobacteria (NTM) (Falkinham 2013). NTMs are responsible of pulmonary infections and display a diverse geographical distribution. Among them, the *Mycobacterium abscessus* complex is described as the most common cause of clinical disease in Asia and Oceania and the second most frequently encountered worldwide after the *Mycobacterium avium* complex (Zweijpfenning, Ingen, and Hoefsloot 2018).

The *M. abscessus* complex comprises three subspecies: *M. abscessus subsp. abscessus*, *M. abscessus subsp. bolletii* and *M. abscessus subsp. massiliense* (Tortoli et al. 2016). The rapidly growing *M. abscessus*, associated with multidrug resistance can be responsible for soft tissue infections related to surgical and aesthetical procedures (Furuya et al. 2008) and tattoos (Griffin et al. 2018). This mycobacterium is also responsible of catheter-related bacteraemia (Rodriguez-Coste et al. 2016) and, more importantly, respiratory disease in individuals with underlying lung disorders such as cystic fibrosis (CF) (Cowman et al. 2019).

3.2 Morphology differences of *M. abscessus*

M. abscessus displays smooth (S) or rough (R) colony morphotypes, which are characterized by the presence or absence of surface-associated glycopeptidolipids (GPL), respectively (Howard et al. 2006). Mutations in the GPL locus, involved in its biosynthesis and transport, are responsible for the loss of GPL that leads to a R variant with a greater aggregation capacity (Medjahed and Reyrat 2009; Bernut et al. 2016). In addition, clinical isolates of *M. abscessus* with R morphotypes have been shown to harbour mutations in the

GPL locus, including *mmpL4a* (Pawlik et al. 2013; Park et al. 2015). However, it remains still unclear how colony morphology affects the prognosis of patients with pulmonary disease.

3.3 Cellular and animal models for the study of *M. abscessus* infections

Experimental evidence in cellular and animal models has associated the R morphotype with increased virulence and persistent infections (Bernut et al. 2017; Rottman et al. 2007) (**Figure 1**).

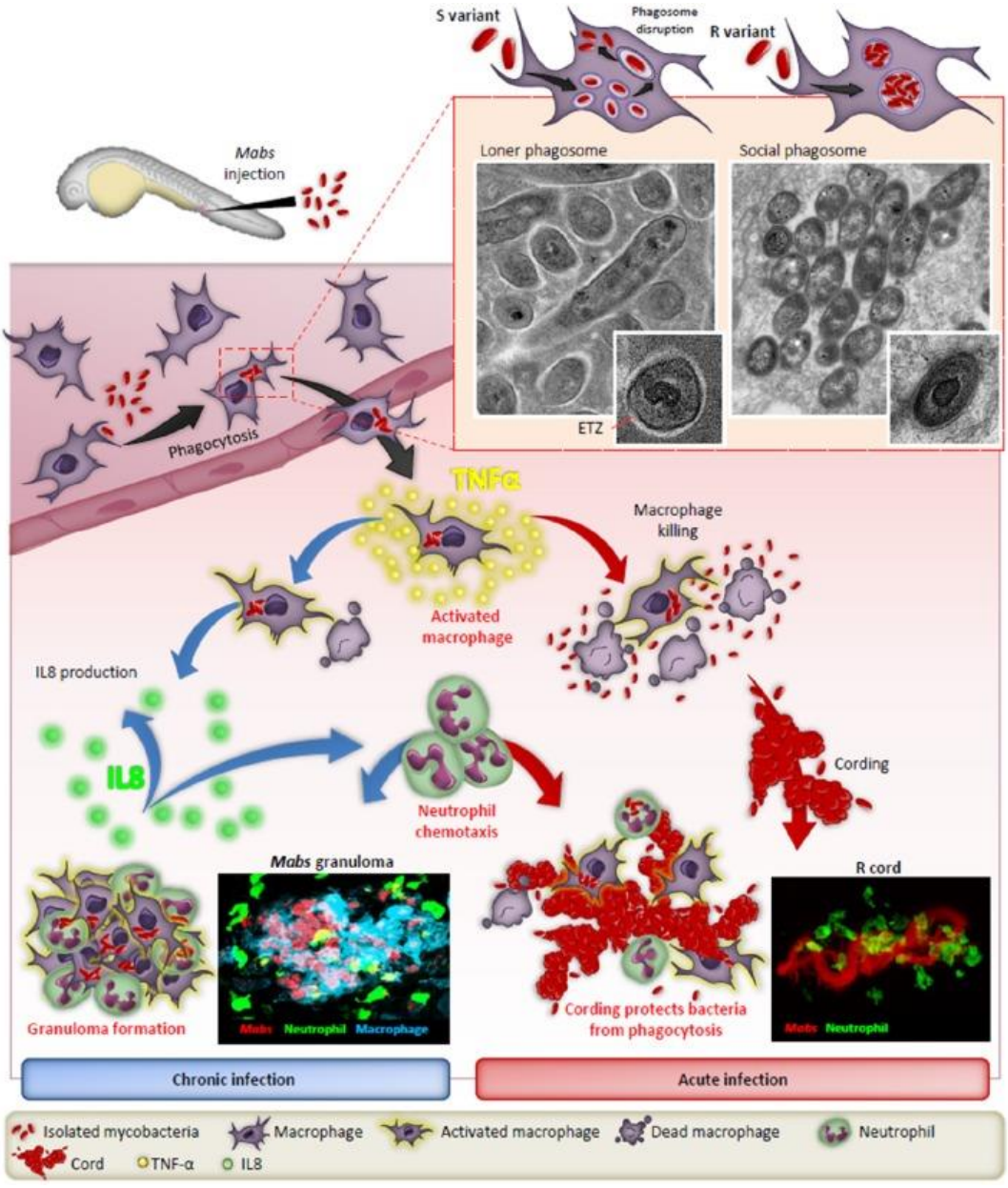

Figure 1. Differences between *M. abscessus* smooth (S) and rough (R) infections in macrophages and zebrafish. Macrophages infected with *M. abscessus* (*Mabs*) are characterized by the presence of loner phagosomes (individually S variant) or social phagosomes (aggregated R variant). Between the phagosome membrane and the mycobacterial cell wall, the visualization of an electron translucent zone (ETZ) depends on

the presence of GPL (S strain). While in the R variant, lacking GPL, this structure is not observed. Additionally, intracytoplasmic release of the S variant can occur after disruption of the phagosome membrane. In zebrafish infected intravenously, macrophages after phagocytizing *Mabs* migrate from the caudal vein to nervous tissues in which the intracellular growth of *Mabs* leads to apoptosis. Released S variant is phagocytosed by newly recruited macrophages which, together with neutrophils, form protective granulomas, resulting in a chronic infection. In contrast, after the release of *Mabs* R, the production of extracellular cords protects bacteria from phagocytosis by macrophages and neutrophils, leading to the formation of abscesses with tissue destruction and acute infection. Additionally, TNF-α production by activated macrophages is responsible for the bactericidal response against *Mabs*. Furthermore, the production of IL-8 mediates the recruitment of neutrophils at the site of infection for the development and maintenance of protective granulomas (Bernut et al. 2017).

Studies have demonstrated the ability of aggregated R bacilli to infect macrophages and grow inside phagocytic vesicles forming social phagosomes. *M. abscessus* R infected cells release large amounts of proinflammatory cytokines (TNF-α and IL-6) unlike macrophages infected with the S variant in which only trace amounts of cytokines can be detected. In addition, it has been described that bacteria forming clumps inside the phagocytic vesicles kill macrophages, subsequently releasing large aggregates of bacilli in the extracellular space. In contrast, the S morphotype can persist within macrophages by blocking phago-lysosomal fusion and resisting apoptosis and autophagy (Brambilla et al. 2016; Roux et al. 2016). Concordant results have been found in the zebrafish model on infection in which the S variant fails to kill the infected embryos. The R morphotype, thanks to the ability to clump and form packed structures designated as “cords”, evades phagocytosis and progresses towards the formation of abscesses that lead to uncontrolled infection and larval death (Bernut, Herrmann, et al. 2014). In general, immunocompetent mice rapidly clear the infection (Bernut, Le Moigne, et al. 2014). However, infection with *M. abscessus* has been shown to persist in several immunocompromised mouse models, such as T-cell-depleted, athymic (nude), severe combined immunodeficiency (SCID), granulocyte-macrophage colony-stimulating factor (GMCSF) knockout, and IFN-γ knockout (GKO) mice. In these models, the characteristic histopathological signs of necrotizing and non-necrotizing granulomas in the lungs has been shown (Obregón-Henao et al. 2015), but without distinguishing the pathological differences between morphotypes S and R. However, these animal models show disadvantages to study the entire course of lung disease caused by *M.*

abscessus. For instance, zebrafish do not possess lungs. Although in this model the development of abscesses can occur throughout the body, there is an important tropism for the central nervous system (CNS) (Bernut, Herrmann, et al. 2014) whereas CNS infections in humans have only been documented rarely (Talati et al. 2008). The main difficulty in the murine model is the rapid clearance of *M. abscessus* that requires the use of immunocompromised models (Bernut et al. 2017).

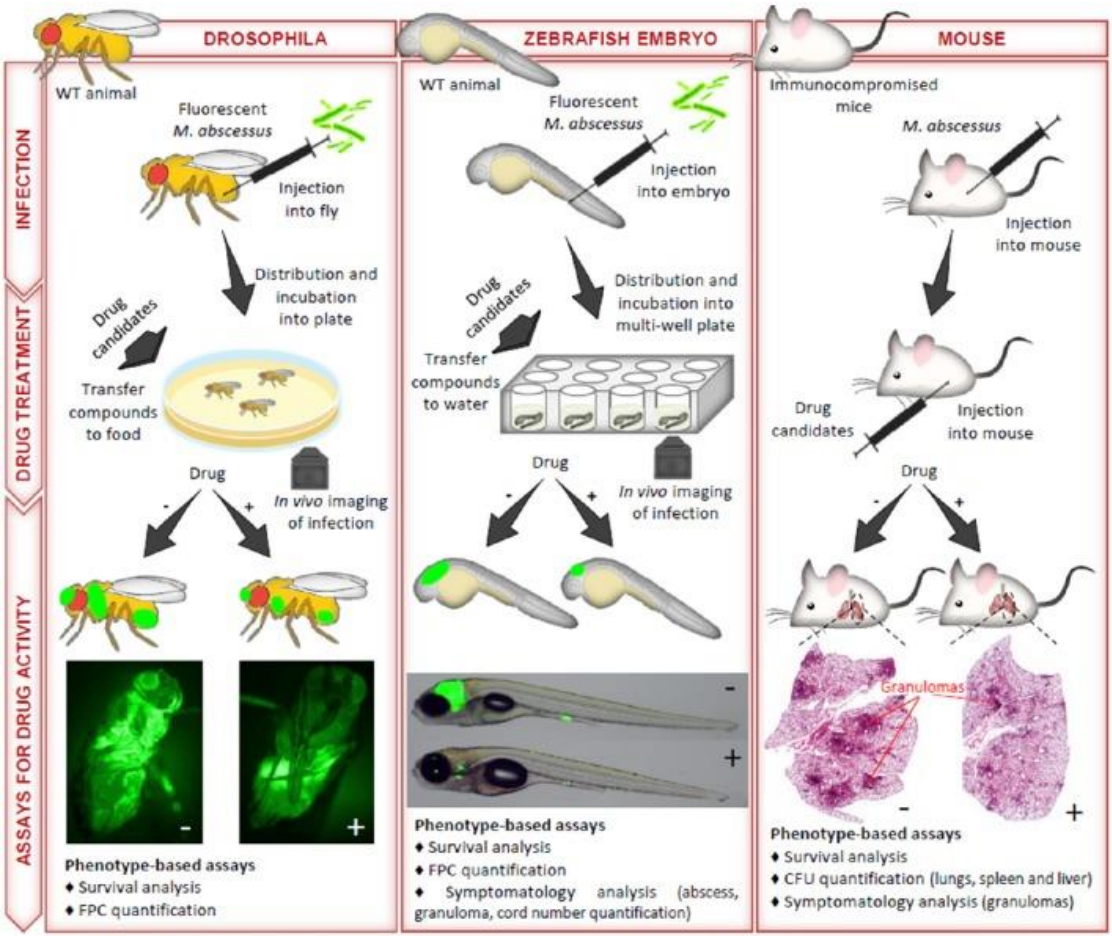

Figure 2. Diverse models available for the *in vivo* study of compounds against *M. abscessus*. The methods of infection, the drug treatment conditions and the assays used to monitor drug activity of anti- *M. abscessus* compounds in drosophila, zebrafish embryos and immunocompromised mice are illustrated. CFU, colony-forming unit; FPC, fluorescent pixel count (Bernut et al. 2017).

In addition to zebrafish and mice, permissive models such as *Drosophila melanogaster* and *Galleria mellonella* are proposed for drug screening against *M. abscessus* (Meir, Grosfeld, and Barkan 2018; Oh et al. 2013) (**Figure 2**). Particularly, *G. mellonella* was used to briefly differentiate the infection outcome between S and R which includes granuloma-like

structures that result in the death of the larvae. However, a faster mortality was observed for the R morphotype (Meir, Grosfeld, and Barkan 2018). These are promising models that can be used for the evaluation of *M. abscessus* mutants involved in pathogenesis or drug resistance mechanisms.

3.4 MmpL proteins and their role in cell wall biosynthesis and drug resistance

Mycobacteria contain a large number of Mycobacterial Membrane Protein Large (MmpL), proposed as multi-substrate efflux pumps (Viljoen et al. 2017). These inner membrane proteins belong to a family of Resistance Nodulation Cell Division (RND) permeases and are driven by the proton motive force (Ruggerone, Murakami, and Vargiu 2013). They can mediate the transport of a wide variety of substrates across the mycobacterial cell membrane, including lipids and drugs (Chalut 2016; Székely and Cole 2016) (**Figure 3**).

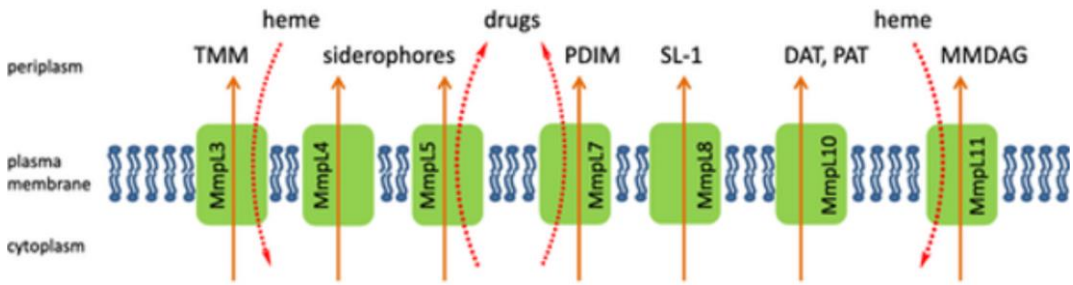

Figure 3. ***M. tuberculosis*** **MmpL proteins with known function.** TMM, trehalose monomycolate; PDIM, phthiocerol dimycocerosate; SL1, sulfolipid-1; DAT, diacyl trehaloses; PAT, pentacyl trehaloses; MMDAG, monomeromycolyl diacylglycerol (Székely and Cole 2016).

Slow and rapid growing mycobacteria have different members of *mmpL* genes in their genomes (Viljoen et al. 2017). While *M. tuberculosis* has 14 of these transporters, 31 are present in *M. abscessus*. **Figure 4** shows the phylogenetic distribution and function of MmpL between *M. tuberculosis* and *M. abscessus*.

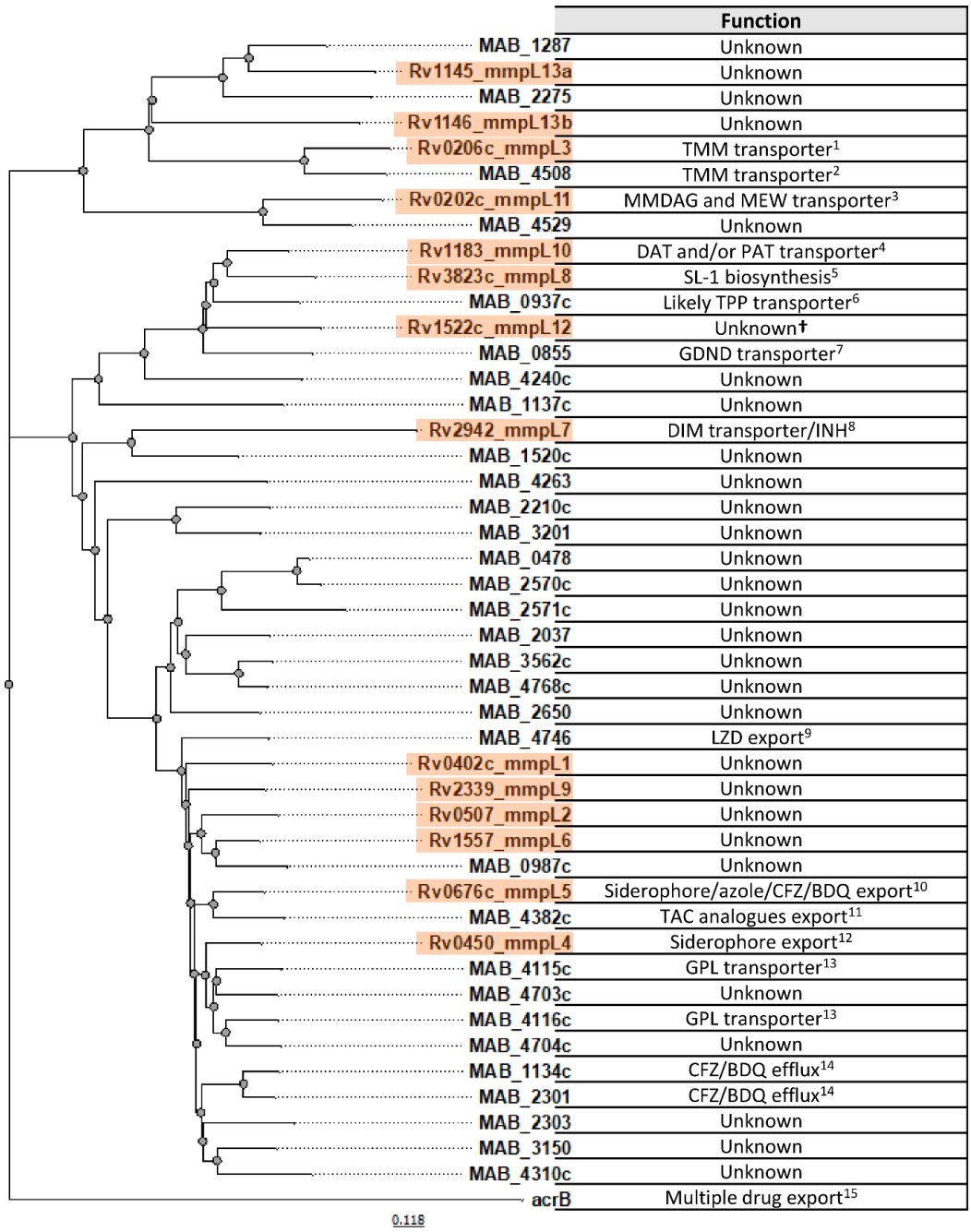

Figure 4. Homology tree and function of all *M. tuberculosis* and *M. abscessus* MmpL. PHYLIP Neighbor joining phylogenetic tree based on a MUSCLE multiple alignment of the amino acid sequences of MmpL efflux pumps. The scale bar below the tree indicates 0.118 amino acids substitutions per site. The tree was rooted to *Escherichia coli* AcrB (RND Efflux Pump). In orange MmpL from *M. tuberculosis*.

TMM: trehalose monomycolate, MMDAG: monomeromycolyl diacylglycerol, MEW: mycolate ester wax, DAT: diacyltrehalose, PAT: polyacyltrehalose, SL-1: sulfolipid-1 biosynthesis, TPP: trehalose polyphleates, GDND: glycosyl diacylated nonadecyl diol, DIM: phthiocerol dimycocerosate, INH: isoniazid, LZD: linezolid, CFZ: clofazimine, BDQ: bedaquiline, TAC: thiacetazone, GPL: glycopeptidolipids. **1**: Grzegorzewicz et al. 2012; **2**: Dupont et al. 2016; **3**: Pacheco et al. 2013; **4**: Belardinelli et al. 2014; **5**: Converse et al. 2003; Domenech et al. 2004; **6**: Burbaud et al. 2016; **7**: Dubois et al. 2018; **8**: Cox et al. 1999; Camacho et al. 2001; Rodrigues et al. 2012; **9**: Ye et al. 2019; **10**: Milano et al. 2009; Wells et al. 2013; Hartkoorn, Uplekar, and Cole 2014; **11**: Halloum et al. 2017; **12**: Wells et al. 2013; **13**: Medjahed and Reyrat 2009; **14**: Richard et al. 2019; Gutiérrez et al. 2019; **15**: Yu, Aires, and Nikaido 2003.

†Controversly related with Lipooligosaccharides transport, based in protein homology with *M. canetti*, *M. marinum*, *M. kansasii* and *M. smegmatis*, however *M. tuberculosis* do not produce this lipid (Etienne et al. 2009).

Proteins of the RND family, in addition to being involved in cell wall biosynthesis and drug resistance, are also important for the efflux of metals and detergents. The high abundance of MmpL proteins could be explained as an adaptative mechanism in response to adverse and changing conditions in the environment or in the various hosts (Delmar, Su, and Yu 2014). Some of the advantages that MmpL may confer to *M. abscessus* are: i) phagocytosis survival by amoebae (Drancourt 2014) and macrophages, ii) resistance to sterilization methods used in clinical settings (Neves et al. 2016), iii) resistance to salts in aquatic environments and in sputum of patients with CF (Asmar et al. 2016) and, iv) protection from the antibiotics produced by environmental competitors (Szumowski et al. 2013).

Since MmpLs are found in the inner membrane and because their substrates (e.g., lipids) are exported to the outer membrane (Chalut 2016), the continuity of this process is very likely to require accessory proteins acting together with the MmpL proteins. Mycobacterial Membrane Protein Small (MmpS) are proposed as possible partners in the efflux pump activity of the MmpLs (Wells et al. 2013). However, it is not clear how these proteins interact with each other and how MmpS contribute to the transport of cell wall lipids or antimycobacterial compounds.

Evidence of the contribution of MmpS and MmpL in *M. abscessus* drug resistance mechanisms was demonstrated in a previous study, in which thiacetazone (TAC) analogues, exhibiting potent activity against *M. abscessus*, were used to elucidate the intrinsic resistance mechanisms of these compounds. Mutants resistant to TAC analogues harboured mutations in the TetR transcriptional regulator (MAB_4384); this led to overexpression of MAB_4383c/MAB_4382c (Halloum et al. 2017), which are the homologs of the MmpS5/MmpL5 system described in resistance to clofazimine and beaquiline in *M. tuberculosis* (Hartkoorn, Uplekar, and Cole 2014).

3.5 MmpL regulation by TetR transcriptional regulators

In mycobacteria, two main families of regulators involved in antibiotic resistance are the Multiple Antibiotic Resistance Regulator (MarR) and the Tetracycline Regulator (TetR). Both regulators share structural and functional characteristics, such as the helix–turn–helix motif for binding to the target DNA (Gong et al. 2019). The mechanism of antibiotic resistance associated to these regulators often includes mutations that affect the DNA-binding domain of the regulator, resulting in overexpression of the target genes (Seoane and Levy 1995; Kisker et al. 1995; Alekshun, Kim, and Levy 2000; Gibson et al. 2010). The MarR and TetR families are present in human pathogenic bacteria but more abundant in environmental bacteria and probably acquired via horizontal transfer (Szczepanowski et al. 2004). These two regulator families are overrepresented in *M. abscessus*, 21 MarR (Gong et al. 2019) and 138 putative TetR proteins (Cuthbertson and Nodwell 2013), emphasizing the importance and these regulatory process in this species. Interestingly in *M. abscessus*, *mmpL* genes are more often present in the genomic vicinity of *tetR* than in *marR* (**Table 1**). However, it cannot be excluded that *mmpLs* lacking a gene encoding a regulator in their genomic neighbourhood may depend on a different regulatory system.

MmpL	Transcriptional Regulator in the vicinity
MAB_0478	MAB_0476c (**tetR**)/MAB_0479 (marR)*
MAB_0855	MAB_0856c (**tetR**)
MAB_0937c	No neighbouring regulator †
MAB_0987c	MAB_0989 (**tetR**)/MAB_0986 (arsR)
MAB_1134c	MAB_1136 (**tetR**)
MAB_1137c	MAB_1136 (**tetR**)/MAB_1138c (marR)*
MAB_1287	MAB_1288 (tetR)*
MAB_1520c	MAB_1522 (luxR)
MAB_2037	No neighbouring regulator †
MAB_2210c	No neighbouring regulator †
MAB_2275	MAB_2276c (embR)
MAB_2301	MAB_2299c (**tetR**)
MAB_2303	MAB_2299c (**tetR**)
MAB_2570c	No neighbouring regulator †
MAB_2571c	No neighbouring regulator †
MAB_2650	MAB_2648c (marR)
MAB_3150	MAB_3151 (tetR)*
MAB_3201	MAB_3199c (**tetR**)
MAB_3562c	MAB_3565 (**tetR**)
MAB_4115c	MAB_4118 (XRE)
MAB_4116c	MAB_4118 (XRE)
MAB_4240c	No neighbouring regulator †
MAB_4263	No neighbouring regulator †
MAB_4310c	MAB_4312 (**tetR**)
MAB_4382c	MAB_4384 (**tetR**)/MAB_4381c (lysR)*
MAB_4508	MAB_4510c (**tetR**)
MAB_4529	No neighbouring regulator †
MAB_4703c	No neighbouring regulator †
MAB_4704c	No neighbouring regulator †
MAB_4746	MAB_4744c (araC)
MAB_4768c	MAB_4765 (**tetR**)/MAB_4772 (**tetR**)

Table 1. MmpL and their neighbouring transcriptional regulators. The predominant presence of TetRs (in bold) possibly involved in the regulation of its neighbour *mmpL*. Additional families of regulators that are in the *mmpL* vicinity or distantly located could be involved in their regulation. **ArsR**: transcriptional repressor involved in resistance to heavy metal ions (Busenlehner, Pennella, and Giedroc 2003). **LuxR**: transcriptional activator involved in cellular signalling pathways and also related to pathogenesis, response to hypoxia and cellular response to nitrosative stress (Santos et al. 2012). **EmbR**: a phosphorylation-dependent transcriptional activator for the arabinosyltransferases operon in *M. tuberculosis* and influencing ethambutol resistance (Sharma et al. 2006). **XRE**: xenobiotic response element involved in the regulation of stress tolerance and virulence in pathogenic Gram-positive bacteria (Hu et al. 2019). **LysR**: transcriptional activators or repressors, among the regulated functions there is metabolism, cell division, quorum sensing, virulence, motility, nitrogen fixation, oxidative stress responses, toxin production, attachment and secretion (Maddocks and Oyston 2008). **AraC**: transcriptional activator involved in the regulation of carbon metabolism, stress responses and pathogenesis (Tobes and Ramos 2002).
*Unlikely to be related to the regulation since it is not divergently oriented.
†Despite some MmpL genes do not possess any regulatory protein nearby, it cannot be discarded that other regulatory network can be involved.

3.6 Drug resistance mechanisms in *M. abscessus*

M. abscessus is considered as one of the most difficult to treat NTM species. The first barrier of resistance to antibiotics relies on the impermeable cell envelope (L. Nguyen and Thompson 2006). Furthermore, *M. abscessus* possesses numerous enzymes that can modify and/or degrade antibiotics or alter their targets. These enzymes are of great importance for intrinsic resistance to various antibiotics classes (Luthra, Rominski, and Sander 2018) (**Figure**

5). Alternative mechanisms of drug resistance include, mutations of targeted genes (Wallace et al. 1996) and drug extrusion by other efflux pumps (Schmalstieg et al. 2012) among which MmpL proteins may contribute. In addition, resistance to amikacin, clarithromycin, erythromycin, and tetracycline has been linked to the transcriptional master activator WhiB7 (Pryjma et al. 2017).

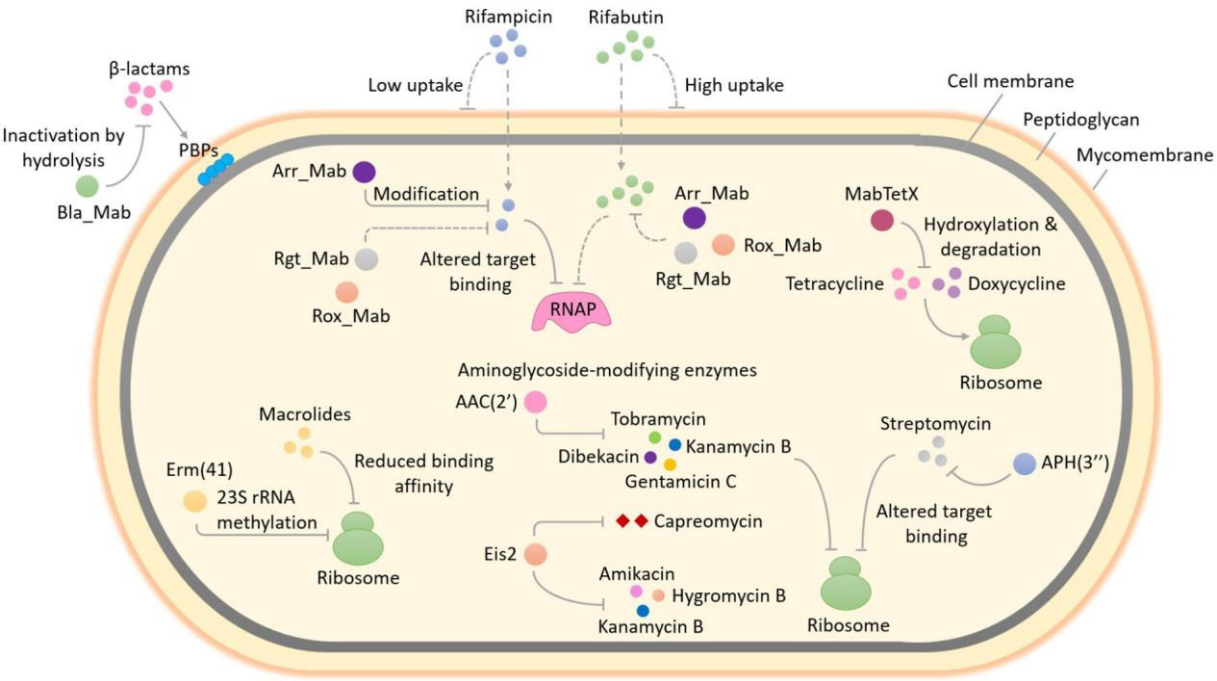

Figure 5. Overview of the diverse enzymes involved in the intrinsic antibiotic resistance in *M. abscessus*. Inducible resistance to macrolides is associated with the methylation of 23S rRNA by **Erm(41)** and the subsequent decrease in the binding affinity of macrolides for the ribosome exit tunnel. Two putative acetyltransferases (**AAC(2′)** and **Eis2)** and one putative phosphotransferase (**APH(3″))** can modify aminoglycoside molecules by adding acyl or phosphate groups, thus preventing the binding of aminoglycoside to its ribosomal target due to steric interruption, resulting in resistance. In addition to aminoglycosides, Eis2 can also modify other ribosome-targeting antibiotics such as capreomycin. Resistance to rifampicin and other rifamycin antibiotics in *M. abscessus* involves ribosylation of the drug by **Arr_Mab**. Additional rifampicin inactivation mechanisms in environmental bacteria include glycosylation, phosphorylation and decomposition of rifampicin by monooxygenation. In *M. abscessus* it is proposed that rifampicin glycosylation and the monooxygenation are driven by the enzymes **Rgt_Mab** and **Rox_Mab**, respectively. *M. abscessus* also produces a flavin monooxygenase that degrades tetracycline, **MabTetX,** which activates molecular oxygen to hydroxylate and destabilize the antibiotic, which subsequently undergoes non-enzymatic decomposition, thereby conferring resistance. Moreover, *M. abscessus* produces a hydrolytic β-lactamase enzyme, **Bla_Mab,** which degrades a wide range of β-lactams including extended-spectrum cephalosporins and carbapenems. RNAP, RNA polymerase; PBPs, penicillin-binding proteins; AAC(2′), 2′-N-acetyltransferase; Eis2, enhanced intracellular survival protein 2; APH(3″), aminoglycoside 3″-O-phosphotransferase (Luthra, Rominski, and Sander 2018).

In particular, the inducible resistance to macrolides associated with 23S RNA methyltransferase encoded by *erm(41)*, which is inactivated in *M. massiliense*, leading to macrolide sensitivity. This remarkable difference is used to simplify the differentiation

between *M. massiliense* from *M. abscessus* or *M. bolletii*. (Kim et al. 2010).

New therapeutic approaches such as the repurposing of clofazimine and bedaquiline, used for the treatment of multi-drug resistant TB have recently been introduced as alternatives for the treatment of *M. abscessus* pulmonary infections (Ruth et al. 2019). The current drug pipeline regarding *M. abscessus* and *M. avium* as well as the status of various clinical trials conducted with repurposed drugs is shown in **Figure 6.**

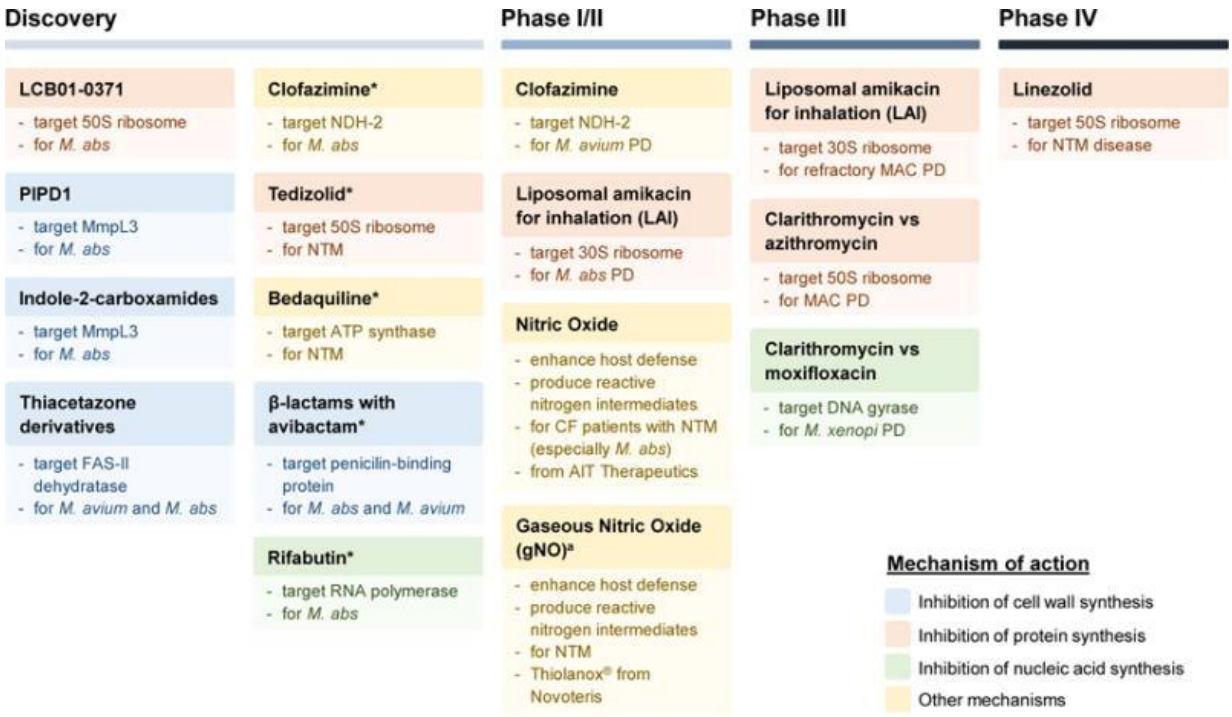

Figure 6. Non-tuberculous mycobacteria (NTM) drug pipeline. Compounds in current discovery (from literature) for NTM treatment are shown. The asterisks (*) indicate repurposed drugs. Drugs under 'Phase I–IV' are from https://clinicaltrials.gov. There are currently no drug candidates for NTM in preclinical development. [a]Gaseous nitric oxide is composed of 0.5% NO and 99.5% nitrogen. Abbreviations: *M. abs*, *M. abscessus*; MAC, *Mycobacterium avium* complex; PD, pulmonary disease; CF, cystic fibrosis; FAS-II, type II fatty acid synthase; NDH-2, type II NADH-quinone oxidoreductase (Wu et al. 2018).

Objectives

Our limited knowledge regarding the molecular mechanisms of intrinsic resistance to antibiotics and pathogenesis in *M. abscessus* has motivated this research study, by following 3 major objectives.

- First, a review focused on the influence of GPL on the biology and pathophysiology of the *M. abscessus* complex is presented. This is followed by a case report study based on two CF patients co-infected with S and R variants. We describe the heterogeneity between the isolates in the same patient and discus the implications for future treatments.

- Second, considering that *M. abscessus* is refractory to genetic manipulation, new genetic tools were developed based on the simplification of the selection of the positive clones. The *mmpSL4ab* operon involved in GPL production/transport was used as a target locus to validate these methods and evaluate the virulence of the resulting mutants using the zebrafish model of infection.

- Third, three studies allowed us to expand the knowledge regarding the regulatory mechanisms of MmpL transporters and their participation in drug resistance mechanisms against different antibiotics active against *M. abscessus*.

CHAPTER I

Glycopeptidolipids: Review of literature

Glycopeptidolipids, a double-edged sword of the *Mycobacterium abscessus* complex

Gutiérrez A.V., Viljoen A., Ghigo E., Herrmann J.L. and Kremer L. Review.

Frontiers in microbiology, 9.

4. CHAPTER I: Glycopeptidolipids: Review of literature

Changes in the morphology of prokaryotes represent an important physiological character in response to various selective pressures such as nutrient availability, cell division, and predators (Young 2007). Biochemical stimuli and genetic control can influence the shape, size, and pigment production. These phenotypic characteristics can provoke a combination of responses (attachment to surfaces, passive dispersion, active motility) that impact the physiological adaptation to the environment and the host (Young 2006).

The appearance of the colony may vary between bacterial species and strains. In mycobacteria, the evolution of cell wall composition is an important factor for colony morphology. The differences between the ancient smooth (S) *Mycobacterium kansasii* and *Mycobacterium canettii* and the modern rough (R) *M. tuberculosis* and *Mycobacterium bovis* are based on hydrophobic surface properties acquired by the increased proportion of less polar lipids (Jankute et al. 2017). A more hydrophobic outer membrane is proposed to contribute to the adhesion to solid substrates and the biofilm formation. In addition, the less permeable hydrophobic cell wall can resist disinfection and antibiotic treatments, and increase aerosol transmission capacity (Falkinham 2003).

Initial research on the irreversible change in morphology from S to R in NTM revealed that after prolonged incubation in malic acid medium or after exposure to ultraviolet light, R colonies arose from an unclassified S *Mycobacterium* scotochromogen. This change in morphology was associated with a possible mutation that led to the loss of mycoside D, a glycolipid that was not been widely investigated (Fregnan, Smith, and Randall 1962). NTMs, including *M. abscessus,* follow a similar principle that dictates the S-to-R morphotype transition (Ripoll et al. 2007).

A cluster of genes encoding proteins involved in the biosynthesis and transport of glycopeptidolipids (GPL) is well conserved between the *M. abscessus* complex, *M. smegmatis*

and *M. avium.* However, structural differences in GPL from *M. abscessus* and other NTM species have been reported (Ripoll et al. 2007; Whang et al. 2017). Important physiological properties, such as sliding motility and biofilm formation are depend on GPL production (Brambilla et al. 2016). On the other hand, strains lacking GPL are reported to be hypervirulent in various animal models (Bernut et al. 2017; Howard et al. 2006; E. Catherinot et al. 2007) as well as in humans whereas R infection is associated with a rapid decline in the lung functions (Emilie Catherinot et al. 2009; Jönsson et al. 2007)

The latest findings related to the influence of GPL on the physiology of the *M. abscessus* complex and its interaction with host cells are reviewed below.

frontiers in Microbiology

MINI REVIEW
published: 05 June 2018
doi: 10.3389/fmicb.2018.01145

Glycopeptidolipids, a Double-Edged Sword of the *Mycobacterium abscessus* Complex

*Ana Victoria Gutiérrez[1,2], Albertus Viljoen[1], Eric Ghigo[3], Jean-Louis Herrmann[4] and Laurent Kremer[1,5]**

[1] Centre National de la Recherche Scientifique, Institut de Recherche en Infectiologie de Montpellier, UMR 9004, Université de Montpellier, Montpellier, France, [2] CNRS, IRD 198, INSERM U1095, APHM, Institut Hospitalo-Universitaire Méditerranée Infection, UMR 7278, Aix-Marseille Université, Marseille, France, [3] CNRS, Campus Joseph Aiguier, Marseille, France, [4] 2I, UVSQ, INSERM UMR 1173, Université Paris-Saclay, Versailles, France, [5] INSERM, IRIM, Montpellier, France

Mycobacterium abscessus is a rapidly-growing species causing a diverse panel of clinical manifestations, ranging from cutaneous infections to severe respiratory disease. Its unique cell wall, contributing largely to drug resistance and to pathogenicity, comprises a vast panoply of complex lipids, among which the glycopeptidolipids (GPLs) have been the focus of intense research. These lipids fulfill various important functions, from sliding motility or biofilm formation to interaction with host cells and intramacrophage trafficking. Being highly immunogenic, the induction of a strong humoral response is likely to select for rough low-GPL producers. These, in contrast to the smooth high-GPL producers, display aggregative properties, which strongly impacts upon intracellular survival. A propensity to grow as extracellular cords allows these low-GPL producing bacilli to escape the innate immune defenses. Transitioning from high-GPL to low-GPL producers implicates mutations within genes involved in biosynthesis or transport of GPL. This leads to induction of an intense pro-inflammatory response and robust and lethal infections in animal models, explaining the presence of rough isolates in patients with decreased pulmonary functions. Herein, we will discuss how, thanks to the generation of defined GPL mutants and the development of appropriate cellular and animal models to study pathogenesis, GPL contribute to *M. abscessus* biology and physiopathology.

Keywords: *Mycobacterium abscessus*, glycopeptidolipid, cell wall, pathogenesis, host/pathogen interactions

OPEN ACCESS

Edited by:
Thomas Dick,
Rutgers, The State University of New Jersey, Newark, United States

Reviewed by:
Anil Ojha,
Wadsworth Center, United States
Olivier Neyrolles,
Centre National de la Recherche Scientifique (CNRS), France

***Correspondence:**
Laurent Kremer
laurent.kremer@irim.cnrs.fr

Specialty section:
This article was submitted to Antimicrobials, Resistance and Chemotherapy, a section of the journal Frontiers in Microbiology

Received: *21 March 2018*
Accepted: *14 May 2018*
Published: *05 June 2018*

Citation:
Gutiérrez AV, Viljoen A, Ghigo E, Herrmann J-L and Kremer L (2018) Glycopeptidolipids, a Double-Edged Sword of the Mycobacterium abscessus Complex. Front. Microbiol. 9:1145. doi: 10.3389/fmicb.2018.01145

INTRODUCTION

Mycobacterium abscessus is a fast-growing non-tuberculous mycobacterium (NTM) and an emerging human pathogen that causes nosocomial skin and soft tissue infections (Brown-Elliott et al., 2012) but also pulmonary infections, especially in patients with cystic fibrosis (CF) and other lung disorders (Sermet-Gaudelus et al., 2003; Esther et al., 2010). Recent investigations reported mechanisms of virulence and physiopathological processes characterizing *M. abscessus* infection thanks to (i) genetic tools that allowed generation of defined mutants and transposon libraries, particularly useful to seek out genetic determinants of intracellular survival (Medjahed and Reyrat, 2009; Cortes et al., 2011; Gregoire et al., 2017; Laencina et al., 2018) and (ii) the development of various complementary cellular and animal models, which have allowed delineation of the early

stages of the infection and the role of important cell types participating in controlling the infection and/or in the formation of granulomas (Ordway et al., 2008; Bernut et al., 2014a, 2017; Laencina et al., 2018). Evidence exists that granulomas harbor persistent *M. abscessus* for extended periods of time (Tomashefski et al., 1996; Medjahed et al., 2010). Additionally, these models have been used successfully to test the *in vivo* therapeutic efficacy of compounds against *M. abscessus*, considered as one of the most drug-resistant mycobacterial species (Bernut et al., 2014b; Dubée et al., 2015; Obregón-Henao et al., 2015; Dupont et al., 2016).

Like other NTMs, *M. abscessus* displays smooth (S) or rough (R) colony morphotypes, associated with distinct *in vitro* and *in vivo* phenotypes. This colony-based distinction is dependent on the presence (in S) or absence (in R) of surface-associated glycopeptidolipids (GPLs) (Howard et al., 2006; Medjahed et al., 2010). The presence or lack of GPL considerably influences important physiological and physiopathological aspects, including sliding motility or biofilm formation, interaction with host cells, intracellular trafficking in macrophages and virulence, ultimately conditioning the clinical outcome of the infection. This review gathers some of the most recent findings related to biosynthesis and transport of GPL in *M. abscessus*, the mechanisms driving the S-to-R switch and how this transition influences the surface properties of the bacilli, interaction with host cells, virulence and potentially the mode of transmission of *M. abscessus*.

GENOMICS AND STRUCTURAL ASPECTS OF GPL IN *M. abscessus*

The mycobacterial envelope comprises three layers: a typical plasma membrane, a complex cell wall partly resembling a Gram-positive wall and an outer layer (Daffé and Draper, 1998). Particularly unusual, the cell wall consists of a thick peptidoglycan layer covalently-linked to arabinogalactan, itself esterified by mycolic acids, forming the inner leaflet of the mycomembrane. In addition, a large variety of extractible lipids form the outer leaflet of the mycomembrane. Among these are the GPL, found in many NTM (**Figure 1A**). GPL are subdivided into alkali-stable C-type GPL and alkali-labile serine-containing GPL. The C-type GPL are found in saprophytic mycobacteria such as *Mycobacterium smegmatis* or in opportunistic pathogens like *Mycobacterium avium*, *Mycobacterium chelonae,* or *Mycobacterium abscessus* (Schorey and Sweet, 2008), whereas the alkali-labile serine-containing GPL were found in *Mycobacterium xenopi* (Besra et al., 1993). C-type GPL share a common lipopeptidyl core consisting of a mixture of 3-hydroxy and 3-methoxy C28-30 fatty acids amidated by a tripeptide-amino-alcohol core of D-Phe-D-*allo*-Thr-D-Ala-L-alaninol. This lipopeptide core is glycosylated with the *allo*-Thr linked to a 6-deoxy-α-L-talose and the alaninol linked to an α-L-rhamnose. These di-glycosylated GPL make up the less polar species (**Figure 1A**). In the case of *M. avium*, the 6-deoxytalose is non-methylated or 3-*O*-methylated, and the rhamnose is either 3-*O*-methylated or 3,4-di-*O*-methylated. *M. avium* GPL can also be *O*-acetylated at various locations, depending on the strain. In contrast, *M. smegmatis*, *M. chelonae,* and *M. abscessus* produce di-glycosylated GPL that contain a 3,4-di-*O*-acetylated 6-deoxytalose and a 3,4-di-*O*-methylated or 2,3,4-tri-*O*-methylated rhamnose (Villeneuve et al., 2003; Ripoll et al., 2007; Whang et al., 2017). These species also produce more polar GPL by the addition of a 2,3,4-tri-hydroxylated rhamnose to the alaninol-linked 3,4-di-*O*-methyl rhamnose. Although being structurally identical, triglycosylated GPL are more abundant in *M. abscessus* than in *M. smegmatis* (Ripoll et al., 2007). GPL are heterogenous in structure and vary according to the fatty acyl chain length and the degree of hydroxylation or *O*-methylation of the glycosidic moieties (**Figure 1B**).

The *gpl* locus is highly conserved in *M. smegmatis*, *M. abscessus,* and *M. avium* (**Figure 1C**) but differences exist, like the presence of an IS1096 in *M. smegmatis.* The tripeptide-aminoalcohol moiety of GPL is assembled by the products of *mps1* and *mps2* (Billman-Jacobe et al., 1999). The genes *gtf1* and *gtf2* catalyze glycosylation of the lipopeptide core whereas *gtf3* adds the extra rhamnose defining triglycosylated GPL. The genes *rmt2*, *rmt3,* and *rmt4* participate in *O*-methylation of the rhamnose and *fmt*, absent in *M. avium*, in *O*-methylation of the lipid moiety. In contrast to *M. smegmatis* which possesses a single *atf* gene involved in acetylation of the two positions of the deoxytalose, two genes, *atf1* and *atf2*, transfer the acetyl residues in a sequential manner in *M. abscessus* (Ripoll et al., 2007). Separated by *gtf3*, *rmlA* and *rmlB* are responsible for monosaccharide activation and epimerization. On the proximal end of the *gpl* locus is found *mmpS4*, *mmpL4a* and *mmpL4b* in an operon and encoding membrane proteins required for the transport of GPL across the plasma membrane (Medjahed and Reyrat, 2009; Deshayes et al., 2010; Bernut et al., 2016b). MmpS4 has been proposed to mediate formation of the GPL biosynthesis/transport machinery megacomplex located at the bacterial pole (Deshayes et al., 2010). GPL transport requires also the integral membrane protein Gap in *M. smegmatis* (Sondén et al., 2005) (**Figure 1A**). How GPL are translocated from the periplasmic space to the outer membrane, however, remains unknown. Additionally, a block of eight genes [*MSMEG_0406* (*fadE5*) to *MSMEG_0413* (*gap-like*)] in *M. smegmatis*, originally proposed to catalyze the lipid synthesis and attachment to the tripeptide-aminoalcohol moiety of GPL (Ripoll et al., 2007) was recently reattributed to the synthesis of trehalose polyphleates (TPP) (Burbaud et al., 2016). In *M. abscessus*, this cluster is far away from the main *gpl* locus with *Rv0926* and *fadE5* being scattered in the *M. abscessus* chromosome (**Figure 1C**).

MOLECULAR MECHANISMS OF THE SMOOTH-TO-ROUGH TRANSITION AND ASSOCIATED PHENOTYPES

Comparative genomics to understand the molecular basis of the S and R phenotypes using isogenic S and R pairs revealed multiple indels or single nucleotide polymorphisms within the *gpl* locus (Pawlik et al., 2013). A single nucleotide deletion in *mmpL4b* and nucleotide insertions in *mps1* were identified in the R variants

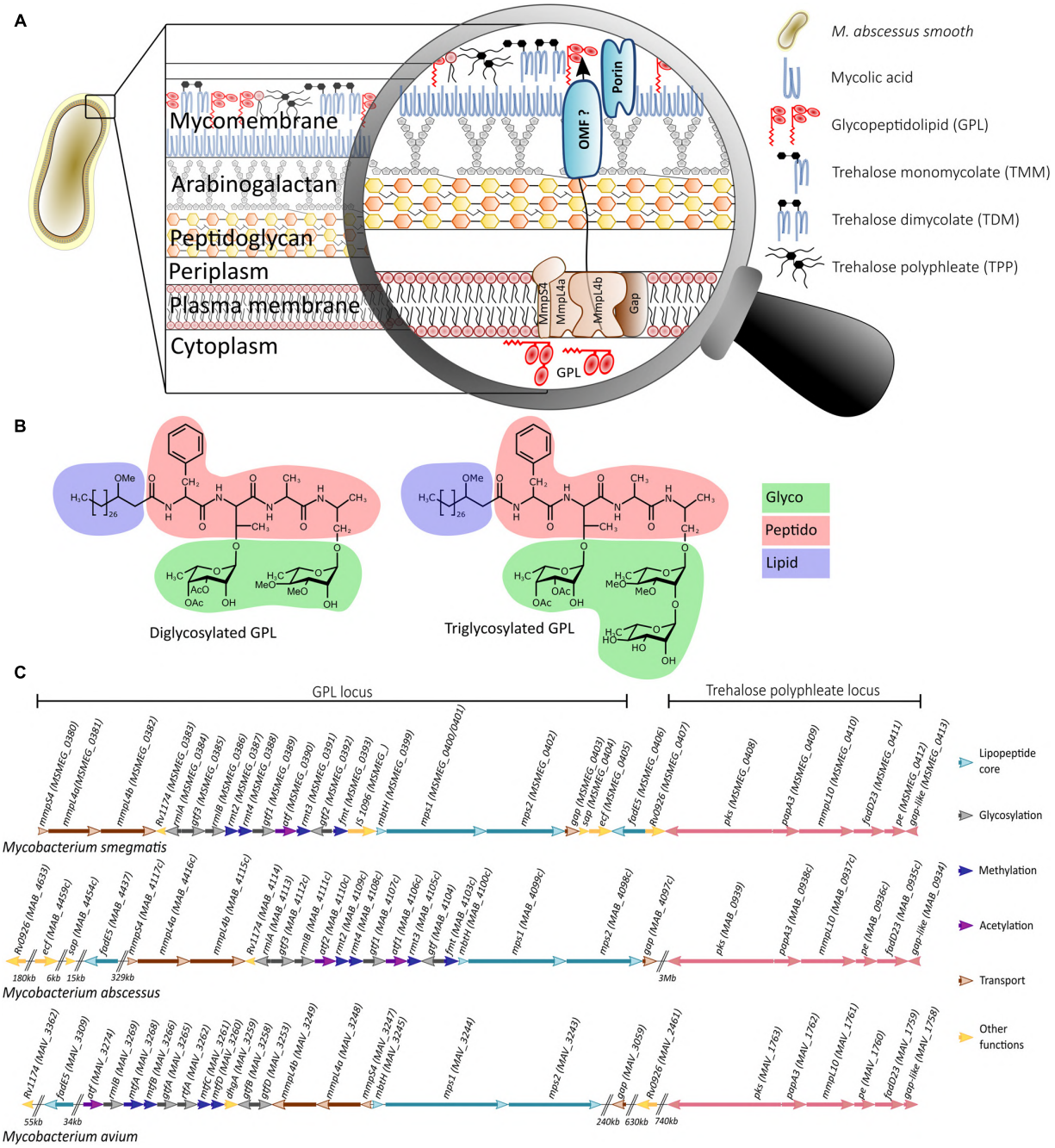

FIGURE 1 | Cell wall localization, structure, and genomics of GPL. **(A)** Schematic representation of the *Mycobacterium abscessus* envelope, with a special focus on the plasma membrane proteins participating in the transport of GPL and on the inner and outer leaflets of the mycomembrane impregnated with various extractible lipids such as GPL. **(B)** Structure of the diglycosylated (apolar) and triglycosylated (polar) GPL. As GPL represent a highly heterogenous population of lipids, only one structure is depicted. Modifications can occur in the lipid chain length or in the hydroxylation/*O*-methylation status of the various monosaccharides. **(C)** Genomic organization of the *gpl* and *tpp* loci in *Mycobacterium smegmatis, Mycobacterium abscessus,* and *Mycobacterium avium*. Arrows indicating the transcription orientation of the different genes are drawn to scale. A color code has been used to specify the participation of these genes in synthesis of the lipopeptide core, glycosylation, methylation, acetylation, transport and other biological functions, as indicated. Genes in the *tpp* locus are displayed in pink.

when compared to the S variants from the three different isogenic S/R couples. Moreover, RNA sequencing demonstrated that S and R isogenic strains differed considerably at the transcriptomic level, with the transcriptional extinction of *mps1*, *mps2,* and *gap* in the R strain caused by an insertion in the 5′-end of *mps1* (Pawlik et al., 2013). Additional mutations in *mps2*, *mmpL4a,* and *mmpS4* were subsequently identified in R strains isolated from later disease stages (Park et al., 2015). Disruption of *mmpL4b* in

M. abscessus S was initially reported to abrogate GPL production, leading to a rough colonial morphotype (Medjahed and Reyrat, 2009; Nessar et al., 2011) (**Figure 2A**). Point mutations in MmpL4a at Tyr842 or MmpL4b at Tyr854, corresponding to two critical residues presumably involved in the proton-motive force of the MmpL proteins, were also associated with loss of GPL production (Bernut et al., 2016b) (**Figure 2A**), suggesting that no functional redundancy exists between MmpL4a and MmpL4b.

Hydrophilic and hydrophobic properties of bacteria can influence surface adhesion and biofilm formation (Krasowska and Sigler, 2014). As shown in *M. smegmatis* (Recht and Kolter, 2001), *M. abscessus* (Howard et al., 2006) and *M. bolletii* (Bernut et al., 2016b) the presence of GPL in the S variants facilitates sliding across the surface of motility agar and biofilm formation on the liquid medium/air interface whereas lack of GPL promotes bacterial aggregation (Brambilla et al., 2016) and cording (Howard et al., 2006; Bernut et al., 2014a, 2016b). However, whether *M. abscessus* R fails at producing biofilms was recently readdressed and proposed that it can grow in biofilm-like structures, which, like S biofilms, are significantly more tolerant than planktonic cultures to acidic pH, hydrogen peroxide, and drugs (Clary et al., 2018). In *M. smegmatis,* the nucleoid-associated protein Lsr2 negatively regulates GPL production (Kocíncová et al., 2008) and plays a role during the initial stages of biofilm development (Yang et al., 2017). Despite the presence of an *lsr2* gene in *M. abscessus,* which is up-regulated in the R variant (Pawlik et al., 2013), the contribution of Lsr2 in regulating GPL expression, sliding motility and biofilm formation remains to be established.

External factors, such as sub-inhibitory antibiotic concentrations, can promote a transient S-to-R change with more aggregated cultures and a higher resistance to phagocytosis (Tsai et al., 2015). Strangely, these phenotypes were neither linked to a loss of GPL production nor to the differential expression of genes within the *gpl* cluster, but were rather mediated by *MAB_3508c*, homologous to *whiB7* and conferring extreme resistance to antibiotics in *M. abscessus* (Hurst-Hess et al., 2017). In contrast, another study reported that sub-inhibitory amikacin treatment, also leading to a S-to-R transition, was associated with decreased GPL, resulting from down-regulation of several *gpl* biosynthetic genes (Lee et al., 2017). Overall, these results suggest that exposure to sub-inhibitory amikacin doses may induce alterations in GPL content, increase virulence and influence the outcome of the infection as well as the therapeutic efficacy of drugs.

PRESENCE OR LOSS OF GPL CONDITIONS BACTERIAL SURFACE PROPERTIES AND INTERACTIONS WITH HOST CELLS

The S and R variants interact differently with host cells and exhibit different intracellular behaviors, as first reported in human monocytes with the R variant persisting longer in these cells (Byrd and Lyons, 1999) and then confirmed in other phagocytes (Howard et al., 2006; Roux et al., 2016). Macrophages encountering the aggregative R strain, are incapable of engulfing clumps of R bacteria, which remain embedded in phagocytic cups on the exterior of the cells (Roux et al., 2016). However, smaller clumps are phagocytosed, resulting in social phagosomes (containing numerous bacilli) that rapidly fuse with lysosomes. In addition, R variant-containing THP1 cells were more acidified, more autophagic and more apoptotic than those infected with the S variant. In contrast, in the majority of S variant-containing phagosomes, a continuous tight apposition is maintained between the phagosome membrane and the mycobacterial cell envelope, leading to phagosome maturation blockage and the absence of acidification in S-infected macrophages. Another conspicuous trait of the S-containing phagosomes is the occurrence of a large electron translucent zone (ETZ) enclosing the bacilli (**Figure 2B**). This ETZ is barely detected in R-containing phagosomes or in phagosomes containing S strains mutated in either *mmpL4a* or *mmpL4b*, indicating that the ETZ relies on the presence of cell surface GPL (Bernut et al., 2016b; Roux et al., 2016). Interestingly, infection with *M. abscessus* S, but not R, leads to phagosome membrane lesions, suggesting that, similarly to pathogenic slow-growing mycobacteria, this variant has the capacity to induce phagosome–cytosol communications (Simeone et al., 2012), through a mechanism that likely involves the type VII secretion system ESX-4 (Laencina et al., 2018).

The distinct mechanisms responsible for the S- and R-induced responses in macrophages are being delineated, highlighting a model whereby the loss of GPL at the surface unmasks underlying phosphatidyl-*myo*-inositol dimannoside (PIM_2) (Rhoades et al., 2009) and lipoproteins (Roux et al., 2011). These TLR-2 agonists stimulate the expression of TNF and intense inflammation. Exacerbation of this response can also lead to tissue lesions associated with R strains. In S strains, by covering underlying immunostimulatory cell wall components, GPL may delay the activation of the immune response during early infection stages and facilitate colonization by preventing TLR-2 signaling in the respiratory epithelial cells (Davidson et al., 2011).

Apoptosis represents an innate response of cells to restrict multiplication of intracellular pathogens (Lamkanfi and Dixit, 2010). *M. abscessus* R was found to be more apoptotic than *M. abscessus* S in different types of macrophages (Roux et al., 2016; Whang et al., 2017). Supporting these findings, purified GPL from *M. abscessus* S inhibits macrophage apoptosis, presumably by suppressing the production of radical oxygen species (ROS), the release of cytochrome c and by preserving the mitochondrial transmembrane potential (Whang et al., 2017) (**Figure 2B**). This mechanism appears to be mediated by targeting of acetylated GPL to the mitochondria where they interact with cyclophilin D, a component of the mitochondrial permeability transition pore (MPTP), inhibiting the MPTP that results in a block on cell death in similar fashion to cyclosporin A. That exogenous GPL-dependent apoptosis inhibition restricts intracellular growth and spreading of *M. abscessus* R, suggests also that GPL may limit *M. abscesssus* virulence (Whang et al., 2017).

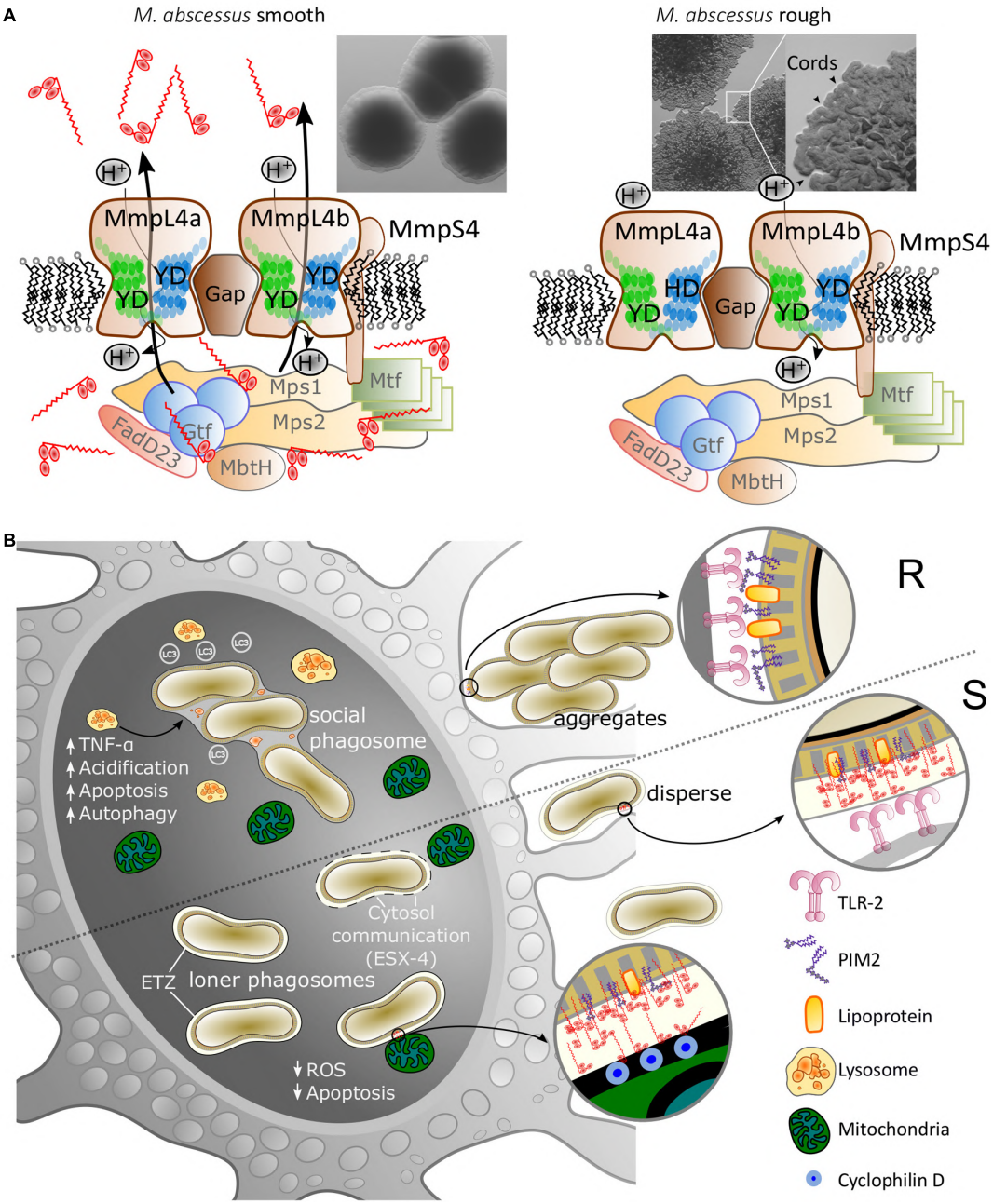

FIGURE 2 | Glycopeptidolipid (GPL) composition influences the colonial morphology and host cell interactions of *M. abscessus*. **(A)** Morphology of the high-GPL producing smooth (S) morphotype (left panel) and low-GPL producing rough (R) morphotype (right panel). The production and transport of GPL requires multiple cytosolic biosynthetic enzymes and transmembrane proteins. Mutations in genes involved in GPL production/transport occurring *in vivo* or introduction of point mutations of crucial Tyr/Asp (Y/D) couples in MmpL4a/MmpL4b participating in the proton relay lead to the arrest of lipid transport and a rough morphotype (right panel). R strains are typified by the production of serpentine cords (inset, arrowheads). **(B)** Inhibition of the macrophage apoptotic response by GPL covering *M. abscessus* S occurs through mitochondrial targeting and interaction with cyclophilin D, reduced production of radical oxygen species (ROS) and limitation of the spread of *M. abscessus* among macrophages. In contrast, the loss of GPL in *M. abscessus* R uncovers immunostimulatory TLR-2 agonists, such as PIM_2 and lipoproteins, leading to an exacerbated pro-inflammatory response that contributes to acute and severe infections.

Collectively, these observations emphasize the diversity of the infection programs orchestrated by S and R variants. While the S variant is promptly phagocytosed by macrophages without immediately affecting cell survival, phagocytosis of the R variant is more harmful to macrophage viability and, following apoptosis, the released bacteria replicate extracellularly in the form of serpentine cords (**Figure 2A**).

IMPACT OF THE GPL CONTENT ON VIRULENCE

Epidemiological surveys document the prominence of the R strain in patients with severe pulmonary infections (Catherinot et al., 2009) and with chronic colonization of the airways in CF patients (Jönsson et al., 2007), but the exact proportions of S and R forms in these populations remain largely unknown. This distinction is, however, of crucial importance considering that the cord-forming R variant causes much more aggressive and invasive pulmonary disease that ends in severe respiratory failure. Further alarm is raised by several studies using various cellular and animal models, confirming the increased virulence of the R over the S form (Bernut et al., 2017). Among these models, the zebrafish (*Danio rerio*) has been proposed as a relevant and genetically tractable host–pathogen conjugate for dissecting *M. abscessus* interactions with host cells (Bernut et al., 2015). This led to important breakthroughs regarding mechanisms of *M. abscessus* pathogenesis, involving cording and granuloma formation (Bernut et al., 2014a) or the importance of the TNF response in controlling the infection and establishment of protective granulomas (Bernut et al., 2016a). S-to-R transitioning is associated with exacerbation of the bacterial burden, the formation of massive serpentine cords, abscess formation, notably in the central nervous system, and increased larval killing (Bernut et al., 2014a). Deletion of *MAB_4780*, encoding a dehydratase required for cording, resulted in extreme attenuation in wild-type and immunocompromized larvae (Halloum et al., 2016), further incriminating cording as a major virulence determinant in strains lacking GPL. Replacing the endogenous *mmpS4-mmpL4a-mmpL4b* promoter with the leaky acetamidase promoter from *M. smegmatis* in *M. abscessus* S resulted in a strain with low-GPL levels, but still aggregating in culture with a rough appearance, similar to R strains. In zebrafish, this mutant exhibited an intermediate virulence phenotype with a delay in killing compared to the R strain. Moreover, the number and size of the abscesses in larvae infected with this low-GPL producing strain were significantly reduced compared to the R strain (Viljoen et al., 2018). This indicates that low-GPL levels impede the induction of the physiopathological signs and virulence of *M. abscessus* R, confirming the opposite relationship between the amount of GPL and virulence. In addition, the S variant is more hydrophilic than the R variant or the rough low-GPL producing strain. This suggests that lack of the hydrophilic GPL components is responsible for their increased hydrophobicity over the S strain and confirm a positive correlation between GPL production and hydrophilicity.

Supporting the theory of transmission *via* aerosols from the environment, *M. abscessus,* along with other NTM, was isolated from household water and shower aerosols in the homes of patients with pulmonary disease (Thomson et al., 2013). Importantly, a direct person-to-person transmission of *M. abscessus* by aerosol inhalation has been asserted in recent world-wide surveys, although the link between morphology/GPL profile and mode of transmission remains to be investigated (Bryant et al., 2013, 2016).

CONCLUSION AND PERSPECTIVES

Fundamental aspects of the *M. abscessus* lifecycle rely on the beneficial effects of GPL in promoting and facilitating the early stages of colonization of the S variant, presumably the major form existing in the environment. By covering the bacilli, the highly immunogenic GPL induce a strong humoral response in infected individuals and it is possible that this strong immune pressure leads to selection of GPL-deficient strains, allowing *M. abscessus* to escape the anti-GPL response and the emergence of R bacilli. The lack of GPL, in turn, leads to increased apoptosis, promoting extracellular replication and cording, acute infection and the most severe forms of the disease. This has also detrimental consequences for the host since, by unmasking other pro-inflammatory cell-surface components, the loss of GPL translates to severe inflammation and lung damage. Therefore, the double edged sword effect of GPL allows *M. abscessus* to efficiently transition between a colonizing environmental micro-organism to an invasive human pathogen. Given the importance of the GPL content in driving the interaction with host cells and in conditioning the issue of the infection, it appears important to pay more attention to the variant (S or R) selected for experimental infections and to systematically report the morphotype of the strains isolated in clinical studies.

Important unsolved questions remain on GPL in *M. abscessus*. Future investigations should describe the complete GPL export machinery since, while transfer of GPL across the plasma membrane has been addressed to some extent, additional unidentified outer-membrane proteins are likely to participate in this important physiological process. So far, the literature only reports the effects of near total loss of GPL in *M. abscessus*, portraying an incomplete picture of the functions of these lipids in the physiology of this pathogen. Polar GPL species in *M. smegmatis* are only produced under carbon starvation and induce smooth-colony formation (Ojha et al., 2002) opening up the possibility that in *M. abscessus* GPL composition is modulated in response to changing environments. Therefore, studies are required to address whether GPL composition affects *M. abscessus* persistence and/or host inflammation, as well as how the dynamics of GPL production, potentially mediated by yet unidentified factors, influences adaptation of *M. abscessus* to its host.

AUTHOR CONTRIBUTIONS

AG designed the figures. All authors contributed to writing the manuscript.

FUNDING

LK acknowledges the support by the Fondation pour la Recherche Médicale (FRM) (DEQ20150331719) and the Infectiopôle Sud Méditerranée for funding the Ph.D. Fellowship of AG.

REFERENCES

Bernut, A., Dupont, C., Sahuquet, A., Herrmann, J.-L., Lutfalla, G., and Kremer, L. (2015). Deciphering and imaging pathogenesis and cording of *Mycobacterium abscessus* in zebrafish embryos. *J. Vis. Exp.* 103:e53130. doi: 10.3791/53130

Bernut, A., Herrmann, J.-L., Kissa, K., Dubremetz, J.-F., Gaillard, J.-L., Lutfalla, G., et al. (2014a). *Mycobacterium abscessus* cording prevents phagocytosis and promotes abscess formation. *Proc. Natl. Acad. Sci. U.S.A.* 111, E943–E952. doi: 10.1073/pnas.1321390111

Bernut, A., Le Moigne, V., Lesne, T., Lutfalla, G., Herrmann, J.-L., and Kremer, L. (2014b). *In vivo* assessment of drug efficacy against *Mycobacterium abscessus* using the embryonic zebrafish test system. *Antimicrob. Agents Chemother.* 58, 4054–4063. doi: 10.1128/AAC.00142-14

Bernut, A., Herrmann, J.-L., Ordway, D., and Kremer, L. (2017). The diverse cellular and animal models to decipher the physiopathological traits of *Mycobacterium abscessus* infection. *Front. Cell. Infect. Microbiol.* 7:100. doi: 10.3389/fcimb.2017.00100

Bernut, A., Nguyen-Chi, M., Halloum, I., Herrmann, J.-L., Lutfalla, G., and Kremer, L. (2016a). *Mycobacterium abscessus*-induced granuloma formation is strictly dependent on TNF signaling and neutrophil trafficking. *PLoS Pathog.* 12:e1005986. doi: 10.1371/journal.ppat.1005986

Bernut, A., Viljoen, A., Dupont, C., Sapriel, G., Blaise, M., Bouchier, C., et al. (2016b). Insights into the smooth-to-rough transitioning in *Mycobacterium bolletii* unravels a functional Tyr residue conserved in all mycobacterial MmpL family members. *Mol. Microbiol.* 99, 866–883. doi: 10.1111/mmi.13283

Besra, G. S., McNeil, M. R., Rivoire, B., Khoo, K. H., Morris, H. R., Dell, A., et al. (1993). Further structural definition of a new family of glycopeptidolipids from *Mycobacterium xenopi*. *Biochemistry* 32, 347–355. doi: 10.1021/bi00052a043

Billman-Jacobe, H., McConville, M. J., Haites, R. E., Kovacevic, S., and Coppel, R. L. (1999). Identification of a peptide synthetase involved in the biosynthesis of glycopeptidolipids of *Mycobacterium smegmatis*. *Mol. Microbiol.* 33, 1244–1253. doi: 10.1046/j.1365-2958.1999.01572.x

Brambilla, C., Llorens-Fons, M., Julián, E., Noguera-Ortega, E., Tomàs-Martínez, C., Pérez-Trujillo, M., et al. (2016). Mycobacteria clumping increase their capacity to damage macrophages. *Front. Microbiol.* 7:1562. doi: 10.3389/fmicb.2016.01562

Brown-Elliott, B. A., Nash, K. A., and Wallace, R. J. (2012). Antimicrobial susceptibility testing, drug resistance mechanisms, and therapy of infections with nontuberculous mycobacteria. *Clin. Microbiol. Rev.* 25, 545–582. doi: 10.1128/CMR.05030-11

Bryant, J. M., Grogono, D. M., Greaves, D., Foweraker, J., Roddick, I., Inns, T., et al. (2013). Whole-genome sequencing to identify transmission of *Mycobacterium abscessus* between patients with cystic fibrosis: a retrospective cohort study. *Lancet* 381, 1551–1560. doi: 10.1016/S0140-6736(13)60632-7

Bryant, J. M., Grogono, D. M., Rodriguez-Rincon, D., Everall, I., Brown, K. P., Moreno, P., et al. (2016). Emergence and spread of a human-transmissible multidrug-resistant nontuberculous mycobacterium. *Science* 354, 751–757. doi: 10.1126/science.aaf8156

Burbaud, S., Laval, F., Lemassu, A., Daffé, M., Guilhot, C., and Chalut, C. (2016). Trehalose polyphleates are produced by a glycolipid biosynthetic pathway conserved across phylogenetically distant mycobacteria. *Cell Chem. Biol.* 23, 278–289. doi: 10.1016/j.chembiol.2015.11.013

Byrd, T. F., and Lyons, C. R. (1999). Preliminary characterization of a *Mycobacterium abscessus* mutant in human and murine models of infection. *Infect. Immun.* 67, 4700–4707.

Catherinot, E., Roux, A.-L., Macheras, E., Hubert, D., Matmar, M., Dannhoffer, L., et al. (2009). Acute respiratory failure involving an R variant of *Mycobacterium abscessus*. *J. Clin. Microbiol.* 47, 271–274. doi: 10.1128/JCM.01478-08

Clary, G., Sasindran, S. J., Nesbitt, N., Mason, L., Cole, S., Azad, A., et al. (2018). *Mycobacterium abscessus* smooth and rough morphotypes form antimicrobial-tolerant biofilm phenotypes but are killed by acetic acid. *Antimicrob. Agents Chemother.* 62, e1782-17. doi: 10.1128/AAC.01782-17

Cortes, M., Singh, A. K., Reyrat, J.-M., Gaillard, J.-L., Nassif, X., and Herrmann, J.-L. (2011). Conditional gene expression in *Mycobacterium abscessus*. *PLoS One* 6:e29306. doi: 10.1371/journal.pone.0029306

Daffé, M., and Draper, P. (1998). The envelope layers of mycobacteria with reference to their pathogenicity. *Adv. Microb. Physiol.* 39, 131–203. doi: 10.1016/S0065-2911(08)60016-8

Davidson, L. B., Nessar, R., Kempaiah, P., Perkins, D. J., and Byrd, T. F. (2011). *Mycobacterium abscessus* glycopeptidolipid prevents respiratory epithelial TLR2 signaling as measured by HβD2 gene expression and IL-8 release. *PLoS One* 6:e29148. doi: 10.1371/journal.pone.0029148

Deshayes, C., Bach, H., Euphrasie, D., Attarian, R., Coureuil, M., Sougakoff, W., et al. (2010). MmpS4 promotes glycopeptidolipids biosynthesis and export in *Mycobacterium smegmatis*. *Mol. Microbiol.* 78, 989–1003. doi: 10.1111/j.1365-2958.2010.07385.x

Dubée, V., Bernut, A., Cortes, M., Lesne, T., Dorchene, D., Lefebvre, A.-L., et al. (2015). β-Lactamase inhibition by avibactam in *Mycobacterium abscessus*. *J. Antimicrob. Chemother.* 70, 1051–1058. doi: 10.1093/jac/dku510

Dupont, C., Viljoen, A., Dubar, F., Blaise, M., Bernut, A., Pawlik, A., et al. (2016). A new piperidinol derivative targeting mycolic acid transport in *Mycobacterium abscessus*. *Mol. Microbiol.* 101, 515–529. doi: 10.1111/mmi.13406

Esther, C. R., Esserman, D. A., Gilligan, P., Kerr, A., and Noone, P. G. (2010). Chronic *Mycobacterium abscessus* infection and lung function decline in cystic fibrosis. *J. Cyst. Fibros.* 9, 117–123. doi: 10.1016/j.jcf.2009.12.001

Gregoire, S. A., Byam, J., and Pavelka, M. S. (2017). *galK*-based suicide vector mediated allelic exchange in *Mycobacterium abscessus*. *Microbiology* 163, 1399–1408. doi: 10.1099/mic.0.000528

Halloum, I., Carrère-Kremer, S., Blaise, M., Viljoen, A., Bernut, A., Le Moigne, V., et al. (2016). Deletion of a dehydratase important for intracellular growth and cording renders rough *Mycobacterium abscessus* avirulent. *Proc. Natl. Acad. Sci. U.S.A.* 113, E4228–E4237. doi: 10.1073/pnas.1605477113

Howard, S. T., Rhoades, E., Recht, J., Pang, X., Alsup, A., Kolter, R., et al. (2006). Spontaneous reversion of *Mycobacterium abscessus* from a smooth to a rough morphotype is associated with reduced expression of glycopeptidolipid and reacquisition of an invasive phenotype. *Microbiology* 152, 1581–1590. doi: 10.1099/mic.0.28625-0

Hurst-Hess, K., Rudra, P., and Ghosh, P. (2017). *Mycobacterium abscessus* WhiB7 regulates a species-specific repertoire of genes to confer extreme antibiotic resistance. *Antimicrob. Agents Chemother.* 61, e1347-17. doi: 10.1128/AAC.01347-17

Jönsson, B. E., Gilljam, M., Lindblad, A., Ridell, M., Wold, A. E., and Welinder-Olsson, C. (2007). Molecular epidemiology of *Mycobacterium abscessus*, with focus on cystic fibrosis. *J. Clin. Microbiol.* 45, 1497–1504. doi: 10.1128/JCM.02592-06

Kocíncová, D., Singh, A. K., Beretti, J.-L., Ren, H., Euphrasie, D., Liu, J., et al. (2008). Spontaneous transposition of IS1096 or ISMsm3 leads to glycopeptidolipid overproduction and affects surface properties in *Mycobacterium smegmatis*. *Tuberculosis* 88, 390–398. doi: 10.1016/j.tube.2008.02.005

Krasowska, A., and Sigler, K. (2014). How microorganisms use hydrophobicity and what does this mean for human needs? *Front. Cell. Infect. Microbiol.* 4:112. doi: 10.3389/fcimb.2014.00112

Laencina, L., Dubois, V., Le Moigne, V., Viljoen, A., Majlessi, L., Pritchard, J., et al. (2018). Identification of genes required for *Mycobacterium abscessus* growth *in vivo* with a prominent role of the ESX-4 locus. *Proc. Natl. Acad. Sci. U.S.A.* 115, E1002–E1011. doi: 10.1073/pnas.1713195115

Lamkanfi, M., and Dixit, V. M. (2010). Manipulation of host cell death pathways during microbial infections. *Cell Host Microbe* 8, 44–54. doi: 10.1016/j.chom.2010.06.007

Lee, S.-Y., Kim, H.-Y., Kim, B.-J., Kim, H., Seok, S.-H., Kim, B.-J., et al. (2017). Effect of amikacin on cell wall glycopeptidolipid synthesis in *Mycobacterium abscessus*. *J. Microbiol.* 55, 640–647. doi: 10.1007/s12275-017-6503-7

Medjahed, H., Gaillard, J.-L., and Reyrat, J.-M. (2010). *Mycobacterium abscessus*: a new player in the mycobacterial field. *Trends Microbiol.* 18, 117–123. doi: 10.1016/j.tim.2009.12.007

Medjahed, H., and Reyrat, J.-M. (2009). Construction of *Mycobacterium abscessus* defined glycopeptidolipid mutants: comparison of genetic tools. *Appl. Environ. Microbiol.* 75, 1331–1338. doi: 10.1128/AEM.01914-08

Nessar, R., Reyrat, J.-M., Davidson, L. B., and Byrd, T. F. (2011). Deletion of the *mmpL4b* gene in the *Mycobacterium abscessus* glycopeptidolipid biosynthetic pathway results in loss of surface colonization capability, but enhanced ability to replicate in human macrophages and stimulate their innate immune response. *Microbiology* 157, 1187–1195. doi: 10.1099/mic.0.046557-0

Obregón-Henao, A., Arnett, K. A., Henao-Tamayo, M., Massoudi, L., Creissen, E., Andries, K., et al. (2015). Susceptibility of *Mycobacterium abscessus* to

antimycobacterial drugs in preclinical models. *Antimicrob. Agents Chemother.* 59, 6904–6912. doi: 10.1128/AAC.00459-15

Ojha, A. K., Varma, S., and Chatterji, D. (2002). Synthesis of an unusual polar glycopeptidolipid in glucose-limited culture of *Mycobacterium smegmatis*. *Microbiology* 148, 3039–3048. doi: 10.1099/00221287-148-10-3039

Ordway, D., Henao-Tamayo, M., Smith, E., Shanley, C., Harton, M., Troudt, J., et al. (2008). Animal model of *Mycobacterium abscessus* lung infection. *J. Leukoc. Biol.* 83, 1502–1511. doi: 10.1189/jlb.1007696

Park, I. K., Hsu, A. P., Tettelin, H., Shallom, S. J., Drake, S. K., Ding, L., et al. (2015). Clonal diversification and changes in lipid traits and colony morphology in *Mycobacterium abscessus* clinical isolates. *J. Clin. Microbiol.* 53, 3438–3447. doi: 10.1128/JCM.02015-15

Pawlik, A., Garnier, G., Orgeur, M., Tong, P., Lohan, A., Le Chevalier, F., et al. (2013). Identification and characterization of the genetic changes responsible for the characteristic smooth-to-rough morphotype alterations of clinically persistent *Mycobacterium abscessus*. *Mol. Microbiol.* 90, 612–629. doi: 10.1111/mmi.12387

Recht, J., and Kolter, R. (2001). Glycopeptidolipid acetylation affects sliding motility and biofilm formation in *Mycobacterium smegmatis*. *J. Bacteriol.* 183, 5718–5724. doi: 10.1128/JB.183.19.5718-5724.2001

Rhoades, E. R., Archambault, A. S., Greendyke, R., Hsu, F.-F., Streeter, C., and Byrd, T. F. (2009). *Mycobacterium abscessus* glycopeptidolipids mask underlying cell wall phosphatidyl-myo-inositol mannosides blocking induction of human macrophage TNF-α by preventing interaction with TLR2. *J. Immunol.* 183, 1997–2007. doi: 10.4049/jimmunol.0802181

Ripoll, F., Deshayes, C., Pasek, S., Laval, F., Beretti, J.-L., Biet, F., et al. (2007). Genomics of glycopeptidolipid biosynthesis in *Mycobacterium abscessus* and *M. chelonae*. *BMC Genomics* 8:114. doi: 10.1186/1471-2164-8-114

Roux, A.-L., Ray, A., Pawlik, A., Medjahed, H., Etienne, G., Rottman, M., et al. (2011). Overexpression of proinflammatory TLR-2-signalling lipoproteins in hypervirulent mycobacterial variants. *Cell. Microbiol.* 13, 692–704. doi: 10.1111/j.1462-5822.2010.01565.x

Roux, A.-L., Viljoen, A., Bah, A., Simeone, R., Bernut, A., Laencina, L., et al. (2016). The distinct fate of smooth and rough *Mycobacterium abscessus* variants inside macrophages. *Open Biol.* 6:160185. doi: 10.1098/rsob.160185

Schorey, J. S., and Sweet, L. (2008). The mycobacterial glycopeptidolipids: structure, function, and their role in pathogenesis. *Glycobiology* 18, 832–841. doi: 10.1093/glycob/cwn076

Sermet-Gaudelus, I., Le Bourgeois, M., Pierre-Audigier, C., Offredo, C., Guillemot, D., Halley, S., et al. (2003). *Mycobacterium abscessus* and children with cystic fibrosis. *Emerg. Infect. Dis.* 9, 1587–1591. doi: 10.3201/eid0912.020774

Simeone, R., Bobard, A., Lippmann, J., Bitter, W., Majlessi, L., Brosch, R., et al. (2012). Phagosomal rupture by *Mycobacterium tuberculosis* results in toxicity and host cell death. *PLoS Pathog.* 8:e1002507. doi: 10.1371/journal.ppat.1002507

Sondén, B., Kocíncová, D., Deshayes, C., Euphrasie, D., Rhayat, L., Laval, F., et al. (2005). Gap, a mycobacterial specific integral membrane protein, is required for glycolipid transport to the cell surface. *Mol. Microbiol.* 58, 426–440. doi: 10.1111/j.1365-2958.2005.04847.x

Thomson, R., Tolson, C., Carter, R., Coulter, C., Huygens, F., and Hargreaves, M. (2013). Isolation of nontuberculous mycobacteria (NTM) from household water and shower aerosols in patients with pulmonary disease caused by NTM. *J. Clin. Microbiol.* 51, 3006–3011. doi: 10.1128/JCM.00899-13

Tomashefski, J. F., Stern, R. C., Demko, C. A., and Doershuk, C. F. (1996). Nontuberculous mycobacteria in cystic fibrosis. An autopsy study. *Am. J. Respir. Crit. Care Med.* 154, 523–528. doi: 10.1164/ajrccm.154.2.8756832

Tsai, S.-H., Lai, H.-C., and Hu, S.-T. (2015). Subinhibitory doses of aminoglycoside antibiotics induce changes in the phenotype of *Mycobacterium abscessus*. *Antimicrob. Agents Chemother.* 59, 6161–6169. doi: 10.1128/AAC.01132-15

Viljoen, A., Gutiérrez, A. V., Dupont, C., Ghigo, E., and Kremer, L. (2018). A simple and rapid gene disruption strategy in *Mycobacterium abscessus*: on the design and application of glycopeptidolipid mutants. *Front. Cell. Infect. Microbiol.* 8:69. doi: 10.3389/fcimb.2018.00069

Villeneuve, C., Etienne, G., Abadie, V., Montrozier, H., Bordier, C., Laval, F., et al. (2003). Surface-exposed glycopeptidolipids of *Mycobacterium smegmatis* specifically inhibit the phagocytosis of mycobacteria by human macrophages. Identification of a novel family of glycopeptidolipids. *J. Biol. Chem.* 278, 51291–51300. doi: 10.1074/jbc.M306554200

Whang, J., Back, Y. W., Lee, K.-I., Fujiwara, N., Paik, S., Choi, C. H., et al. (2017). *Mycobacterium abscessus* glycopeptidolipids inhibit macrophage apoptosis and bacterial spreading by targeting mitochondrial cyclophilin D. *Cell Death Dis.* 8:e3012. doi: 10.1038/cddis.2017.420

Yang, Y., Thomas, J., Li, Y., Vilchèze, C., Derbyshire, K. M., Jacobs, W. R., et al. (2017). Defining a temporal order of genetic requirements for development of mycobacterial biofilms. *Mol. Microbiol.* 105, 794–809. doi: 10.1111/mmi.13734

Conflict of Interest Statement: The authors declare that the research was conducted in the absence of any commercial or financial relationships that could be construed as a potential conflict of interest.

CHAPTER II

Co-infection with smooth and rough colony variants of *Mycobacterium abscessus* in cystic fibrosis patients

The genomic heterogeneity of co-infecting *Mycobacterium abscessus* smooth and rough colony variants in cystic fibrosis patients.

Gutiérrez A.V., Baron S., Sardi F., Reynaud-Gaubert M., Saad J., Drancourt M.

In progress.

5. CHAPTER II: Co-infection with smooth and rough colony variants of *Mycobacterium abscessus* in cystic fibrosis patients

The first description of *M. abscessus* causing clinical disease was published more than 60 years ago in a case report of an elderly women with chronic knee infection. The multidrug resistant *M. abscessus*, no yet discovered, was misdiagnosed with TB and the classical treatment failed. Despite the failure of treatment, the remission of the infection by this atypical mycobacteria was reported after 18 months (Moore and Frerichs 1953), controversially with current reports, which consider this infection incurable in some cases if surgical resection is not performed (Nathavitharana et al. 2019). This isolate is currently used worldwide as the type strain of *M. abscessus* (known as ATCC 19977).

Nowadays, *M. abscessus* is particularly known for causing pulmonary disease in patients with CF and in individuals with other underlying lung disorders. Clearance of this mycobacterium is not an option among these patients, which often requires adapted treatments according to clinical progress and limited by antibiotic toxicity (Nathavitharana et al. 2019). The *M. abscessus* complex include three subspecies, the intrinsic resistance to macrolides in *M. abscessus* and *M. bolletii* is attributed to the ribosomal methylase encoded by *(erm)41*. In contrast, *M. massiliense* contains a truncated *erm(41)* gene, explaining why this subspecies remains susceptible to macrolides. The increased interest in the use of whole-genome sequencing (WGS) to differentiate subspecies of *M. abscessus* could contribute to better guide the clinician for the most adapted treatments and to increase our understanding regarding the differences in the virulence phenotypes between these (sub)species.

During the last 20 years *M. abscessus* has gained popularity as a public health problem with a preference for airway colonization in CF patients, although cases of *M. abscessus* have been reported in patients without CF, with the *M. avium* complex remaining the most frequently identified NTM in this CF patients (Jönsson et al. 2007).

M. abscessus displays smooth (S) or rough (R) colony morphotypes, which are characterized by the presence or absence of surface-associated GPL, respectively (Howard et al. 2006). In the cellular and in the zebrafish animal model, the difference between the progression of infection S and R has been studied, in which the S morphotype is considered the chronic form while the R is hypervirulent and causes invasive infections (Bernut et al. 2017). In clinical research it has been observed that wound isolates mainly exhibit S colony morphology, while R morphology is associated with chronic airway colonization (Jönsson et al. 2007; Kim et al. 2008). In contrast with previous reports that suggest the S variant as the initial airway colonizer (Emilie Catherinot et al. 2009). The presence of the R variant is also often associated with an increase in the severity of the symptoms (Emilie Catherinot et al. 2009; Kreutzfeldt et al. 2013; Dedrick et al. 2019; Jönsson et al. 2007) and a disseminated disease with a fatal outcome (Sanguinetti et al. 2001).

We present here two cases of airways co-infection with *M. abscessus* S and R variants, in two unrelated patients with CF. Genetic analysis after WGS suggests colonization by two different strains in one patient, while in the second patient both strains were closely related, indicating a morphological conversion, although this R strain did not show any change in the GPL profile. Aminoglycoside treatment is proposed as a possible trigger on the conversion of the S P9530 strain to the R P9529 strain. We present new SNPs in S and R isolates that could possible influence the morphological change.

Lastly, we propose the use of WGS for the precise identification of different strains in the same patient using the integration of Antibiotic Resistance Gene databases such as ResFinder (Xavier et al. 2016), CARD (Jia et al. 2017) and ARG-ANNOT (Gupta et al. 2014). These databases could detect genetic determinants of antimicrobial resistance that we believe may positively influence the treatment outcome.

Beyond phenotype: The genomic heterogeneity of co-infecting *Mycobacterium abscessus* smooth and rough colony variants in cystic fibrosis patients.

Ana Victoria Gutiérrez[1,2], Sophie Alexandra Baron[1,2], Feyrouz Sonia Sardi[1,2], Martine Reynaud-Gaubert[3,4], Jamal Saad[1,2], x Michel Drancourt[1,2*]

[1]Aix Marseille Univ., IRD, MEPHI, Marseille, France.

2 IHU Méditerranée Infection, Marseille, France.

3 Aix-Marseille University, Faculté de médecine, Marseille, France.

4 Department of Respiratory Diseases, Lung Transplant Team, University Hospital of Marseille, Marseille, France.

[*]Corresponding author: Prof. Michel Drancourt michel.drancourt@univ-amu.fr

Keywords: *Mycobacterium abscessus*, Whole-genome sequencing, morphotype, co-infection.

Summary

Background The nontuberculous *Mycobacterium abscessus* have gain worldwide popularity in the last 20 years for causing opportunistic infections especially in cystic fibrosis (CF) patients. *M. abscessus* infection in a single patient by heterogeneous clones might negatively impact the treatment outcome and progression of disease.

Methods We present a case report of two unrelated CF patients co-infected with *M. abscessus* smooth and rough phenotypes. We used whole-genome sequencing (WGS) to identify co-infection and diversification of *M. abscessus* isolates and further description of genetic determinants related to morphology changes.

Findings Genomic analysis showed for one patient co-infection while for the other patient infection by one clone diversified in two morphologies. The rough isolate from the first patient had novel SNPs that could be involved in smooth-to-rough morphology change. In the second patient both smooth and rough isolates were presenting glycopeptidolipids, which prompt us to identify four genes only present in the smooth isolate. In addition, we obtained different susceptibility profile in the four clinical isolates.

Interpretation Smooth *M. abscessus* is proposed as the infecting form, subsequent loose of glycopeptidolipids in the host leads to rough phenotype. We opened a new paradigm describing a CF patient infected with two different clones including a rough isolate and additionally identifying a rough *M. abscessus* clone without loose of GPL. We propose WGS for the identification of heterogenic isolates and genetic determinants of antimicrobial resistance that we believe will positively influence the treatment prognosis.

Funding Agence Nationale de la Recherche, and European funding FEDER PRIMI.

INTRODUCTION

Mycobacterium abscessus complex are among the most frequent respiratory tract opportunistic pathogens in cystic fibrosis patients.[1] Their taxonomic classification has changed several times: *M. abscessus* was initially described as a new species,[2] it has then been re-classified as a subspecies of *M. chelonae* [3] and is being included in the *M. abscessus* complex which comprises *M. abscessus* subsp. *abscessus, M. abscessus* subsp. *bolletii* and *M. abscessus* subsp. *massiliense*[4], hereinafter referred as *M. abscessus, M. bolletii* and *M. massiliense*. Their phenotypic and genotypic identification represents a challenge since the morphology, protein profile and 16S rRNA gene sequence do not vary between these three species; whereas *rpoB, hsp65* and *erm(41)* gene sequences seem unique to each one of these three species. Furthermore, colonies of *M. abscessus, M. bolletii* and *M. massiliense* exhibit two different morphotypes, smooth and rough.[5–7] Previous studies using *ex vivo* and *in vivo* models suggested that rough morphotype exhibited increased virulence as compared to smooth morphotype,[8,9] yet these experimental observations poorly translated in clinical observations and the actual characterization of clinical isolates. In particular such clinical isolates have not been genome sequenced in order to more deeply interpret phenotypic data.

Here, we are describing two cases of pulmonary tract co-infection with *M. abscessus* smooth and rough phenotypes, in two unrelated cystic fibrosis patients. We used whole genome sequencing (WGS) to precisely identify the isolates and describe any genetic differences that support the possible virulence factors between these two phenotypes and understand the phenotypic traits that mask the heterogeneity.

MATERIAL AND METHODS

Patients specimens and microbiological procedures.

Clinical histories of patients were anonymized from their computerized medical records, in agreement with the advice of the IHU Méditerranée Infection Ethics Committee n°

2016-024 (dated 19 October, 2016). Decontaminated sputum were inoculated on a homemade 5% sheep blood Columbia agar (COS)-modified medium (COSMO12, Eurobio, Culture-Top, Courtaboeuf, France) and incubated for 30 days at 37°C. Colonies were identified using matrix assisted laser desorption ionization-time of flight mass spectrometry (MALDI-TOS MS) as previously described.[10] Minimal inhibitory concentration (MIC) was performed using E-test gradient strip method (bioMérieux, Marcy l'Etoile, France) on COS medium incubated at 30°C. The following antibiotics were tested: amikacin, clarithromycin (reading after 7 days), ofloxacin, linezolid, cotrimoxazole, tigecycline, ethambutol and doxycycline. In parallel, the salinity of sputum was performed as previously described.[11]

Patients

Patient n°1, was a 34-year-old patient with a history of cystic fibrosis, bilateral agenesis of vas deferens and subacute diverticular cholecystitis with lithiasis. He was known to be pulmonary chronically colonized with *M. abscessus*, *Staphylococcus aureus* and *Pseudomonas aeruginosa* since 2014 and was long-term treated with colistin, pristinamycin and doxycycline. In 2014, *M. abscessus* was isolated for the first time from sputum on liquid method with the Bactec/Alert procedure (Becton-Dickinson, Le Pon t-de-Claix, France). Partial *rpoB* gene sequencing confirmed species affiliation to *M. abscessus.* and this bacterium was again isolated on liquid medium in 2016. In 2017, a sputum sample was inoculated on agar medium and two types of colonies were observed after 10-day incubation here designated as P9527 and P9528 (Figure 1). The first colony (P9527) appeared white, dry and rough, whereas the other colony (P9528) was round, white, shiny and smooth. Identification with MALDI-TOF allow us to classify these two colonies in the *M. abscessus* complex group with a score of 1·823 and 1·932 for the R and the S colonies, respectively. Partial *rpoB* sequencing identified *M. abscessus* subsp. *abscessus* (Genbank accession number MF471859) with 100% coverage and 100% similarity (568/568 bp). Antibiotic susceptibility tests were performed on the two morphotypes and were similar, with exception

of clarithromycin which showed a resistant profile in the P9527 strain and a sensitive profile in the P9528 strain (Table 1). The sputum salinity measurement was 21·5 grams per liter.

Patient n°2 was a 25-year-old patient with cystic fibrosis. The patient was chronically colonized with *Aspergillus fumigatus*, *Stenotrophomonas maltophilia*, *S. aureus* and *Haemophilus parainfluenzae* since 2014. *M. abscessus* was firstly isolated in a sputum in 2019 after a follow-up consultation. Similar as the previous patient, a white, dry and rough colony designated as P9529 and a white, shiny and smooth colony named P9530 were obtained after 6-day incubation on agar medium (Figure 1). MALDI-TOF identification gave a *M. abscessus* complex score of 2·025 and 1·779 for the S and the R colonies, respectively. At the time of the isolation, the patient was long-term treated with an antibiotic rotation of 15 days tobramycin and 15 days colistin and daily doxycycline and azithrom ycin. The antibiotic susceptibility test showed differences for amikacin presenting a resistant phenotype in P9530 (12 $\mu g \cdot mL^{-1}$) in contrast of P9529 (1·5 $\mu g \cdot mL^{-1}$), additional differences were found for tigecycline in which P9529 showed sensitivity (1 $\mu g \cdot mL^{-1}$) and P9530 an intermediate susceptibility profile (3 $\mu g \cdot mL^{-1}$). The sputum salinity measurement was 12 grams per liter.

Lipid analysis.

M. abscessus S and R CIP104536^{T} and the four clinical isolates (P9527, P9528, P9529 and P9530) were grown exponentially, adjusted to OD_{600} 1, plated on 7H10^{OADC} agar and incubated for 5 days at 37 °C. A dense layer of bacterial growth was collected from the agar, added 2 mL of MeOH-0.3% NaCl (10:1) and heated for 5 min at 100°C. The polar lipids were extracted by adding 2.3 mL of chloroform-MeOH-0.3% NaCl (9:10:3) and mixing for 1 h at room temperature, additionally was re-extracted the residue with 750 µL of chloroform-MeOH-0.3% NaCl (5:10:4) for 30 min, both fractions were combined and mixed with 1·3 mL of chloroform and 1·3 mL of 0·3% NaCl for 5 min. The lower-organic phase was evaporated and suspended in chloroform/MeOH (2:1). Apolar lipids were analysed by thin-layer liquid chromatography as previously described.[12]

Whole genome sequence bioinformatic analysis.

Genomic DNA of the clinical isolate strains were extracted using InstaGen matrix (Biorad, Marnes-la-Coquette, France). DNA was quantified by Qubit assay with the high sensitivity kit (Life technologies, Carlsbad, CA, USA) and 0·2 µg/µL of the DNA was sequenced on Illumina MiSeq runs using the paired-end application (Illumina Inc., San Diego, USA). Paired-end sequencing and automated cluster generation of 11 run, with dual indexed 2× 251-bp reads were performed for 40 hrs. Total information was obtained from a 462 k/mm2 cluster density with a cluster passing quality control filters of 95·5%. Assembly was performed on trimmed or raw data with a pipeline incorporating different software (SPAdes software 3·5·0[13] and Trimmomatic[14] for trimmed data). Then scaffolds which size was under 800 bp and low coverage were removed (identified by BLAST as contaminants). Genomes were annotated using Prokka.[15] Roary pangenome pipeline in Galaxy software (https://usegalaxy.org.au./) was used to generate the pan-genome analysis of the genomes with minimum percentage identity for Blastp 95% and percentage of isolates a gene must be in to be core 99%. Genome to Genome Distance Calculator (GGDC) was employed for similarity estimation between compared genomes (http://ggdc.dsmz.de), formula 2 was recommended into account to interpret the results of the draft genome analyzed. Single-nucleotide polymorphisms (SNP) in the glycopeptidolipid (GPL) locus were identified manually after alignment between S and R isolates from the same patient using MUSCLE in the alignment editor Unipro UGENE v1·32·0.[16] Identification of mutations related to resistance to macrolides[17,18] was done in *erm(41)* and *rrl* genes using the same tool. All the sequences were obtained from the WGS data. Genome sequences have been deposited into the EMI database under the following accession numbers: P9527 (ERS3527803), P9528 (ERS3527804), P9529 (ERS3527805), and P9530 (ERS3527806).

RESULTS

Genomic analysis

In silico DNA-DNA hybridization of these four isolates estimated by comparing them with reference genomes (Table 2) using GGDC version 2·0 online tool yielded 99·8% between P9529 (R) and P9530 (S) with 0·22% of G+C content difference, but 94·6% between P9527 (R) and P9528 (S) with 1·12% of G+C content difference. Moreover, pangenome analysis of the four isolates showed that P9529 and P9530 grouped together with high similarity at the level of global genome profile, but the P9527 and P9528 isolates showed significantly heterogeneity at level of dispensable genome (Figure 2).

Genomic comparison using two different tools showed that patient n°1 was infected by two different clones, with rough (P9527) and smooth (P9528) colony morphology, but the patient n°2 was infected by one clone with two form rough (P9529) and smooth (P9530).

In order to genotypically associate the possible S to R conversion in the patient "number 2" to the previously reported indels (insertion /deletion) in the *mps1, mps2, gap, mmpS4a, mmpL4a* and *mmpL4b* genes,[19,20] all the GPL loci[21] were analysed. Although no indels (insertion/deletion) were detected, a comparison between the S and R strains P9530/P9529 identified a discrete amount of nonsynonymous SNP including *mmpL4b* (A212C), *mps1* (C2369G), *mps2* (A1400G, C1534G, G2041C, G6194T, G7534C) and *gap* (G11A, G50T). Other SNPs in the GPL locus that have not been previously reported and might be involved in the switch smooth to rough were found in the P9527 clinical isolate and are listed in Table 3.

By last, thin layer chromatography (TLC) was performed on the extracts from four clinical isolates. As expected, the P9527 strain presenting R morphology did not show bands corresponding to GPL. Surprisingly, in the rough strain P9529 the GPL remain intact (Figure 3), therefore, the previous SNP identified in the P9529 strains are not responsible of the rough morphotype conversion.

Additional analysis using the bioinformatic online tool Phandango[22] allowed us to visualize the gene distribution between our four clinical isolates and identify possible unique genes for differentiate smooth from rough colony morphology (Figure 2). Four genes were found only in the smooth strains P9528 and P9530 and not in the rough isolates. Nucleotide BLAST alignment of these genes showed: (1) a hypothetical protein presenting a partial match up with *MAB_3888* corresponding to a putative RNA polymerase sigma-70 factor, (2) a PE family immunomodulator PE5 having a complete match up with *MAB_0046*, (3) a putative PPE family protein PPE2 showing a complete match up with *MAB_0809c* and (4) a hypothetical protein presenting a partial match up with *MAB_4691c* corresponding to a probable non-ribosomal peptide synthetase PstA (Table 4).

A further analysis was done in another promising area of the pangenome showing a differential pattern between smooth and roug h (Figure 4), but non common marker was found between smooth and rough morphotypes in this area (Table 5).

Genotypic characterization of *erm(41)* and *rrl* genes in four clinical isolates.

The four clinical isolates did not present mutations at the nucleotide positions 2058 and 2059 in the *rrl* gene. Further analysis was done in the *erm(41)* gene, only the strain P9528 which showed a sensitive phenotype to clarithromycin was carrying a non-functional Erm(41) (C28 sequevar) while the three other strains known for be resistant to clarithromycin were identified with a T28 sequevar. On the other hand, for all strains an additional mutation (V80I) was found (Table 6), a previous study in Korea that included 152 resistant strains to clarithromycin associated this mutation with most of the resistant strains.[23]

DISCUSSION

We report two cases of unrelated cystic fibrosis patients presenting respiratory tract colonization caused by *M. abscessus* with two rough/smooth colony variants for each in the same sputum sample. The salinity of the respiratory samples was concordant with a previous study that showed a higher salinity in the sputum of cystic fibrosis patients.[11] The mean

salinity of cystic fibrosis patients in this study was 10.5 grams per liter compared to control group (7·4 grams per liter). *M. abscessus* isolates are salt-tolerated species that can survive in environment with >4% salt.[24] This high tolerance to salt could explain the special affinity for this species to colonize the respiratory tract of cystic fibrosis patients.

The identification was firmly ensured by WGS analysis as the three *M. abscessus* complex species are closely related in a morphological, and in a comparative genomic analysis,[25] currently is still not clear how each species contributes to pathogenicity and further studies need to be addressed. *rpoB, erm(41)* and *hsp65* are three genes that can be sequenced to help the identification at the subspecies level.[26] We sequenced both the rough and the smooth forms of the isolates to compare their genomes. While it is well known that *M. abscessus* complex present two colonies morphologies, the two morphotypes are non-commonly reported in the same sample of a patient. Previous studies have shown a low frequency of this mixed phenotype in *M. abscessus*[5,27] and *M. bolletii* pulm onary infections[5] and more recently seems to become a new concern due to different resistance profiles between isolates.[5,28] To our knowledge, mixed colonies in *M. massiliense* have not been reported yet. The smooth non cording and the rough cording morphotype differences rely on the presence/absence of GPL, respectively.[29] Within the GPL locus in the *M. abscessus* complex, the *msp1, msp2, gap, mmpS4, mmpL4a and mmpL4b* genes have shown to play an important role in the GPL production. Insertion of a CG nucleotides in the *msp1* gene was proven to lead to transcriptional arrest of the *msp1-msp2-gap* operon.[19] Additional indels (insertions and deletion) and SNPs in the *msp1, msp2, gap, mmpS4, mmpL4a and mmpL4b* have also been related to the loss of production of GPL leading to rough morphotype in clinical isolates.[20] The previous reported insertions across the GPL locus were not present in our P9527, however multiple novel SNP were found in this locus (Table 3) including *rmlA* (3 SNP), *atf2* (1 SNP), *atf1* (3 SNP), *rmt3* (1 SNP), *gtf* (1 SNP), *mps1* (8 SNP), *mps2* (3 SNP) which could be linked to the loss of GPL and the rough morphology. Additional findings

after comparison between the smooth and rough isolates open the possibility that there may be other factors that influence morphology change. A recent report explained the effect of aminoglycosides as streptomycin, amikacin or kanamycin to change smooth *M. abscessus* to rough morphology without producing depletion of GPL,[30] confirming that the rough morphology is not only due to the absence of GPL. In our study the patient n°2 was treated with tobramycin, this aminoglycoside may have an influence in the diversification of the smooth P9530 strain to the rough P9529 strain which did not presented any change in the GPL profile.

There is propose the existence of a second GPL-like locus[19] possibly also implicated in the GPL production and smooth to rough transition. This locus contains two non-ribosomal peptide synthase *pst*A genes (*MAB_4690c- MAB_4691c*) similar to *mps1* and *mps2* from the GPL locus. We have identified four genes only present in the smooth clinical isolates of this study but not in the rough strains, one of them encoding for a hypothetical protein homologous with MAB_4691c, opening the possibility of new markers for smooth to rough transitioning.

Our genetic analysis suggests colonization by two distinct strains in one patient, while in the second patient, both smooth and rough strains were closely related indicating morphology conversion. It has been proposed that smooth to rough conversion occurs in the host by clonal diversification. In a follow-up study in patients chronically infected with *M. abscessus* was found initial isolation of the smooth morphotype and later isolation of rough morphotype,[20] nevertheless it is no being considered whether this event could be due to initial colonization with smooth morphotype and a consequent re-colonization with a secondary rough strain. Despite having multiple *ex vivo* and *in vivo* reports that relate the severity of the infection to morphology,[8] it is still not clear how this change from smooth to rough morphology could affect the patient's prognosis.

M. abscessus is a difficult to threat mycobacteria presenting resistance to most of

available drugs.[31] In the 1990's before being describe the inducible resistance to macrolides, clarithromycin was used as a successful therapy.[32] Acquired macrolide resistance was known to be conferred by mutation at position 2058 or 2059 in the *rrl* gene encoding the peptidyltransferase domain of the 23S rRNA but with low frequency in *M. abscessus.* A novel mechanism was introduced 10 years ago, inducible resistance to macrolides attributed to *erm(41),* this methylase is proposed to monomethylate the adenine at position 2058 (A2058) in the 23S rRNA conferring resistance.[33] Loss of function of *erm(41)* linked to sensitive phenotype to clarithromycin is being describe by the T28C mutation.[18] In this study we describe a patient coinfected with two different *M. abscessus* strains having each a different genotype concordant with the clarithromycin phenotype. In another hand, in the patient n°2 we obtained one clone with two different morphologies that showed differences in susceptibility to amikacin and tigecycline, this diversification as the colonization by two different strains can have implications in the susceptibility profile increasing the difficulty to select the proper therapy and that could impact in the disease outcome. Another unexplored possibility is the co-infection by multiple *M. abscessus* complex strains without difference in colony morphology that go unnoticed. We propose the use of WGS to guarantee the identification of different strains in the same patient and apply the most appropriate treatment according to antibiotic resistance genotypes.

Funding information: This work was supported by the French Government under the « Investissements d'avenir » (Investments for the Future) program managed by the Agence Nationale de la Recherche (ANR, fr: National Agency for Research), (reference: Méditerranée Infection 10-IAHU-03). This work was supported by Région Provence Alpes Côte d'Azur and European funding FEDER PRIMMI.

Transparency declaration: MD is a co-founder and shareholder of the start-up Culture-Top cited in this manuscript. The other authors declare that they have no competing interests.

Authors' contributions: SB and MDr designed the study, drafted and revised the manuscript. MRG performed medical examinations. AVG, FSS, and JS performed microbiology analyses. AVG performed the SNP identification on GPL locus and *erm(41)* and *rrl* genes; lipid extraction and analysis; and wrote the paper. JS performed WGS and analyses. All authors have read and approved the final manuscript.

References

1. Lopeman RC, Harrison J, Desai M, Cox JAG. *Mycobacterium abscessus*: Environmental Bacterium Turned Clinical Nightmare. Microorganisms. 2019 Mar 22;7(3).

2. Moore M, Frerichs JB. An unusual acid-fast infection of the knee with subcutaneous, abscess-like lesions of the gluteal region; report of a case with a study of the organism, *Mycobacterium abscessus*, n. sp. J Invest Dermatol. 1953 Feb;20(2):133–69.

3. Kubica GP, Baess I, Gordon RE, Jenkins PA, Kwapinski JB, McDurmont C, et al. A co-operative numerical analysis of rapidly growing mycobacteria. J Gen Microbiol. 1972 Nov;73(1):55–70.

4. Leao SC, Tortoli E, Euzéby JP, Garcia MJ. Proposal that *Mycobacterium massiliense* and *Mycobacterium bolletii* be united and reclassified as *Mycobacterium abscessus subsp. bolletii comb. nov.*, designation of *Mycobacterium abscessus subsp. abscessus subsp. nov*. and emended description of *Mycobacterium abscessus.* Int J Syst Evol Microbiol. 2011 Sep;61(Pt 9):2311–3.

5. Rüger K, Hampel A, Billig S, Rücker N, Suerbaum S, Bange F-C. Characterization of rough and smooth morphotypes of *Mycobacterium abscessus* isolates from clinical specimens. J Clin Microbiol. 2014 Jan;52(1):244–50.

6. Kim B-J, Yi S-Y, Shim T-S, Do SY, Yu H-K, Park Y-G, et al. Discovery of a novel hsp65

genotype within *Mycobacterium massiliense* associated with the rough colony morphology. PLoS ONE. 2012;7(6):e38420.

7. Bernut A, Viljoen A, Dupont C, Sapriel G, Blaise M, Bouchier C, et al. Insights into the smooth-to-rough transitioning in *Mycobacterium bolletii* unravels a functional Tyr residue conserved in all mycobacterial MmpL family members. Mol Microbiol. 2016 Mar;99(5):866–83.

8. Bernut A, Herrmann J-L, Ordway D, Kremer L. The Diverse Cellular and Animal Models to Decipher the Physiopathological Traits of *Mycobacterium abscessus* Infection. Front Cell Infect Microbiol. 2017;7:100.

9. Malcolm KC, Caceres SM, Pohl K, Poch KR, Bernut A, Kremer L, et al. Neutrophil killing of *Mycobacterium abscessus* by intra- and extracellular mechanisms. PLoS ONE. 2018;13(4):e0196120.

10. Afouda P, Ndongo S, Khelaifia S, Labas N, Cadoret F, Di Pinto F, et al. Noncontiguous finished genome sequence and description of *Prevotella phocaeensis sp. nov.*, a new anaerobic species isolated from human gut infected by *Clostridium difficile*. New Microbes New Infect. 2017 Jan;15:117–27.

11. Grandjean Lapierre S, Phelippeau M, Hakimi C, Didier Q, Reynaud-Gaubert M, Dubus J-C, et al. Cystic fibrosis respiratory tract salt concentration: An Exploratory Cohort Study. Medicine (Baltimore). 2017 Nov;96(47):e8423.

12.Besra GS. Preparation of cell-wall fractions from mycobacteria. Methods Mol Biol. 1998;101:91–107.

13. Bankevich A, Nurk S, Antipov D, Gurevich AA, Dvorkin M, Kulikov AS, et al. SPAdes: a new genome assembly algorithm and its applications to single-cell sequencing. J Comput Biol. 2012 May;19(5):455–77.

14. Bolger AM, Lohse M, Usadel B. Trimmomatic: a flexible trimmer for Illumina sequence data. Bioinformatics. 2014 Aug 1;30(15):2114–20.

15. Seemann T. Prokka: rapid prokaryotic genome annotation. Bioinformatics. 2014 Jul 15;30(14):2068–9.

16. Okonechnikov K, Golosova O, Fursov M, UGENE team. Unipro UGENE: a unified bioinformatics toolkit. Bioinformatics. 2012 Apr 15;28(8):1166–7.

17. Kim H-Y, Kim BJ, Kook Y, Yun Y-J, Shin JH, Kim B-J, et al. *Mycobacterium massiliense* is differentiated from *Mycobacterium abscessus* and *Mycobacterium bolletii* by erythromycin ribosome methyltransferase gene (erm) and clarithromycin susceptibility patterns. Microbiology and Immunology. 2010;54(6):347–53.

18. Bastian S, Veziris N, Roux A-L, Brossier F, Gaillard J-L, Jarlier V, et al. Assessment of clarithromycin susceptibility in strains belonging to the *Mycobacterium abscessus* group by erm(41) and rrl sequencing. Antimicrob Agents Chemother. 2011 Feb;55(2):775–81.

19. Pawlik A, Garnier G, Orgeur M, Tong P, Lohan A, Le Chevalier F, et al. Identification and characterization of the genetic changes responsible for the characteristic smooth-to-rough morphotype alterations of clinically persistent *Mycobacterium abscessus*. Mol Microbiol. 2013 Nov;90(3):612–29.

20. Park IK, Hsu AP, Tettelin H, Shallom SJ, Drake SK, Ding L, et al. Clonal Diversification and Changes in Lipid Traits and Colony Morphology in M*ycobacterium abscessus* Clinical Isolates. J Clin Microbiol. 2015 Nov;53(11):3438–47.

21. Gutiérrez AV, Viljoen A, Ghigo E, Herrmann J-L, Kremer L. Glycopeptidolipids, a Double-Edged Sword of the *Mycobacterium abscessus* Complex. Front Microbiol. 2018;9:1145.

22. Hadfield J, Croucher NJ, Goater RJ, Abudahab K, Aanensen DM, Harris SR. Phandango: an interactive viewer for bacterial population genomics. Bioinformatics. 2017 Sep 25;

23. Lee SH, Yoo HK, Kim SH, Koh W-J, Kim CK, Park YK, et al. The drug resistance profile of *Mycobacterium abscessus* group strains from Korea. Ann Lab Med. 2014 Jan;34(1):31–7.

24. Asmar S, Sassi M, Phelippeau M, Drancourt M. Inverse correlation between salt tolerance and host-adaptation in mycobacteria. BMC Res Notes. 2016 Apr 29;9:249.

25. Sassi M, Drancourt M. Genome analysis reveals three genomospecies in *Mycobacterium abscessu*s. BMC Genomics. 2014 May 12;15:359.

26. Blauwendraat C, Dixon GLJ, Hartley JC, Foweraker J, Harris KA. The use of a two-gene sequencing approach to accurately distinguish between the species within the *Mycobacterium abscessus* complex and *Mycobacterium chelonae*. Eur J Clin Microbiol Infect Dis. 2012 Aug;31(8):1847–53.

27. Kim H-Y, Kook Y, Yun Y-J, Park CG, Lee NY, Shim TS, et al. Proportions of *Mycobacterium massiliense and Mycobacterium bolletii* strains among Korean *Mycobacterium chelonae-Mycobacterium abscessus* group isolates. J Clin Microbiol. 2008 Oct;46(10):3384–90.

28. Shaw LP, Doyle RM, Kavaliunaite E, Spencer H, Balloux F, Dixon G, et al. Children with cystic fibrosis are infected with multiple subpopulations of *Mycobacterium abscessus* with different antimicrobial resistance profiles. Clin Infect Dis. 2019 Jan 26;

29. Howard ST, Rhoades E, Recht J, Pang X, Alsup A, Kolter R, et al. Spontaneous reversion of *Mycobacterium abscessus* from a smooth to a rough morphotype is associated with reduced expression of glycopeptidolipid and reacquisition of an invasive phenotype. Microbiology (Reading, Engl). 2006 Jun;152(Pt 6):1581–90.

30. Tsai S-H, Lai H-C, Hu S-T. Subinhibitory Doses of Aminoglycoside Antibiotics Induce Changes in the Phenotype of *Mycobacterium abscessus.* Antimicrob Agents Chemother. 2015 Oct;59(10):6161–9.

31. Nessar R, Cambau E, Reyrat JM, Murray A, Gicquel B. *Mycobacterium abscessus:* a new antibiotic nightmare. J Antimicrob Chemother. 2012 Apr;67(4):810–8.

32. Mushatt DM, Witzig RS. Successful treatment of *Mycobacterium abscessus i*nfections with multidrug regimens containing clarithromycin. Clin Infect Dis. 1995 May;20(5):1441–2.

33. Nash KA, Brown-Elliott BA, Wallace RJ. A novel gene, erm(41), confers inducible macrolide resistance to clinical isolates of Mycobacterium abscessus but is absent from *Mycobacterium chelonae*. Antimicrob Agents Chemother. 2009 Apr;53(4):1367–76.

Figures legends

Figure 1: Morphologic appearance of four clinical isolates of *M. abscessus* and the reference strains smooth and rough after 4 days on 7H10 agar at 37°C.

Figure 2: Pan-genome tree of *Mycobacterium abscessus* strains study. Identification of a possible marker to differentiate between smooth and rough morphotypes. Numbers designation for each marker are described in the table 2. Rough (R), Smooth (S).

Figure 3: Lipid profile of *M. abscessus* strains showing the P9527 strain as the only clinical isolate sharing a deficient GPL profile. Equal weights of total lipid extracts from *M. abscessus* Swt, Rwt, P9527, P9528, P9529 and P9530 strains were analysed by thin-layer chromatography using chloroform/methanol/water (9:10:1, v/v/v). GPLs are indicated with a black box.

Figure 4: Pan-genome analysis between four clinical isolates showed a differential pattern but not related with smooth and rough morphotypes. The description of the signalled area is described in detail in the table 5. Rough (R), Smooth (S).

Figure 1

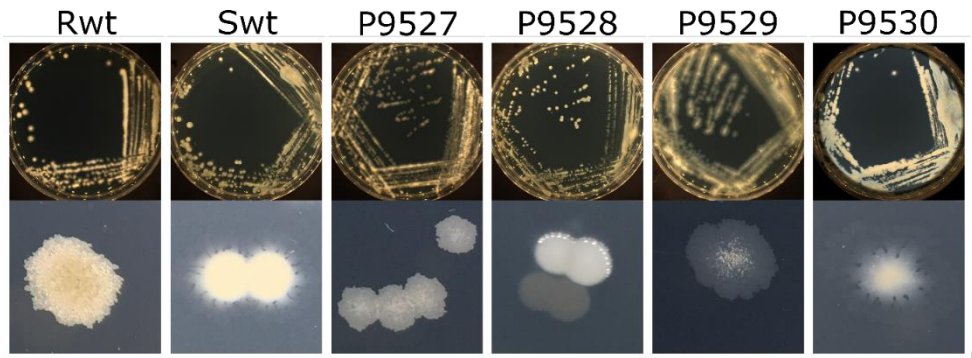

Figure 2

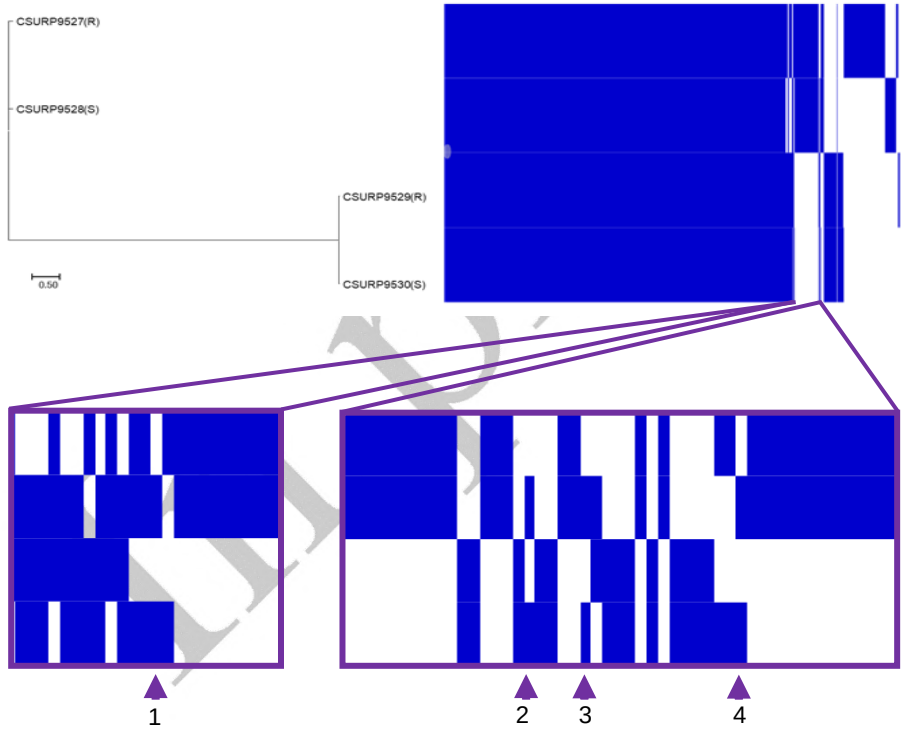

Figure 3

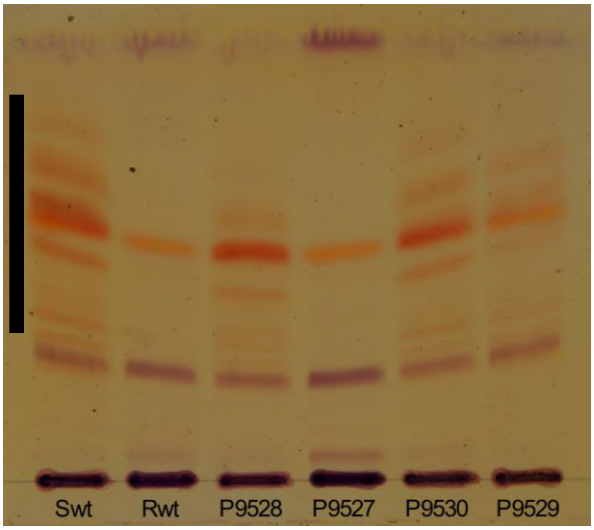

Figure 4

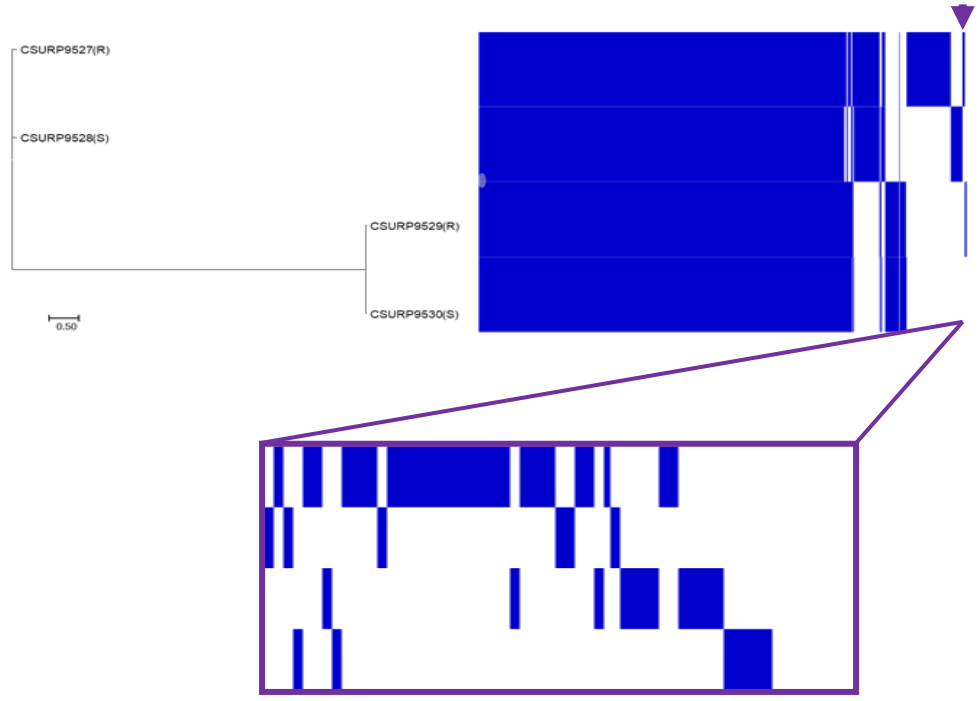

Table 1: Minimum inhibitory concentration (MIC) of selected antibiotics against clinical isolates of *M. abscessus*. MIC values are given in µg/mL

	P9527	P9528	P9529	P9530
Amikacin	12 (R)	12 (R)	1.5 (S)	12 (R)
Clarithromycin	8 (R)	3 (S)	>256 (R)	6 (R)
Ofloxacin	>32 (R)	>32 (R)	>32 (R)	>32 (R)
Linezolid	>256 (R)	>256 (R)	256 (R)	>256 (R)
Bactrim	>32 (R)	>32 (R)	>32 (R)	>32 (R)
Tigecycline	1 (S)	1 (S)	1 (S)	3 (I)
Doxycycline	>256 (R)	>256 (R)	>256 (R)	>256 (R)

I, intermediate; S, susceptible; R, resistant

Table 2: DNA-DNA hybridization values between the four clinical isolates and between references genomes.

Strains	Subject strain	dDDH (d4, %)	G+C content difference (%)
'CSURP9527'	'CSURP9528'	94.6	1.16
'CSURP9528'	'CSURP9529'	95.1	0.44
'CSURP9527'	'CSURP9529'	94.3	1.6
'CSURP9529'	'CSURP9530'	99.8	0.22
'CSURP9528'	'CSURP9530'	95	0.22
'CSURP9527'	'CSURP9530'	94.2	1.39
'CSURP9528'	*Mycobacterium abscessus subsp. massiliense CCUG 48898*	76.2	0.19
'CSURP9529'	*Mycobacterium abscessus subsp. massiliense CCUG 48898*	76.1	0.25
'CSURP9530'	*Mycobacterium abscessus subsp. massiliense CCUG 48898*	76	0.03
'CSURP9527'	*Mycobacterium abscessus subsp. massiliense CCUG 48898*	75.5	1.35
'CSURP9528'	*Mycobacterium abscessus subsp. massiliense JCM 15300*	76.1	0.19
'CSURP9530'	*Mycobacterium abscessus subsp. massiliense JCM 15300*	76	0.03
'CSURP9529'	*Mycobacterium abscessus subsp. massiliense JCM 15300*	76	0.25
'CSURP9527'	*Mycobacterium abscessus subsp. massiliense JCM 15300*	75.5	1.35
'CSURP9528'	*'Mycobacterium subsp. massiliense str. GO 06'*	76.7	0.42
'CSURP9529'	*'Mycobacterium subsp. massiliense str. GO 06'*	76.5	0.02
'CSURP9527'	*'Mycobacterium subsp. massiliense str. GO 06'*	76.5	1.59
'CSURP9530'	*'Mycobacterium subsp. massiliense str. GO 06'*	76.4	0.2
'CSURP9529'	*Mycobacteroides abscessus ATCC 19977*	95.6	0.19
'CSURP9530'	*Mycobacteroides abscessus ATCC 19977*	95.5	0.03
'CSURP9528'	*Mycobacteroides abscessus ATCC 19977*	94.8	0.25
'CSURP9527'	*Mycobacteroides abscessus ATCC 19977*	94.3	1.41

Digital DNA-DNA hybridization (dDDH)

Table 3. Mutations across the glycopeptidolipids (GPL) locus in four clinical isolates. Characteristics of a rough-like clinical isolate (P9529) compared to the smooth clinical isolates (P9530) and comparison of P9528/P9527 clones. Single nucleotide polymorphisms (SNP) were identified in the GPL locus and corresponding amino acid changes are also indicated.

Strains	Gene	SNP	AA change
P9527 (Rough)	*mmpS4*	..	..
	mmpL4a	..	..
	mmpL4b	..	..
	Rv1174	..	..
	rmlA	A154T G166C A170C	I52F A56P D57A
	gtf3	..	..
	rmlB	..	..
	atf2	A334G	T112A
	rmt2	..	..
	rmt4	..	..
	gtf1	..	..
	atf1	G539C C947G G1072A	G180A A316G A358T
	rmt3	G635T	L212R
	gtf	G1237A	G413S
	fmt	..	..
	mbtH	..	..
	mps1	A634G A1773C T2130G G4595A A7273G G8041A G8231A T9536A	M212V E591D D710E G1532E T2425A V2681I R2744Q M3179K
	mps2	G1621A C3173T A4012C	V541I A1058V T1348P
	gap	..	..
P9529 (Rough)	*mmpS4*	..	..
	mmpL4a	..	..
	mmpL4b	A212C	D71A
	Rv1174	..	..
	rmlA	..	..
	gtf3	T743C	L248P
	rmlB	T531G	S177R
	atf2	..	..
	rmt2	..	..
	rmt4	..	..
	gtf1	G664T	G222W
	atf1	..	..
	rmt3	..	..
	gtf	..	..
	fmt	..	..
	mbtH	..	..
	mps1	C2369G	A790G
	mps2	A1400G C1534G G2041C G6194T G7534C	D467G R512G G681R G2065V E2512Q
	gap	G11A G50T	G4E G17V

Table 4. Identification of a possible marker to differentiate between smooth and rough morphotypes.

Annotation	BLAST Analysis	Function	P9527	P9528	P9529	P9530
1. Hypothetical protein	Partial match up with MAB_3888 corresponding to a Putative RNA polymerase sigma-70 factor	Interacts transiently with the RNA polymerase catalytic core formed by RpoA, RpoB, RpoC and RpoZ to form the RNA polymerase holoenzyme that can initiate transcription	..	P9528_02843	..	P9530_03875
2. PE family immunomodulator PE5	Complete match up with MAB_0046 corresponding to a Probable PE family protein	In M. tb modulate innate immunity and mediate bacillary survival in macrophages	..	P9528_04911	..	P9530_04558
3. Putative PPE family protein PPE2	Complete match up with MAB_0809c corresponding to a Conserved hypothetical PPE family protein	PPE2 prolongs intracellular survival by inhibiting *inos* gene transcription and limiting nitric oxide (NO) production	..	P9528_03754	..	P9530_02145
4. Hypothetical protein	Partial match up with MAB_4691c corresponding to a Probable non-ribosomal peptide synthetase PstA	PstA is a homologous of Mps2 a protein involved in the biosynthesis of GPL. Mutations in Mps2 lead to smooth to rough switch	..	OINCFHIL_04913	..	P9530_04758

Table 5. Gene distribution across the pangenome visualization in figure 4. Non common marker was found between smooth and rough morphotypes in this area. In the isolate columns are presented each gene numbers that were visualized as a blue pattern.

BLAST match	P9527 (Rough)	P9528 (Smooth)	P9529 (Rough)	P9530 (Smooth)
	04992	..	..	..
	..	03098	..	..
ESAT-6-like protein EsxG	..	..		03304
	05318	..	..	..
	05316	..	..	..
Putative PPE family protein PPE2	..	..	01674	..
ESAT-6-like protein EsxH	..	..	..	03305
	02932	..	..	..
	05298	..	..	..
	02194	..	..	..
	05089	..	..	..
		03870	..	..
	02095	..	..	..
	01064	..	..	..
	03970	..	..	..
	00668	..	..	..
	05327	..	..	..
	01675	..	..	..
	03975	..	..	..
	01366	..	..	..
	01365	..	..	..
	01363	..	..	..
	01369	..	..	..
	02882	..	..	..
	02884	..	..	..
Hypothetical protein	..	..	00764	..
	05319	..	..	..
	05320	..	..	..
	03507	..	..	..
	05157	..	..	..
	..	03175	..	..
	..	03176	..	..
	05266	..	..	..
	01100	..	..	..
Hypothetical protein	..	..	02097	..
	05331	..	..	..
	..	01877	..	..
Hypothetical protein	..	..	03029	..
Hypothetical protein	..	..	03577	..
Hypothetical protein	..	..	03704	..
Hypothetical protein	..	..	04334	..
	01516	..	..	..
	02995	..	..	..
Hypothetical protein	..	..	04653	..
Hypothetical protein	..	..	04687	..
Hypothetical protein	..	..	04727	..
Hypothetical protein	..	..	04744	..
Hypothetical protein	..	..	04745	..
Hypothetical protein	..	..	..	00431
Hypothetical protein	..	..	..	00790
Hypothetical protein	..	..	..	01445
Hypothetical protein	..	..	..	01642
Hypothetical protein	..	..	..	02921

For the BLAST match were considered only the genes from the diversified clone since these two isolates are the closest related.

Table 6. Genotypes in the *erm(41)* gene among the clinical isolates. Single nucleotide polymorphisms (SNP) were identified in *erm(41)* gene and corresponding amino acid changes are also indicated. In bold is showed the SNP linked to a non-functional Erm(41).

Strains	SNP	AA change
P9527_R	T159C	··
	A238G	V80I
	G255A	··
	G279T	··
	A330C	··
	T336C	··
P9528_S	T28C	R10W
	T159C	··
	A238G	V80I
	A330C	··
P9529_R	T159C	··
	A238G	V80I
	G255A	··
	A330C	··
P9530_S	T159C	··
	A238G	V80I
	G255A	··
	A330C	··

The type strain ATCC 19977 was used as reference.

CHAPTER III

Development of new techniques for the generation of mutants in *M. abscessus*

A simple and rapid gene disruption strategy in *Mycobacterium abscessus*: on the design and application of glycopeptidolipid mutants.

Viljoen A., Gutiérrez A.V., Dupont C., Eric Ghigo and Kremer L.

Frontiers in cellular and infection microbiology, 8, p.69.

6. CHAPTER III: Development of new techniques for the generation of mutants in *M. abscessus.*

The development of vaccines and novel drugs for mycobacterial species has been possible thanks to the use of genetic engineering that has largely contributed to decipher the function of genes and evaluate their impact on the physiology, drug resistance mechanisms and pathogenesis in bacteria (Lamrabet and Drancourt 2012).

Little is known about the mechanisms by governing multi-drug resistance in *M. abscessus*. The single cross-over step techniques developed in this study offer a new set of tools to easily generate gene disruption in *M. abscessus*. These tools could potentially be applied to study antibiotic resistance and virulence in *M. abscessus*, an could possibly be applied to other NTMs know to be refractory to genetic manipulation.

The suicide plasmids described in this study have been designed to contain the *tdTomato* red fluorescent marker which simplifies the selection of positive clones and allows infections to be monitored in real time in cellular models or in transparent zebrafish embryos.

To evaluate the potency of this tool (pXU1), the *mmpL4a* gene involved in GPL production/transport was chosen as a target, because its disruption would be accompanied by the S-to-R transition, which is easy to monitor on agar plates. The R phenotype is associated with lethal infections in zebrafish, due to their high propensity to produce cords, which subsequently protect the bacilli from being phagocytosed by macrophages (Bernut, Herrmann, et al. 2014). A conditional system (pXU3) was also designed using an acetamide-inducible promoter cloned upstream of the *mmpS4-mmpL4a-mmpL4b* gene cluster for a fine-tuning control GPL expression. This led to colonies with a R morphotype but with reduced levels of GPL. This S/R hybrid strain may be particularly interesting to further dissect the mechanisms that govern the S-to-R switch and responsible for the establishment of acute infections.

In conclusion, we developed genetic tools that could contribute to further elucidating important aspects in mycobacterial physiology and/or the validation of new chemotherapeutic targets.

frontiers in Cellular and Infection Microbiology

ORIGINAL RESEARCH
published: 14 March 2018
doi: 10.3389/fcimb.2018.00069

A Simple and Rapid Gene Disruption Strategy in *Mycobacterium abscessus*: On the Design and Application of Glycopeptidolipid Mutants

*Albertus Viljoen[1], Ana Victoria Gutiérrez[1,2], Christian Dupont[1], Eric Ghigo[3] and Laurent Kremer[1,4]**

[1] Centre National de la Recherche Scientifique UMR 9004, Institut de Recherche en Infectiologie de Montpellier, Université de Montpellier, Montpellier, France, [2] Unité de Recherche Microbes, Evolution, Phylogeny and Infection (MEPHI), Institut Hospitalier Universitaire Méditerranée-Infection, Marseille, France, [3] Centre National de la Recherche Scientifique, Marseille, France, [4] IRIM, 34293, Institut National de la Santé et de la Recherche Médicale, Montpellier, France

Little is known about the disease-causing genetic determinants that are used by *Mycobacterium abscessus*, increasingly acknowledged as an important emerging pathogen, notably in cystic fibrosis. The presence or absence of surface exposed glycopeptidolipids (GPL) conditions the smooth (S) or rough (R) *M. abscessus* subsp. *abscessus* (*M. abscessus*) variants, respectively, which are characterized by distinct infective programs. However, only a handful of successful gene knock-out and conditional mutants have been reported in *M. abscessus,* testifying that genetic manipulation of this mycobacterium is difficult. To facilitate gene disruption and generation of conditional mutants in *M. abscessus*, we have designed a one-step single cross-over system that allows the rapid and simple generation of such mutants. Cloning of as small as 300 bp of the target gene allows for efficient homologous recombination to occur without additional exogenous recombination-promoting factors. The presence of tdTomato on the plasmids allows easily sifting out the large background of mutants spontaneously resistant to antibiotics. Using this strategy in the S genetic background and the target gene *mmpL4a*, necessary for GPL synthesis and transport, nearly 100% of red fluorescent clones exhibited a rough morphotype and lost GPL on the surface, suggesting that most red fluorescent colonies obtained after transformation incorporated the plasmid through homologous recombination into the chromosome. This system was further exploited to generate another strain with reduced GPL levels to explore how the presence of these cell wall-associated glycolipids influences *M. abscessus* hydrophobicity as well as virulence in the zebrafish model of infection. This mutant exhibited a more pronounced killing phenotype in zebrafish embryos compared to its S progenitor and this effect correlated with the production of abscesses in the central nervous system. Overall, these results suggest that the near-complete absence of GPL on the bacterial surface is a necessary condition for optimal pathogenesis of this mycobacterium. They also suggest that GPL content affects hydrophobicity of *M. abscessus,* potentially altering the aerosol transmission, which is of particular importance from an epidemiological and clinical perspective.

Keywords: gene disruption, *Mycobacterium abscessus*, zebrafish, virulence, glycopeptidolipid

OPEN ACCESS

Edited by:
Stephane Canaan, Centre National de la Recherche Scientifique (CNRS), France

Reviewed by:
Franck Biet, INRA Centre Val de Loire, France
Florian Maurer, Forschungszentrum Borstel (LG), Germany

***Correspondence:**
Laurent Kremer
laurent.kremer@irim.cnrs.fr

Received: *16 December 2017*
Accepted: *27 February 2018*
Published: *14 March 2018*

Citation:
Viljoen A, Gutiérrez AV, Dupont C, Ghigo E and Kremer L (2018) A Simple and Rapid Gene Disruption Strategy in Mycobacterium abscessus: On the Design and Application of Glycopeptidolipid Mutants. Front. Cell. Infect. Microbiol. 8:69. doi: 10.3389/fcimb.2018.00069

INTRODUCTION

Mycobacterium abscessus subsp. *abscessus* (*M. abscessus*) is an emerging pathogen increasingly recognized as a serious threat to cystic fibrosis (CF) patients who show a marked vulnerability to infections with this bacterium, which is exacerbated by *M. abscessus*'s extraordinary intrinsic tolerance toward many antibiotics (van Dorn, 2017). Notably, *M. abscessus* is phenotypically resistant to most antitubercular drugs (Nessar et al., 2012). Despite being a member of the rapid-growing environmental phylogeny of mycobacteria, which contain at worst some opportunistic pathogens, *M. abscessus* is considered as a true pathogen that can cause difficult-to-manage, persistent and even deadly infections in otherwise healthy individuals (Varghese et al., 2012; Jeong et al., 2017). It is clear that novel strategies are urgently needed in the fight against *M. abscessus*-induced diseases (van Dorn, 2017).

New approaches to combat *M. abscessus* infections may rely on the discovery of completely new chemical entities that inhibit essential pathways in this bacterium (Viljoen et al., 2017). This may involve the improvement of available compounds to better inhibit putative molecular targets in *M. abscessus*, which may have slightly different structures or functions compared to orthologs efficiently inhibited in other bacteria. It may also involve the discovery of molecules that act in synergy or render efficient available drugs used to treat mycobacterial infections (Singh et al., 2014; Kaushik et al., 2015; Lefebvre et al., 2017). Whatever the case, the development of new anti-*M. abscessus* drugs would benefit immensely from information on the genetic and biochemical vulnerabilities of this bacterium, information which at the current time is very cryptic. Although *M. abscessus* shares many virulence features of *M. tuberculosis* (Ripoll et al., 2009; Choo et al., 2014), recent studies have highlighted common genetic vulnerabilities and drug resistance mechanisms between the two bacteria involving unrelated compounds (Dupont et al., 2016; Halloum et al., 2017; Kozikowski et al., 2017). These data further warrant studies aimed at deciphering the physiology of *M. abscessus* from the genetic level upwards. Information provided by such studies would likely bring answers to questions such as why *M. abscessus* is so resistant to such a large variety of drugs and why, despite being an environmental mycobacterium, it is capable of causing serious infections in humans. Indeed, recent years have seen the development of genetic tools to inactivate *M. abscessus* genes in a site-specific manner (Medjahed and Reyrat, 2009; Halloum et al., 2016; Gregoire et al., 2017; Rominski et al., 2017) as well as to generate conditional gene expression mutants (Cortes et al., 2011). This has led to the identification of a yet small number of genes that are downright essential for virulence or intracellular survival (Bernut et al., 2014, 2016; Halloum et al., 2016) or playing more important roles during certain stages of infection, such as the establishment of infection (Bakala N'Goma et al., 2015) or during the chronic stage of infection (Viljoen et al., 2016).

The present study was undertaken to develop a simple and rapid gene-knock-out strategy as an alternative to approaches relying on double homologous recombination particularly suitable for use in *M. abscessus*. We have focused our study on the *mmpS4-mmpL4a-mmpL4b* gene locus, the products of which participate in the biosynthesis and transport of glycopeptidolipids (GPL) from the bacterial cytosol where they are produced to the outer layers of the cell wall where they are interspersed in the mycomembrane (Deshayes et al., 2010). Indeed, GPL is the major determinant of the smooth colonial morphotype, characteristic of *M. abscessus* environmental forms (Medjahed et al., 2010). Upon the loss of GPL production, *M. abscessus* converts to a rough colonial morphology and loses attributes that are reminiscent of environmental mycobacteria, such as the ability to form biofilms and sliding motility (Howard et al., 2006).

The availability of new suitable genetic tools described here should undoubtedly further facilitate and stimulate the characterization of new virulence factors and/or the discovery of new drug targets in this emerging pathogen.

MATERIALS AND METHODS

Reagents and Growth Conditions

Unless otherwise stated, all reagents were from Sigma Aldrich. *Escherichia coli* XL1-blue was used for cloning and was routinely maintained at 37°C with shaking at 100–250 rpm. *M. abscessus* CIP104536 was grown in Sauton's broth medium (0.5 g/L K_2HPO_4, 0.5 g/L $MgSO_4$, 4 g/L L-asparagine monohydrate, 0.05 g/L ferric ammonium citrate, 2 g/L citric acid, 6 % (v/v) glycerol, 1 mg/L $ZnSO_4$), Middlebrook 7H9 (Becton Dickinson) or LB broth; and on agar using LB agar. Both liquid and solid media were, in some instances, supplemented with oleic acid/albumin/dextrose/oleic acid (OADC) enrichment or 0.2% (w/v) glycerol and with the detergent tyloxapol at 0.025% (v/v). Antibiotics used to propagate plasmids in *E. coli* were hygromycin (75 μg/mL), kanamycin (25 μg/mL) and zeocine (25 μg/mL). The concentration of kanamycin used to select *M. abscessus* transformants was 250 μg/mL, but was dropped to 100 μg/mL to maintain the plasmids once integration by homologous recombination was confirmed.

For complementation studies, *mmpL4a*::pUX1 transformed with the pMV306-zeo plasmids was cultured in liquid broth and on LB plates containing 50 μg/mL kanamycin and 25 μg/mL zeocine. In order to investigate the rate at which reversion to a wild-type genotype occurred in *mmpL4a*::pUX1 mutants, logarithmic phase cultures of the three mutants (generated with pUX1 plasmids containing varying sizes of the *mmpL4* insert) were first collected by centrifugation and washed three times with PBS. These bacteria were then used to inoculate fresh cultures with and without the antibiotic kanamycin to an $OD_{600} = 0.01$. The cultures were incubated at 37°C for with slow shaking for 7 days until early stationary phase was reached ($OD_{600} > 1$). Subsequently, they were used to inoculate fresh medium with or without kanamycin to an $OD_{600} = 0.01$ and the culturing, sub-culturing process was repeated five more times. After each passage, with and without kanamycin, an aliquot was taken and diluted appropriately in order to view approximately 10,000 colonies by spreading out 100 μL of the diluted suspension on LB agar plates (non-supplemented with kanamycin).

Construct Generation

All specific oligonucleotides and plasmids produced in this study are listed in **Table 1**. All cloned fragments were amplified using purified *M. abscessus* genomic DNA and Phusion polymerase (Finnzymes). To produce the backbone vector used to generate single cross-over gene disruptions, the NheI restriction site in the vector pMV261 (Stover et al., 1991) was first replaced with an AflII site by self-ligating the T4 polynucleotide kinase (NEB) phosphorylated PCR product obtained with the primer set pMV3′ and pMV(NheI-AflII) and pMV261 as template. Subsequently, the obtained plasmid (pMV261-AflII) was digested with XmnI and ligated to the T4 DNA polymerase (Invitrogen) blunted SpeI fragment of pTEC27 containing the tdTomato and hygromycin resistance cassettes (Takaki et al., 2013). The resulting construct, pUX1, contained neither a mycobacterial origin of replication nor features necessary for integration into the mycobacterial chromosome. For simple cloning into pUX1, it contains the convenient restriction enzymes BamHI, AflII, PvuII, NheI, and SpeI, the latter two creating compatible ends, which will also accept XbaI overhangs. pUX2, containing the mWasabi green fluorescent protein gene instead of tdTomato, was obtained in a similar fashion using pTEC15 (Takaki et al., 2013). The plasmid for single cross-over recombination containing the acetamidase promoter, pUX3, was made by replacing the NheI-BamHI fragment of pUX1 containing the hygromycin resistance cassette with the NheI-BamHI fragment of pSD26 (Daugelat et al., 2003) containing the acetamidase promoter.

In order to produce the pUX1 derivatives to inactivate *mmpL4a,* different size PCR products of a sequence internal to the *mmpL4a* gene was first obtained using the primers mmpL4a_Fw_SpeI and mmpL4a_Rev_BamHI_100, or mmpL4a_Rev_BamHI_500, or mmpL4a_Rev_BamHI_1000, or mmpL4a_Rev_BamHI_1500 (**Table 1**). These amplicons were subsequently treated with SpeI and BamHI and ligated to NheI-BamHI-linearized pUX1. To generate the pUX2-*mmpL4a*_1500bp derivative, the SpeI-NheI restriction product of pUX2, containing the *oriE* and mWasabi was ligated to the SpeI-XbaI fragment of pUX1-*mmpL4a*_1500bp containing the kanamycin cassette. pMV306-zeo-*mmpL4a-mmpL4b* was made by first amplifying the *mmpL4a* and *mmpL4b* operon of *M. abscessus*, using the primers mmpL4a-mmpL4b_left and mmpL4a-mmpL4b_right_HindIII (**Table 1**). The PCR product was subsequently EcoRI-HindIII digested and ligated to EcoRI-HindIII-linearized pMV306-zeo-*mmpL4a* (Bernut et al., 2016). To generate the pUX3 derivative used to replace the *mmpS4* promoter with the acetamidase promoter and

TABLE 1 | Oligonucleotides and plasmids generated and used in the study.

Name	Sequence/Description
OLIGONUCLEOTIDES	
pMV3′	GCCTGGCAGTCGATCGTACG
pUX1-NheI	ACGGCATGGACGAGCTGTAC
pMV(NheI-AflII)[a]	CCGCGGTGATCAGCTTAAGCCAACAAAGCGAC
mmpL4a_Fw_SpeI	TGTGACTAGTCAGATGGGGAAGGTCTTTCA
mmpL4a_Rev_BamHI_100	CAAGAAGGATCCCGTAATACTTGTGCGCATCGTCTCC
mmpL4a_Rev_BamHI_500	GAGAGGATCCCGGTGAACAACAGGATGATG
mmpL4a_Rev_BamHI_1000	GAGAGGATCCCGGTGTAGCTGGGGTTGTAT
mmpL4a_Rev_BamHI_1500	GTGTGGATCCTGTTTGAGCATGTCGTCCAT
mmpL4a_conf_left	CTTCCGTGGTCCGTCAAAT
mmpL4a_conf_right	CATTCGTGAGACCAGCAACA
mmpS4_Fw_BamHI	GAGTAGGATCCATGCGTCTGTGGATTCCGCTG
mmpS4_Rev_AflII	GAGTACTTAAGCATGATGCTTCCCACCGCG
mmpS4_conf_left	GGATACCCAGTGGCTTGAAA
mmpL4a-mmpL4b_left	TGCGTCTGTGGATTCCGCTG
mmpL4a-mmpL4b_right_HindIII	GAGAGAAAGCTTAGTACGTCATCCCGGTGTTC
PLASMIDS	
pMV261	Multicopy *E. coli* - mycobacterium shuttle vector, kan^r (Stover et al., 1991)
pMV261-AflII	Variant of pMV261 in which the NheI site of the polylinker was changed to an AflII by site-directed mutagenesis, kan^r
pMV306-zeo-*mmpL4a*	Integrative *E. coli* - mycobacterium shuttle vector, zeo^r, contains *M. abscessus* subsp. *abscessus mmpL4a* under the control of the *hsp60* promoter (Bernut et al., 2016)
pUX1	Plasmid produced by ligating the *colE1* origin and kan^r cassettes-containing XmnI fragment of pMV261-AflII to the blunted SpeI fragment from pTEC27 (Takaki et al., 2013) containing the tdTomato and hyg^r cassettes.
pUX2	Plasmid produced by ligating the *colE1* origin and kan^r cassettes-containing XmnI fragment of pMV261-AflII to the blunted SpeI fragment from pTEC15 (Takaki et al., 2013) containing the mWasabi and hyg^r cassettes.
pUX3	Plasmid produced by replacing the hyg^r cassette flanked by NheI and BamHI sites of pUX1 with the acetamidase inducer elements of pSD26 (Daugelat et al., 2003).

[a] *Underlined are restriction enzyme recognition sequences.*

regulatory elements of *M. smegmatis*, a 300 bp 5′-portion of the *mmpS4* gene was first amplified by PCR using the primers mmpS4_Fw_BamHI mmpS4_Rev_AflII (**Table 1**), subsequently digested with BamHI and AflII and ligated to BamHI-AflII-linearised pUX3.

Preparation of Electrocompetent Mycobacteria and Transformation

To obtain highly electrocompetent *M. abscessus*, a single colony was used to inoculate Sauton's medium supplemented with OADC and tyloxapol (Sauton^{OADC}). This culture was grown at 37°C with gentle agitation (<60 rpm) until an OD_{600} of about 5 was reached (in the case of the R variant, bacteria were grown for a similar duration and then concentrated to about 5 OD_{600}), then aliquoted into 1 mL volumes and frozen at −80°C. A single such aliquot was thawed and used to inoculate 200 mL Sauton^{OADC} in an Erlenmeyer flask, which was shaken overnight at 100 rpm and 37°C until an OD_{600} reading of approximately 0.8 was achieved. Bacteria were then chilled on icy water for 1–2 h, collected by centrifugation (3,000 × g, 15 min, 4°C) and washed four times with gradually decreasing volumes (50, 25, 10, and 5 mL) of ice-cold wash solution (10% glycerol (v/v), 0.025% tyloxapol). Electrocompetent bacteria were resuspended in 1 mL wash solution and, in the case of the R variant, deaggregated by 15 passages through a 26 GA syringe needle. For high yield of transformants, 1–10 μg plasmid DNA were added to 200 μl of fresh electrocompetent bacilli, which were then transferred to a chilled 0.2 cm electrode gap GenePulser eletroporation cuvette (Bio-Rad) and subjected to electrotransformation using a GenePulser Cxell electroporator (Bio-Rad) and the following settings: 2.5 kV, 1,000 Ω and 25 μF. Electroporated bacteria were recovered in 1 mL ice cold Sauton^{OADC}, transferred to 15 mL centrifuge tubes and incubated for 2–16 hrs at 37°C with gentle shaking. The bacteria were then plated out on LB agar plates containing the appropriate antibiotic and incubated at 37°C until colonies appeared (around 3–5 days later). Using this protocol, we routinely obtained efficiencies of 2–5 × 10^4 CFU/μg DNA transformed and 10–100 red fluorescent single cross-over colonies. Cryogenic storage of electrocompetent bacteria at −80°C, preceded by snap freezing of cells on liquid nitrogen, resulted in about a log decrease in electro-transformation efficiency, which was still high enough to obtain single cross-over red fluorescent rough colonies, but at a lower frequency.

GPL Extraction and Analysis

GPL extraction was performed as reported previously (Villeneuve et al., 2003) with some modifications. In brief, bacteria were cultured to Log growth phase (OD_{600}, 0.6–1.2) in 7H9^{OADC} (30 mL) without agitation and without detergent. After centrifugation, lipids were extracted from the bacterial pellets first with chloroform/methanol (1:2, v/v) and then three times by chloroform/methanol (1:1, v/v). Lipid extracts were pooled and dried under a stream of nitrogen prior to resuspension in chloroform. Lipids were then washed at least four times with a volume of H_2O equal to the volume of chloroform, dried, re-dissolved in dichloromethane and subjected to thin layer chromatography (TLC) analysis using Silica gel 60 F_{254} plates (Merck). GPLs were separated using chloroform/methanol (9:1, v/v), sprayed with orcinol/sulphuric acid vapor prior to revelation by charring.

Hexadecane Partitioning

Briefly exponentially growing mycobacteria were collected by centrifugation and washed twice with PUM (100 mM K_2HPO_4, 54 mM KH_2PO_4, 30 mM urea, 0.8 mM $MgCl_2$) buffer prior to carrying out hexadecane partitioning, as previously described (Jankute et al., 2017).

Zebrafish Care and Ethics Statements

All zebrafish experiments were approved by the Direction Sanitaire et Vétérinaire de l'Hérault et Comité d'Ethique pour l'Expérimentation Animale de la région Languedoc Roussillon under the reference CEEA-LR-1145. Experiments were done using the *golden* mutant (Lamason et al., 2005) crossed with wild-type AB zebrafish, maintained as described earlier (Bernut et al., 2014). Ages of embryos are expressed as hours post fertilization (hpf).

Zebrafish Embryo Infections

The various *M. abscessus* strains expressing tdTomato were prepared, injected and monitored according to protocols reported previously (Bernut et al., 2015). In brief, infections were performed by microinjection of bacterial suspensions (≈2 nL containing 150–200 bacteria) intravenously in dechorionated and anesthetized 30 hpf embryos. The size of the inoculum was verified *a posteriori* by injecting 2 nL of each bacterial suspension in sterile PBS^T and plating on 7H10^{OADC}. For kill kinetics, infected larvae were transferred into 12 well plates (3 embryos/well) and incubated at 28.5°C. Survival curves were drawn by counting dead embryos every day for up to 13 days. To analyze abscess size induced by different strains of *M. abscessus*, the largest abscess in each infected fish was first marked off on scale-set microscope images of whole embryos using the polygon selection tool of the Fiji software. Next, the measure function was used in order to obtain abscess area in μm^2.

RESULTS

Efficacy of Single Cross-Over Homologous Recombination at the GPL Locus

In this simple single cross-over strategy, a PCR amplicon of a region within the target gene is cloned into pUX1 or pUX2 (**Figure 1A**), neither of which contain a mycobacterial origin of replication nor the integrase and *attP* site necessary for integration into the mycobacterial chromosome. Once *M. abscessus* is electro-transformed with such a plasmid, the sole means by which this plasmid could be propagated within the dividing bacteria is by inserting itself into the bacterial chromosome through homologous recombination with the target gene, resulting in specific gene disruption, as depicted in **Figure 1B**. We further reasoned that owing to the high rate of spontaneous resistance to selective antibiotics seen for *M. abscessus*, the presence of a brightly fluorescing marker, such

as tdTomato (red) or mWasabi (green), on the plasmid may largely facilitate subsequent screening of electro-transformed putative knock-out colonies. To make the cloning step of the internal gene fragment easy, the backbones of pUX1 and pUX2 (**Figure 1B**) were designed to contain the convenient restriction sites for BamHI, AflII and PvuII flanked by kanamycin and hygromycin cassettes. On the opposite side of the kanamycin and hygromycin cassettes lie the NheI and SpeI restriction sites, allowing replacement of one of the resistance cassettes with the cloned target gene sequence.

We chose to exploit the *mmpL4a* gene that encodes one of the constituents of the GPL biosynthesis/transport apparatus, as recently demonstrated in *Mycobacterium abscessus* subsp. *bolletii* (Bernut et al., 2016), as a target gene. Knock-outs of this gene

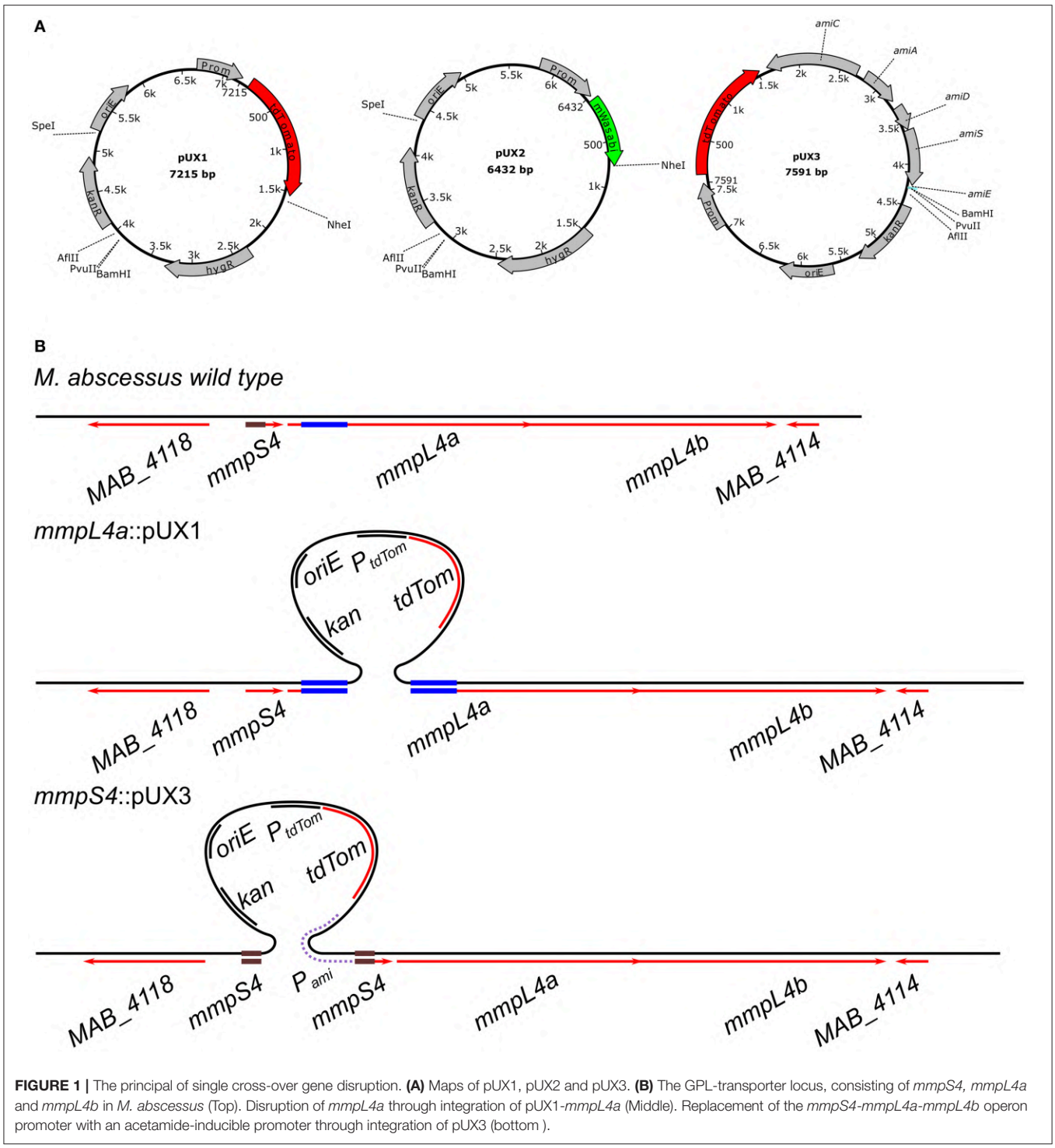

FIGURE 1 | The principal of single cross-over gene disruption. **(A)** Maps of pUX1, pUX2 and pUX3. **(B)** The GPL-transporter locus, consisting of *mmpS4, mmpL4a* and *mmpL4b* in *M. abscessus* (Top). Disruption of *mmpL4a* through integration of pUX1-*mmpL4a* (Middle). Replacement of the *mmpS4-mmpL4a-mmpL4b* operon promoter with an acetamide-inducible promoter through integration of pUX3 (bottom).

would be easily tractable after transformation due to their distinct R colony morphology clearly setting them apart from S colonies that appear either due to spontaneous resistance or illegitimate recombinational uptake of transformed plasmid. Since smaller sizes of cloned fragment may be less prone to homologous recombination, which could be particularly problematic when smaller genes are targeted, we started by cloning internal fragments of *mmpL4a* ranging from 100–1,500 bp in length. As detailed in **Table 2**, with an electroporation efficiency just exceeding 10^4 CFU/μg plasmid, which is more than a log lower usually obtained with *M. smegmatis* mc^2155 (Parish and Stoker, 1998), transforming the same preparation of electrocompetent *M. abscessus* S with pUX1-*mmpL4a* yielded an unexpectedly large number of red-fluorescent colonies. Importantly, all these red-fluorescent colonies appeared with a distinct R morphology, while spontaneous resistant colonies presented the clear S morphology of the progenitor S strain (**Figure 2A**). Screening of several randomly chosen R and red fluorescent colonies using appropriate PCR/sequencing confirmed the presence of pUX1 within the chromosomal *mmpL4a* locus in all selected clones (**Figure 2B**). This indicates that uptake of pUX1-*mmpL4a* occurred exclusively through homologous recombination of the plasmid with the chromosomal *mmpL4a* locus. Indeed, no red-fluorescent kanamycin resistant *M. abscessus* colonies could be obtained by transformation with the empty pUX1 despite several attempts (data not shown). These results suggest (i) that homologous recombination occurs at a higher frequency in *M. abscessus* than that reported for other commonly investigated mycobacterial species, such as *M. smegmatis* (Pavelka and Jacobs, 1999), *M. bovis* BCG (Sander et al., 2001) and *M. tuberculosis* (Parish et al., 1999) and (ii) that illegitimate recombination events between pUX1 and the *M. abscessus* chromosome occurs at a very low level or not at all. As expected, the frequency of red fluorescent R colonies obtained with pUX1-*mmpL4a* containing a 1,500 bp cloned fragment of *mmpL4a* was much greater than the frequency obtained with constructs carrying smaller sizes (500 bp) of the cloned fragment (**Table 2**). After several attempts, we failed to isolate a single R red fluorescent colony from bacteria transformed with pUX1-*mmpL4a* containing a 100 bp cloned-fragment of the gene (**Table 2**). To test the vector pUX2, which is essentially exactly the same as pUX1 except that it contains mWasabi instead of tdTomato, we made a version of this vector containing the 1500 bp *mmpL4a* insert as for pUX1-*mmpL4a*_1500bp. As anticipated, transforming *M. abscessus* with this plasmid yielded green fluorescent R colonies (**Figure 2A**).

Mutants Generated by Single Cross-Over Homologous Recombination Exhibit Expected Phenotypes

S and R morphotypes are often associated with the presence or absence, respectively, of GPL in mycobacteria (Billman-Jacobe et al., 1999; Eckstein et al., 2000; Recht and Kolter, 2001), including *M. abscessus* and *M. abscessus* subsp. *bolletii* (Howard et al., 2006; Bernut et al., 2016). This prompted us to analyze the GPL profile in the *mmpL4a::*pUX1 mutants by thin-layer chromatography (TLC). As anticipated, and similarly to the *M. abscessus* CIP104526 R type strain, all the mutated R fluorescent mutants were characterized by the loss of GPL production (**Figure 2C**). Abrogation of GPL production/transport occurred in all mutants generated with the pUX1 constructs harboring different sizes of the *mmpL4a* fragment. We next aimed to complement the *mmpL4a*::pUX1 mutant by transforming *mmpL4a*::pUX1_500bp with the pMV306-zeo-*mmpL4a* plasmid (**Figure 2D**). Re-introduction of a copy of *mmpL4a* on the integrative vector did not confer a S colony morphology. It was thus possible that integration of pUX1 into the *mmpL4a* gene had a polar effect also on *mmpL4b*, which is located downstream of *mmpL4a* in a possible operon configuration. We thus constructed a new plasmid, pMV306-zeo-*mmpL4a-mmpL4b*, and introduced it in the mutant. Re-introduction of both *mmpL4a* and *mmpL4b* fully restored the wild-type S colony morphology in the *mmpL4a*::pUX1_500bp mutant (**Figure 2D**), proving that pUX1 exerted a polar effect on the expression of a gene downstream in the operon of the targeted gene for mutation.

Since homologous integration of pUX1-*mmpL4a* into the chromosome resulted in the duplication of the central cloned gene fragment (**Figure 1B**), it is conceivable that by a second homologous recombination event between the 5′ and 3′ truncated parts of the *mmpL4a* gene with the pUX1 insertion, pUX1-*mmpL4a* could be lost from the chromosome, hence resulting in reversion to the wild-type genotype. We thus assayed the possibility of such a reversion to occur by serially sub-culturing the different *mmpL4a*::pUX1 mutants in the presence or absence of the selective antibiotic kanamycin, preparing serial dilutions of the cultures after each passage and plating these

TABLE 2 | Frequency of plasmid uptake by homologous recombination.

Size of cloned fragment in pUX1/3 (bp)	100[b]	300[c]	500[b]	1,000[b]	1,500[b]
N° Red fluorescent colonies	0	3	5	43	147
% Colonies PCR positive	0	100	100	100	100
% Efficiency[a]	0	100	100	100	100
Transformation efficiency	1.45×10^4 CFU/μg DNA				

[a] *Percentage of total number of colonies that are red fluorescent and PCR positive.*
[b] *Cloned into pUX1.*
[c] *Cloned into pUX3.*

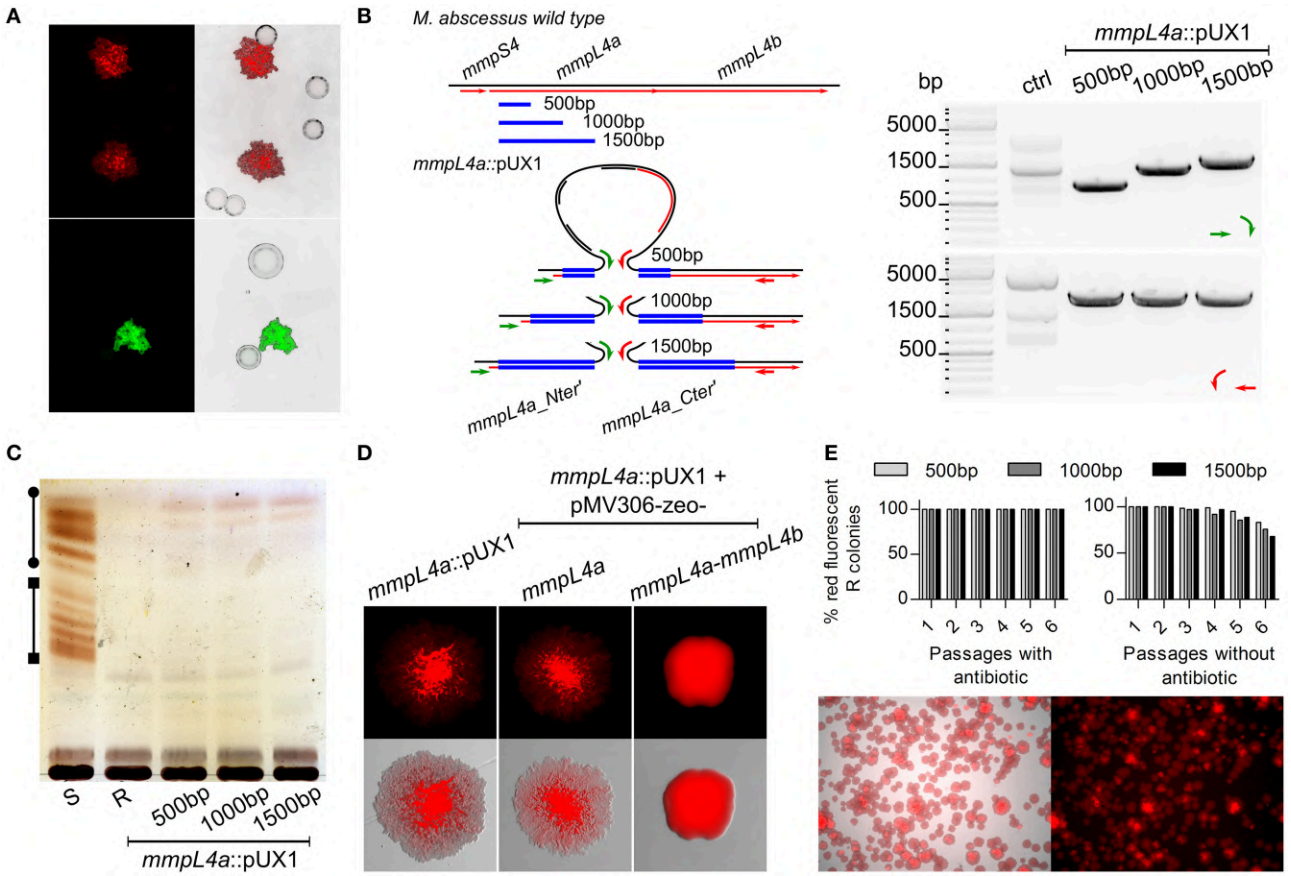

FIGURE 2 | Single cross-over gene disruption of *mmpL4a*. **(A)** Representative fluorescence and overlay images showing the selection of red fluorescent colonies with exclusively a R morphotype after transformation of *M. abscessus* S with pUX1-*mmpL4a* (Top) or pUX2-*mmpL4a* (Bottom). Colonies arising as a result of spontaneous resistance to the selective antibiotic are non-fluorescent and smooth. **(B)** PCR screening and sequencing strategy employed to easily confirm correct integration of the pUX1 plasmid into the target gene, *mmpL4a*. Expected amplicon size generated with the green primer set are 922 bp (*mmpL4a*::pUX1_500bp), 1462 bp (*mmpL4a*::pUX1_1000bp) and 1790 bp (*mmpL4a*::pUX1_1500bp), while the expected size for the red primer amplicon is 2444 bp (the same size for all three mutants). **(C)** TLC showing disappearance of glycopeptidolipids (GPL) in *mmpL4a*::pUX1 mutants. The line with circle caps indicate diglycosylated GPL, while the line with the square caps indicate triglycosylated GPL. **(D)** Representative fluorescence and overlay images showing that complementation of *mmpL4a*::pUX1 with *mmpL4a* alone does not restore a S colony morphology while complementation with *mmpL4a* and *mmpL4b* does. **(E)** Stability of pUX1 integration into the target gene *mmpL4a* was assessed by passaging *mmpL4a*::pUX1 (500, 1,000, and 1,500 bp insert) strains in the presence (top left) or absence (top right) of selective kanamycin, followed by serially diluting aliquots and plating these on LB agar without kanamycin in order to observe up to 10,000 single colonies. Bottom. Representative fluorescence and composite images showing purely rough red fluorescent colonies of *mmpL4a* after two passages in liquid medium in the absence of selective kanamycin.

out on LB agar so as to observe single colonies after 4–5 days of incubation. Reversion to the wild-type phenotype could be easily observed in the loss of R morphology and red fluorescence. After six serial passages in the presence of kanamycin not a single S, non-fluorescent colony could be observed among at least 10,000 colonies. In the absence of kanamycin, no wild-type reversions were observed after two passages. However, after a third passage, between 1 and 3% of colonies observed were S and non-fluorescent and, after six passages, this percentage had increased to between 15 and 35% of the total number of colonies observed (**Figure 2E**). In addition, the rate of reversion appeared to be directly related to the size in nucleotide bases of the cloned fragment in pUX1. These data attest to the stability of pUX1 integration in the presence of selective antibiotic and the relative stability even in the absence of antibiotic pressure.

Taken together, these results show that pUX1-based single cross-over targeted inactivation of genes is simple and occurs at a high frequency in *M. abscessus*.

Generation of a Low-Level GPL Producing Rough Variant

Next, we aimed to extend the single cross-over strategy to generation of conditional mutants. A derivative of pUX1, designated pUX3, that contains the promoter and a truncated portion of the coding sequence of the *M. smegmatis amiE* gene (Parish et al., 1997) as well as the acetamide responsive elements, *amiA*, *amiC*, *amiD*, and *amiS* was constructed (**Figure 1A**). A polylinker within the truncated *amiE* coding sequence allows simple cloning of a 5′ fragment of a gene of interest in frame with the *amiE* coding sequence. Subsequent transformation of bacteria

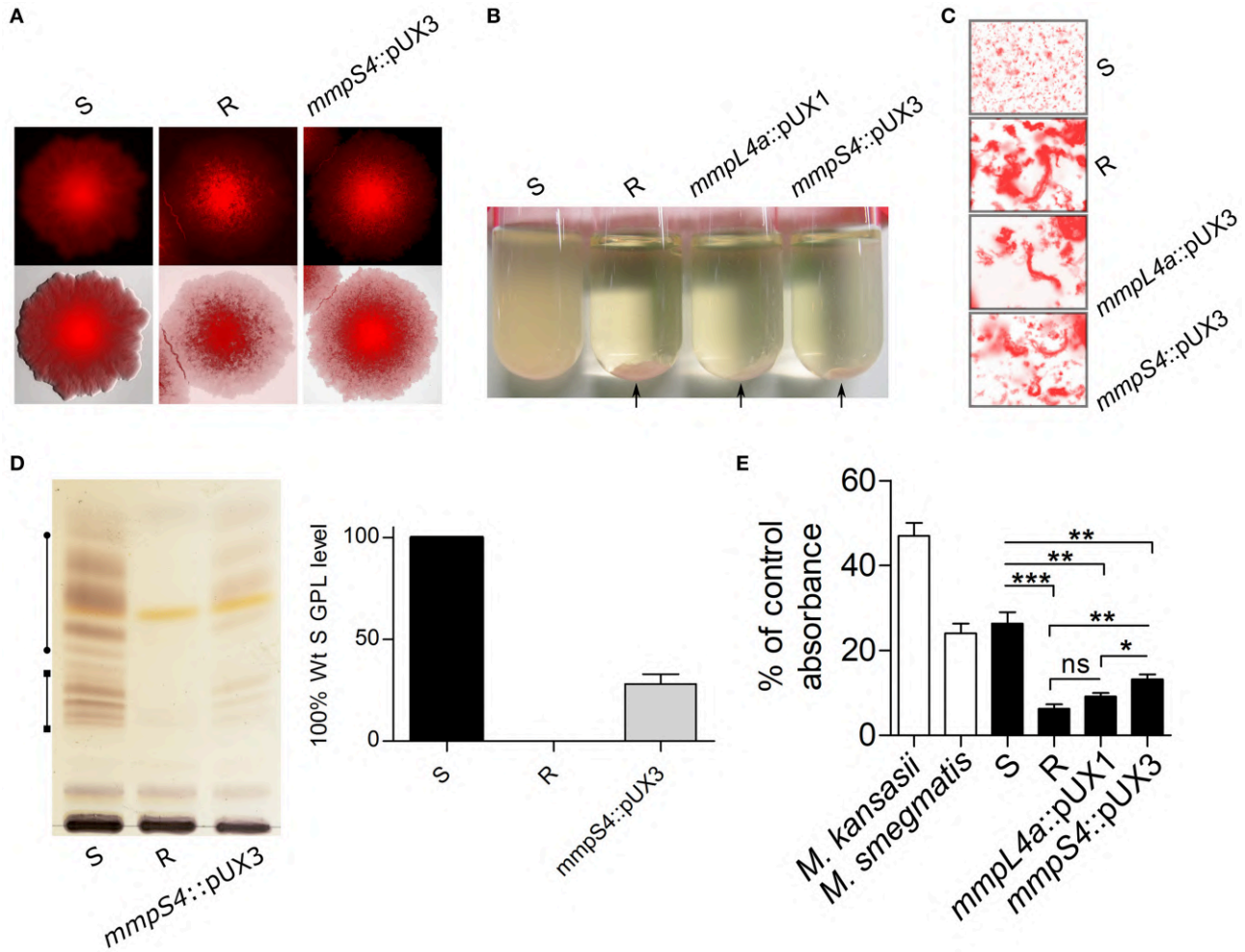

FIGURE 3 | Single cross-over promoter replacement of *mmpS4*. **(A)** Representative bright field, fluorescence and composite images showing the rough colony morphology associated with the *mmpS4*::pUX3 strain. **(B)** Like the R, but unlike the S variant, *mmpS4*::pUX3 sediments rapidly in liquid culture. Exponentially growing cultures ($OD_{600} = 1$) were transferred to glass tubes and allowed to sediment for 10 min before pictures were taken. Arrows indicate the sedimented bacterial aggregates. **(C)** Representative fluorescence images showing serpentine cords in broth culture of *M. abscessus* R, *mmpL4a*::pUX1 and *mmpS4*::pUX3 but not of *M. abscessus* S. **(D)** Left: Low-level GPL production is maintained in *mmpS4*::pUX3 as assessed by TLC, despite its rough colonial phenotype and aggregative properties. The line with circle caps indicate diglycosylated GPL, while the line with the square caps indicate triglycosylated GPL. Right: TLCs produced as in the left from four independent experiments were subjected to a densitometric analysis in order to determine the relative level of GPL present in the *mmpS4*::pUX3 mutant. Shown is the mean and standard deviation calculated from these experiments. **(E)** *M. abscessus* R is more hydrophobic than S, while the *mmpS4*::pUX3 mutant strain's hydrophobicity is between S and R, as assessed by hexadecane partitioning and shown as hydrophobicity index (in percentage of aqueous phase OD prior to partitioning). Histograms and error bars are means and standard deviations of at least three independent experiments. Differences between means were analyzed for significance using a two-tailed Student's *T*-test employing Welch's correction for unequal variances. Ns, non-significant, $^{*}p < 0.05$, $^{**}p < 0.01$, $^{***}p < 0.001$.

allowing homologous recombination between the gene of interest and pUX3 results in replacement of the native gene promoter with the acetamide responsive elements of pUX3 (**Figure 1B**).

To test the efficacy of the pUX3 acetamide-inducible conditional mutant system, we again focused on the locus in *M. abscessus* that is responsible for GPL export, consisting of the genes *mmpS4*, *mmpL4a,* and *mmpL4b*. Since these three genes are arranged in an operon configuration and, hence, it is likely that the three genes are transcribed as a single mRNA transcript, a 300 bp fragment of the *mmpS4* gene was cloned into pUX3 (**Figure 1B**). Transformation of the *M. abscessus* S variant with this plasmid, pUX3-*mmpS4*, yielded red-fluorescent colonies with a rough morphology (**Figure 3A**). PCR/sequencing analysis confirmed the proper replacement of the *mmpS4* promoter with the acetamidase elements of pUX3 (data not shown). Moreover, the *mmpS4*::pUX3 mutant, like the R reference strain, aggregated in liquid culture and failed to produce homogenous suspensions that typify *M. abscessus* S cultures (**Figure 3B**). Importantly, serpentine cords, a hallmark of *M. abscessus* R virulence (Bernut et al., 2014), were observed in liquid cultures of *mmpS4*::pUX3 as for *mmpL4a*::pUX1 and *M. abscessus* R, but not for *M. abscessus* S (**Figure 3C**).

Several tests employing acetamide as supplement were then performed in order to induce MmpS4-MmpL4a-MmpL4b expression and GPL production both in broth and on solid agar culture. However, stable high-level GPL production supporting S phenotypes was not fully achieved, despite testing various acetamide concentrations and medium compositions (data not shown). In addition to colony morphology and bacterial aggregation phenotypes, GPL profiles of cultures were also assessed by TLC. As shown in **Figure 3D**, the *mmpS4*::pUX3 strain still produced low levels of GPL compared to the S progenitor (approximately 30% of S levels), even in the absence of inducer. Therefore, despite our inability to generate a strain for which GPL production and the R-to-S transition could be conditionally induced by the presence or absence of an inducer (acetamide), we ascertained a new *M. abscessus* mutant that behaved like the R variant, aggregating in culture and producing rough and dry colonies, but still producing and exporting low levels of GPL.

GPL Loss Is a Determinant of Mycobacterial Hydrophobicity

Partitioning of mycobacterial cultures between hexadecane and an aqueous buffer has recently been used as a quantitative marker of hydrophobicity in *Mycobacterium tuberculosis* evolution and pathogenicity, ranging from hydrophilic environmental low-pathogenicity ancestors *Mycobacterium kansasii* and *Mycobacterium canettii* to highly hydrophobic virulent tubercle bacilli (Minnikin et al., 2015; Jankute et al., 2017). Given the important difference in the morphotype and aggregative properties characterizing the *M. abscessus* variants, hexadecane-aqueous buffer partitioning was applied to the S, R and the different *M. abscessus* mutants generated in this study to unveil a possible link between hydrophobicity and GPL content. In addition, *M. kansasii* Hauduroy (ATCC12478), included as an internal control strain, was found to be highly hydrophilic, as reported previously (Jankute et al., 2017; **Figure 3E**). The S variant shared comparable partitioning profiles in hexadecane, with *M. smegmatis* mc^2155 and both were significantly more hydrophilic than the R variant or the *mmpL4a*::pUX1 mutant. This indicates that lack of the hydrophilic GPL components in the parental R strain or the *mmpL4a*::pUX1 mutant is responsible for the increased hydrophobicity of these strains. Interestingly, the *mmpS4*::pUX3 derivative, which produces low levels of GPL but expresses rough and aggregative properties, exhibited intermediate levels of partitioning and hydrophobic properties as compared to the S and R strains (**Figure 3E**), further confirming a positive correlation between GPL production and hydrophilicity.

Low-Level GPL Production Impedes Virulence of a Rough Variant

The zebrafish embryo was recently used as a relevant animal model to describe the chronology of the events leading to acute infection with *M. abscessus* and to compare the increased virulence of the R over the S variant (Bernut et al., 2014, 2015). Herein, we further exploited this model to compare the virulence and the physiopathological symptoms of the parental S and R strains with the *mmpS4*::pUX3 mutant. Around 200 CFU of the tdTomato-expressing strains were injected in the caudal vein of embryos at 30 h post-fertilization (hpf). Mortality was monitored at a daily basis for 13 days. Consistent with previous findings (Bernut et al., 2014, 2016), injection of the S form failed to induce larval mortality whereas intravenous injection of the R variant was associated with a robust infection that led to about 60% of mortality at 10 dpi (**Figure 4A**). In contrast, the survival curve of embryos infected with *mmpS4*::pUX3 showed an intermediate profile, characterized by a delay in killing as compared to infection with the R strain and with a reduced mortality rate (around 30% at 13 dpi). The transparency of the embryos was next exploited to count and characterize the abscesses, considered as typical pathophysiological markers of severity of the infection in this animal model (Bernut et al., 2014, 2015, 2016). The proportion of embryos infected with the S strain and developing abscesses remains low as compared to the one infected with the R variant, as reported earlier (Bernut et al., 2014, 2015, 2016). However, abscesses were detected in around 60% of the *mmpS4*::pUX3-infected embryos over 9 dpi and this was significantly reduced as compared to the R-infected animals (**Figure 4B**). In all infected groups, the majority of the abscesses were found within the central nervous system, mainly in the brain (**Figure 4C**). Careful inspection of the infected embryos unraveled significant differences in the size of the abscesses in the R- or *mmpS4*::pUX3-infected embryos (**Figure 4C**). A quantitative analysis was done by measuring the area of the abscesses, thus mirroring their size/volume, in individuals of both groups of infected animals. This clearly revealed that the size of the abscesses was highly heterogenous in both the R- and the *mmpS4*::pUX3-infected populations (**Figure 4D**). However, the median size of the abscesses in the former group was significantly more pronounced than the one in the *mmpS4*::pUX3-infected group. This latter group also contained a large number of embryos with no or very small abscesses (**Figures 4C,D**).

Overall, these results further support the direct relationship between the GPL content and virulence of *M. abscessus* and that low-level GPL production impedes the induction of the physiopathological symptoms and virulence of a R variant.

DISCUSSION

In comparison to the large number of studies dedicated to delineating the pathophysiology of *M. tuberculosis*, non-tuberculous mycobacteria (NTM) have been largely neglected as pathological organisms. However, in recent years *M. abscessus*, one such NTM, has been witnessed as a serious and emerging infectious agent, surpassing tuberculosis in many industrialized countries. Not only is it responsible for severe post-surgical and pulmonary infections (Jeong et al., 2017; Koh et al., 2017), but it is also intrinsically resistant to most currently available antibiotics (Medjahed et al., 2010; Nessar et al., 2012). This situation is worsened by the recent whole-genome sequencing studies of *M. abscessus* in CF patients indicating a possible

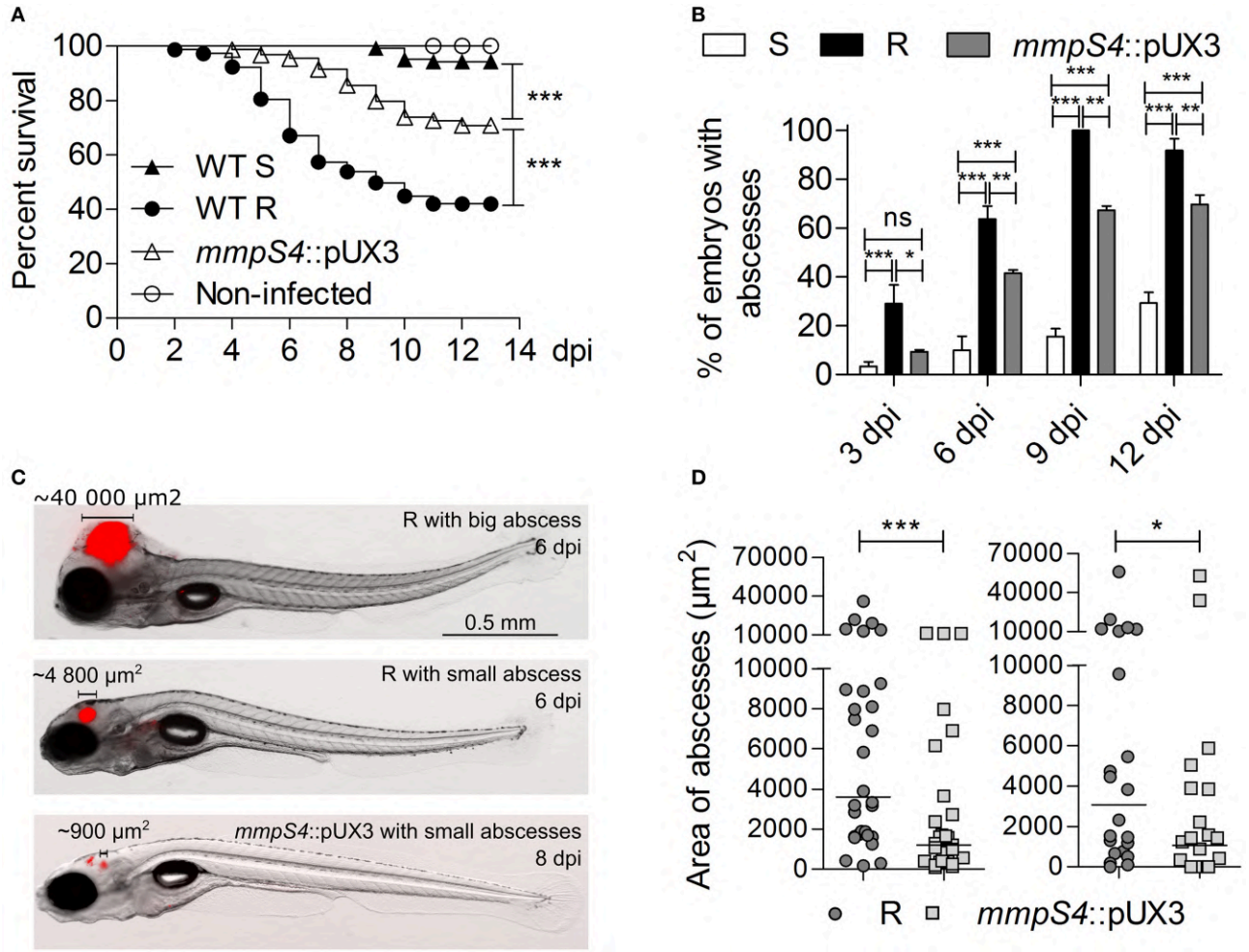

FIGURE 4 | Low-level GPL producing *mmpS4*::pUX3 is more virulent than the S variant in zebrafish embryos, but not as virulent as the R variant. **(A)** Survival curves of zebrafish embryos infected with different strains. Killing of zebrafish embryos over the course of the experiment by different mycobacterial strains were compared using the Mantel-Cox log rank test. Shown is the pooled data from five independent experiments. In each experiment, 25–30 embryos were injected each with 200 ± 50 cfu. **(B)** Kinetic of abscess appearance in the population of infected embryos over a 12-day infection period showing retarded abscess appearance in *mmpS4*::pUX3-infected embryos compared to embryos infected with the R variant. Histograms and error bars represent means and their associated standard errors calculated from two independent experiments using 20 embryos per bacterial strain on each occasion. Data was analyzed by two-way ANOVA and Bonferroni post-tests. Ns, non-significant, $^{*}p < 0.05$, $^{**}p < 0.01$, $^{***}p < 0.001$. **(C)** Representative images of embryos infected with the R variant at 6 dpi and *mmpS4*::pUX3 at 8 dpi showing smaller abscesses in the case of *mmpS4*::pUX3. **(D)** Scatterplots from two independent experiments showing sizes in area of the largest abscess per infected embryo over the 12-days infection period ($n = 20$ per bacterial strain in each experiment). Median abscess area between the R variant and *mmpS4*::pUX3 were statistically compared using a one-tailed Mann Whitney test. $^{*}p < 0.05$, $^{***}p < 0.001$.

human-to-human transmission of this infection (Bryant et al., 2013, 2016). The treatment duration being very long (lasting for 1–2 years) and associated with multi-drug regimens leading often to disappointing results, it resembles that of XDR-TB. In addition, *M. abscessus* can provoke latent infections and persist silently for many years in lesions before re-emerging to produce an acute infection (Tomashefski et al., 1996; Cullen et al., 2000; Medjahed et al., 2010). Unfortunately, despite its increasing importance as a true pathogen, the lack of efficient genetic methods to easily manipulate *M. abscessus* has contributed to the little knowledge on its genetic requirements to establish acute and chronic infections and to adapt to its various environments and hosts. In this context, the present study was undertaken to provide an alternative to the standard recombineering strategy. It is based on a very simple method to disrupt genes by single homologous recombination occurring between the gene targeted for disruption and a suicide plasmid with a cloned internal fragment of the target gene. Cloning of only a single PCR product is required to generate the single cross-over substrate plasmid, no induction of recombineering proteins is required prior to preparation of electrocompetent cells and the presence of the tdTomato red (or mWasabi green) fluorescent marker on the plasmid eliminates the very high background of spontaneous resistant mutants, thus avoiding

fastidious and time-consuming screening procedures. However, careful attention should be paid during design of PCR amplicons for cloning of internal target gene fragments and in the case it is required to clone smaller (<500 bp) sequences of target genes, several transformation attempts may be required to obtain knock-outs. In addition, use of this technique to disrupt genes found in operons may have undesired polar effects on the genes located downstream of the target gene, although this issue can be subsequently addressed by appropriate complementation studies. Another major advantage of this method is that it avoids the subsequent time-consuming curing procedures of the mutated strains that characterizes the recombineering strategy, which relies on the use of a plasmid carrying the exonucleases from phage Che9c (van Kessel and Hatfull, 2007). In addition, the one-step procedure described here allows to directly integrate a red fluorescent marker into the mutant, which is particularly useful for subsequent *in vivo* imaging in infected cells and/or zebrafish embryos (Bernut et al., 2017).

In mycobacteria that produce and elaborate GPL on the bacterial surface, the synthesis of these lipids inside the cytosol and the transport across the plasma membrane is coupled and relies on a set of biosynthetic enzymes and lipid transporters, which form a large complex at the plasma membrane (Deshayes et al., 2010). It was previously demonstrated that the transmembrane protein MmpS4 is necessary for the proper complex formation of the GPL biosynthesis/transport machinery in *M. smegmatis* (Deshayes et al., 2010). On the other hand, the efflux pump protein MmpL4b was implicated in the transport of GPL in *M. abscessus* (Medjahed and Reyrat, 2009) and, more recently, it was shown that both MmpL4a and MmpL4b are required for the export of GPL in this mycobacterium (Bernut et al., 2016). Exploiting the genetic tools produced in this study, we inactivated the *mmpL4a-mmpL4b* gene couple and reproduced several of the phenotypes associated with the R colony morphotype of *M. abscessus*, including the loss of GPL. In addition, by replacing the endogenous promoter of *mmpS4* with an acetamide inducible promoter that is prone to poor repression in the absence of the inducer acetamide, we unintentionally obtained a low-level GPL producer that still exhibited phenotypes associated with the GPL-deficient rough variant of *M. abscessus*, notably aggregation and cord formation. Since genetic alterations within the GPL biosynthetic locus preceding R colony onset in clinical isolates were previously reported (Park et al., 2015), we further exploited this hybrid mutant that produces low GPL levels and exhibiting a R morphotype to investigate its virulence attributes using zebrafish embryos.

Since the R form of *M. abscessus* is considered more aggressive than the S form as it is often associated with more severe infections and decline of pulmonary functions in patients (Jönsson et al., 2007; Catherinot et al., 2009), we recently adapted the zebrafish infection model to understand why this is the case (Bernut et al., 2014, 2015, 2017). Using this animal model, we could explain the hypervirulent phenotype of the R through our observations that the R form has the ability to form serpentine cords, which serve as an efficient mechanism of immune evasion allowing this form to thrive extracellularly causing rapid larval death (Bernut et al., 2014, 2015, 2017; Halloum et al., 2016). However, the short duration of the zebrafish infection experiment, which lasts for no longer than 2 weeks and the low CFU with which the larvae are injected have been barriers to study the dynamics of the S-to-R transition as it occurs in real time *in vivo*. Using a set of *M. abscessus* strains exhibiting high (S strain), low (*mmpS4*::pUX3) or no (R strain) GPL, we further confirm the impact of the GPL profile on pathogenicity of *M. abscessus* and demonstrate that the presence of even low levels of this lipid strongly impacts on larval killing of a cord-forming R variant. It is, however, noteworthy that data obtained in zebrafish cannot necessarily be translated directly to human disease as embryos present disadvantages over mammalian models, including important anatomical differences as well as the lack of adaptive immunity in the early development stages, thereby affecting the outcome of the infection. Whereas embryos appear also more adapted to study acute infection with *M. abscessus,* the effect of the GPL profile on the chronic stages of the disease would be better modeled in other mammalian models such using immuno-compromised mice.

The same *M. abscessus* strains were also used to demonstrate a positive correlation between GPL production and hydrophilicity of *M. abscessus.* These results are analogous to those reported recently to demonstrate the implication of hydrophobicity in the evolution of *M. tuberculosis* pathogenicity, mainly related by the increased proportion of less polar lipids in the outer membrane (Minnikin et al., 2015; Jankute et al., 2017). Among all the strains tested, *M. kansasii* Hauduroy was the most hydrophilic strain due to the presence of large amounts of multiglycosylated phenolic glycolipids and lipooligosaccharides and restricted amounts or absence of important apolar lipids that characterize *M. tuberculosis* such diacyl trehalose, pentacyl trehalose or sulfoglycolipids. *M. abscessus* S, although being less hydrophilic than *M. kansasii*, was significantly more hydrophilic than *M. abscessus* R. In contrast, low GPL expression in *mmpS4*::pUX3 was associated with an intermediate phenotype. Changes in the cell wall associated lipids have been proposed to enhance the capability for aerosol transmission of *M. tuberculosis*. Whether this holds true for *M. abscessus*, *i.e.* that the hydrophobic R strain has acquired an increased propensity for aerosol transmission compared to the hydrophilic S strain is tempting. Supporting this view, epidemiological studies have documented the presence of the R variant in acute respiratory failure (Catherinot et al., 2009) and a significant association between an R phenotype and chronic colonization of the airways in CF patients (Jönsson et al., 2007). The possibility of aerosol transmission has recently been raised in world-wide surveys of *M. abscessus* infections (Bryant et al., 2013, 2016) but the possible link between this mode of transmission with the colony morphology/hydrophobicity has not been addressed and requires additional investigations. Since the evolutionary transformation from a hydrophilic, environmental, low-pathogenicity *M. abscessus* S to a hydrophobic, virulent *M. abscessus* R is particularly definite, the distinction between S and R variants should be better addressed and taken into account in epidemiological studies as this may help to

better understand/anticipate transmission of *M. abscessus* among human populations that are exposed or vulnerable to *M. abscessus* infections.

AUTHOR CONTRIBUTIONS

AV conceived the idea of the project, conducted experiments, analyzed the data and wrote the paper. AG conducted experiments, analyzed the data. CD conducted experiments, analyzed the data. EG analyzed the data and participating in writing the paper. LK conceived the idea of the project, analyzed the data and wrote the paper.

FUNDING

LK acknowledges the support by the Fondation pour la Recherche Médicale (FRM) (DEQ20150331719), the Infectiopôle Sud Méditerranée for funding the PhD fellowship of AG and the National Research Agency (ANR-15-CE18-0007-02) for funding CD.

REFERENCES

Bakala N'Goma, J. C., Le Moigne, V., Soismier, N., Laencina, L., Le Chevalier, F., Roux, A.-L., et al. (2015). *Mycobacterium abscessus* phospholipase C expression is induced during coculture within amoebae and enhances *M. abscessus* virulence in mice. *Infect. Immun.* 83, 780–791. doi: 10.1128/IAI.02032-14

Bernut, A., Dupont, C., Sahuquet, A., Herrmann, J.-L., Lutfalla, G., and Kremer, L. (2015). Deciphering and imaging pathogenesis and cording of *Mycobacterium abscessus* in zebrafish embryos. *J. Vis. Exp.* 103:e53130. doi: 10.3791/53130

Bernut, A., Herrmann, J.-L., Kissa, K., Dubremetz, J.-F., Gaillard, J.-L., Lutfalla, G., et al. (2014). *Mycobacterium abscessus* cording prevents phagocytosis and promotes abscess formation. *Proc. Natl. Acad. Sci. U.S.A.* 111, E943–E952. doi: 10.1073/pnas.1321390111

Bernut, A., Herrmann, J.-L., Ordway, D., and Kremer, L. (2017). The diverse cellular and animal models to decipher the physiopathological traits of *Mycobacterium abscessus* infection. *Front. Cell. Infect. Microbiol.* 7:100. doi: 10.3389/fcimb.2017.00100

Bernut, A., Viljoen, A., Dupont, C., Sapriel, G., Blaise, M., Bouchier, C., et al. (2016). Insights into the smooth-to-rough transitioning in *Mycobacterium bolletii* unravels a functional Tyr residue conserved in all mycobacterial MmpL family members. *Mol. Microbiol.* 99, 866–883. doi: 10.1111/mmi.13283

Billman-Jacobe, H., McConville, M. J., Haites, R. E., Kovacevic, S., and Coppel, R. L. (1999). Identification of a peptide synthetase involved in the biosynthesis of glycopeptidolipids of *Mycobacterium smegmatis*. *Mol. Microbiol.* 33, 1244–1253. doi: 10.1046/j.1365-2958.1999.01572.x

Bryant, J. M., Grogono, D. M., Greaves, D., Foweraker, J., Roddick, I., Inns, T., et al. (2013). Whole-genome sequencing to identify transmission of *Mycobacterium abscessus* between patients with cystic fibrosis: a retrospective cohort study. *Lancet Lond. Engl.* 381, 1551–1560. doi: 10.1016/S0140-6736(13)60632-7

Bryant, J. M., Grogono, D. M., Rodriguez-Rincon, D., Everall, I., Brown, K. P., Moreno, P., et al. (2016). Emergence and spread of a human-transmissible multidrug-resistant nontuberculous mycobacterium. *Science* 354, 751–757. doi: 10.1126/science.aaf8156

Catherinot, E., Roux, A.-L., Macheras, E., Hubert, D., Matmar, M., Dannhoffer, L., et al. (2009). Acute respiratory failure involving an R variant of *Mycobacterium abscessus*. *J. Clin. Microbiol.* 47, 271–274. doi: 10.1128/JCM.01478-08

Choo, S. W., Wee, W. Y., Ngeow, Y. F., Mitchell, W., Tan, J. L., Wong, G. J., et al. (2014). Genomic reconnaissance of clinical isolates of emerging human pathogen *Mycobacterium abscessus* reveals high evolutionary potential. *Sci. Rep.* 4:4061. doi: 10.1038/srep04061

Cortes, M., Singh, A. K., Reyrat, J.-M., Gaillard, J.-L., Nassif, X., and Herrmann, J.-L. (2011). Conditional gene expression in *Mycobacterium abscessus*. *PloS ONE* 6:e29306. doi: 10.1371/journal.pone.0029306

Cullen, A. R., Cannon, C. L., Mark, E. J., Colin, A. A. (2000). *Mycobacterium abscessus* infection in cystic fibrosis. Colonization or infection? *Am. J. Respir. Crit. Care Med.* 161, 641–645. doi: 10.1164/ajrccm.161.2.9903062

Daugelat, S., Kowall, J., Mattow, J., Bumann, D., Winter, R., Hurwitz, R., et al. (2003). The RD1 proteins of *Mycobacterium tuberculosis*: expression in *Mycobacterium smegmatis* and biochemical characterization. *Microbes Infect.* 5, 1082–1095. doi: 10.1016/S1286-4579(03)00205-3

Deshayes, C., Bach, H., Euphrasie, D., Attarian, R., Coureuil, M., Sougakoff, W., et al. (2010). MmpS4 promotes glycopeptidolipids biosynthesis and export in *Mycobacterium smegmatis*. *Mol. Microbiol.* 78, 989–1003. doi: 10.1111/j.1365-2958.2010.07385.x

Dupont, C., Viljoen, A., Dubar, F., Blaise, M., Bernut, A., Pawlik, A., et al. (2016). A new piperidinol derivative targeting mycolic acid transport in *Mycobacterium abscessus*. *Mol. Microbiol.* 101, 515–529. doi: 10.1111/mmi.13406

Eckstein, T. M., Inamine, J. M., Lambert, M. L., and Belisle, J. T. (2000). A genetic mechanism for deletion of the *ser2* gene cluster and formation of rough morphological variants of *Mycobacterium avium*. *J. Bacteriol.* 182, 6177–6182. doi: 10.1128/JB.182.21.6177-6182.2000

Gregoire, S. A., Byam, J., and Pavelka, M. S. (2017). *galK*-based suicide vector mediated allelic exchange in *Mycobacterium abscessus*. *Microbiol. Read. Engl.* 163, 1399–1408. doi: 10.1099/mic.0.000528

Halloum, I., Carrère-Kremer, S., Blaise, M., Viljoen, A., Bernut, A., Le Moigne, V., et al. (2016). Deletion of a dehydratase important for intracellular growth and cording renders rough *Mycobacterium abscessus* avirulent. *Proc. Natl. Acad. Sci. U.S.A.* 113, E4228–E4237. doi: 10.1073/pnas.1605477113

Halloum, I., Viljoen, A., Khanna, V., Craig, D., Bouchier, C., Brosch, R., et al. (2017). Resistance to thiacetazone derivatives active against *Mycobacterium abscessus* involves mutations in the MmpL5 transcriptional repressor MAB_4384. *Antimicrob. Agents Chemother.* 61:e02509-16. doi: 10.1128/AAC.02509-16

Howard, S. T., Rhoades, E., Recht, J., Pang, X., Alsup, A., Kolter, R., et al. (2006). Spontaneous reversion of *Mycobacterium abscessus* from a smooth to a rough morphotype is associated with reduced expression of glycopeptidolipid and reacquisition of an invasive phenotype. *Microbiol. Read. Engl.* 152, 1581–1590. doi: 10.1099/mic.0.28625-0

Jankute, M., Nataraj, V., Lee, O. Y.-C., Wu, H. H. T., Ridell, M., Garton, N. J., et al. (2017). The role of hydrophobicity in tuberculosis evolution and pathogenicity. *Sci. Rep.* 7:1315. doi: 10.1038/s41598-017-01501-0

Jeong, S. H., Kim, S.-Y., Huh, H. J., Ki, C.-S., Lee, N. Y., Kang, C.-I., et al. (2017). Mycobacteriological characteristics and treatment outcomes in extrapulmonary *Mycobacterium abscessus* complex infections. *Int. J. Infect. Dis.* 60, 49–56. doi: 10.1016/j.ijid.2017.05.007

Jönsson, B. E., Gilljam, M., Lindblad, A., Ridell, M., Wold, A. E., and Welinder-Olsson, C. (2007). Molecular epidemiology of *Mycobacterium abscessus*, with focus on cystic fibrosis. *J. Clin. Microbiol.* 45, 1497–1504. doi: 10.1128/JCM.02592-06

Kaushik, A., Makkar, N., Pandey, P., Parrish, N., Singh, U., and Lamichhane, G. (2015). Carbapenems and rifampin exhibit synergy against *Mycobacterium tuberculosis* and *Mycobacterium abscessus*. *Antimicrob. Agents Chemother.* 59, 6561–6567. doi: 10.1128/AAC.01158-15

Koh, W.-J., Jeong, B.-H., Kim, S.-Y., Jeon, K., Park, K. U., Jhun, B. W., et al. (2017). Mycobacterial characteristics and treatment outcomes in *Mycobacterium abscessus* lung disease. *Clin. Infect. Dis.* 64, 309–316. doi: 10.1093/cid/ciw724

Kozikowski, A. P., Onajole, O. K., Stec, J., Dupont, C., Viljoen, A., Richard, M., et al. (2017). Targeting mycolic acid transport by indole-2-carboxamides for the treatment of *Mycobacterium abscessus* infections. *J. Med. Chem.* doi: 10.1021/acs.jmedchem.7b00582

Lamason, R. L., Mohideen, M.-A., Mest, J. R., Wong, A. C., Norton, H. L., Aros, M. C., et al. (2005). SLC24A5, a putative cation exchanger, affects pigmentation in zebrafish and humans. *Science* 310, 1782–1786. doi: 10.1126/science.1116238

Lefebvre, A.-L., Le Moigne, V., Bernut, A., Veckerl,é, C., Compain, F., Herrmann, J.-L., et al. (2017). Inhibition of the β-lactamase BlaMab by avibactam improves

the *in vitro* and *in vivo* efficacy of imipenem against *Mycobacterium abscessus*. *Antimicrob. Agents Chemother.* 61:e02440-16. doi: 10.1128/AAC.02440-16

Medjahed, H., Gaillard, J.-L., and Reyrat, J.-M. (2010). *Mycobacterium abscessus*: a new player in the mycobacterial field. *Trends Microbiol.* 18, 117–123. doi: 10.1016/j.tim.2009.12.007

Medjahed, H., and Reyrat, J.-M. (2009). Construction of *Mycobacterium abscessus* defined glycopeptidolipid mutants: comparison of genetic tools. *Appl. Environ. Microbiol.* 75, 1331–1338. doi: 10.1128/AEM.01914-08

Minnikin, D. E., Lee, O. Y.-C., Wu, H. H. T., Besra, G. S., Bhatt, A., Nataraj, V., et al. (2015). Ancient mycobacterial lipids: key reference biomarkers in charting the evolution of tuberculosis. *Tuberc. Edinb. Scotl.* 95(Suppl. 1), S133–S139. doi: 10.1016/j.tube.2015.02.009

Nessar, R., Cambau, E., Reyrat, J. M., Murray, A., and Gicquel, B. (2012). *Mycobacterium abscessus*: a new antibiotic nightmare. *J. Antimicrob. Chemother.* 67, 810–818. doi: 10.1093/jac/dkr578

Parish, T., Gordhan, B. G., McAdam, R. A., Duncan, K., Mizrahi, V., and Stoker, N. G. (1999). Production of mutants in amino acid biosynthesis genes of *Mycobacterium tuberculosis* by homologous recombination. *Microbiol. Read. Engl.* 145(Pt 12), 3497–3503. doi: 10.1099/00221287-145-12-3497

Parish, T., Mahenthiralingam, E., Draper, P., Davis, E. O., and Colston, M. J. (1997). Regulation of the inducible acetamidase gene of *Mycobacterium smegmatis*. *Microbiol. Read. Engl.* 143(Pt 7), 2267–2276. doi: 10.1099/00221287-143-7-2267

Parish, T., and Stoker, N. G. (eds.). (1998). "Electroporation of Mycobacteria," in *Mycobacteria Protocols Methods in Molecular Biology* (Totowa, NJ: Humana Press), 129–144.

Park, I. K., Hsu, A. P., Tettelin, H., Shallom, S. J., Drake, S. K., Ding, L., et al. (2015). Clonal diversification and changes in lipid traits and colony morphology in *Mycobacterium abscessus* clinical isolates. *J. Clin. Microbiol.* 53, 3438–3447. doi: 10.1128/JCM.02015-15

Pavelka, M. S., and Jacobs, W., R. (1999). Comparison of the construction of unmarked deletion mutations in *Mycobacterium smegmatis*, *Mycobacterium bovis* bacillus Calmette-Guérin, and *Mycobacterium tuberculosis* H37Rv by allelic exchange. *J. Bacteriol.* 181, 4780–4789.

Recht, J., and Kolter, R. (2001). Glycopeptidolipid acetylation affects sliding motility and biofilm formation in *Mycobacterium smegmatis*. *J. Bacteriol.* 183, 5718–5724. doi: 10.1128/JB.183.19.5718-5724.2001

Ripoll, F., Pasek, S., Schenowitz, C., Dossat, C., Barbe, V., Rottman, M., et al. (2009). Non mycobacterial virulence genes in the genome of the emerging pathogen *Mycobacterium abscessus*. *PLoS ONE* 4:e5660. doi: 10.1371/journal.pone.0005660

Rominski, A., Selchow, P., Becker, K., Brülle, J. K., Dal Molin, M., and Sander, P. (2017). Elucidation of *Mycobacterium abscessus* aminoglycoside and capreomycin resistance by targeted deletion of three putative resistance genes. *J. Antimicrob. Chemother.* 72, 2191–2200. doi: 10.1093/jac/dkx125

Sander, P., Papavinasasundaram, K. G., Dick, T., Stavropoulos, E., Ellrott, K., Springer, B., et al. (2001). *Mycobacterium bovis* BCG *recA* deletion mutant shows increased susceptibility to DNA-damaging agents but wild-type survival in a mouse infection model. *Infect. Immun.* 69, 3562–3568. doi: 10.1128/IAI.69.6.3562-3568.2001

Singh, S., Bouzinbi, N., Chaturvedi, V., Godreuil, S., and Kremer, L. (2014). *In vitro* evaluation of a new drug combination against clinical isolates belonging to the *Mycobacterium abscessus* complex. *Clin. Microbiol. Infect.* 20, O1124–O1127. doi: 10.1111/1469-0691.12780

Stover, C. K., de la Cruz, V. F., Fuerst, T. R., Burlein, J. E., Benson, L. A., Bennett, L. T., et al. (1991). New use of BCG for recombinant vaccines. *Nature* 351, 456–460. doi: 10.1038/351456a0

Takaki, K., Davis, J. M., Winglee, K., and Ramakrishnan, L. (2013). Evaluation of the pathogenesis and treatment of *Mycobacterium marinum* infection in zebrafish. *Nat. Protoc.* 8, 1114–1124. doi: 10.1038/nprot.2013.068

Tomashefski, Jr. J. F., Stern, R. C., Demko, C. A., and Doershuk, C. F. (1996). Nontuberculous mycobacteria in cystic fibrosis. An autopsy study. *Am. J. Respir. Crit. Care Med.* 154, 523–528. doi: 10.1164/ajrccm.154.2.8756832

van Dorn, A. (2017). Multidrug-resistant *Mycobacterium abscessus* threatens patients with cystic fibrosis. *Lancet Respir. Med.* 5:15. doi: 10.1016/S2213-2600(16)30444-1

van Kessel, J. C., and Hatfull, G. F. (2007). Recombineering in *Mycobacterium tuberculosis*. *Nat. Methods* 4, 147–152. doi: 10.1038/nmeth996

Varghese, B., Shajan, S. E., Al, M. O., and Al-Hajoj, S. A. (2012). First case report of chronic pulmonary lung disease caused by *Mycobacterium* abscessus in two immunocompetent patients in Saudi Arabia. *Ann. Saudi Med.* 32, 312–314. doi: 10.5144/0256-4947.2012.312

Viljoen, A., Blaise, M., de Chastellier, C., and Kremer, L. (2016). *MAB_3551c* encodes the primary triacylglycerol synthase involved in lipid accumulation in *Mycobacterium abscessus*. *Mol. Microbiol.* 102, 611–627. doi: 10.1111/mmi.13482

Viljoen, A., Herrmann, J.-L., Onajole, O. K., Stec, J., Kozikowski, A. P., and Kremer, L. (2017). Controlling extra- and intramacrophagic *Mycobacterium abscessus* by targeting mycolic acid transport. *Front. Cell. Infect. Microbiol.* 7:388. doi: 10.3389/fcimb.2017.00388

Villeneuve, C., Etienne, G., Abadie, V., Montrozier, H., Bordier, C., Laval, F., et al. (2003). Surface-exposed glycopeptidolipids of *Mycobacterium smegmatis* specifically inhibit the phagocytosis of mycobacteria by human macrophages. Identification of a novel family of glycopeptidolipids. *J. Biol. Chem.* 278, 51291–51300. doi: 10.1074/jbc.M306554200

Conflict of Interest Statement: The authors declare that the research was conducted in the absence of any commercial or financial relationships that could be construed as a potential conflict of interest.

CHAPTER IV

Study of *M. abscessus* resistance mechanism by the TetR-MmpL system

Mechanistic and Structural Insights Into the Unique TetR-Dependent Regulation of a Drug Efflux Pump in *Mycobacterium abscessus*.

Richard M, Gutiérrez A.V., Viljoen A., Ghigo E., Blaise M. and Kremer L.

Frontiers in microbiology, 9, p.649.

7. CHAPTER IV: Study of *M. abscessus* resistance mechanism by the TetR-MmpL system

7.1 Article 1: Mechanistic and Structural Insights Into the Unique TetR-Dependent Regulation of a Drug Efflux Pump in *Mycobacterium abscessus*.

M. abscessus is known for its natural resistance to multiple antibiotics, including antitubercular drugs such as rifampicin, isoniazid, pyrazinamide and ethambutol (Nessar et al. 2012). That treatment options are limited and associated with a poor clinical response, explains why *M. abscessus* represents a public health problem of increasing importance (Nathavitharana et al. 2019).

Thiacetazone (TAC) is a thiosemicarbazone (PubChem n.d.) responsible for inhibiting mycolic acid cyclopropanation (Alahari et al. 2007) and mycolic acid biosynthesis (Grzegorzewicz, Korduláková, et al. 2012) and previously used for the treatment of *M. tuberculosis* infections. However, due to cutaneous hypersensitivity reactions in patients infected with human immunodeficiency virus (HIV), the World Health Organization (WHO) recommended that it not be included in the first line treatment for TB (Falzon et al. 2014). TAC has been shown to not be efficient against several NTMs including *M. abscessus* (Pang et al. 2015; Halloum et al. 2016), presumably because these species lack the monooxygenase EthA required for activation of the prodrug TAC into metabolically active compounds (Dover et al. 2007).

A previous study (Halloum et al. 2017) identified improved analogues of TAC. Among 38 analogues tested, three were selected against the *M. abscessus* complex and *M. tuberculosis*. To describe the mechanism of resistance to these TAC analogues, spontaneous resistant mutants to these compounds were selected and subjected to WGS. Mutations in *MAB_4384*, a putative TetR transcriptional regulator that controls the expression of *MAB_4383c/MAB_4382c*, close homologs of *mmpS5/mmpL5* in *M. tuberculosis* were identified.

The TetR family of regulators belongs to the family of one-component signal transduction systems, mostly known for regulating antibiotic efflux pumps. However, they can participate in the regulation of enzymes involved in catabolic pathways, antibiotic biosynthesis, osmotic stress and pathogenicity (Cuthbertson and Nodwell 2013). The TetR homodimer is composed of two identical monomers, each of which is folded into 10 α-helices with connecting turns and loops. The N-terminal of each monomer consist of three α-helices that form a helix-turn-helix motif responsible of DNA binding (Orth et al. 2000).

Since the 1960s, the mechanism of tetracycline resistance has been extensively studied in *E. coli* (Izaki, Kiuchi, and Arima 1966; Franklin 1967; Levy and McMurry 1974; Yang, Zubay, and Levy 1976; Beck et al. 1982; Wolfgang Hillen et al. 1983). In the 1990s, a complete model was described that included a TetR and an efflux pump. The *tetR* gene is oriented divergently to the neighbouring efflux pump gene and forms a genetic couple separated by an intergenic region. This region contains a palindromic sequence in which the helix-turn-helix motif of the TetR binds and exerts transcriptional control of the neighbouring efflux pump genes (W. Hillen and Berens 1994).

The spontaneous resistant strains carrying mutations in the TetR MAB_4384 regulator, were used to dissect and link the regulatory mechanisms governing expression of the *mmpS5-mmpL5* efflux pump (*MAB_4383c/MAB_4382c*) with resistance to the TAC analogues.

The MEME suite bioinformatic tool was used to identify a palindromic sequence in the intergenic region between *MAB_4384* and *mmpS5/mmpL5*. The DNA-binding activity of MAB_4384 was studied by electrophoretic mobility shift assays (EMSA) that included also mutated versions of the palindromic sequence and/or MAB_4384 variants harbouring the previously identified mutations (Halloum et al. 2017).

A β-galactosidase reporter system was also developed to define the specificity of MAB_4384 for its operator region. In addition, protein crystallization allowed us to solve the X-ray structure of MAB_4384. We confirmed a typical TetR homodimer structure of

MAB_4384, confirming its belonging to the TetR family of regulators. We identified crucial residues for the DNA-binding activity of MAB_4384 to its DNA target. Additional results suggest that TAC analogues bind to MAB_4384, thereby inducing a decrease in affinity of the regulator to its target, leading to a concomitant overexpression of the MmpS5/MmpL5 efflux pump.

frontiers in Microbiology

ORIGINAL RESEARCH
published: 05 April 2018
doi: 10.3389/fmicb.2018.00649

Mechanistic and Structural Insights Into the Unique TetR-Dependent Regulation of a Drug Efflux Pump in *Mycobacterium abscessus*

Matthias Richard[1], Ana Victoria Gutiérrez[1,2], Albertus J. Viljoen[1], Eric Ghigo[3], Mickael Blaise[1] and Laurent Kremer[1,4]**

[1] CNRS UMR 9004, Institut de Recherche en Infectiologie de Montpellier, Université de Montpellier, Montpellier, France, [2] Unité de Recherche, Microbes, Evolution, Phylogeny and Infection, Institut Hospitalier Universitaire Méditerranée Infection, Marseille, France, [3] Centre National de la Recherche Scientifique, Campus Joseph Aiguier, Marseille, France, [4] Institut National de la Santé et de la Recherche Médicale, Institut de Recherche en Infectiologie de Montpellier, Montpellier, France

Mycobacterium abscessus is an emerging human pathogen causing severe pulmonary infections and is refractory to standard antibiotherapy, yet few drug resistance mechanisms have been reported in this organism. Recently, mutations in *MAB_4384* leading to up-regulation of the MmpS5/MmpL5 efflux pump were linked to increased resistance to thiacetazone derivatives. Herein, the DNA-binding activity of MAB_4384 was investigated by electrophoretic mobility shift assays using the palindromic sequence $IR_{S5/L5}$ located upstream of *mmpS5/mmpL5*. Introduction of point mutations within $IR_{S5/L5}$ identified the sequence requirements for optimal binding of the regulator. Moreover, formation of the protein/$IR_{S5/L5}$ complex was severely impaired for MAB_4384 harboring D14N or F57L substitutions. $IR_{S5/L5}$*/lacZ* reporter fusions in *M. abscessus* demonstrated increased β-galactosidase activity either in strains lacking a functional MAB_4384 or in cultures treated with the TAC analogs. In addition, X-ray crystallography confirmed a typical TetR homodimeric structure of MAB_4384 and unraveled a putative ligand binding site in which the analogs could be docked. Overall, these results support drug recognition of the MAB_4384 TetR regulator, alleviating its binding to $IR_{S5/L5}$ and steering up-regulation of MmpS5/MmpL5. This study provides new mechanistic and structural details of TetR-dependent regulatory mechanisms of efflux pumps and drug resistance in mycobacteria.

Keywords: ***Mycobacterium abscessus,*** **TetR regulator, MmpL, efflux pump, structure, thiacetazone analogs, EMSA**

OPEN ACCESS

Edited by:
Thomas Dick,
Rutgers University, United States

Reviewed by:
Peter Sander,
Universität Zürich, Switzerland
Kyle Rohde,
University of Central Florida, United States

****Correspondence:***
Mickael Blaise
mickael.blaise@irim.cnrs.fr
Laurent Kremer
laurent.kremer@irim.cnrs.fr

Specialty section:
This article was submitted to Antimicrobials, Resistance and Chemotherapy, a section of the journal Frontiers in Microbiology

Received: *13 February 2018*
Accepted: *20 March 2018*
Published: *05 April 2018*

Citation:
Richard M, Gutiérrez AV, Viljoen AJ, Ghigo E, Blaise M and Kremer L (2018) Mechanistic and Structural Insights Into the Unique TetR-Dependent Regulation of a Drug Efflux Pump in Mycobacterium abscessus. Front. Microbiol. 9:649. doi: 10.3389/fmicb.2018.00649

INTRODUCTION

Mycobacterium abscessus is a rapid growing mycobacterium (RGM) that has recently become an important health problem (Mougari et al., 2016). This non-tuberculous mycobacterial (NTM) pathogen can cause serious cutaneous, disseminated or pulmonary infections, particularly in cystic fibrosis (CF) patients. In CF patients, infection with *M. abscessus* is correlated with a decline in lung function and poses important challenges during last-resort lung transplantation (Esther et al., 2010; Smibert et al., 2016). An epidemiological study has recently documented the prevalence

and transmission of *M. abscessus* between hospital settings throughout the world, presumably *via* fomites and aerosols and uncovered the emergence of dominant circulating clones that have spread globally (Bryant et al., 2016). In addition, *M. abscessus* exhibits innate resistance to many different classes of antimicrobial agents, rendering infections with this microorganism extremely difficult to treat (Nessar et al., 2012; van Dorn, 2017). Recent studies have started to unveil the basis of the multi-drug resistance characterizing *M. abscessus,* uncovering a wide diversity of mechanisms or regulatory networks. These involve, for example, the induction of the *erm(41)* encoded 23S rRNA methyltransferase and mutations in the 23S *rRNA* that lead to clarithromycin resistance (Nash et al., 2009), the presence of a broad spectrum β-lactamase that limits the use of imipenem (Dubée et al., 2015; Lefebvre et al., 2016, 2017) or the presence of *eis2,* encoding an acetyltransferase that modifies aminoglycosides, specifically induced by *whiB7*, which contributes to the intrinsic resistance to amikacin (Hurst-Hess et al., 2017; Rominski et al., 2017b). Other studies reported the role of the ADP-ribosyltransferase MAB_0591 as a major contributor to rifamycin resistance (Rominski et al., 2017a) whereas MAB_2385 was identified as an important determinant in innate resistance to streptomycin (Dal Molin et al., 2018).

Recently, we reported the activity of a library of thiacetazone (TAC) derivatives against *M. abscessus* and identified several compounds exhibiting potent activity against a vast panel of clinical strains isolated from CF and non-CF patients (Halloum et al., 2017). High resistance levels to these compounds were linked to mutations in a putative transcriptional repressor MAB_4384, together with a strong up-regulation of the divergently oriented adjacent locus encoding a putative MmpS5/MmpL5 transporter system. That ectopic overexpression of MmpS5/MmpL5 in *M. abscessus* also increased the minimal inhibitory concentration (MIC) to analogs of TAC further suggested that these two proteins may act as an active efflux pump which was sufficient to confer drug resistance (Halloum et al., 2017). In addition to uncovering new leads for future drug developments, this study also highlighted a novel mechanism of drug resistance in *M. abscessus*. Unexpectedly, an important difference relies on the fact that, in *M. tuberculosis*, MmpS5/MmpL5 acts as a multi-substrate efflux pump causing low resistance levels to antitubercular compounds such as clofazimine, bedaquiline, and azoles (Milano et al., 2009; Andries et al., 2014; Hartkoorn et al., 2014) whereas the *M. abscessus* strains overexpressing MmpS5/MmpL5 are very resistant to the TAC analogs but fail to show cross-resistance against clofazimine or bedaquiline (Halloum et al., 2017). This implies that, despite their high primary sequence identity, the MmpS5/MmpL5 orthologs from *M. tuberculosis* and *M. abscessus* do not share the same substrate specificity. Moreover, whereas Rv0678, the cognate regulator of MmpS5/MmpL5 in *M. tuberculosis* belongs to the MarR family (Radhakrishnan et al., 2014), MAB_4384 is part of the TetR family of regulators and the change in the transcriptional level of *mmpS5/mmpL5* was much more pronounced in the *M. abscessus* mutants than in the *M. tuberculosis* mutants (Milano et al., 2009; Hartkoorn et al., 2014).

The TetR transcriptional regulatory factors are common single component signal transduction systems found in bacteria. These proteins possess a conserved helix-turn-helix (HTH) signature at the N-terminal of the DNA-binding domain as well as a ligand binding domain (LBD) located at the C-terminal part (Cuthbertson and Nodwell, 2013). They often act as repressors and interact with a specific DNA target to prevent or abolish transcription in the absence of an effector. In contrast, the binding of a specific ligand to the LBD induces structural changes, conducting the dissociation of the repressor from the target DNA, and the subsequent transcription of the TetR-regulated genes. Being largely associated with resistance to antibiotics and regulation of genes coding for small molecule exporters, TetR regulators also govern expression of antibiotic biosynthesis genes, quorum sensing and in distinct aspects in bacterial physiology/virulence (Cuthbertson and Nodwell, 2013). A recent global analysis indicated that the TetR regulators represent the most abundant class of regulators in mycobacteria, the vast majority remaining uncharacterized (Balhana et al., 2015). In order to provide new insight into the mechanism of gene regulation by TetR regulators in mycobacteria and to describe a new and specific drug resistance mechanism in *M. abscessus*, we focused our efforts on the molecular and structural characterization of the MAB_4384-dependent regulation of MmpS5/MmpL5.

In this study, a combination of genetic and biochemical analyses was applied to determine the specificity of this regulatory system in *M. abscessus* and to describe the contribution of key residues that are important in driving the DNA-binding of MAB_4384 to its operator. We report also the crystal structure of the MAB_4384 TetR regulator. Overall, the results provide new insights into the regulation of members of the MmpL family and on a novel mechanism of drug resistance in *M. abscessus*.

MATERIALS AND METHODS

Plasmids, Strains, Growth Conditions, and Reagents

The *Mycobacterium abscessus* subsp. *abscessus* CIP104536^T reference strain and all derived mutant strains are listed in Supplementary Table S1. Strains were grown in Middlebrook 7H9 broth (BD Difco) supplemented with 0.05% Tween 80 (Sigma-Aldrich) and 10% oleic acid, albumin, dextrose, catalase (OADC enrichment; BD Difco) (7H9$^{T/OADC}$) at 30°C or in Sauton's medium in the presence of antibiotics, when required. On plates, colonies were selected either on Middlebrook 7H10 agar (BD Difco) supplemented with 10% OADC enrichment (7H10^{OADC}) or on LB agar. For drug susceptibility testing, cultures were grown in Cation-Adjusted Mueller-Hinton Broth (CaMHB; Sigma-Aldrich). The TAC analogs D6, D15, and D17 were synthesized as reported previously (Coxon et al., 2013) and dissolved in DMSO. Other antibiotics were purchased from Sigma-Aldrich.

Cloning of Wild-Type and Mutated MAB_4384 and Site-Directed Mutagenesis

MAB_4384 was PCR-amplified from *M. abscessus* CIP104536^T purified genomic DNA using the *MAB_4384_full* primers (Supplementary Table S2) and Phusion polymerase (Thermo Fisher Scientific). The amplicon was cloned into pET32a restricted with KpnI and HindIII (New England Biolabs), enabling the introduction of *MAB_4384* in frame with the thioredoxin and poly-histidine tags as well as a Tobacco Etch Virus protease (TEV) cleavage site between the N-terminus of MAB_4384 and the tags. The *MAB_4384* alleles harboring the g40a (D14N) and t169c (F57L) mutations were PCR-amplified using the primers described above and using the purified genomic DNA of the two spontaneous resistant *M. abscessus* strains to TAC analogs reported previously (Halloum et al., 2017). The double mutant carrying both g40a and t169c mutations was obtained from the *MAB_4384* (g40a) allele using the PCR-driven primer overlap extension method (Aiyar et al., 1996). Briefly, two separate PCR reactions were set up using Phusion polymerase. The first was generated using the forward primer *MAB_4384_full* Fw and a reverse internal primer *MAB_4384_DM* Rev harboring the nucleotide substitution responsible for the mutation. The second PCR was set up with an internal forward primer *MAB_4384_DM* Fw overlapping the internal reverse primer *MAB_4384_DM* Rev and with the original reverse primer *MAB_4384_full* Rev. PCR products were purified, annealed and amplified by a last PCR amplification with the *MAB_4384_full* primers. All mutated genes were cloned into pET32a, as described for wild-type *MAB_4384*.

Expression and Purification of MAB_4384 Variants

The various pET32a-derived constructs containing either the wild-type or the mutated *MAB_4384* gene alleles were used to transform *Escherichia coli* strain BL21 Rosetta 2 (DE3) (Novagen). Cultures were grown in Luria-Bertani (LB) medium containing 200 μg/mL ampicillin and 30 μg/mL chloramphenicol until an optical density at 600 nm (OD_{600}) of between 0.6 and 1.0 was reached. Liquid cultures were then placed on icy water for 30 min prior to the addition of 1 mM isopropyl β-D-1-thiogalactopyranoside (IPTG) and incubation for an additional 20 h at 16°C. Bacteria were then collected by centrifugation (6,000 × *g*, 4°C, 60 min) and the pellets were resuspended in lysis buffer (50 mM Tris-HCl pH 8, 200 mM NaCl, 20 mM imidazole, 5 mM β-mercaptoethanol, 1 mM benzamidine). Cells were opened by sonication and the lysate clarified by centrifugation (28,000 × *g*, 4°C, 45 min) and subjected to a first step of nickel affinity chromatography (IMAC) (Ni-NTA Sepharose, GE Healthcare Life Sciences). After elution, the protein was dialyzed overnight at 4°C in a buffer containing 50 mM Tris-HCl pH 8, 200 mM NaCl, 5 mM β-mercaptoethanol and TEV protease (1 mg of protease/50 mg of total protein) to cleave the thioredoxin and histidine tags from the recombinant proteins. The dialyzed preparations were purified again by IMAC, followed by an anion exchange chromatography step (HiTrap Q Fast Flow, GE Healthcare Life Sciences) as well as a final polishing step using size exclusion chromatography (SEC) (Sephadex^{TM} 75 10/300 GL, GE Healthcare Life Sciences) and a buffer containing 50 mM Tris-HCl pH 8, 200 mM NaCl and 5 mM β-mercaptoethanol.

The selenomethionine-substituted protein was expressed in the methionine auxotroph *E. coli* strain B834 (DE3) (Novagen). A 1L culture was grown very densely in LB medium containing 200 μg/mL ampicillin for 36 h at 37°C. Bacteria were harvested by centrifugation and the pellets resuspended in minimal medium A without antibiotic and methionine traces (M9 medium, trace elements, 0.4% glucose, 1 μM $MgSO_4$, 0.3 mM $CaCl_2$, biotin and thiamine at 1 μg/mL). After an additional wash in medium A, the bacterial pellet was resuspended in 6L of medium A containing 200 μg/mL ampicillin and incubated for 2 h at 37°C. Finally, S/L selenomethionine was added at a final concentration of 100 μg/mL. After 30 min of incubation, expression of the protein was induced with 1 mM IPTG for 5 h at 37°C. The protein was purified using a protocol similar to the one used for the proteins expressed in the *E. coli* strain BL21 Rosetta 2(DE3).

Determination of Oligomeric States of MAB_4384 by Size Exclusion Chromatography

The oligomeric state of MAB_4384 and MAB_4384:DNA complex in solution were assessed on an ENrich^{TM} SEC 650 size exclusion column (Bio-Rad) run on an ÄKTA pure 25M chromatography system (GE Healthcare Life Science). The protein, DNA or protein:DNA complex were eluted with 50 mM Tris-HCl pH 8, 200 mM NaCl and 5 mM β-mercaptoethanol at a flow rate of 0.4 mL/min at 4°C. MAB_4384 (dimer) was concentrated to 3.9 mg/mL, while DNA was at 2.8 mg/mL and complexes were formed at different protein(dimer)/DNA molar ratios of 1:1, 2:1, 3:1. The molecular weights were determined based on a calibration curve generated using the Gel Filtration Markers Kit (Sigma-Aldrich) for proteins ranging from 12,400 to 200,000 Da. The column void volume was assessed with the elution peak of dextran blue. The apparent mass was obtained by plotting the partition coefficient K_{av} against the log values of the molecular weights of the standard proteins.

Disruption of *MAB_4384* and *mmpL5* in *M. abscessus*

To generate *MAB_4384* and *mmpL5* knock-out mutants, internal fragments of the genes were PCR-amplified using Phusion polymerase and the specific oligonucleotide sets: *MAB_4384*::pUX1 Fw with *MAB_4384*::pUX1 Rev and *mmpL5*::pUX1 Fw with *mmpL5*::pUX1 Rev, respectively, digested with NheI and BamHI and ligated to NheI-BamHI-linearized pUX1 (Supplementary Table S1), a suicide vector specifically designed to perform gene inactivation in *M. abscessus* (Viljoen et al., 2018). Electrocompetent *M. abscessus* was transformed with the plasmids pUX1-*MAB_4384* and pUX1-*mmpL5* and plated on 250 μg/mL kanamycin LB plates. After 5 days of incubation at 37°C, red fluorescent colonies were selected and gene disruption resulting from homologous recombination

between the plasmid DNA and the target genes was confirmed by PCR and sequencing with appropriate primers (Supplementary Table S2).

Quantitative Real-Time PCR

Isolation of RNA, reverse transcription and qRT-PCR were done as reported earlier (Halloum et al., 2017) using the primers listed in Supplementary Table S2.

Drug Susceptibility Assessment

The MICs were determined according to the CLSI guidelines (Woods et al., 2011), as reported earlier (Halloum et al., 2017).

Electrophoretic Mobility Shift Assays

First, a typical DNA binding motif recognized by the TetR regulator, often composed of palindromic sequences or inverted repeats, was identified *in silico* within the intergenic region located between *MAB_4384* and the *MAB_4383c (mmpS5$_{Mabs}$)/MAB_4382c (mmpL5$_{Mabs}$)* gene cluster, hereafter referred to as IR$_{S5/L5}$, using the MEME Suite 4.20.0 online tool[1] (Bailey et al., 2009). A 45 bp double stranded DNA fragment (Probe 1) containing the 27 bp palindromic sequence was labeled with fluorescein at their 5′ ends (Sigma-Aldrich). Increasing amounts of purified MAB_4384 protein were co-incubated with 280 nM of the fluorescein-labeled probes in 1X Tris Base/acetic acid/EDTA (TAE) buffer for 1 h at room temperature. The samples were then subjected to 6% native polyacrylamide gel electrophoresis for 30 min at 100 V in 1X TAE buffer. Gel shifts were visualized by fluorescence using an Amersham Imager 600 (GE Healthcare Life Sciences). All additional modified probes listed Supplementary Table S2 and used in this study were synthetized and used in electrophoretic mobility shift assay (EMSA) assays, as described above.

Construction of β-Galactosidase Reporter Strains and β-Gal Assays

The *lacZ* reporter gene encoding the β-galactosidase was amplified from the *E. coli* HB101 using primers listed in Supplementary Table S2. The amplicon was cloned into pMV261 cut with BamHI and HindIII, thus yielding pMV261_P$_{hsp60}$_*lacZ*. The 208 bp intergenic region IR$_{S5/L5}$ was amplified by PCR using *M. abscessus* CIP104536^T genomic DNA and the *MAB_4384*_P$_{S5/L5}$ primers (Supplementary Table S2) and subsequently cut with XbaI and BamHI. The *hsp60* promoter was removed from pMV261_P$_{hsp60}$_*lacZ* construct by restriction using XbaI and BamHI and replaced with IR$_{S5/L5}$, thus creating pMV261_P$_{S5/L5}$_*lacZ*. A promoterless pMV261_*lacZ* construct was also generated by removing the *hsp60* promoter from the pMV261_P$_{hsp60}$_*lacZ* with BamHI and XbaI, blunting the overhang extremities using the T4 DNA Polymerase and self-religation.

The β-galactosidase activity of the *M. abscessus* strains carrying either wild-type or mutated *MAB_4384* alleles and the various β-gal reporter constructs was monitored streaking the strains directly on 7H10^{OADC} agar plates supplemented with 100 μg/mL kanamycin and 50 μg/mL X-gal (Sigma-Aldrich). The quantification of the β-gal activity was also assayed in liquid medium using a protocol adapted from Miller's method. Briefly, a 10 mL culture in Sauton's medium supplemented with 0.025% tyloxapol was grown until the OD_{600} reached 0.6–1. Cultures were collected by centrifugation (4,000 × *g* for 10 min at 4°C) and the bacterial pellets were resuspended in 700 μL 1X phosphate-buffered saline (PBS) prior to mechanical lysis by bead beating (3 min treatment, 30 Hz). Lysates were finally centrifuged at 16,000 × *g* for 10 min at 4°C. 10 μL of clarified lysate were co-incubated 30 min at 37°C with 100 μL of reaction buffer (60 mM Na_2HPO_4, 40 mM NaH_2PO_4, 10 mM KCl, 1 mM $MgSO_4$, 50 mM β-mercaptoethanol) in 96-well plates. Enzymatic reactions were initiated by adding 35 μL of 2-Nitrophenyl β-D-galactopyranoside (ONPG, Sigma-Aldrich) at 4 mg/mL and absorbance was recorded at 420 nm at 34°C using a Multimode Microplate Reader POLARstar Omega (BMG Labtech). The β-galactosidase specific activity ($SA_{\beta-Gal}$) was calculated using the following formula: $SA_{\beta-Gal}$ = (Absorbance$_{420nm}$ × min^{-1})/(OD_{280nm} × liter of culture). To test the β-gal-induction by the TAC analogs, the drugs were added directly to the cultures grown in Sauton's medium (OD_{600} = 0.6–1) and incubated with slow shaking for 96 h at 37°C. The β-gal activity was determined as described above.

Crystallization, Data Collection, and Refinement

The MAB_4384 crystals were grown in sitting drops in MR Crystallization Plates (Hampton Research) at 18°C by mixing 1.5 μl of protein solution concentrated to 4.7 mg/mL with 1.5 μl of reservoir solution made of 100 mM sodium cacodylate pH 6.5, 200 mM $MgCl_2$, 16% PEG 8000 and 5% DMSO. Crystals were briefly soaked in 100 mM Cacodylate buffer pH 6.5, 200 mM $MgCl_2$, 16% PEG 8000, 5% DMSO and 10% PEG 400 prior to being cryo-cooled in liquid nitrogen. The selenomethionine-substituted MAB_4384 crystals were obtained in sitting drops in 96-well SWISSCI MRC plates (Molecular Dimension) at 18°C by mixing 0.8 μl of protein solution concentrated to 2.5 mg/mL with 0.8 μl of reservoir solution consisting of 35% (v/v) 1,4 dioxane. Crystals were cryo-cooled without any additional cryo-protection. Data were processed with *XDS* and scaled and merged with *XSCALE* (Kabsch, 2010). Data collection statistics are presented in **Table 1**. The MAB_4384 structure was solved by the single wavelength anomalous dispersion method. *AutoSol* from the *Phenix* package was used to solve the structure (Adams et al., 2010). Twelve of the fourteen potential selenium sites in the asymmetric unit were found using a resolution cutoff of 3.4 Å for the search of the Se atoms. After density modification, a clear electron density map for the two TetR monomers allowed initial model building. The resulting partial model was used to perform molecular replacement with the 1.9 Å native dataset using *Phaser* (McCoy et al., 2007) from the *Phenix* package (Adams et al., 2010). *Coot* (Emsley et al., 2010) was used for manual rebuilding while structure refinement and validation were performed with

[1]http://meme-suite.org

TABLE 1 | Data collection and refinement statistics.

	MAB_4384 native	Selenium peak
Data collection statistics		
Beamline	ESRF-ID30B	ESRF-ID30B
Wavelength (Å)	0.979	0.979
Resolution range (Å)	36.5–1.9 (1.96–1.9)	47–2.3 (2.38–2.3)
Space group	P 1 21 1	P 1 21 1
Unit cell (Å,°)	40.8 100.8 56.0 90 105.8 90	41.4 99.3 55.7 90 106.9 90
Total reflections	73028 (7378)	126590 (12013)
Unique reflections	31705 (3193)	18983 (1849)
Multiplicity	2.3 (2.3)	6.7 (6.5)
Completeness (%)	92.1 (93.4)	98.6 (98.1)
Mean I/sigma (I)	11.09 (1.06)	11.66 (1.36)
Wilson B-factor (Å^2)	33.9	46.02
R-meas	0.06 (0.92)	0.13 (1.21)
CC1/2	0.99 (0.51)	0.97 (0.67)
CC*	1 (0.82)	0.99 (0.89)
Data refinement statistics		
Reflections used in refinement	31695 (3193)	
Reflections used for R-free	2000 (201)	
R-work	0.184 (0.312)	
R-free	0.213 (0.351)	
Number of non-H atoms	3460	
Macromolecules	3178	
Solvent	282	
Protein residues	402	
RMS bonds (Å)	0.002	
RMS angles (°)	0.45	
Ramachandran favored (%)	98.99	
Ramachandran allowed (%)	1.01	
Ramachandran outliers (%)	0.00	
Rotamer outliers (%)	0.95	
Average B-factor (Å^2)	43.6	
Macromolecules	43.2	
Solvent	47.6	
PDB accession number	5OVY	

The values in parenthesis are for the last resolution shell.

the *Phenix* package (Adams et al., 2010). The statistics for data collection and structure refinement are displayed in **Table 1**. Figures were prepared with PyMOL[2]. The atomic coordinates and the structure factors for the reported MAB_4384 crystal structure has been deposited at the Protein Data bank (accession number 5OVY).

Docking of TAC Analogs Into the Ligand Binding Site

Docking studies was performed with *PyRx* (Dallakyan and Olson, 2015) running *AutoDock Vina* (Trott and Olson, 2010). Search was done with grid dimensions of 39.45, 39.05, 29.25 Å and origin coordinates at $x = -17.8$, $y = 6.9$, $z = 0.63$. The search was performed on chain B of the crystal structure of MAB_4384 without any additional model modification.

[2]www.pymol.org

RESULTS

MAB_4384 Specifically Regulates Susceptibility to TAC Analogs in *M. abscessus*

We recently showed that mutations in the MAB_4384 regulator were associated with the transcriptional induction of the divergently oriented adjacent genes coding for an MmpS5/MmpL5 efflux pump and accounting for high resistance levels toward various TAC analogs (Halloum et al., 2017). To gain more insight into this drug resistance mechanism in *M. abscessus,* detailed genetic, functional and structural characterizations of the MAB_4384 regulator were undertaken. First, the expression profile of 19 *mmpL* genes was analyzed by qRT-PCR using the *M. abscessus* D15_S4 strain which possesses an early stop codon in *MAB_4384* resulting in high resistance levels to the TAC analogs D6, D15 and D17 (MIC > 200 μg/mL), presumably due to derepression of the MmpS5/MmpL5 efflux pump machinery (Halloum et al., 2017). The results clearly showed a pronounced increase in the expression level of *MAB_4382c* (*mmpL5*) mRNA in D15_S4 in comparison to the wild-type strain as reported previously, while no marked effect on the remaining *mmpL* genes was detected **(Figure 1A)**. The expression levels of *tgs1*, encoding the primary triacylglycerol synthase responsible for the accumulation of triglycerides in *M. abscessus* (Viljoen et al., 2016) was included as unrelated gene control. As expected, expression of *tgs1* stayed unchanged **(Figure 1A)**. To further confirm these results, the *MAB_4384* and *MAB_4382c* genes were inactivated by homologous recombination using the recently developed genetic tool dedicated to facilitate gene disruption in *M. abscessus* (Viljoen et al., 2018), as illustrated in Supplementary Figures S1A,B. The mutant strain, designated *MAB_4384*::pUX1, failed to show morphological changes (Supplementary Figure S1C) and grew similarly to its parental strain and the *MAB_4382c*::pUX1 mutant (Supplementary Figure S1D), suggesting that *MAB_4384* does not play a significant role under normal *in vitro* conditions. However, this mutant exhibited high resistance levels to D6, D15, and D17 (MIC > 200 μg/mL, corresponding to >8-, >32-, and >16-fold-increases in MIC levels, respectively) (**Table 2**) similarly to our previous results for D15_S4 (Halloum et al., 2017), thus validating the expected phenotype of the strain. Analysis of the transcriptional profile of all 19 *mmpL* genes in *MAB_4384*::pUX1 confirmed the results obtained in the D15_S4 strain **(Figure 1B)**. Interestingly, expression of *MAB_4384* itself was significantly induced in *MAB_4384*::pUX1, **(Figure 1C)**, albeit lower than the expression level of *mmpL5*, thus indicating that MAB_4384 is self-regulated.

Overall, these results suggest that MAB_4384 is a unique and highly specific regulator controlling expression of *mmpL5* in *M. abscessus*, which was strongly up-regulated in the absence of MAB_4384.

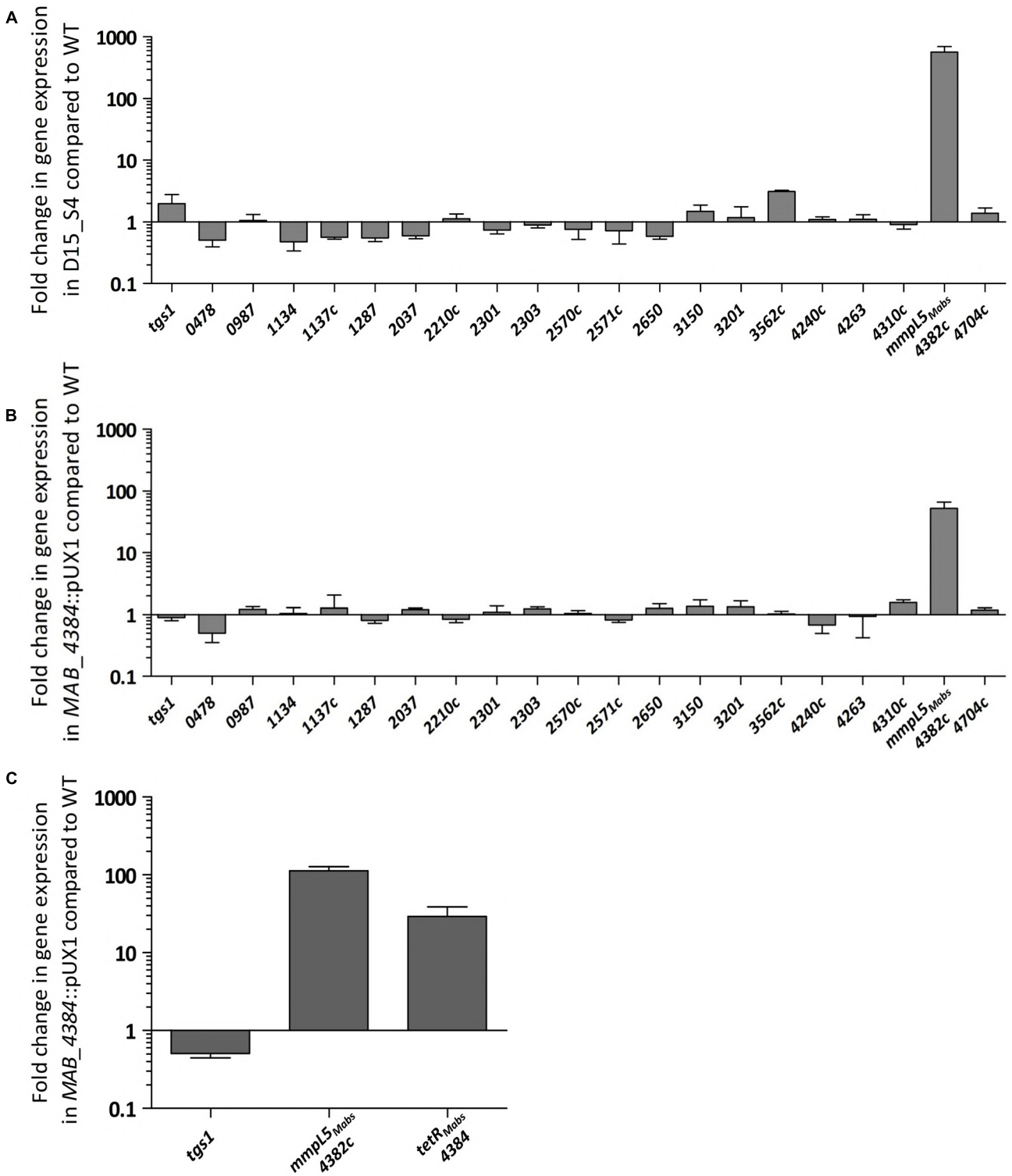

FIGURE 1 | MAB_4384 is a specific repressor of the *mmpS5/mmpL5* locus in *M. abscessus*. Transcriptional profile of 19 *mmpL* in *M. abscessus* expressed in fold induction relative to expression in the wild-type strain (CIP104536^T) in **(A)** the D15_S4 spontaneous mutant resistant to TAC analogs containing a stop codon in *MAB_4384* and in **(B)** *MAB_4384*::pUX1 in which *MAB_4384* has been disrupted by homologous recombination. *tgs1* was included as a non-relevant control gene. Error bars indicate standard deviation. **(C)** Expression of MAB_*4384* in *M. abscessus.* Fold induction levels of *MAB_4384* were calculated in *MAB_4384*::pUX1 relative to the parental strain. Error bars indicate standard deviation. Relative gene expression was calculated using the $\Delta\Delta$Ct method with correction for PCR efficiency. Data is representative of three independent experiments.

TABLE 2 | Drug susceptibility profile of *M. abscessus* S strains inactivated in either *MAB_4384* (*tetR* gene) or *MAB_4382c* (*mmpL5* gene).

	MIC (μg/mL)				
Strain	**D6**	**D15**	**D17**	**CFZ**	**BDQ**
CIP104536^T	25	6.2	12.5	1.6	0.05
MAB_4384::pUX1	>200	>200	>200	1.6	0.05
MAB_4382c::pUX1	12.5	6.2	6.2	1.6	0.05

The MIC (μg/mL) was determined in CaMH medium. Data are representative of three independent experiments. CFZ, clofazimine; BDQ, bedaquiline.

MAB_4384 Negatively Regulates Expression of *mmpS5/mmpL5*

The pMV261_$P_{S5/L5}$_*lacZ* plasmid was constructed, containing the β-galactosidase gene as a reporter in *M. abscessus* to further confirm the negative regulation of MAB_4384 on the target gene (*mmpS5/mmL5* locus) expression. To do this, the 208 bp intergenic region located between *MAB_4384* and *mmpS5/mmpL5* **(Figure 2A)**, designated $IR_{S5/L5}$, was cloned upstream of *lacZ*. pMV261_$P_{S5/L5}$_*lacZ* was subsequently introduced in parental smooth (S) and rough (R) variants of *M. abscessus* as well as in three different strains carrying single point mutations in MAB_4384 (M1A, F57L, and D14N), previously selected for their high resistance phenotype to TAC analogs (Halloum et al., 2017). In addition, pMV261_P_{hsp60}_*lacZ* allowing constitutive expression of *lacZ* under the control of the strong *hsp60* promoter was produced. As expected, pMV261_P_{hsp60}_*lacZ* led to high expression of *lacZ* in the wild-type strain and in the mutants compared to the promoter-less plasmid, as evidenced by the production of intense blue colonies and a strong β-Gal activity (**Figure 2B**). In contrast, whereas $IR_{S5/L5}$ resulted in very low expression of LacZ in the wild-type strains, characterized by a pale blue color on plates and low β-Gal activity in liquid-grown cultures, a pronounced *lacZ* induction was detected in all three mutant strains (**Figure 2B**). Strikingly, the *lacZ* expression levels in these strains was almost comparable to the one observed in the pMV261_P_{hsp60}_*lacZ*-containing strains.

Overall, these results indicate that expression of *lacZ* is strongly repressed in the presence of an intact MAB_4384 regulator and that under derepressed conditions, the promoter driving expression of *mmpS5/mmpL5* appears almost as strong as the *hsp60* promoter.

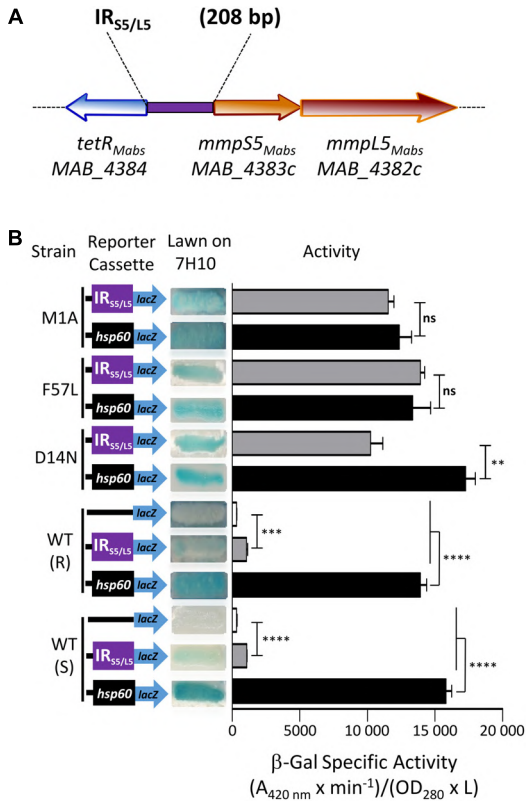

FIGURE 2 | Identification of a MAB_4384-dependent regulatory promoter region in *M. abscessus*. **(A)** Schematic representation of the genome organization of *MAB_4384* and the *mmpS5/mmpL5* gene cluster in *M. abscessus* with the purple rectangle indicating the $IR_{S5/L5}$ intergenic region cloned upstream of the *lacZ* reporter construct. **(B)** The effect of MAB_4384 on *mmpS5/mmpL5* expression was assayed by constructing a plasmid with the *lacZ* reporter under control of $IR_{S5/L5}$. A positive control plasmid consisting of the constitutive expression of *lacZ* under the control of the *hsp60* promoter and a negative control consisting of a promoter-less *lacZ* were also generated. All constructs were introduced into wild-type smooth (S) and rough (R) variants as well as into three different strains harboring single point mutations in MAB_4384 (M1A, D14N and F57L replacements). Exponentially growing *M. abscessus* cultures were streaked onto 7H10 plates containing 100 μg/mL kanamycin and 50 μg/mL X-gal. The plates were subsequently incubated for 3–4 days at 37°C and visualized for their appearance with respect to white-to-blue coloration. The β-galactosidase specific activity ($SA_{\beta-Gal}$) was quantified in liquid cultures using ONPG as a substrate. Results were obtained from three independent experiments and the error bars represent standard deviation. The capped lines indicate the groups compared. For statistical analysis, the Student's *t*-test was applied with ns, **, ***, **** indicating non-significant, $p < 0.01$, $p < 0.001$, and $p < 0.0001$, respectively.

MAB_4384 Binds to a Palindromic Sequence Within $IR_{S5/L5}$

Motif-based sequence analysis using MEME (Bailey et al., 2009) revealed the presence of a 27 bp segment within the divergently oriented $IR_{S5/L5}$ intergenic region and harboring a palindromic sequence **(Figure 3A)**. To test whether this motif represents a DNA binding site for MAB_4384, EMSA was first performed using increasing concentrations of purified MAB_4384 expressed in *E. coli* in the presence of a 45 bp fragment of $IR_{S5/L5}$ (Probe 1; **Figure 3B**) carrying extra nucleotides flanking the palindromic sequence. Under these conditions, a DNA–protein complex was seen **(Figure 3C)**. To confirm the specificity of the binding, a competition assay with increasing concentrations of the corresponding unlabeled probe (cold probe) was carried out, leading to a dose-dependent decrease of the DNA–protein complex **(Figure 3C)**. In addition, in the presence of an excess of a non-related labeled probe, the shift was maintained, thus indicating that a specific protein–DNA complex was seen only when MAB_4384 was incubated with DNA containing the specific inverted repeat sequence. To better define the

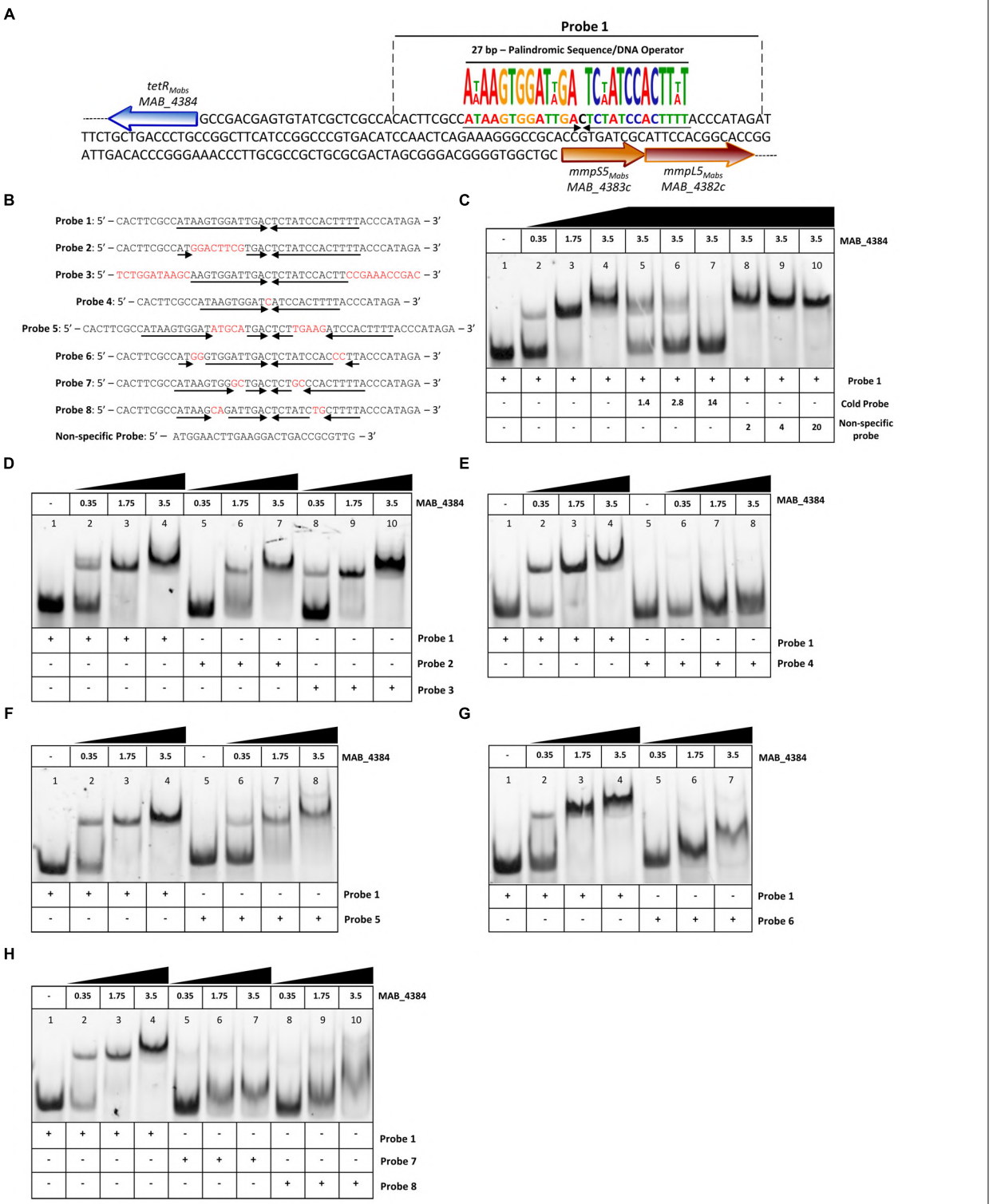

FIGURE 3 | Binding activity of MAB_4384 to a palindromic region within $IR_{S5/L5}$. **(A)** DNA sequence of $IR_{S5/L5}$ and representation of the operator composed of a 27 bp region containing two degenerated inverted sequences of 13 nucleotides each (black arrows) and separated by a one nucleotide spacer. The probe used to perform the EMSA is delimited by dotted lines (Probe 1). **(B)** DNA sequences of all the various 5′ fluorescein-labeled probes used in this study. **(C)** EMSA and competition assay using probe 1. Protein and DNA concentrations are expressed in μM. In competition assays, the concentration of Probe 1 was fixed at 280 nM. Gel shifts were revealed by fluorescence emission. **(D–H)** EMSA using Probes 2 to 8, each time compared to the shift profile obtained with Probe 1. Experiments were reproduced three times with similar results.

minimal motif and the importance of the nucleotides involved in recognition and binding of the protein, a large set of fluorescein-labeled probes differing in their size and/or sequence were next assayed **(Figure 3B).** In the presence of Probe 2, in which only the right inverted sequence was conserved, a delay in the DNA shift was observed (partial in the presence of 1.75 μM of protein as compared to the reaction in the presence of Probe 1). Shifts using Probe 3, where the extra nucleotides surrounding the palindromic sequence were changed randomly were comparable to those obtained with Probe 1 **(Figure 3D)**, indicating that the extra-palindromic sequence does not influence protein binding. With Probe 4, where the inverted repeats were shortened by six nucleotides, the formation of the DNA–protein complex was severely impeded even with the highest concentration of protein tested (3.5 μM) **(Figure 3E)**. Increasing the spacer between the two inverted repeats by 10 nucleotides (Probe 5) negatively impacted the shift **(Figure 3F)**. Substitutions of two nucleotides at the extremities in each repeat sequence (Probe 6) was accompanied by a pronounced shift alteration **(Figure 3G)** and similar results were obtained when di-nucleotide substitutions occurred at other positions within the conserved palindromic sequence (Probes 7 and 8) **(Figure 3H)**.

Overall, these results confirm that a strict preservation of this inverted sequence and space separating these two motifs are crucial for binding of MAB_4384 to its target.

Asp14 and Phe57 Are Critical for Optimal DNA-Binding Activity of MAB_4384

Multiple primary sequence alignments of the MAB_4384 N-terminus with other TetR regulators with known three-dimensional structures indicate that the N-terminus Asp14 residue is well conserved in several other Tet regulators **(Figure 4A)**. Similarly, Phe57 was also found to be part of a highly conserved stretch of amino acids in these proteins, although, in some instances, Phe was replaced by bulky/hydrophobic residues **(Figure 4A)**. The importance of the conservation of these two residues for the function of MAB_4384 and presumably also for that of the other TetR regulators, was next assessed by EMSA using the purified MAB_4384 mutated variants. As compared to the shift profile with wild-type MAB_4384, the production of the DNA–protein complex was severely impaired in the presence of either MAB_4384 (D14N) **(Figure 4C)** or MAB_4384 (F57L) **(Figure 4D)** and fully abrogated in the presence of the double mutant (D14N/F57L) **(Figure 4E)**.

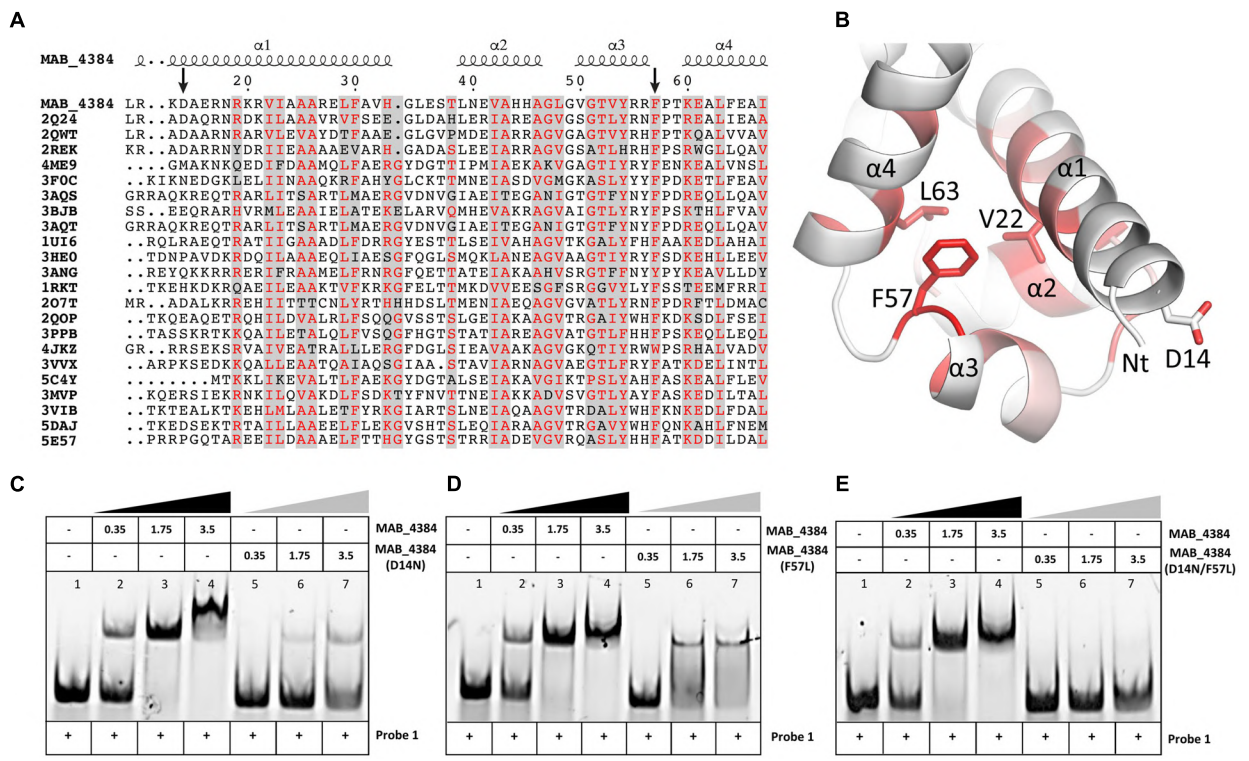

FIGURE 4 | D14N and F57L mutations abrogate binding of MAB_4384 to its palindromic DNA target. **(A)** Multiple primary sequence alignments of MAB_4384 N-terminus with other TetR family members whose crystal structures are known (PDB code indicated) from different microorganisms showing the conservation of the Asp14 and Phe57 residues (indicated with black arrows). **(B)** Mapping of the mutations on the crystal structure of MAB_4384, the degree of residue conservation (obtained from the sequence alignment in **A**) is represented by the coloration, from white (low conservation) to red (high conservation). **(A,B)** Were prepared using the ENDscript server (http://endscript.ibcp.fr/ESPript/ENDscript/). EMSA were performed using increasing concentrations (in μM) of the purified MAB_4384 (D14N) **(C)**, MAB_4384 (F57L) **(D)** or MAB_4384 (D14N/F57L) **(E)** in the presence of Probe 1. Wild-type MAB_4384 was included as a positive control in each assay. The concentration of Probe 1 was fixed at 280 nM. Gel shifts were revealed by fluorescence emission. Three independent experiments were performed with similar results.

Overall, these results support the importance of both residues in the DNA-binding capacity of MAB_4384 and the impaired ability of the mutants to bind to the operator is in agreement with the derepression of *lacZ* transcription in the *M. abscessus* strains carrying the D14N or F57L mutations **(Figure 2B)**.

Oligomeric States of MAB_4384 and MAB_4384:DNA in Solution

To further characterize the MAB_4384:DNA complex formation, we next assessed its stability in solution by SEC **(Figure 5)**. The oligomeric state of MAB_4384 in solution has an apparent 42.6 kDa molecular weight as compared to its 24.7 kDa theoretical molecular mass calculated from its primary sequence, thus highlighting the dimeric state of MAB_4384 in solution. MAB_4384 (dimer) was next incubated with the non-fluorescent DNA Probe 1 **(Figure 3A)** in a 1:1 molar ratio. A stable complex elution peak at 12.6 mL clearly shifted from the elution peak of MAB_4384 and DNA alone **(Figure 5)**, allowing deduction of the molecular mass of the protein:DNA complex at 102 kDa. As the DNA alone in solution appeared on SEC as a 24.5 kDa molecule, these results strongly suggest the existence of two MAB_4384 dimers bound to one DNA molecule as such a complex would possess a molecular mass of 109.7 kDa (2×42.6 kDa + 24.5 kDa). This 2-to-1 binding mode was further corroborated by the fact that an elution peak corresponding to free DNA can be seen at 14.4 mL when we mixed the MAB_4384 dimer and DNA in a 1:1 ratio. Moreover, increasing the molar ratio of the MAB_4384 dimer:DNA complex (2:1 and 3:1) did not yield larger protein:DNA complexes (data not shown), suggesting that, at a 1:1 molar ratio, the operator is already saturated by the protein. This observation is not unique as two TetR dimers have been shown to bind their DNA targets in other microorganisms, such as in *Staphylococcus aureus* (Grkovic et al., 2001) or in *Thermus thermophilus* (Agari et al., 2012).

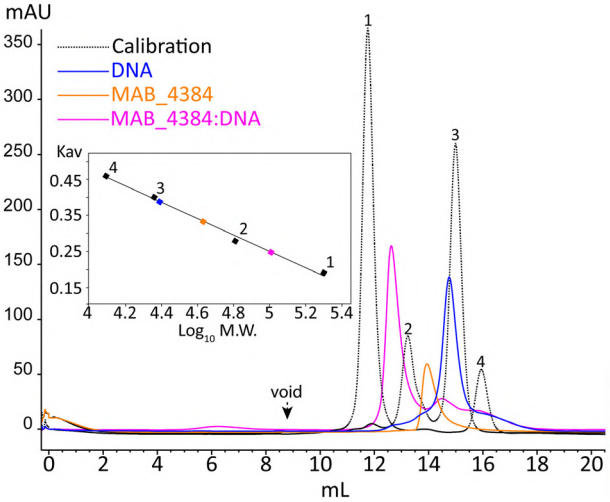

FIGURE 5 | Oligomerization of MAB_4384 and the MAB_4384:DNA complex in solution. The oligomeric states of MAB_4384 alone or complexed to its DNA target were determined by size exclusion chromatography. The elution profile of the proteins, used for the calibration is displayed as a dashed black line. Calibration was established using β-amylase (200 kDa) (1), bovine serum albumin (66 kDa) (2), carbonic anhydrase (29 kDa) (3), and cytochrome C (12.4 kDa) (4), eluting with estimated volumes of 11.7, 13.2, 14.9, 15.9 mL, respectively. The void volume was determined with the elution volume (8.8 mL) of dextran blue. MAB_4384 (dimer) was at a concentration of 3.9 mg/mL. The elution profiles of MAB_4384 dimer, DNA target and MAB_4384 bound to the DNA target are shown in orange, blue, and pink and their respective elution peaks were at 13.9, 14.7, and 12.6 mL. K_{av} indicates the partition coefficient.

Crystal Structure of MAB_4384

To understand, at a molecular basis, how the D14N or F57L mutations generate resistance to TAC analogs, we first crystallized and determined the X-ray structure of MAB_4384. Although the structure of the protein could not be solved by molecular replacement, the phase problem was overcome with the SAD method using crystals of selenomethionine-substituted MAB_4384 **(Table 1)**. The crystal structure of the native protein was subsequently solved with the partial model obtained from the SAD data and refined to a resolution of 1.9 Å. The asymmetric unit contains two subunits. Chain A was modeled from residues Asp14 to Thr213, indicating that the first thirteen residues, one residual Gly residue from the tag and the last eight residues in the C-terminus were not visible in the electron density. Chain B showed also disordered regions as the first ten residues, one Gly residue from the tag in N-terminus as well as the last nine residues in the C-terminus, could not be modeled. Analysis of the crystal packing using the *PISA* server (Krissinel and Henrick, 2007) predicted the existence of a stable homodimer formed within the crystal, consistent with other TetR regulators (Cuthbertson and Nodwell, 2013) and with the SEC profile of MAB_4384 in solution **(Figure 5)**.

The two subunits are very similar as their superposition leads to a root mean square deviation (r.m.s.d.) of 0.53 Å over 198 aligned residues. The N-terminus comprises the DNA binding domain (DBD), followed by the LBD. The DBD is composed of three α-helices α1: residues 12–33, α2: 39–46, and α3: 50–56, where helices 2 and 3 form a helix-turn-helix (HTH) motif. The LBD is made of seven α-helices, α4: 60–82, α5: 88–104, α6: 107–114, α7: 121–143, α8: 155–170, α9: 178–188, and α10: 205–211 **(Figure 6A)**. The surface of dimerization of about 1,700 $Å^2$ is mediated by 31 residues mainly from helices α8 and α9 of each subunit and involves numerous interactions notably five salt bridges, fourteen hydrogen bonds and van der Waals interactions.

Interestingly, we noticed the presence of extra electron density in the LBD of chain B in a rather hydrophobic pocket **(Figure 6B)**. Although we could not interpret this density, we hypothesize that it may correspond to a compound present in the crystallization solution, such as PEG. Search for structural homologs in the PDBeFold server indicated that the closest structure to MAB_4384 corresponds to the LfrR TetR transcriptional regulator from *Mycobacterium smegmatis* bound to proflavin (PDB id : 2V57) (Bellinzoni et al., 2009) with an r.m.s.d. of 2.6 Å and sharing 16% primary sequence identity with MAB_4384. However, only one subunit of each structure could

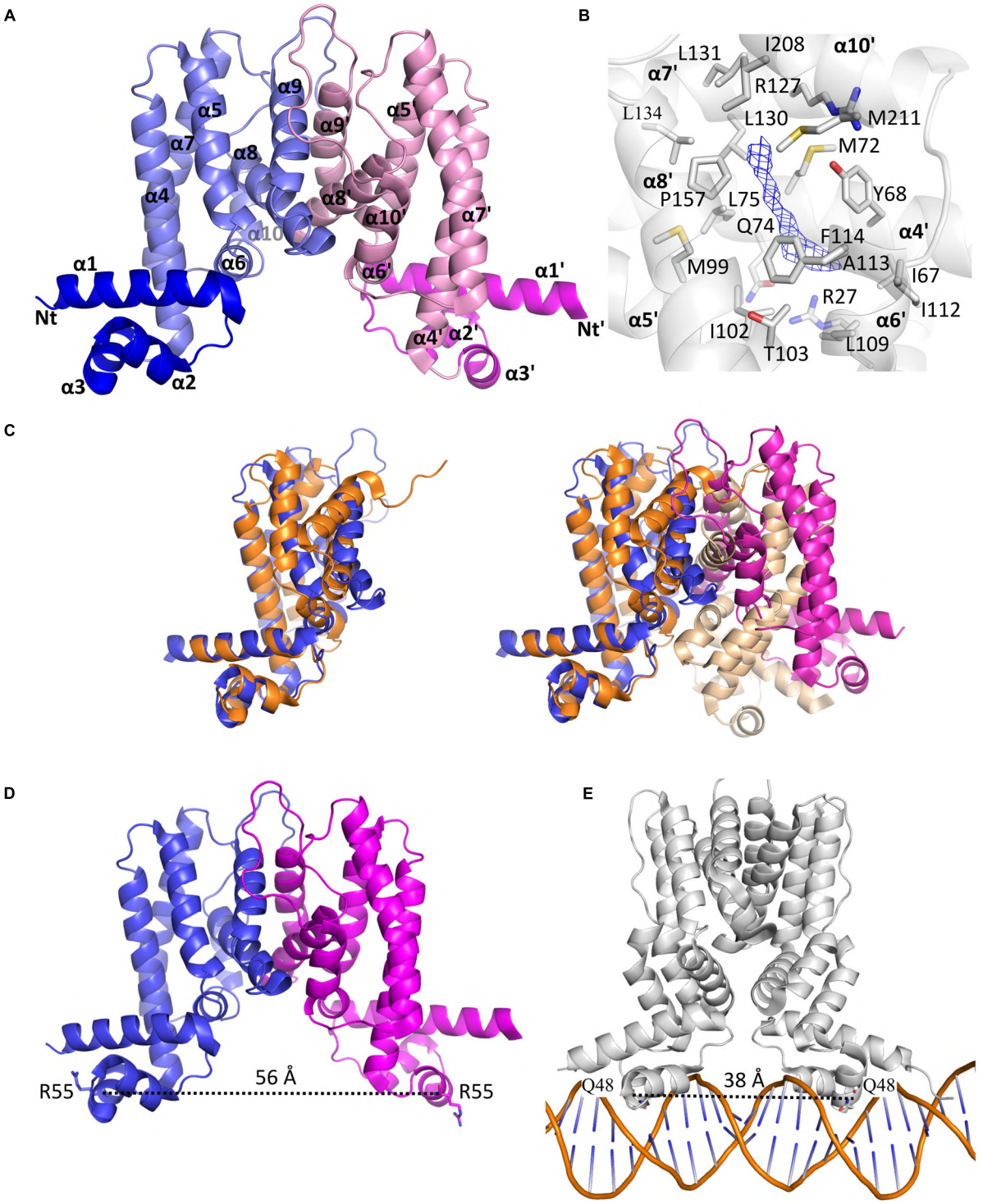

FIGURE 6 | The homodimeric crystal structure of MAB_4384. **(A)** Overall structure of the MAB_4384 dimer displayed as cartoon representation. The LBDs of each subunit are colored in slate and pink while the DNA binding domains are colored in blue and magenta. Helices are indicated by the α signs followed by numbers, Nt and Ct stands for N-terminus and C-terminus and ' is for chain B. **(B)** Putative ligand binding pocket in the LBD of MAB_4384. The Fo-Fc simulated annealed omit map contoured at 3 σ level is shown in blue. Residues that are 4 Å around the electron density blob and that are potential amino acids of the ligand binding site are shown as sticks. **(C)** Structural comparison of MAB_4384 with the crystal structure of the *M. smegmatis* LfrR repressor (PDB id: 2V57). The left panel represents the superposition of one monomer of MAB_4384 (in blue) on one monomer of LfrR (in orange). The superposition of the two homodimers is shown on the right panel, the two subunits of MAB_4384 are in blue and magenta and the two monomers of LfrR are in orange and wheat. **(D,E)** The figures compare the distance between the two DNA binding domains in MAB_4384 **(D)** and in the crystal structure of the *M. smegmatis* TetR Ms6564 protein bound to its DNA target (PDB id: 4JL3).

be superposed as the overall dimers differed largely **(Figure 6C)**. LrfR represses the expression of the LfrA efflux pump (Buroni et al., 2006) and mediates resistance to ethidium bromide, acriflavine, and fluoroquinolones (Takiff et al., 1996).

Due to the occurrence of an extra electron density within the LBD of MAB_4384 and that the closest structure of MAB_4384 is LfrR in its ligand bound form, it is very likely that MAB_4384 was crystallized in its open conformation, i.e., its derepressed form that is not able to interact with DNA. This was assessed by determining the distance between two residues from the DBD susceptible to interact with DNA. Residues Arg55 from chains A and B are about 56 Å apart **(Figure 6D)**. In comparison, the distances between the equivalent residues in various TetR:DNA complexes are largely reduced. In the TetR:DNA complex (PDB id: 4PXI) from *Streptomyces coelicolor* this distance is 45 Å (Bhukya et al., 2014), in the TetR:DNA complex from *M. smegmatis* (PDB id: 4JL3) (Yang et al., 2013) **(Figure 6E)**, *E. coli* (PDB id: 1QPI) (Orth et al., 2000), *Corynebacterium glutamicum* (PDB id: 2YVH) (Itou et al., 2010) or *Staphylococcus aureus* (PDB id: 1JT0) (Schumacher et al., 2002) the distances are 38 Å, 30 Å, 42 Å, and 37 Å, respectively. From these results it can be inferred that the DBDs of MAB_4384 are too far from each other to bind to the DNA groove. These observations combined with the presence of an unidentified ligand in the LBD strongly suggest that the MAB_4384 structure is in an open conformation.

Structural Basis of the Resistant Phenotype of the Mutants

To determine the impact of the mutations in the spontaneous resistant *M. abscessus* mutants, the D14N and F57L residues were mapped on the crystal structure of MAB_4384. Asp14 is located at the beginning of helix α1 and is conserved in several TetR protein members **(Figures 4A,B)**. Residues from helix α1 are often found in contact with DNA as seen in several TetR:DNA crystal structures. Nonetheless, due to the acidic nature of Asp, it is more likely that this residue repulses DNA. We, therefore, hypothesize that it may instead contribute to the correct positioning of other residues located in its close vicinity. Alternatively, repulsion may promote important interactions of DNA with other residues. Indeed, in other collected datasets at lower resolution (data not shown), Asp14 was found to establish a salt bridge interaction, thereby stabilizing the side chain of Arg17 that could interact with DNA. In the absence of a crystal structure of MAB_4384 bound to DNA it is, however, difficult to convincingly affirm the impact of the D14N substitution. However, neither the repulsion of DNA nor the establishment of a salt bridge would be possible if Asn is present instead of Asp, presumably explaining the loss of DNA binding activity of the TetR D14N mutant.

The role of Phe57 situated on helix α3 is more obvious as this position appears always occupied by bulky residues (Phe, Tyr, or Trp) in numerous TetR proteins **(Figure 4A)**. The side chain of Phe57 contacts the side chains of Val22 from helix α1 and Leu63 from helix α4 **(Figure 4B)**. Phe57 is very likely to perform an important structural role in stabilizing the DBD. Replacement with a less bulky side chain such as Leu would abolish these contacts with helices α1 and α4 residues, thus perturbing the overall structural fold of this domain and suppressing the DNA-binding capacity of MAB_4384.

Drug Recognition of MAB_4384 Induces Expression of MmpS5/MmpL5

TetR regulators can respond to small molecules and the best characterized member of this family of regulators is *E. coli* TetR itself. It confers resistance to tetracycline by regulating the expression of the tetracycline TetA efflux pump (Hillen and Berens, 1994). When tetracycline binds to TetR, the regulator loses affinity for the operators, conducting derepression of *tetA* and extrusion of tetracycline out of the bacteria (Lederer et al., 1995). To investigate whether TAC derivatives could bind to the LBD of MAB_4384, *in silico* docking was performed. Despite using a large grid box covering the entire LBD, all three compounds seem to be accommodated by the same binding pocket **(Figure 7A)**. Interestingly, this pocket positioned exactly where the extra electron density was seen in the LBD **(Figure 6B)**. All the compounds bind with similar energies in the aforementioned hydrophobic binding pocket. A slightly stronger interaction for the most hydrophobic derivative D17 was nonetheless observed. D17 and D6 that seem to bind stronger are more hydrophobic and in their best docking poses their thiosemicarbazide group is differently oriented as compared to D15.

Next, we determined whether expression of *mmpS5/mmpL5* can be conditionally induced by the substrates that are extruded by the efflux pump system. This was achieved by determining the effect of the D6, D15, and D17 analogs on LacZ production using the pMV261_$P_{S5/L5}$_*lacZ* reporter strain in *M. abscessus* incubated in Sauton's medium with various drug concentrations consisting of 1X, 2.5X, and 5X the MIC for D15 and of 0.5X, 1X, and 2.5X for D6 and D17. Kinetic studies indicated that optimal expression was obtained after 96 h of treatment (data not shown). The LacZ assay showed that transcription was induced by the TAC analogs in a dose-dependent manner whereas non-related drugs such as amikacin or the DMSO control had no effects **(Figure 7B)**. In comparison with the basal transcriptional level in Sauton's medium (no drug control), the addition of TAC derivatives in the cultures resulted in a reproducible 2.5- to 5-fold increase in the detection of β-Gal activity with D17 being the most potent inducer at 2.5X MIC. However, ethionamide, an antitubercular drug that, like the TAC and TAC analogs, requires to be activated by the EthA monooxygenase (Baulard et al., 2000; DeBarber et al., 2000; Dover et al., 2007; Halloum et al., 2017) failed to induce *lacZ* at 5X MIC (previously determined at 16 μg/ml). Induction of *lacZ* by D17 treatment was further confirmed at a transcriptional level from the pMV261_$P_{S5/L5}$_*lacZ* cultures treated with 2.5× MIC of D17 for 8 h **(Figure 7C**, left). This effect was specific to D17 as no gene induction was observed in the DMSO-treated cultures. Consistently, transcription profiling of *mmpS5* and *mmpL5* in the D17-exposed cultures clearly showed a marked induction level as compared to the DMSO-treated cultures and no effect on *tgs1* expression **(Figure 7C**, right).

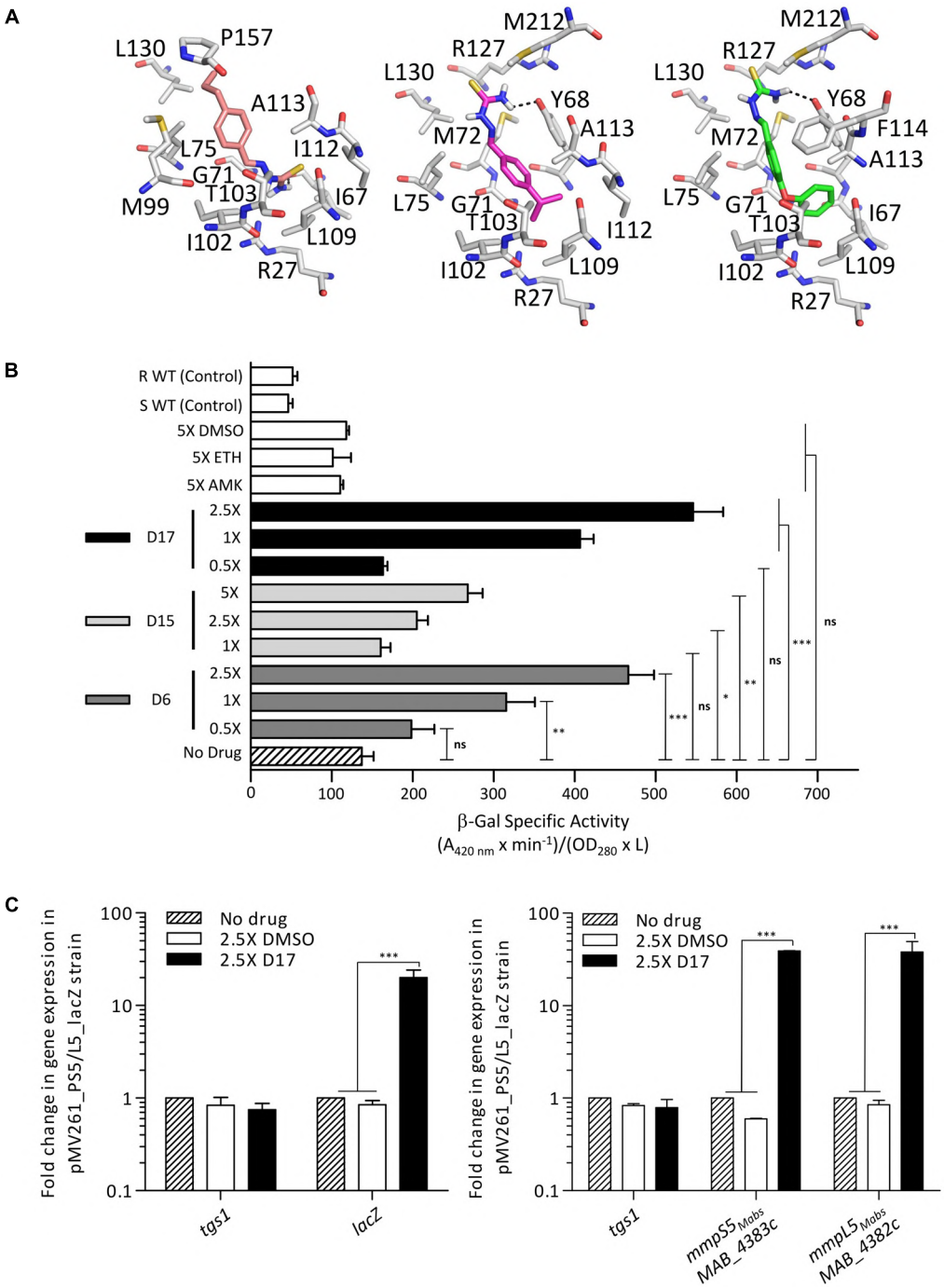

FIGURE 7 | $IR_{S5/L5}$ can be induced by structural analogs of thiacetazone. **(A)** Docking of TAC derivatives in the ligand binding site of MAB_4384. All the residues involved in van der Waals, hydrophobic bonds or hydrogen bonds (in black dashes) are displayed as sticks. D15 in salmon has a binding energy of ΔG = –6.6 kcal/mol, D6 in magenta has a ΔG = –7.3 kcal/mol, and D17 seems to bind slightly stronger with a ΔG = –8.3kcal/mol. **(B)** Conditional induction of *lacZ* by structural analogs of TAC in *M. abscessus*. Induction of β-Gal activity in wild-type *M. abscessus* S carrying pMV261_$P_{S5/L5}$_*lacZ* was assayed using mid-log phase cultures incubated with increasing drug concentrations varying from 1X to 5X the MIC for D15 and varying from 0.5X to 2.5X the MIC for D6 and D17. Inductions were performed for 96 h at 37°C. The β-galactosidase specific activity ($SA_{\beta-Gal}$) was quantified in liquid cultures using ONPG as a substrate. Amikacin (AMK) and ethionamide (ETH) were included as unrelated drug controls. **(C)** Transcriptional profile of *lacZ* in the *M. abscessus* pMV261_$P_{S5/L5}$_*lacZ* reporter strain exposed to 2.5X the MIC of D17 for 8 h (left). *tgs1* was included as a non-relevant control. Replacing D17 by an equal volume of DMSO had no effect on *lacZ* transcription. Transcriptional induction of $mmpS5_{Mabs}$ and $mmpL5_{Mabs}$ following exposure to 2.5X the MIC of D17 for 8 h (right). Results were obtained from three independent experiments and the error bars represent standard deviation. For statistical analysis the Student's *t*-test was applied with ns, *, **, ***, **** indicating non-significant, $p < 0.05$, $p < 0.01$, $p < 0.001$, and $p < 0.0001$, respectively.

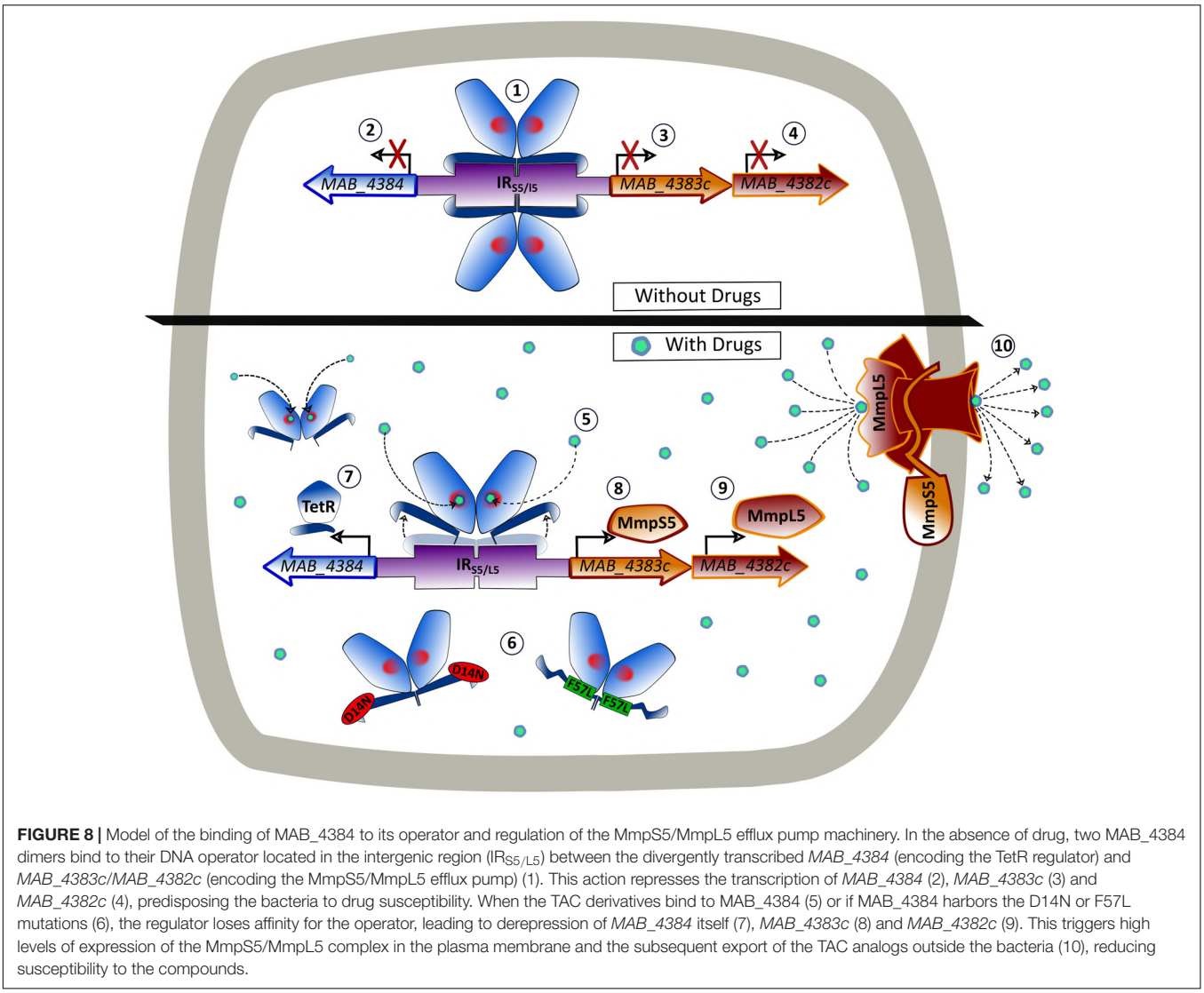

FIGURE 8 | Model of the binding of MAB_4384 to its operator and regulation of the MmpS5/MmpL5 efflux pump machinery. In the absence of drug, two MAB_4384 dimers bind to their DNA operator located in the intergenic region ($IR_{S5/L5}$) between the divergently transcribed *MAB_4384* (encoding the TetR regulator) and *MAB_4383c/MAB_4382c* (encoding the MmpS5/MmpL5 efflux pump) (1). This action represses the transcription of *MAB_4384* (2), *MAB_4383c* (3) and *MAB_4382c* (4), predisposing the bacteria to drug susceptibility. When the TAC derivatives bind to MAB_4384 (5) or if MAB_4384 harbors the D14N or F57L mutations (6), the regulator loses affinity for the operator, leading to derepression of *MAB_4384* itself (7), *MAB_4383c* (8) and *MAB_4382c* (9). This triggers high levels of expression of the MmpS5/MmpL5 complex in the plasma membrane and the subsequent export of the TAC analogs outside the bacteria (10), reducing susceptibility to the compounds.

Together, these results support the view that TAC analogs, which are substrates of MmpS5/mmpL5, are also effectors of MAB_4384-induced transcription of *mmpS5/mmpL5*.

DISCUSSION

Herein, a combination of genetic, biochemical and structural studies was used to demonstrate that MAB_4384 is part of the TetR family of regulators, which represses the transcriptional expression of the MmpS5/MmpL5 efflux pump. MAB_4384 belongs to the type I class TetR family of regulators, characterized by a divergent orientation to one of the adjacent target genes (Cuthbertson and Nodwell, 2013). In *M. tuberculosis,* MmpS5/MmpL5 is under the control of the MarR repressor Rv0678 (Radhakrishnan et al., 2014) and mutations in this regulator leads to drug resistance (Andries et al., 2014; Hartkoorn et al., 2014; Zhang et al., 2015). EMSA indicated a direct binding of Rv0678 to the intergenic region located between *mmpS5* and *Rv0678*. However, shifts were also found using the promoter regions of *mmpS2-mmpL2*, *mmpS4-mmpL4,* and *Rv0991-Rv0992* (Radhakrishnan et al., 2014), suggesting that a single regulator can control expression of several *mmpS/mmpL* loci. Our analysis indicates that, despite the fact that *M. abscessus* possesses the highest number of *mmpL* genes among all mycobacterial species studied (Viljoen et al., 2017), the MAB_4384 regulator is highly specific to the *mmpS5/mmpL5* pair as demonstrated by the lack of transcriptional regulation of a large set of *mmpL* genes and the presence of a unique inverted DNA sequence target that was not found elsewhere in the chromosome. This unique trait might also be reflected by the modest structural homology of MAB_4384 with other TetR crystal structures. The tight regulation and the high specificity of interaction with its target DNA, however, cannot be solely explained on the basis of the MAB_4384 crystal structure and the structure of the MAB_4384:DNA complex is, therefore, greatly warranted to dissect these underlying mechanisms. Nevertheless, our structural analysis underscores the strategy employed by *M. abscessus* to acquire mutations

impacting the DNA-binding capacity or the folding/stability of the DBD of MAB_4384 to become resistant.

EMSA and *lacZ* reporter fusions confirmed that D14N and F57L mutations, alleviating the DNA-binding activity of MAB_4384, cause a strong up-regulation of *mmpS5/mmpL5* gene expression, in agreement with our previous qRT-PCR analyses (Halloum et al., 2017). This leads to extrusion of the TAC derivatives out of the cells, contributing to the high MIC values for TAC derivatives against these mutants, as illustrated in **Figure 8**. Expression of multi-drug resistant efflux pumps can also be conditionally induced using structurally diverse substrates (Kaatz and Seo, 1995; Rosenberg et al., 2003; Buroni et al., 2006). This induction is caused by the direct interaction of these substrates with the repressors, interfering with binding of the repressors to their target operators and resulting in increased expression of the pumps. Here, we show inducible β-galactosidase activity following treatment with D6, D15, or D17, a mechanism that is very likely to be meditated by MAB_4384. This view is reinforced by the fact that docking studies highlighted the possibility that all three analogs could be accommodated in the LBD of the protein, which perfectly coincided with the extra electron density observed. Since, the LBD are remote from the DBD, the derepression of TetR family regulators involves allosteric mechanisms that include conformational changes transmitted largely within the same subunit (Ramos et al., 2005). The interaction of ligands with the LBD captures a conformational state where the DBD is repositioned relative to the LBD in a way that the dimer is prevented from binding to its target DNA. However, definitive proof of this mechanism awaits the elucidation of the crystal structure of the D17-bound form of MAB_4384, as reported for instance with the hexadecyl octanoate-bound EthR repressor (Frénois et al., 2004) or the LfrR regulator complexed with proflavine (Bellinzoni et al., 2009). Lack of inducible *lacZ* expression in *M. abscessus* cultures exposed to amikacin, for which mutations in 16S rRNA represent a major mechanism of resistance (Prammananan et al., 1998), indicates that MmpL5-mediated efflux cannot mediate resistance toward this antibiotic in line with the lack of cross-resistance toward amikacin observed for TAC derivative-spontaneous resistant mutants (Halloum et al., 2017). The specificity of the MAB_4384-driven resistance mechanism described herein is further supported by the lack of *lacZ* induction during exposure to ETH, that similarly to TAC and TAC analogs, requires bio-transformation by EthA, whose expression is also dependent on the EthR regulator belonging to the TetR family (Baulard et al., 2000; Engohang-Ndong et al., 2004; Halloum et al., 2017). Together, these findings strongly suggest that when TAC analogs bind to MAB_4384, the regulator loses affinity for its DNA target, resulting in up-regulation of *mmpS5/mmpL5* and export of the drugs from the cells **(Figure 8)**. These results also point out the selectivity of this efflux-based mechanism. Indeed, no change in the MIC of clofazimine or bedaquiline were noticed in a *MAB_4384*-disrupted strain, which appears intriguing as MmpL5 has been reported as a multi-substrate efflux pump responsible for low-level resistance to both of these drugs in *M. tuberculosis* (Hartkoorn et al., 2014). The LBD of MAB_4384 potentially can accommodate bulky molecules and might thus indicate that MAB_4384 is involved in efflux of other types of compounds in addition to TAC analogs. However, we could neither dock clofazimine nor bedaquiline in the LBD of MAB_4384 (not shown). Several reasons can be put forth to explain these species-specific variations. In *M. tuberculosis*, expression of MmpL5 is under the control of a MarR regulator rather than a TetR regulator. Alternatively, we have previously reported the occurrence in *M. abscessus* of three *mmpS5/mmpL5* paralogs (Halloum et al., 2017), thus, it remains possible that either of the two remaining genes may participate in co-resistance to these drugs in *M. abscessus*.

The highly pronounced expression of *lacZ* under derepressed conditions found in the M1A, F57L, or D14N mutant strains, almost at levels similar to those driven by the strong and constitutive *hsp60* promoter, confirmed the very high expression levels of *mmpS5* and *mmpL5* detected by qRT-PCR and probably explains the very high level of resistance of the mutants (MIC $>$ 200 μg/mL). This contrasts also with findings where MmpL5 mediates only low-levels of resistance in *M. tuberculosis* (Andries et al., 2014; Hartkoorn et al., 2014), presumably because expression of *mmpL5* is driven by a weaker promoter than in *M. abscessus*. That *mmpS5/mmpL5* expression is tightly controlled suggests that the MmpS5/MmpL5 machinery may exert an important function in the assembly and/or maintenance of the cell wall by exporting a yet unidentified lipid, as already reported for several MmpL transporters in *M. tuberculosis* (Chalut, 2016; Viljoen et al., 2017). Alternatively, they may participate in adaptation during the infection process. However, the growth curves of the wild-type or the strain constitutively expressing high levels of MmpL5 (due to the M1A mutation in MAB_4384) were comparable *in vitro*. In addition, microinjections of the different strains were done in the zebrafish embryo, an animal model previously developed to study the early events of the *M. abscessus* infection (Bernut et al., 2014, 2015). No differences in virulence were noticed between the wild-type and MAB_4384 (M1A) strains (Supplementary Figure S2). Interestingly, the *mmpS5/mmpL5* locus was found to be induced when *M. abscessus* was exposed to a defined, synthetic medium that mimics the composition of CF sputum (Miranda-CasoLuengo et al., 2016). This may be part of a complex adaptive transcriptional response to the mucus layer of the CF airways that leads to the chronic infections of *M. abscessus*.

In summary, this study provides new functional and structural insights into TetR-dependent regulation of MmpL efflux pumps in mycobacteria. Considering the exceptionally high abundance of TetR transcriptional regulators (more than 130) as well as the important MmpL repertoire (around 30) in *M. abscessus*, one can anticipate that mechanisms similar to the one described here are exploited by this pathogen to express its intrinsic resistance level to other antibiotics.

ETHICS STATEMENT

Zebrafish experiments were done at IRIM, according to European Union guidelines for handling of laboratory animals

(http://ec.europa.eu/environment/chemicals/lab_animals/home_en.htm) and approved by the Direction Sanitaire et Vétérinaire de l'Hérault and Comité d'Ethique pour l'Expérimentation Animale de la Région Languedoc Roussillon (CEEA-LR) under the reference CEEA-LR-1145.

AUTHOR CONTRIBUTIONS

MR, AVG, AV, MB, and LK acquired and analyzed the data. EG, MB, and LK wrote the manuscript. LK conceived and designed the study.

FUNDING

This work was supported by the Fondation pour la Recherche Médicale (FRM) (grant number DEQ20150331719 to LK; grant number ECO20160736031 to MR) and by the InfectioPôle Sud for funding the Ph.D. Fellowship of AVG.

ACKNOWLEDGMENTS

The authors wish to thank G. S. Coxon for the generous gift of the TAC analogs. The crystallographic data were collected on beamline ID30B at the European Synchrotron Radiation Facility (ESRF), Grenoble, France. The authors are grateful to Local Contact at the ESRF for providing assistance in using beamline ID30B.

SUPPLEMENTARY MATERIAL

The Supplementary Material for this article can be found online at: https://www.frontiersin.org/articles/10.3389/fmicb.2018.00649/full#supplementary-material

REFERENCES

Adams, P. D., Afonine, P. V., Bunkóczi, G., Chen, V. B., Davis, I. W., Echols, N., et al. (2010). *PHENIX*: a comprehensive Python-based system for macromolecular structure solution. *Acta Crystallogr. D Biol. Crystallogr.* 66, 213–221. doi: 10.1107/S0907444909052925

Agari, Y., Sakamoto, K., Kuramitsu, S., and Shinkai, A. (2012). Transcriptional repression mediated by a TetR family protein, PfmR, from *Thermus thermophilus* HB8. *J. Bacteriol.* 194, 4630–4641. doi: 10.1128/JB.00668-12.

Aiyar, A., Xiang, Y., and Leis, J. (1996). Site-directed mutagenesis using overlap extension PCR. *Methods Mol. Biol.* 57, 177–191. doi: 10.1385/0-89603-332-5:177

Andries, K., Villellas, C., Coeck, N., Thys, K., Gevers, T., Vranckx, L., et al. (2014). Acquired resistance of *Mycobacterium tuberculosis* to bedaquiline. *PLoS One* 9:e102135. doi: 10.1371/journal.pone.0102135

Bailey, T. L., Boden, M., Buske, F. A., Frith, M., Grant, C. E., Clementi, L., et al. (2009). MEME SUITE: tools for motif discovery and searching. *Nucleic Acids Res.* 37, W202–W208. doi: 10.1093/nar/gkp335

Balhana, R. J. C., Singla, A., Sikder, M. H., Withers, M., and Kendall, S. L. (2015). Global analyses of TetR family transcriptional regulators in mycobacteria indicates conservation across species and diversity in regulated functions. *BMC Genomics* 16:479. doi: 10.1186/s12864-015-1696-9

Baulard, A. R., Betts, J. C., Engohang-Ndong, J., Quan, S., McAdam, R. A., Brennan, P. J., et al. (2000). Activation of the pro-drug ethionamide is regulated in mycobacteria. *J. Biol. Chem.* 275, 28326–28331. doi: 10.1074/jbc.M003744200

Bellinzoni, M., Buroni, S., Schaeffer, F., Riccardi, G., De Rossi, E., and Alzari, P. M. (2009). Structural plasticity and distinct drug-binding modes of LfrR, a mycobacterial efflux pump regulator. *J. Bacteriol.* 191, 7531–7537. doi: 10.1128/JB.00631-09

Bernut, A., Dupont, C., Sahuquet, A., Herrmann, J.-L., Lutfalla, G., and Kremer, L. (2015). Deciphering and imaging pathogenesis and cording of *Mycobacterium abscessus* in zebrafish embryos. *J. Vis. Exp.* 103:53130. doi: 10.3791/53130

Bernut, A., Herrmann, J.-L., Kissa, K., Dubremetz, J.-F., Gaillard, J.-L., Lutfalla, G., et al. (2014). *Mycobacterium abscessus* cording prevents phagocytosis and promotes abscess formation. *Proc. Natl. Acad. Sci. U.S.A.* 111, E943–E952. doi: 10.1073/pnas.1321390111

Bhukya, H., Bhujbalrao, R., Bitra, A., and Anand, R. (2014). Structural and functional basis of transcriptional regulation by TetR family protein CprB from *S. coelicolor* A3(2). *Nucleic Acids Res.* 42, 10122–10133. doi: 10.1093/nar/gku587

Bryant, J. M., Grogono, D. M., Rodriguez-Rincon, D., Everall, I., Brown, K. P., Moreno, P., et al. (2016). Emergence and spread of a human-transmissible multidrug-resistant nontuberculous mycobacterium. *Science* 354, 751–757. doi: 10.1126/science.aaf8156

Buroni, S., Manina, G., Guglierame, P., Pasca, M. R., Riccardi, G., and De Rossi, E. (2006). LfrR is a repressor that regulates expression of the efflux pump LfrA in *Mycobacterium smegmatis*. *Antimicrob. Agents Chemother.* 50, 4044–4052. doi: 10.1128/AAC.00656-06

Chalut, C. (2016). MmpL transporter-mediated export of cell-wall associated lipids and siderophores in mycobacteria. *Tuberclosis* 100, 32–45. doi: 10.1016/j.tube.2016.06.004

Coxon, G. D., Craig, D., Corrales, R. M., Vialla, E., Gannoun-Zaki, L., and Kremer, L. (2013). Synthesis, antitubercular activity and mechanism of resistance of highly effective thiacetazone analogues. *PLoS One* 8:e53162. doi: 10.1371/journal.pone.0053162

Cuthbertson, L., and Nodwell, J. R. (2013). The TetR family of regulators. *Microbiol. Mol. Biol. Rev.* 77, 440–475. doi: 10.1128/MMBR.00018-13

Dal Molin, M., Gut, M., Rominski, A., Haldimann, K., Becker, K., and Sander, P. (2018). Molecular mechanisms of intrinsic streptomycin resistance in *Mycobacterium abscessus*. *Antimicrob. Agents Chemother.* 62:e01427-17. doi: 10.1128/AAC.01427-17

Dallakyan, S., and Olson, A. J. (2015). Small-molecule library screening by docking with PyRx. *Methods Mol. Biol.* 1263, 243–250. doi: 10.1007/978-1-4939-2269-7_19

DeBarber, A. E., Mdluli, K., Bosman, M., Bekker, L. G., and Barry, C. E. (2000). Ethionamide activation and sensitivity in multidrug-resistant *Mycobacterium tuberculosis*. *Proc. Natl. Acad. Sci. U.S.A.* 97, 9677–9682. doi: 10.1073/pnas.97.17.9677

Dover, L. G., Alahari, A., Gratraud, P., Gomes, J. M., Bhowruth, V., Reynolds, R. C., et al. (2007). EthA, a common activator of thiocarbamide-containing drugs acting on different mycobacterial targets. *Antimicrob. Agents Chemother.* 51, 1055–1063. doi: 10.1128/AAC.01063-06

Dubée, V., Bernut, A., Cortes, M., Lesne, T., Dorchene, D., Lefebvre, A.-L., et al. (2015). β-Lactamase inhibition by avibactam in *Mycobacterium abscessus*. *J. Antimicrob. Chemother.* 70, 1051–1058. doi: 10.1093/jac/dku510

Emsley, P., Lohkamp, B., Scott, W. G., and Cowtan, K. (2010). Features and development of coot. *Acta Crystallogr. D Biol. Crystallogr.* 66, 486–501. doi: 10.1107/S0907444910007493

Engohang-Ndong, J., Baillat, D., Aumercier, M., Bellefontaine, F., Besra, G. S., Locht, C., et al. (2004). EthR, a repressor of the TetR/CamR family implicated in ethionamide resistance in mycobacteria, octamerizes cooperatively on its operator. *Mol. Microbiol.* 51, 175–188. doi: 10.1046/j.1365-2958.2003.03809.x

Esther, C. R., Esserman, D. A., Gilligan, P., Kerr, A., and Noone, P. G. (2010). Chronic *Mycobacterium abscessus* infection and lung function decline

in cystic fibrosis. *J. Cyst. Fibros.* 9, 117–123. doi: 10.1016/j.jcf.2009.12.0001

Frénois, F., Engohang-Ndong, J., Locht, C., Baulard, A. R., and Villeret, V. (2004). Structure of EthR in a ligand bound conformation reveals therapeutic perspectives against tuberculosis. *Mol. Cell* 16, 301–307. doi: 10.1016/j.molcel.2004.09.020

Grkovic, S., Brown, M. H., Schumacher, M. A., Brennan, R. G., and Skurray, R. A. (2001). The staphylococcal QacR multidrug regulator binds a correctly spaced operator as a pair of dimers. *J. Bacteriol.* 183, 7102–7109. doi: 10.1128/JB.183.24.7102-7109.2001

Halloum, I., Viljoen, A., Khanna, V., Craig, D., Bouchier, C., Brosch, R., et al. (2017). Resistance to thiacetazone derivatives active against *Mycobacterium abscessus* involves mutations in the MmpL5 transcriptional repressor MAB_4384. *Antimicrob. Agents Chemother.* 61:11e01225-17. doi: 10.1128/AAC.02509-16

Hartkoorn, R. C., Uplekar, S., and Cole, S. T. (2014). Cross-resistance between clofazimine and bedaquiline through upregulation of MmpL5 in *Mycobacterium tuberculosis*. *Antimicrob. Agents Chemother.* 58, 2979–2981. doi: 10.1128/AAC.00037-14

Hillen, W., and Berens, C. (1994). Mechanisms underlying expression of Tn10 encoded tetracycline resistance. *Annu. Rev. Microbiol.* 48, 345–369. doi: 10.1146/annurev.mi.48.100194.002021

Hurst-Hess, K., Rudra, P., and Ghosh, P. (2017). *Mycobacterium abscessus* WhiB7 regulates a species-specific repertoire of genes to confer extreme antibiotic resistance. *Antimicrob. Agents Chemother.* 61:e01347-17. doi: 10.1128/AAC.01347-17

Itou, H., Watanabe, N., Yao, M., Shirakihara, Y., and Tanaka, I. (2010). Crystal structures of the multidrug binding repressor *Corynebacterium glutamicum* CgmR in complex with inducers and with an operator. *J. Mol. Biol.* 403, 174–184. doi: 10.1016/j.jmb.2010.07.042

Kaatz, G. W., and Seo, S. M. (1995). Inducible NorA-mediated multidrug resistance in *Staphylococcus aureus*. *Antimicrob. Agents Chemother.* 39, 2650–2655. doi: 10.1128/AAC.39.12.2650

Kabsch, W. (2010). Integration, scaling, space-group assignment and post-refinement. *Acta Crystallogr. D Biol. Crystallogr.* 66, 133–144. doi: 10.1107/S0907444909047374

Krissinel, E., and Henrick, K. (2007). Inference of macromolecular assemblies from crystalline state. *J. Mol. Biol.* 372, 774–797. doi: 10.1016/j.jmb.2007.05.022

Lederer, T., Takahashi, M., and Hillen, W. (1995). Thermodynamic analysis of tetracycline-mediated induction of Tet repressor by a quantitative methylation protection assay. *Anal. Biochem.* 232, 190–196. doi: 10.1006/abio.1995.0006

Lefebvre, A.-L., Dubée, V., Cortes, M., Dorchêne, D., Arthur, M., and Mainardi, J.-L. (2016). Bactericidal and intracellular activity of β-lactams against *Mycobacterium abscessus*. *J. Antimicrob. Chemother.* 71, 1556–1563. doi: 10.1093/jac/dkw022

Lefebvre, A.-L., Le Moigne, V., Bernut, A., Veckerlé, C., Compain, F., Herrmann, J.-L., et al. (2017). Inhibition of the β-lactamase BlaMab by avibactam improves the *in vitro* and *in vivo* efficacy of imipenem against *Mycobacterium abscessus*. *Antimicrob. Agents Chemother.* 61:e02440-16. doi: 10.1128/AAC.02440-16

McCoy, A. J., Grosse-Kunstleve, R. W., Adams, P. D., Winn, M. D., Storoni, L. C., and Read, R. J. (2007). *Phaser* crystallographic software. *J. Appl. Crystallogr.* 40, 658–674. doi: 10.1107/S0021889807021206

Milano, A., Pasca, M. R., Provvedi, R., Lucarelli, A. P., Manina, G., Ribeiro, A. L., et al. (2009). Azole resistance in *Mycobacterium tuberculosis* is mediated by the MmpS5-MmpL5 efflux system. *Tuberclosis* 89, 84–90. doi: 10.1016/j.tube.2008.08.003

Miranda-CasoLuengo, A. A., Staunton, P. M., Dinan, A. M., Lohan, A. J., and Loftus, B. J. (2016). Functional characterization of the *Mycobacterium abscessus* genome coupled with condition specific transcriptomics reveals conserved molecular strategies for host adaptation and persistence. *BMC Genomics* 17:553. doi: 10.1186/s12864-016-2868-y

Mougari, F., Guglielmetti, L., Raskine, L., Sermet-Gaudelus, I., Veziris, N., and Cambau, E. (2016). Infections caused by *Mycobacterium abscessus*: epidemiology, diagnostic tools and treatment. *Expert Rev. Anti Infect. Ther.* 14, 1139–1154. doi: 10.1080/14787210.2016.1238304

Nash, K. A., Brown-Elliott, B. A., and Wallace, R. J. (2009). A novel gene, *erm(41)*, confers inducible macrolide resistance to clinical isolates of *Mycobacterium abscessus* but is absent from *Mycobacterium chelonae*. *Antimicrob. Agents Chemother.* 53, 1367–1376. doi: 10.1128/AAC.01275-08

Nessar, R., Cambau, E., Reyrat, J. M., Murray, A., and Gicquel, B. (2012). *Mycobacterium abscessus*: a new antibiotic nightmare. *J. Antimicrob. Chemother.* 67, 810–818. doi: 10.1093/jac/dkr578

Orth, P., Schnappinger, D., Hillen, W., Saenger, W., and Hinrichs, W. (2000). Structural basis of gene regulation by the tetracycline inducible Tet repressor-operator system. *Nat. Struct. Biol.* 7, 215–219. doi: 10.1038/73324

Prammananan, T., Sander, P., Brown, B. A., Frischkorn, K., Onyi, G. O., Zhang, Y., et al. (1998). A single 16S ribosomal RNA substitution is responsible for resistance to amikacin and other 2-deoxystreptamine aminoglycosides in *Mycobacterium abscessus* and *Mycobacterium chelonae*. *J. Infect. Dis.* 177, 1573–1581. doi: 10.1086/515328

Radhakrishnan, A., Kumar, N., Wright, C. C., Chou, T.-H., Tringides, M. L., Bolla, J. R., et al. (2014). Crystal structure of the transcriptional regulator Rv0678 of *Mycobacterium tuberculosis*. *J. Biol. Chem.* 289, 16526–16540. doi: 10.1074/jbc.M113.538959

Ramos, J. L., Martínez-Bueno, M., Molina-Henares, A. J., Terán, W., Watanabe, K., Zhang, X., et al. (2005). The TetR family of transcriptional repressors. *Microbiol. Mol. Biol. Rev.* 69, 326–356. doi: 10.1128/MMBR.69.2.326-356.2005

Rominski, A., Roditscheff, A., Selchow, P., Böttger, E. C., and Sander, P. (2017a). Intrinsic rifamycin resistance of *Mycobacterium abscessus* is mediated by ADP-ribosyltransferase MAB_0591. *J. Antimicrob. Chemother.* 72, 376–384. doi: 10.1093/jac/dkw466

Rominski, A., Selchow, P., Becker, K., Brülle, J. K., Dal Molin, M., and Sander, P. (2017b). Elucidation of *Mycobacterium abscessus* aminoglycoside and capreomycin resistance by targeted deletion of three putative resistance genes. *J. Antimicrob. Chemother.* 72, 2191–2200. doi: 10.1093/jac/dkx125

Rosenberg, E. Y., Bertenthal, D., Nilles, M. L., Bertrand, K. P., and Nikaido, H. (2003). Bile salts and fatty acids induce the expression of *Escherichia coli* AcrAB multidrug efflux pump through their interaction with Rob regulatory protein. *Mol. Microbiol.* 48, 1609–1619. doi: 10.1046/j.1365-2958.2003.03531.x

Schumacher, M. A., Miller, M. C., Grkovic, S., Brown, M. H., Skurray, R. A., and Brennan, R. G. (2002). Structural basis for cooperative DNA binding by two dimers of the multidrug-binding protein QacR. *EMBO J.* 21, 1210–1218. doi: 10.1093/emboj/21.5.1210

Smibert, O., Snell, G. I., Bills, H., Westall, G. P., and Morrissey, C. O. (2016). *Mycobacterium abscessus* complex - a particular challenge in the setting of lung transplantation. *Expert Rev. Anti Infect. Ther.* 14, 325–333. doi: 10.1586/14787210.2016.1138856

Takiff, H. E., Cimino, M., Musso, M. C., Weisbrod, T., Martinez, R., Delgado, M. B., et al. (1996). Efflux pump of the proton antiporter family confers low-level fluoroquinolone resistance in *Mycobacterium smegmatis*. *Proc. Natl. Acad. Sci. U.S.A.* 93, 362–366. doi: 10.1073/pnas.93.1.362

Trott, O., and Olson, A. J. (2010). AutoDock Vina: improving the speed and accuracy of docking with a new scoring function, efficient optimization, and multithreading. *J. Comput. Chem.* 31, 455–461. doi: 10.1002/jcc.21334

van Dorn, A. (2017). Multidrug-resistant *Mycobacterium abscessus* threatens patients with cystic fibrosis. *Lancet Respir. Med.* 5:15. doi: 10.1016/S2213-2600(16)30444-1

Viljoen, A., Blaise, M., de Chastellier, C., and Kremer, L. (2016). MAB_3551c encodes the primary triacylglycerol synthase involved in lipid accumulation in *Mycobacterium abscessus*. *Mol. Microbiol.* 102, 611–627. doi: 10.1111/mmi.13482

Viljoen, A., Dubois, V., Girard-Misguich, F., Blaise, M., Herrmann, J.-L., and Kremer, L. (2017). The diverse family of MmpL transporters in mycobacteria: from regulation to antimicrobial developments. *Mol. Microbiol.* 104, 889–904. doi: 10.1111/mmi.13675

Viljoen, A., Gutiérrez, A. V., Dupont, C., Ghigo, E., and Kremer, L. (2018). A simple and rapid gene disruption strategy in *Mycobacterium abscessus*: on the design and application of glycopeptidolipid mutants. *Front. Cell. Infect. Microbiol.* 8:69. doi: 10.3389/fcimb.2018.00069

Woods, G. L., Brown-Elliott, B. A., Conville, P. S., Desmond, E. P., Hall, G. S., Lin, G., et al. (2011). *Susceptibility Testing of Mycobacteria, Nocardiae and Other Aerobic Actinomycetes: Approved Standard*, 2nd Edn. Wayne, PA: Clinical and Laboratory Standards Institute.

Yang, S., Gao, Z., Li, T., Yang, M., Zhang, T., Dong, Y., et al. (2013). Structural basis for interaction between *Mycobacterium smegmatis* Ms6564, a TetR family master regulator, and its target DNA. *J. Biol. Chem.* 288, 23687–23695. doi: 10.1074/jbc.M113.468694

Zhang, S., Chen, J., Cui, P., Shi, W., Zhang, W., and Zhang, Y. (2015). Identification of novel mutations associated with clofazimine resistance in *Mycobacterium tuberculosis*. *J. Antimicrob. Chemother.* 70, 2507–2510. doi: 10.1093/jac/dkv150

Conflict of Interest Statement: The authors declare that the research was conducted in the absence of any commercial or financial relationships that could be construed as a potential conflict of interest.

CHAPTER IV

Study of *Mycobacterium abscessus* resistance mechanism by the TetR-MmpL system

Mutations in the MAB_2299c TetR regulator confer cross-resistance to clofazimine and bedaquiline in *Mycobacterium abscessus*.

Richard, M., Gutiérrez, A.V., Viljoen, A., Rodriguez-Rincon, D., Roquet-Baneres, F., Blaise, M., Everall, I., Parkhill, J., Floto, R.A. and Kremer, L.

Antimicrobial agents and chemotherapy, 63(1), pp.e01316-18.

7. CHAPTER IV: Study of *Mycobacterium abscessus* resistance mechanism by the TetR-MmpL system

7.2. Article 2: Mutations in the MAB_2299c TetR regulator confer cross-resistance to clofazimine and bedaquiline in *Mycobacterium abscessus.*

The efficacy of current recommended treatments for the *M. abscessus* complex is debatable according to different epidemiological studies. Moreover, *M. abscessus sensu stricto* was reported as the species with the highest relapse rates among the *M. abscessus* complex subspecies (van Ingen et al. 2013). Therefore, new therapeutic approaches are needed to shorten the duration of treatment. Novel therapeutic strategies rely on the development of new chemical entities and the repositioning of known drugs (Wu et al. 2018).

Clofazimine is a riminophcnazine dye (2-/)-chloranilino-5-/)-chlorophenyl-3: 5-dihydro-3-isopropyliminophenazine) that was initially designed for the treatment of *M. tuberculosis* (Barry et al. 1957). Despite the antitubercular success of this red dye in murine models, it was not use to treat human TB (Silva et al. 2018) but was used for the treatment of leprosy (McDOUGALL et al. 1980; Garrelts 1991). Clofazimine targets type II NADH-quinone oxidoreductase, an important element in the electron transport chain by competing for electrons with menaquinone (Yano et al. 2011). Additional mechanisms are proposed for its antimycobacterial activity that involve membrane disruption and compromise of ATPase activity. Due to the cationic amphiphilic nature of this drug, a multitargeted function could explain the low level of resistance to this drug (Cholo et al. 2017). The main mutation associated with clofazimine resistance in *M. tuberculosis* is found in *Rv0678* that encodes the MarR transcriptional regulator of *mmpS5-mmpL5*. Additional mutations were also found in *Rv2535c,* encoding a putative PepQ peptidase and in *Rv1979c* encoding a permease possibly involved in amino acid transport (Zhang et al. 2015). The clinical success of clofazimine for infections caused by the *M. avium* complex draws attention to the future potential of this drug

to treat other NTM. To date, several clinical studies have reported the success in the introduction of clofazimine for the treatment of *M. abscessus* pulmonary disease (Wu et al. 2018).

The new antitubercular drug, bedaquiline, 1-(6-bromo-2-methoxy-quinolin-3- yl)-4-dimethylamino-2-naphthalen-1-yl-1- phenyl-butan-2-ol is a diarylquinoline approved by the United States Food and Drug Administration and the European Medicines Agency for the treatment of multidrug-resistant TB (Wolfson et al. 2015). The mode of action of this drug points to the interruption of H^+ transfer and subsequent impairment of ATP production, by joining the subunit C of the mitochondrial adenosine triphosphate synthase encoded by *atpE* (Andries et al. 2005). Mutations in this gene have been associated with resistance to bedaquiline in *M. tuberculosis* (Segala et al. 2012). In addition, bedaquiline shares cross-resistance with clofazimine though mutations in *Rv0678* and *Rv2535c* (T. V. A. Nguyen et al. 2018). Bedaquiline is a promising alternative to be included in the treatment of *M. abscessus* and other NTM infections although it exerts bacteriostatic activity *in vitro* and *in vivo* (Lounis et al. 2009; Lerat et al. 2014; Dupont et al. 2017). The combined treatment of clofazimine/bedaquiline has shown a synergistic interaction against *M. abscessus*. However, special attention should be given to this dual therapy, as it could promote the emergence of resistance to bedaquiline (Ruth et al. 2019).

With the current need to include more efficient treatments and the availability of clofazimine and bedaquiline as new alternatives, we were interested in describing the mechanisms of resistance to clofazimine. Six clofazimine resistant mutants were generated *in vitro*. WGS allowed to identify mutations in *MAB_2299c* in all 6 resistors. *MAB_2299c* encodes a putative TetR regulator adjacent to two pairs of genes that encode the putative *mmpS/mmpL* transporters, *MAB_2300-MAB_2301* and *MAB_2302-MAB_2303*. All six clofazimine-resistant mutants were cross-resistant to bedaquiline. Moreover, the DNA-binding target that contains two palindromic motifs was identified thanks to bioinformatics

tools and EMSA were performed to evaluate the formation of DNA-protein complex. The results obtained clearly indicated that MAB_2299c was involved in the overexpression of the efflux pump system MAB_2300-MAB_2301 but not MAB_2302-MAB_2303.

In addition, the genetic tool to generate mutants using a two-step homologous recombination system based on our previous suicide plasmid that carries *tdTomato* as positive selection marker (Viljoen et al. 2018) was improved by adding *katG* as a counter-selection marker. This technique allowed to generate an unmarked deletion of *MAB_2299c* and subsequently confirm its participation in cross-resistance to clofazimine/bedaquiline as a consequence of up-regulation of the MAB_2300-MAB_2301 efflux pump system.

In conclusion, we demonstrated the implication of MAB_2299c in the repression of the efflux pump system MAB_2300-MAB_2301 and its contribution in the cross-resistance to clofazimine and bedaquiline.

AMERICAN SOCIETY FOR MICROBIOLOGY | Antimicrobial Agents and Chemotherapy®

Mutations in the MAB_2299c TetR Regulator Confer Cross-Resistance to Clofazimine and Bedaquiline in *Mycobacterium abscessus*

Matthias Richard,[a] Ana Victoria Gutiérrez,[a,c] Albertus Viljoen,[a] Daniela Rodriguez-Rincon,[d] Françoise Roquet-Baneres,[a] Mickael Blaise,[a] Isobel Everall,[e] Julian Parkhill,[e] R. Andres Floto,[d] Laurent Kremer[a,b]

[a]Institut de Recherche en Infectiologie de Montpellier (IRIM), Université de Montpellier, CNRS UMR 9004, Montpellier, France
[b]INSERM, IRIM, Montpellier, France
[c]Unité de Recherche Microbes, Evolution, Phylogeny and Infection (MEPHI), Institut Hospitalier Universitaire Méditerranée-Infection, Marseille, France
[d]Molecular Immunity Unit, Department of Medicine, University of Cambridge, MRC Laboratory of Molecular Biology, Cambridge, United Kingdom
[e]Wellcome Trust Sanger Institute, Hinxton, United Kingdom

ABSTRACT New therapeutic approaches are needed against *Mycobacterium abscessus*, a respiratory mycobacterial pathogen that evades efforts to successfully treat infected patients. Clofazimine and bedaquiline, two drugs used for the treatment of multidrug-resistant tuberculosis, are being considered as alternatives for the treatment of lung diseases caused by *M. abscessus*. With the aim to understand the mechanism of action of these agents in *M. abscessus*, we sought herein to determine the means by which *M. abscessus* can develop resistance. Spontaneous resistant strains selected on clofazimine, followed by whole-genome sequencing, identified mutations in *MAB_2299c*, encoding a putative TetR transcriptional regulator. Unexpectedly, mutants with these mutations were also cross-resistant to bedaquiline. MAB_2299c was found to bind to its target DNA, located upstream of the divergently oriented *MAB_2300-MAB_2301* gene cluster, encoding MmpS/MmpL membrane proteins. Point mutations or deletion of *MAB_2299c* was associated with the concomitant upregulation of the *mmpS* and *mmpL* transcripts and accounted for this cross-resistance. Strikingly, deletion of *MAB_2300* and *MAB_2301* in the *MAB_2299c* mutant strain restored susceptibility to bedaquiline and clofazimine. Overall, these results expand our knowledge with respect to the regulatory mechanisms of the MmpL family of proteins and a novel mechanism of drug resistance in this difficult-to-treat respiratory mycobacterial pathogen. Therefore, *MAB_2299c* may represent an important marker of resistance to be considered in the treatment of *M. abscessus* diseases with clofazimine and bedaquiline in clinical settings.

KEYWORDS EMSA, MmpL, *Mycobacterium abscessus*, TetR regulator, bedaquiline, clofazimine, drug resistance mechanisms, efflux pumps

Mycobacterium abscessus is an emerging nontuberculous mycobacterium (NTM) commonly associated with contaminated traumatic skin wounds or postsurgical soft tissue infections (1). Among the rapid growers, *M. abscessus* also represents the most frequently isolated species in cystic fibrosis (CF) patients, with a prevalence of 3% to 6% in this population (2), or in patients with other underlying lung disorders, such as non-CF bronchiectasis and chronic obstructive pulmonary disease (COPD), resulting in nodular and cavitary granulomas and persistent lung infection (3–6). CF patients with chronic *M. abscessus* infection have higher rates of lung function decline than those with no NTM infections (7). Recent surveys have identified *M. abscessus* to be a major threat in many CF centers worldwide (5), and this alarming situation is worsened by

Citation Richard M, Gutiérrez AV, Viljoen A, Rodriguez-Rincon D, Roquet-Baneres F, Blaise M, Everall I, Parkhill J, Floto RA, Kremer L. 2019. Mutations in the MAB_2299c TetR regulator confer cross-resistance to clofazimine and bedaquiline in *Mycobacterium abscessus*. Antimicrob Agents Chemother 63:e01316-18. https://doi.org/10.1128/AAC.01316-18.

Address correspondence to Laurent Kremer, laurent.kremer@irim.cnrs.fr.

M.R. and A.V.G. contributed equally to this article.

Received 20 June 2018
Returned for modification 3 August 2018
Accepted 9 October 2018
Accepted manuscript posted online 15 October 2018
Published 21 December 2018

epidemiological studies documenting the transmission of dominant circulating *M. abscessus* clones that have spread globally between hospitals (8). In addition, lung infections caused by *M. abscessus* remain extremely difficult to treat, mainly because of its natural resistance to most currently available antibiotics (9). The prognosis of pulmonary infections is poor, particularly in the context of CF, with a cure rate of 30% to 50%, in spite of lengthy courses of antibiotics often complemented by surgery (10). In contrast to many other NTM infections, antibiotherapy against *M. abscessus* often fails, leading to lasting sputum culture positivity, and no antibiotic regimen reliably cures these infections (3, 11–14).

There is an important medical need to discover and develop more efficient and safer treatments to fight against *M. abscessus*. The proposed strategy for fueling a drug pipeline can rely on (i) *de novo* drug discovery to identify new pharmacophores and targets, (ii) repurposing of known drugs as new treatments of *M. abscessus* infections, or (iii) the repositioning of antibiotics that act against pharmacologically validated targets but that have been developed for the treatment of other infectious diseases (15). Among the repositioned drugs over which there is increasing interest, clofazimine (CFZ) and bedaquiline (BDQ) are currently being evaluated in clinical trials for their activities against *M. abscessus* pulmonary infections.

The riminophenazine clofazimine (CFZ) is a lipophilic agent with cationic amphiphilic properties used as an antileprosy drug and currently repurposed as an antituberculosis (anti-TB) drug (16). CFZ also has unique characteristics, such as a slow metabolic elimination, preferential accumulation inside macrophages, and a low incidence of drug resistance (16). In *M. tuberculosis*, CFZ acts as a prodrug which is reduced by the NADH dehydrogenase (Ndh2) and, upon spontaneous reoxidation by O_2, releases reactive oxygen species (ROS) (17), explaining why high levels of resistance to CFZ are rare. Due to the recent widespread emergence of *M. abscessus*, there has been a renewed interest in the repurposing of CFZ for the treatment of *M. abscessus* infections. *In vitro* studies reported the efficacy of CFZ in multidrug regimens for the treatment of *M. abscessus* infections, in which it showed synergistic activity with amikacin (18) or tigecycline (19). CFZ was also found to prevent the regrowth of *M. abscessus* exposed to clarithromycin and amikacin (13). Although CFZ has increasingly been used in the treatment of lung diseases in clinical practice (10, 20), only limited data on its effectiveness are available. In one study, CFZ was found to be safe, reasonably tolerated, and active when given orally for the treatment of NTM infections, including *M. abscessus* infections, and was proposed to be an alternative drug for the treatment of NTM diseases (21). In another study, CFZ-containing regimens also showed improved treatment outcomes in patients with pulmonary diseases due to *M. abscessus* (22).

BDQ is a diarylquinoline antibiotic that has been approved by the Food and Drug Administration and the European Medicines Agency for the treatment of multidrug-resistant tuberculosis (MDR-TB) (23). BDQ acts by targeting the c subunit of the essential F_oF_1 ATP synthase (24–27), and studies have also proposed that it may inhibit the ATP synthase via another mechanism involving the ε subunit of the enzyme, in addition to binding to its c subunit (28, 29). BDQ exhibits very low MICs against various NTM, including *M. abscessus* clinical isolates from CF and non-CF patients (27, 30, 31), but despite being an excellent growth inhibitor at low doses, it lacks bactericidal activity against *M. abscessus* (27). Studies in immunocompromised mouse models led to conflictual conclusions, reporting, on the one hand, a benefit of BDQ in reducing bacterial loads in gamma interferon knockout mice (32) and, on the other hand, no decrease in the bacillary loads in the lungs or an inability to prevent death in nude mice (33). However, BDQ is highly efficient in reducing pathophysiological signs, such as abscesses and cords in *M. abscessus*-infected zebrafish, and in protecting zebrafish larvae from death (27). The mode of action of BDQ in *M. abscessus* relies on rapid ATP depletion and was demonstrated by genetically transferring single point mutations into *atpE*, which conferred high levels of resistance to the drug (27). Preliminary results of studies using BDQ as salvage therapy for pulmonary infections with *M. avium* or *M. abscessus* suggested that BDQ has clinical activity but its efficacy appears to be

TABLE 1 Drug susceptibility profiles and genotypes of 6 spontaneous CFZ-resistant *M. abscessus* strains[a]

Strain	MIC_{99} (μg/ml)			Mutation in *MAB_2299c*	
	CFZ	BDQ	AMK	SNP/indel	Amino acid change
Wild type	4	0.5	8		
CFZ-R1	8	2	8	T119G	L40W
CFZ-R3	8	2	8	C276del	P92fs
CFZ-R4	8	2	8	G541T	E181stop
CFZ-R6	8	2	8	ins318A	D106fs
CFZ-R7	8	2	8	T452C	L151P
CFZ-R9	8	2	8	G643A	G215S

[a]The mutants were derived from the ATCC 199177 S parental strain and selected in the presence of CFZ. MIC_{99} values were determined on Middlebrook 7H10 agar. Single nucleotide polymorphisms (SNP) and/or indels were identified in *MAB_2299c*. The corresponding amino acid changes are also indicated. CFZ, clofazimine; BDQ, bedaquiline; AMK, amikacin; del, deletion; ins, insertion; fs, frameshift.

relatively moderate, as suggested by a low sputum culture conversion rate (34). Therefore, the clinical utility of BDQ against *M. abscessus* infections requires more studies.

To further delineate the mechanism of action of CFZ and BDQ in *M. abscessus*, we sought to determine how *M. abscessus* develops resistance to these agents. Herein, mutations were identified in a new TetR regulator, MAB_2299c. These mutations were associated with low levels of resistance to both CFZ and BDQ. Genetic and biochemical analyses were applied to determine the specificity of this regulatory system in *M. abscessus* and to describe the contribution of a key residue important in driving the DNA-binding activity of MAB_2299c to its operator. The results expand our knowledge with respect to the regulatory mechanisms of the MmpL family of efflux pumps and on a novel mechanism of drug resistance in *M. abscessus*.

RESULTS

Mutations in *MAB_2299c* confer coresistance to CFZ and BDQ. With the aim of identifying the mechanism of resistance to CFZ in *M. abscessus*, 6 spontaneous CFZ-resistant mutants were first reared in passages of the reference *M. abscessus* ATCC 19977 S strain in liquid medium containing increasing concentrations of CFZ and then isolated on solid 7H11 medium supplemented with oleic acid-albumin-dextrose-catalase (OADC) ($7H11^{OADC}$ medium). All 6 resistors exhibited low resistance levels (MIC, 8 μg/ml) compared to the resistance level of the parental strain (MIC, 4 μg/ml) (Table 1). Spontaneous resistant mutants arose at a frequency of $\approx 2 \times 10^{-7}$. Whole-genome sequencing identified mutations in the *MAB_2299c* locus in all 6 mutants, which were subsequently confirmed by PCR amplification and Sanger sequencing. This approach identified single nucleotide polymorphisms (SNP) in mutants CFZ-R1 (L40W replacement), CFZ-R4 (stop codon), CFZ-R7 (L151P replacement), and CFZ-R9 (G215S replacement), as well as a single nucleotide deletion in CFZ-R3 or a single nucleotide insertion in CFZ-R6 leading to frameshift mutations (Table 1). These observations converge to a prominent role of MAB_2299c in the CFZ resistance phenotype. Interestingly, all 6 CFZ-resistant mutants were also coresistant to BDQ with MIC levels of 2 μg/ml, corresponding to a 4-fold increased MIC compared to that for the parental strain (Table 1). In contrast, all mutants remained susceptible to amikacin (AMK). These results imply that mutations in *MAB_2299c* confer cross-resistance to CFZ and BDQ but not to AMK, pointing out a unique resistance mechanism.

***MAB_2299c* encodes a TetR repressor controlling expression of a specific MmpS/MmpL pair.** Sequence alignments and BLAST analyses indicated that *MAB_2299c* encodes a putative TetR transcriptional regulator. TetR family members possess a conserved N-terminal helix-turn-helix (HTH) DNA-binding domain and a C-terminal ligand regulatory domain and are commonly associated with antibiotic resistance by regulating expression of genes coding for multidrug resistance efflux pumps (35). Interestingly, the two gene pairs (*MAB_2300-MAB_2301* and *MAB_2302-MAB_2303*)

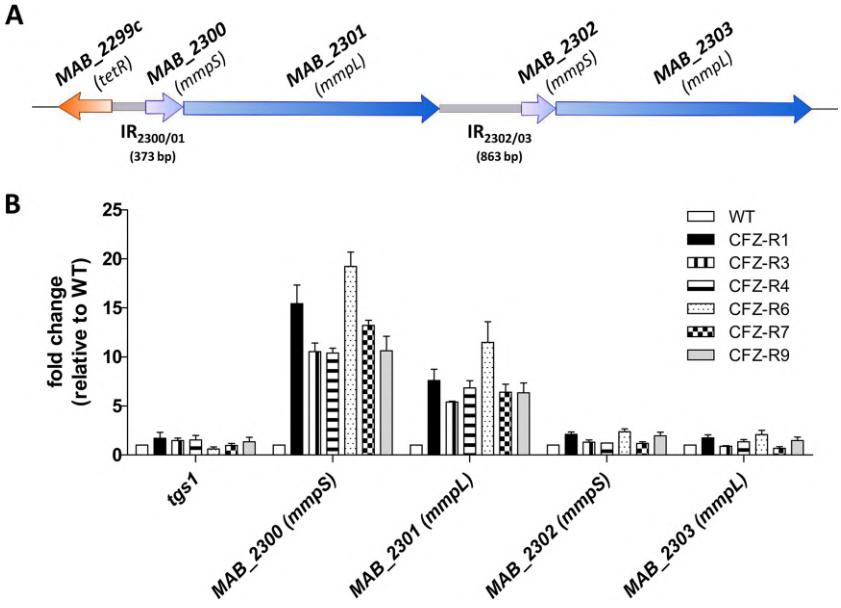

FIG 1 *MAB_2299c* regulates expression of the *MAB_2300-MAB_2301* locus. (A) Schematic representation of the genetic environment of *MAB_2299c* and its two adjacent *mmpS-mmpL* gene pairs (*MAB_2300-MAB_2301* and *MAB_2302-MAB_2303*). The sizes and positions of the two intergenic regions ($IR_{2300/01}$ and $IR_{2302/03}$) are indicated. (B) Transcriptional expression of the *MAB_2300-MAB_2303* genes in the parental *M. abscessus* strain and in 6 spontaneous CFZ-resistant mutants harboring mutations in *MAB_2299c*. The results are expressed as the fold change in mRNA levels between the mutant strains and the parental strain. Error bars indicate the standard deviation. Relative gene expression was calculated using the $2^{-\Delta\Delta CT}$ threshold cycle (C_T) method with PCR efficiency correction. The data are representative of those from three independent experiments.

adjacent to *MAB_2299c* and transcribed in the opposite direction code for MmpS (*MAB_2300* and *MAB_2302*) and MmpL (*MAB_2301* and *MAB_2303*) integral membrane proteins (Fig. 1). MmpL proteins are part of the superfamily of resistance, nodulation, and division (RND) transporters and were reported to act as efflux pumps for azoles, CFZ, and BDQ in *M. tuberculosis* (36, 37) and for thiacetazone analogues in *M. abscessus* (38, 39).

To explore whether the TetR regulator MAB_2299c controls the expression of the neighboring *mmpS* and *mmpL* genes, quantitative reverse transcription-PCR (qRT-PCR) was first performed both in the parental *M. abscessus* S strain and in the 6 CFZ- and BDQ-resistant derivatives harboring the various *MAB_2299c* alleles. The results clearly showed the induction of both the *MAB_2300* and the *MAB_2301* transcripts in all 6 mutants (Fig. 1B). The expression levels of *tgs1*, which encodes the triacylglycerol synthase, involved in the synthesis and accumulation of triglycerides in *M. abscessus* (40), and which was included as an unrelated gene control, were found to remain unchanged in the various strains tested (Fig. 1B). In contrast, no induction of the expression levels of *MAB_2302* and *MAB_2303* transcripts was observed in the different mutant strains (Fig. 1B). This suggests that MAB_2299c represses expression of only the *MAB_2300-MAB_2301* (*mmpS-mmpL*) pair.

MAB_2299c binds to a palindromic sequence upstream of *MAB_2300*. Using MEME, a motif-based sequence analysis tool (41), a 64-bp DNA segment within the 373-bp intergenic region between *MAB_2299c* and *MAB_2300* ($IR_{2300/01}$) harboring two palindromic sequences as well as two degenerated repeat motifs was identified (Fig. 2A). To test whether this 64-bp fragment represents a DNA-binding site for MAB_2299c, electrophoretic mobility shift assays (EMSA) were performed using increasing concentrations of purified MAB_2299c in the presence of the corresponding labeled fragment (probe A; Fig. 2B). Under these conditions, a DNA-protein complex was detected. The specificity of binding was demonstrated in a competition assay by adding increasing concentrations of the corresponding unlabeled DNA fragment (cold

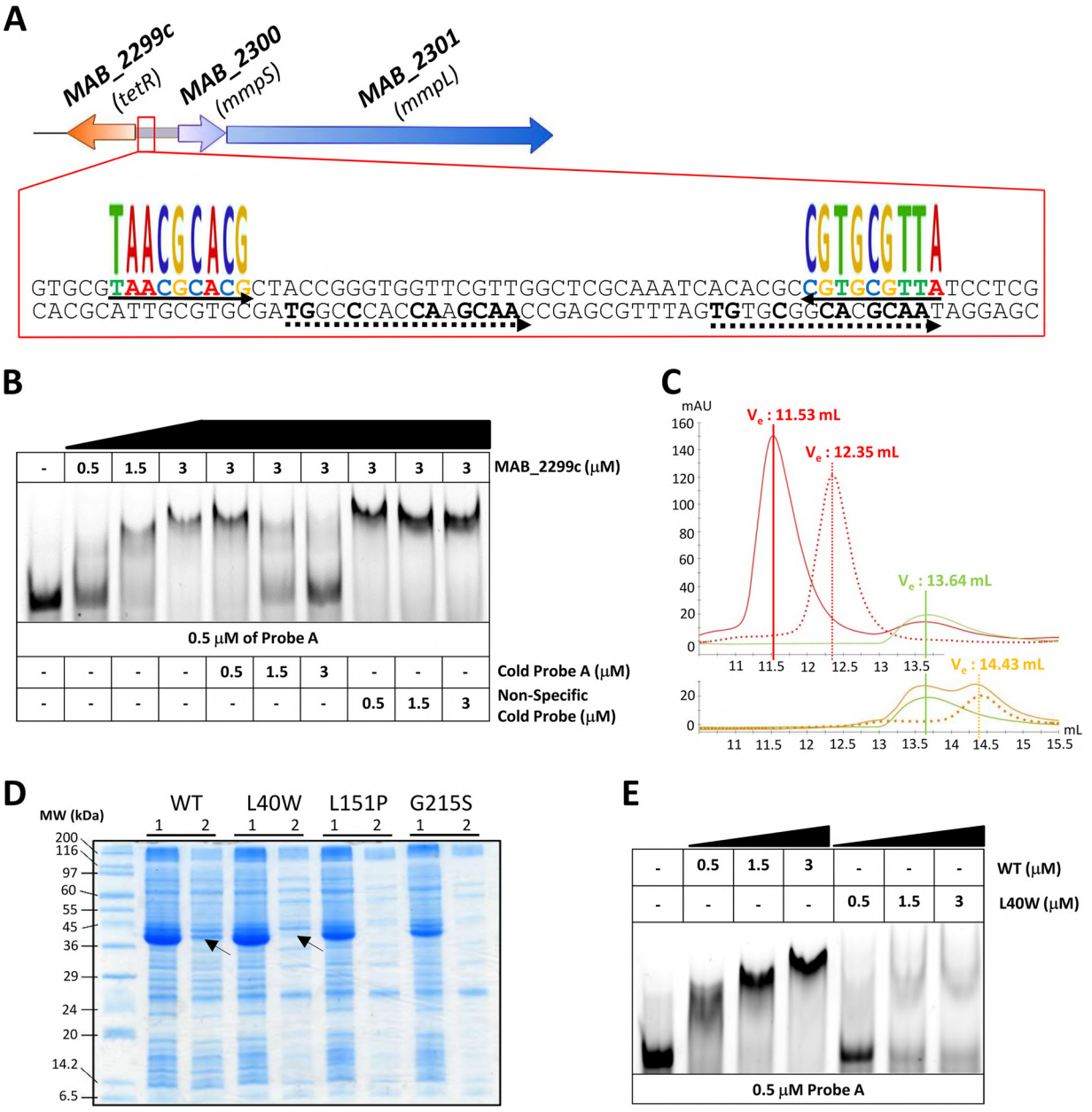

FIG 2 Binding activity of MAB_2299c to the intergenic region upstream of *MAB_2300-MAB_2301*. (A) Schematic representation of the 64-bp DNA operator identified within $IR_{2300/01}$ corresponding to the sequence of probe A. The oligonucleotides recognized by MAB_2299c are composed of two palindromes (underlined by arrows) and two degenerated double repeats (underlined by dashed arrows). (B) EMSA and competition assays using probe A and purified MAB_2299c. Gel shifts were revealed by fluorescence emission using a 5′ fluorescein-labeled probe A. (C) Gel filtration profiles of free probe A, free MAB_2299c, and the TetR-DNA complex. Probe A (red dotted line) and *MAB_2299c* (green line) were isolated individually by size exclusion chromatography and displayed elution volumes (V_e) of 12.35 ml and 13.64 ml, respectively. When mixed together, a stable MAB_2299c-probe A complex (red line) with an elution volume of 11.53 ml was observed. The MAB_4384-specific palindromic sequence (orange dotted line) eluted at 14.43 ml. However, when mixed together with MAB_2299c, no protein-DNA complex was formed and both the DNA and protein were eluted separately (orange line) as two distinct peaks, with the elution volumes corresponding exactly to those for the MAB_4384 palindrome and MAB_2299c protein alone. mAU, milli-absorbance units. (D) Expression of the various MAB_2299c variants in *E. coli*. Lanes 1, total crude extract; lanes 2, clarified/soluble extract. The theoretical molecular mass of MAB_2299c-6His-TrxA is 41,420 Da. MW, molecular weight. (E) Impaired DNA-binding activity of the MAB_2299c L40W mutant, as shown by EMSA using either the soluble MAB_2299c (WT) or MAB_2299c (L40W) protein. Gel shifts were revealed by the fluorescence emission thanks to fluorescein-labeled probe A.

probe), which led to a dose-dependent decrease in DNA-protein complex formation (Fig. 2B). Moreover, the shift was maintained in the presence of an excess of a nonrelated probe, further indicating that a specific protein-DNA complex was formed only when the TetR regulator was incubated with DNA containing its specific target.

These results were also confirmed by size exclusion chromatography (SEC), where the MAB_2299c-probe A complex eluted at 11.53 ml and could be readily separated from the protein alone (which eluted at 13.64 ml) or the DNA target (which eluted at 12.35 ml) (Fig. 2C, top). In contrast, no protein-DNA complex was eluted when MAB_2299c was incubated with the DNA target from MAB_4384, a previously characterized TetR regulator in *M. abscessus* (38, 39) (Fig. 2C, bottom), further highlighting the specificity of the MAB_2299c/$IR_{2300/01}$ interaction. In addition, the pronounced shift impairment using mutated derivatives of probe A lacking either the palindromic sequence (ΔPalin) or the degenerated double repeats (ΔDR), generated by replacing the original sequences with random nucleotides, suggests that both the palindrome and the double repeats are required for the optimal binding of MAB_2299c to its operator (see Fig. S1 in the supplemental material).

Screening of the entire 863-bp $IR_{2302/03}$ located upstream of the second *mmpS-mmpL* pair (Fig. 1A) using MEME failed to identify inverted repeats that looked similar to the ones found in $IR_{2300/01}$, suggesting that the regulator is unlikely to recognize a DNA-binding sequence in the upstream region of *MAB_2302-MAB_2303*. To confirm this hypothesis, EMSAs were done by incubating increasing concentrations of MAB_2299c with 3 overlapping probes covering the entire $IR_{2302/03}$ region (Fig. S2A). Even at the highest protein concentration tested, no protein-DNA complexes were observed with either of the three probes (Fig. S2B). These results are in agreement with the qRT-PCR results (Fig. 1B) and support the view that MAB_2299c is unable to bind to $IR_{2302/03}$ and to regulate the expression of this second *mmpS-mmpL* pair.

Overall, these results confirm the strict DNA sequence requirements for the optimal binding of MAB_2299c to $IR_{2300/01}$.

Leu40 is critical for optimal DNA-binding activity of MAB_2299c. To get insights into the mechanisms by which the different point mutations in CFZ-R1, CFZ-R7, and CFZ-R9 confer resistance to CFZ and BDQ, the three corresponding *MAB_2299c* alleles were cloned into pET32a and introduced into *E. coli* for expression. Figure 2D shows that although the 3 mutated proteins were highly expressed, only a very small fraction of the L40W protein was found in the soluble fraction, whereas the vast majority of the L151P and G215S mutants remained insoluble. Despite many attempts and by using large *E. coli* cultures, we failed to obtain enough soluble L151P and G215S proteins for subsequent purification but succeeded in generating the L40W derivative in a soluble form. Due to its localization within the N-terminal domain of the TetR regulator, known to participate in the DNA-binding activity of the protein (35), we addressed whether the L40W substitution conferring resistance to CFZ and BDQ affects the DNA-binding activity of MAB_2299c. EMSAs were therefore performed using purified MAB_2299c (L40W) and probe A. Compared to the shift profile with wild-type (WT) MAB_2299c, the formation of the DNA-protein complex was severely impaired in the presence of the mutated protein, even at high protein concentrations (Fig. 2E).

Overall, these results support the importance of Leu40 in the DNA-binding capacity of MAB_2299c and explain the reduced ability of the mutants to bind to the operator region, in agreement with the derepression of *MAB_2300-MAB_2301* transcription in the CFZ-R1 *M. abscessus* strain carrying the L40W substitution (Fig. 1B).

An unmarked deletion of *MAB_2299c* leads to upregulation of the *MAB_2300-MAB_2301* efflux pump and coresistance to CFZ and BDQ. Because point mutations or premature stop codons in the *MAB_2299c* mutants did not prevent the altered proteins from interacting with other protein partners/DNA sequences and eventually generating aberrant phenotypes, we further confirmed the contribution of *MAB_2299c* in the profile of susceptibility/resistance to CFZ and BDQ by generating an *M. abscessus* deletion mutant. To achieve this aim, we first improved a flexible suicide vector that we previously created, pUX1 (43), by cloning into it the *M. tuberculosis katG*, which was recently demonstrated as an efficient counterselectable marker in *M. abscessus* in the presence of isoniazid (INH) (42). Through the positive selection afforded by kanamycin resistance and tdTomato markers and the negative selection afforded by *katG*, this

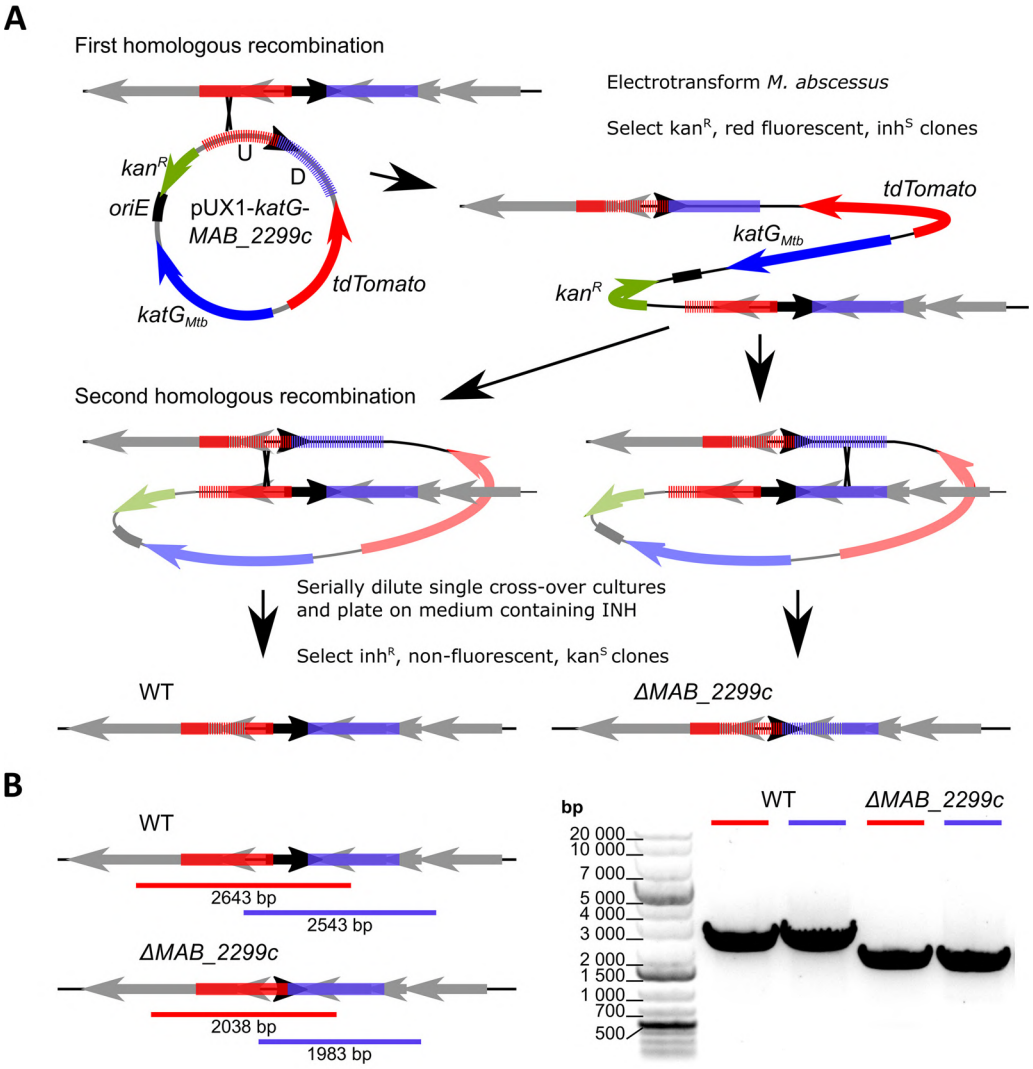

FIG 3 Generation of an unmarked *MAB_2299c* deletion mutant in *M. abscessus*. (A) Line drawing illustrating the general protocol followed to ascertain the Δ*MAB_2299c* mutant. $katG_{Mtb}$, *M. tuberculosis katG*. (B) (Left) Line drawing of the genomic context in the *M. abscessus* WT and Δ*MAB_2299c* mutant that also illustrates the PCR strategy followed to confirm the deletion of *MAB_2299c*. Red and blue bars, the PCR products obtained during the screening of potential mutant clones; black arrow, *MAB_2299c*. (Right) A gel confirming the Δ*MAB_2299c* genotype. The red and blue bars correspond to the amplicons obtained in the left panel. These amplicons were subjected to sequencing analysis to confirm the correct deletion of the *MAB_2299c* gene.

vector, pUX1-*katG*, could be used in a two-step homologous recombination procedure to generate scarless unmarked deletion mutants in *M. abscessus*. The different steps of this method leading to an unmarked *MAB_2299c* deletion are depicted in Fig. 3A. As a first step, sequences of approximately 1 kb directly upstream and downstream of a 560-bp internal fragment of the 666-bp *MAB_2299c* open reading frame were cloned adjacently into pUX1-*katG*. After transformation of *M. abscessus* with pUX1-*katG-MAB_2299c*, colonies that had undergone a first homologous recombination between the plasmid and the bacterial chromosome either up- or downstream of the *MAB_2299c* gene were easily identified by their red fluorescence against a large background of colonies spontaneously resistant to the selective antibiotic. After a single passage in liquid culture without kanamycin, the *MAB_2299c* single-crossover clones were serially diluted and the dilutions were plated on INH-containing solid medium. Clones that were INH resistant, nonfluorescent, and kanamycin sensitive arose at an approximate frequency of 10^{-4} to 10^{-3} CFU/ml. These clones were selected and subsequently

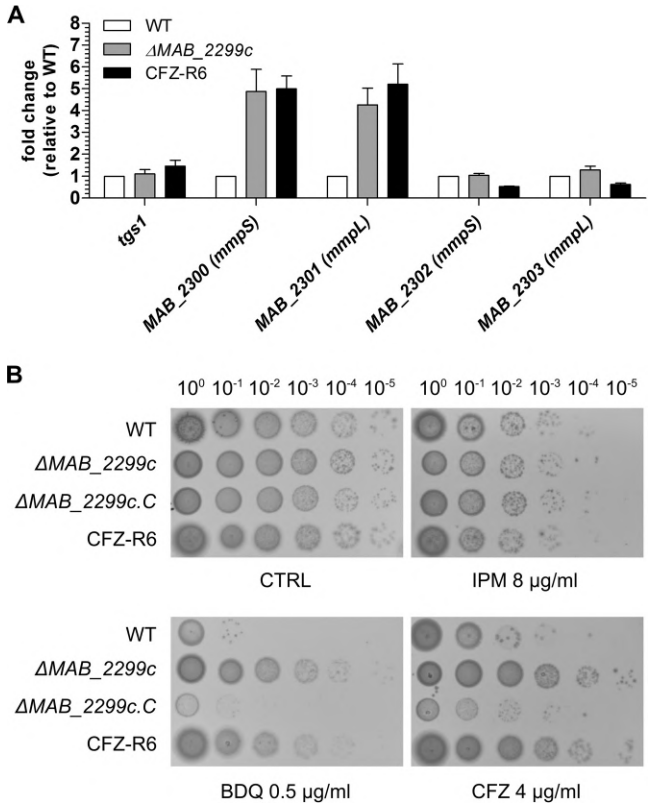

FIG 4 Deletion of *MAB_2299c* confers resistance to both CFZ and BDQ. (A) Results of a qRT-PCR experiment showing the induction levels of the *mmpS-mmpL* (*MAB_2300-MAB_2301*) pair but not *MAB_2302-MAB_2303* when *MAB_2299c* is deleted from the *M. abscessus* genome. (B) Profile of the susceptibility or resistance of *M. abscessus* WT, *M. abscessus* Δ*MAB_2299c*, and the complemented derivative of Δ*MAB_2299c* (Δ*MAB_2299c.C*) to BDQ, CFZ, or IPM. Five microliters of 10-fold serially diluted bacterial suspensions of exponentially growing cultures was spotted on Middlebrook 7H10 plates in the absence (control [CTRL]) or presence of drugs at the indicated concentrations. The plates were incubated at 37°C for 4 days.

genotyped to confirm the correct unmarked deletion of *MAB_2299c* by PCR/sequencing analysis (Fig. 3B). No observable changes in the colony morphology or in the *in vitro* growth rate were noticed in this unmarked deletion mutant, subsequently designated Δ*MAB_2299c* (Fig. S3). Δ*MAB_2299c* was then subjected to qRT-PCR analysis. The results in Fig. 4A clearly show a 5-fold increase in the transcription level of *MAB_2300* and *MAB_2301*, but not that of *MAB_2302* and *MAB_2303*. Interestingly, these induction levels were comparable to those found in CFZ-R6. In agreement with the qRT-PCR results performed using the various CFZ spontaneous mutants, the *MAB_2299c* gene deletion did not affect expression of the *MAB_2302-MAB_2303* pair. As expected, the CFZ and BDQ susceptibility pattern of the Δ*MAB_2299c* mutant was comparable to that of CFZ-R6 (Fig. 4B). Importantly, both the Δ*MAB_2299c* and CFZ-R6 mutants displayed enhanced growth on agar supplemented with 0.5 μg/ml BDQ or 4 μg/ml CFZ (Fig. 4B, bottom), whereas, under the same conditions, the growth of the parental *M. abscessus* strain was severely inhibited. That this resistance phenotype was restricted to CFZ and BDQ only was supported by the similar growth and susceptibility to imipenem (IPM) of all strains. As anticipated, complementation of the Δ*MAB_2299c* mutant by introducing a pMV261-*MAB_2299c* construct (leading to Δ*MAB_2299c*.C) fully restored susceptibility to both CFZ and BDQ (Fig. 4B). In contrast, the susceptibility profile of the Δ*MAB_2299c* mutant to anti-TB front-line drugs (INH, ethambutol, or rifampin) was comparable to that of the WT and complemented strains (Table S3). Together, these results confirm the importance of MAB_2299c in resistance to CFZ and BDQ.

Deletion of *MAB_2300-MAB_2301* in the Δ*MAB_2299c* mutant restores susceptibility to CFZ and BDQ. To address whether resistance to CFZ and BDQ is directly

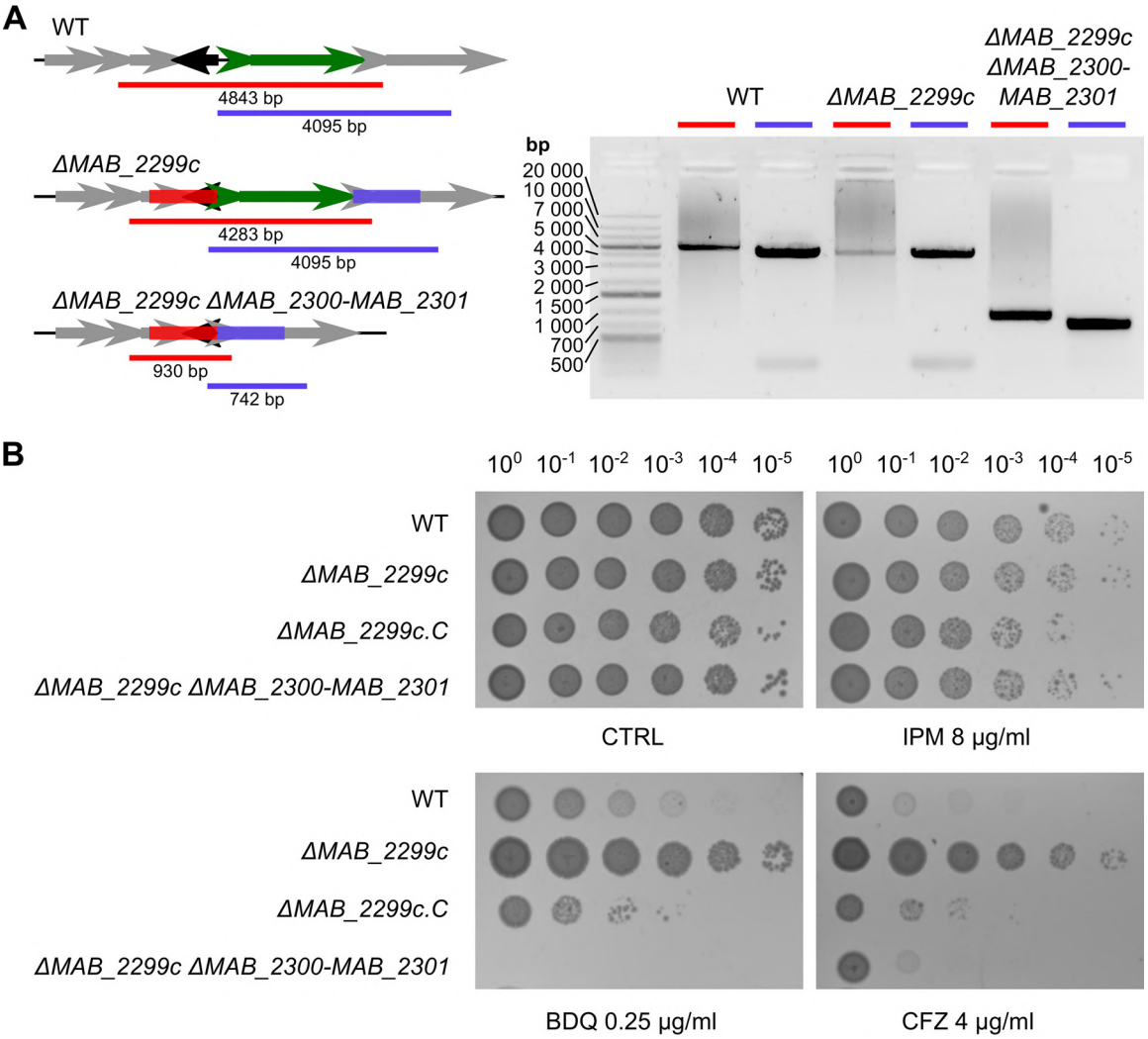

FIG 5 Deletion of *MAB_2300* and *MAB_2301* in Δ*MAB_2299c* restores sensitivity to CFZ and BDQ. (A) Line drawing (left) of the *MAB_2299c-MAB_2301* genomic context in the *M. abscessus* WT, Δ*MAB_2299c*, and Δ*MAB_2299c* Δ*MAB_2300-MAB_2301* strains. Also illustrated is the PCR strategy followed to confirm the deletion of *MAB_2300* and *MAB_2301*. Black arrow, *MAB_2299c*; small and large green arrows, *MAB_2300* and *MAB_2301*, respectively. (B) Profile of susceptibility of the Δ*MAB_2299c* Δ*MAB_2300-MAB_2301* triple-knockout strain to BDQ, CFZ, or IPM compared to the other strains reared in this study. Five microliters of 10-fold serially diluted bacterial suspensions obtained from exponentially growing cultures was spotted on Middlebrook 7H10 plates in the absence (control [CTRL]) or presence of drugs at the indicated concentrations. The plates were incubated at 37°C for 4 days.

mediated by an MmpS/MmpL-dependent efflux machinery which is induced in Δ*MAB_2299c*, both *MAB_2300* and *MAB_2301* were deleted in the Δ*MAB_2299c* mutant. The simultaneous knockout of *MAB_2300* and *MAB_2301* in the unmarked *MAB_2299c* deletion mutant was achieved using a strategy similar to the one used to construct the Δ*MAB_2299c* mutant. The Δ*MAB_2299c* Δ*MAB_2300-MAB_2301* genotype of this triple-knockout mutant was confirmed by PCR, as illustrated in Fig. 5A. Importantly, whereas the susceptibility of the triple mutant to CFZ was reverted to WT levels, the MIC of BDQ for this mutant was even lower than the MIC observed for the WT strain (Fig. 5B and Table S3). This indicates that abolition of the MAB_2300-MAB_2301 efflux pump system rendered the Δ*MAB_2299c* mutant sensitive to both drugs. As expected, the triple mutant's sensitivity to IPM remained similar to that of the Δ*MAB_2299* progenitor (Fig. 5B and Table S3).

Overall, these results suggest that both CFZ and BDQ are specific substrates of the MAB_2301 (MmpL) efflux pump and that the sole deletion of this MmpS/MmpL system is sufficient to reverse the CFZ and BDQ resistance phenotype of the Δ*MAB_2299c* mutant.

DISCUSSION

M. abscessus has recently emerged as one of the most clinically relevant NTM (8, 14) and accounts for more than 80% of all pulmonary infections caused by rapidly growing mycobacteria (44). It poses a serious threat, particularly in patients suffering from lung disorders, such as CF or bronchiectasis (14, 44). Occasional fatalities due to *M. abscessus* infections (44, 45) can be a result of the extreme difficulty with the treatment of patients as a result of the intrinsic and broad antibiotic resistance of this bacterium conferred by an impermeable cell envelope, the presence of drug-modifying enzymes and a large abundance of efflux pumps (3, 11, 46). Therefore, to reach an unmet medical need in the treatment of *M. abscessus* diseases, the repositioning of the anti-TB drugs CFZ and BDQ has recently been evaluated in retrospective case series, although data related to their mode of action and/or resistance mechanisms in *M. abscessus* remain scarce.

In this study, whole-genome sequencing of *in vitro*-selected mutants showing cross-resistance to CFZ and BDQ identified mutations in *MAB_2299c* that were subsequently confirmed by PCR/sequencing. MAB_2299c belongs to the TetR family of transcriptional regulators, representing the most abundant family of regulators in mycobacteria (47). In line with the general observation that 60% of TetR regulators are divergently oriented with the genes that they control, *MAB_2299c* was found in the opposite orientation relative to that of its *MAB_2300* and *MAB_2301* target genes. That the different point mutations identified (L40W, L151P, and G215S) were associated with similar fold increases in the upregulation of *MAB_2300-MAB_2301* in the mutants carrying premature stop codons suggested a loss of DNA-binding activity, resulting in derepression of *MAB_2300-MAB_2301* gene expression. This hypothesis was confirmed by EMSA, which clearly demonstrated an impaired DNA-binding activity of the L40W mutant, with Leu40 being located in the N-terminal domain, which carries the DNA-binding activity in TetR regulators (35). The L151P and G215S mutated proteins, albeit being expressed in high yields in *E. coli*, remained largely insoluble, suggesting that the L151 and G215 residues play a role in the folding and/or stability of the MAB_2299c multimer. Therefore, substitution of these important residues is very likely to affect the overall structure of the regulator and, consequently, its biological function. During preparation of the manuscript, an independent study identified mutations in several genes, including *MAB_2299c*, in CFZ-resistant *M. abscessus* strains selected *in vitro* (48). Whereas most mutations conferred a loss of function caused by indels or stop codons, three amino acid replacements differing from ours were found, namely, C110Y, H173R, and A214S. Interestingly, the mutation at position A214 is located next to G215, found in our study, further emphasizing an important role of this region in the activity/structure of the regulator. However, despite the lack of any mechanistic data regarding the involvement of these mutations in the function of MAB_2299c and in MmpS/MmpL expression and a potential link with BDQ resistance, the study by Chen et al. (48) strongly supports our findings regarding the implication that MAB_2299c is a major determinant of resistance to CFZ and BDQ. Our results are also reminiscent of those of previous work describing a similar cross-resistance to both BDQ and CFZ identified by a whole-genome sequencing comparison of initial and relapse isolates of *Mycobacterium intracellulare* which occurred during a trial of BDQ as salvage therapy for *M. intracellulare* lung disease (49). Mutations in MmpT5, another TetR member controlling expression of the adjacent *mmpS5-mmpL5* drug efflux operon, was identified as the cause for this cross-resistance. Susceptibility testing indicated that *mmpT5* mutations are associated with 2- to 8-fold increases in MICs for BDQ and CFZ (49).

MAB_2300-MAB_2301 encodes an MmpS/MmpL efflux pump system which is separated by an intergenic region from *MAB_2302-MAB_2303*, encoding a second putative efflux pump system. Whether MAB_2299c controls the expression of the first, the second, or both MmpS/MmpL pairs was addressed by qRT-PCR. Our results clearly indicate that only *MAB_2300-MAB_2301* is under the control of MAB_2299c, and this specificity of regulation was further confirmed by functional complementation exper-

iments with a *MAB_2299c* deletion mutant. Restoration of the CFZ and BDQ susceptibility profile to WT levels was achieved following ectopic expression of MAB_2299c in the deletion mutant. Strikingly, deletion of the *MAB_2300-MAB_2301* locus in Δ*MAB_2299c* abrogated the resistance to both drugs, thus suggesting that the MmpS/MmpL machinery encoded by *MAB_2300-MAB_2301* acts as a multisubstrate efflux pump that is responsible for the drug resistance phenotype in *M. abscessus*. Similarly, studies in *M. tuberculosis* showed resistance to azoles, CFZ, and BDQ involving a wide set of mutations in *Rv0678*, encoding a transcriptional regulator from the MarR family, causing overexpression of the MmpS5/MmpL5 efflux pump (36, 37, 50–52). In addition, the level of resistance to both drugs in the *M. tuberculosis Rv0678* mutants was similar to that found in the *M. abscessus MAB_2299c* mutants. To explain why the MAB_2300/MAB_2301 pair participates in BDQ and CFZ extrusion while the MAB_4383c/MAB_4382c pair that we previously identified to be the closest ortholog in *M. abscessus* of MmpS5/MmpL5, rather, excludes thiacetazone derivatives and not BDQ and CFZ (38), we performed multiple-sequence alignments and subsequent sequence identity determination of the nucleotide and protein sequences of the 17 MmpS/MmpL pairs encoded by the *M. abscessus* genome (see Table S4 in the supplemental material). The identity scores at both the nucleotide and protein levels supported our previous observations that MAB_4383c/MAB_4382c is the closest orthologous pair to MmpS5/MmpL5 from *M. tuberculosis*. Interestingly, considering the protein sequence identity, MAB_2301 is the second closest ortholog to MmpL5 from *M. tuberculosis* after MAB_4382c, explaining the functional similarity in CFZ and BDQ export. However, a full explanation of the differences in substrate specificity that exist between MmpS5/MmpL5 orthologs/paralogs will rely on the elucidation of the high-resolution three-dimensional structures of MmpS5/MmpL5 alone and, more pertinently, in complex with their substrates. Given the very high relatedness between MAB_2300/MAB_2301 and other MmpS-MmpL pairs in *M. abscessus* (Table S4), one cannot exclude the possibility that other MmpS-MmpL efflux pumps mediate cross-resistance to CFZ and BDQ. This can be investigated thanks to the new suicide vector pUX1-*katG*, described in this study, which allows the easy and rapid generation of scarless genetic alterations in the *M. abscessus* chromosome, facilitated by the presence of the brightly red fluorescent tdTomato positive selectable marker and the KatG counterselectable marker.

In *M. tuberculosis*, efflux inhibition using efflux pump inhibitors such as verapamil or reserpine decreases the MICs of BDQ and CFZ *in vitro* (52, 53). Whether these inhibitors would also potentiate the effect of CFZ and/or BDQ in resistant *M. abscessus* strains remains to be established. However, in both organisms, the resistance levels were low and were about 4-fold greater than those of their parental strains. This may be linked to the low induction level of the *MAB_2300-MAB_2301* gene cluster under derepressed conditions (in the *MAB_2299c* mutants or deletion strain). This also contrasts with the very high induction level reported previously for *mmpS5-mmpL5* in mutants or a deletion strain of *MAB_4384*, which also accounted for very high levels of resistance to thiacetazone analogues (38, 39). Overall, these observations, combined with the fact that *M. abscessus* possesses a very large *mmpL* repertoire (54) and also a high abundance of TetR transcriptional regulators, allow us to speculate that similar drug resistance mechanisms are employed by this pathogen to express its natural pattern of resistance to many more antimicrobial agents.

In summary, this study adds new functional and mechanistic insights into the TetR-dependent regulation mechanisms responsible for cross-resistance to CFZ and BDQ in *M. abscessus*, which may have important clinical implications. Future studies should help to elucidate whether the emergence of *MAB_2299c* variants occurs during BDQ or CFZ treatment in patients with *M. abscessus* lung disease.

MATERIALS AND METHODS

Strains, growth conditions, and reagents. All *M. abscessus* strains used in this study are listed in Table S1 in the supplemental material. The strains were grown in Middlebrook 7H9 broth (BD Difco) supplemented with 0.05% Tween 80 (Sigma-Aldrich) and 10% oleic acid, albumin, dextrose, catalase (OADC enrichment; BD Difco) ($7H9^{T/OADC}$) at 30°C (unless otherwise stated) or in Sauton's medium in the

presence of antibiotics, when required. On plates, colonies were selected on Middlebrook 7H10 or 7H11 agar (BD Difco) supplemented with 10% OADC enrichment (7H10^{OADC} or 7H11^{OADC}, respectively) or on LB agar. All drugs were purchased from Sigma-Aldrich.

Drug susceptibility testing. MICs were determined on cation-adjusted Mueller-Hinton broth using the microdilution method or on Middlebrook 7H10^{OADC} agar plates. The MIC_{99} was defined as the minimal drug concentration required to inhibit 99% growth and was recorded by counting the colonies obtained after 3 to 4 days of incubation at 30°C. All experiments were done on three independent occasions. The frequency of spontaneous resistance was determined by counting the number of resistant colonies growing on 7H10^{OADC} and 7H11^{OADC} agar supplemented with 8 μg/ml CFZ after plating 5×10^7 CFU.

Generating clones resistant to clofazimine. Resistance to CFZ was induced by subjecting an *M. abscessus* ATCC 19977 susceptible clone to sub-MICs of the antibiotic. The bacteria were grown in 7H9 supplemented with albumin-dextrose-catalase (ADC; 10%) and glycerol (0.04%) containing sub-MICs of CFZ for 5 days. The bacteria were then spun in a centrifuge at 3,000 $\times$ *g* and washed with phosphate-buffered saline. Bacteria that grew at the highest concentration of CFZ were used to inoculate new cultures containing increasing concentrations of CFZ. The bacteria were then grown in 7H9 supplemented with ADC (10%) and glycerol (0.04%) without CFZ for 5 days and streaked on 7H11 agar plates supplemented with OADC (10%) and glycerol (0.04%) containing CFZ. Single colonies isolated from these plates were subjected to MIC determinations and DNA extraction and sequencing. All growth was done at 37°C.

Whole-genome sequencing and target identification. DNA from six spontaneous resistant mutants and one susceptible isolate was sequenced on an Illumina MiSeq platform, producing 150-bp paired-end reads. The raw reads were subsequently mapped to the *M. abscessus* reference genome using the BWA-MEM algorithm (55). Variants were called using the SAMtools (v.1.2) and BCFtools (v.1.2) packages and the parameters described previously (56, 57). Single nucleotide polymorphisms (SNP) were identified in *MAB_2299c*, and confirmation of these mutations was done by PCR amplification and sequencing.

DNA constructs. All constructs used in this study are listed in Table S1. For expression of MAB_2299c in *E. coli*, *MAB_2299c* was PCR amplified from pure genomic DNA of *M. abscessus* CIP104536^T using primers MAB_2299c_Fw and MAB_2299c_Rv (Table S2) and Phusion polymerase (Thermo Fisher Scientific). The allele carrying the L40W mutation was amplified from strain CFZ-R1 using the same primers. The PCR products were then cloned into pET32a that had been cut with KpnI and HindIII, allowing introduction of thioredoxin and polyhistidine tags at the N terminus of the protein. A tobacco etch virus (TEV) cleavage site was also incorporated before the 1st amino acid of the protein to remove the N-terminal tags from the rest of the protein. To complement the *M. abscessus* Δ*MAB_2299c* mutant, *MAB_2299c* was PCR amplified using the Compl_MAB_2299c primers (Table S2), digested with EcoRI, and ligated into pMV261 that had been digested with MscI and EcoRI, allowing the constitutive overexpression of *MAB_2299c* under the control of the *hsp60* promoter, thus yielding pMV261-*MAB_2299c* (Table S1).

Quantitative real-time PCR. Isolation of RNA, reverse transcription, and qRT-PCR were done as reported earlier (38), using the primers listed in Table S2.

Expression and purification of MAB_2299c variants. The *E. coli* BL21(DE3) strain (New England Biolabs) containing the pRARE2 vector was transformed with the pET32a constructs containing either the wild-type (WT) or the mutated *MAB_2299c* gene harboring the L40W mutation. Protein expression was done in lysogeny broth (LB) medium containing 200 μg/ml ampicillin and 30 μg/ml chloramphenicol. When an optical density at 600 nm of 0.6 to 1 was reached, the cultures underwent a 30-min cold shock in icy water prior to protein synthesis induction with 1 mM isopropyl-β-D-1-thiogalactopyranoside (IPTG). Cultures were then grown for 20 h at 16°C prior to centrifugation (6,000 $\times$ *g*, 4°C, 20 min). Bacterial pellets were resuspended in lysis buffer (50 mM Tris-HCl, pH 8, 200 mM NaCl, 20 mM imidazole, 1 mM benzamidine, 5 mM β-mercaptoethanol), and the cells were disrupted by sonication before the lysates were clarified by an additional centrifugation (16,000 $\times$ *g*, 4°C, 45 min). Proteins were then purified by a first ion metal affinity chromatography (IMAC) step (Ni-nitrilotriacetic acid Sepharose; GE Healthcare Life Sciences). To remove the two N-terminal tags (thioredoxin, His tag), the eluted proteins were mixed in a 1:50 ratio with the TEV protease and dialyzed overnight at 4°C against 50 mM Tris-HCl, pH 8, 200 mM NaCl, and 5 mM β-mercaptoethanol. The dialyzed proteins were subjected to a second IMAC step before being further dialyzed against a buffer consisting of 50 mM Tris-HCl, pH 8, and 5 mM β-mercaptoethanol. The proteins were then purified by cation exchange chromatography (HiTrap SP Sepharose Fast Flow; GE Healthcare Life Sciences) and eluted in the same buffer using a linear NaCl gradient. Size exclusion chromatography (SEC; ENrich SEC 650; Bio-Rad) was then performed using an elution buffer containing 50 mM Tris-HCl, pH 8, 200 mM NaCl, and 5 mM β-mercaptoethanol to generate highly pure proteins.

EMSA. Using the MEME suite 4.20.0 online tool, a DNA operator of 64 nucleotides containing two perfect palindromes and a degenerated double repeat sequence was identified within the intergenic region between *MAB_2299c* and *MAB_2300*. Thus, the 64-bp double-stranded sequence (probe A) was labeled at the 5′ end with fluorescein (Sigma-Aldrich) and incubated for 1 h at room temperature in 1$\times$ Tris base-acetic acid-EDTA (TAE) buffer with increasing amounts of MAB_2299c or MAB_2299c (L40W). After 30 min of electrophoresis in 1$\times$ TAE buffer at 100 V, gel shifts were revealed by fluorescence using an Amersham Imager 600 imager (GE Healthcare Life Sciences). This native DNA operator as well as mutated probes are listed in Table S2. The 373-bp intergenic region located between *MAB_2299c* and *MAB_2300* and the three overlapping probes covering the entire intergenic region between *MAB_2301*

and *MAB_2302* (Table S2) were amplified using a similar strategy and subjected to electrophoretic mobility shift assays (EMSA) using purified MAB_2299c.

Isolation of the MAB_2299c-probe A complex by SEC. Protein-DNA complex formation was assessed by high-performance liquid chromatography (HPLC) using an Akta Pure 25M chromatography system (GE Healthcare Life Sciences) on an ENrich SEC 650 column (Bio-Rad). The DNA alone, the protein alone, and the protein-DNA mixture were eluted at 4°C at a flow rate of 0.4 ml/min in a buffer containing 50 mM Tris-HCl, pH 8, 200 mM NaCl, 5 mM β-mercaptoethanol. Probe A (60 μg) and MAB_2299c (186 μg) were independently loaded onto the column. A mixture of 60 μg probe A and 186 μg MAB_2299c was coincubated for 1 h at room temperature and loaded onto the column. As a negative control, 21 μg of a 45-bp DNA operator targeted by the TetR regulator MAB_4384 was coincubated with 186 μg MAB_2299c and loaded onto the column.

Generation of *MAB_2299c* and *MAB_2300-MAB_2301* recombination plasmids. To generate pUX1-*katG*, used to perform gene disruption by two-step homologous recombination, the *M. tuberculosis katG* gene was first PCR amplified using the overlap extension mutagenesis approach (58) to introduce a synonymous mutation in the gene, removing an NheI restriction site. Briefly, two separate PCR mixtures containing either the primer set katG_outer_Fw and katG_inner_Rev or the primer set katG_inner_Fw and katG_outer_Rev, purified genomic DNA from *M. tuberculosis*, and Phusion polymerase (Thermo Fisher Scientific) were set up. The PCR products were purified and added (10 ng each) to a new Phusion polymerase PCR mixture without any primers or genomic DNA. This mixture was then subjected to two cycles of 95°C for 30 s, 55°C for 2 min, and 72°C for 3 min before the outer primers were added and 25 more cycles of 95°C for 10 s, 55°C for 30 s, and 72°C for 2 min were performed. The final PCR product was AvrII digested and ligated to AvrII-XmnI-linearized pUX1 to produce pUX1-*katG*. To generate pUX1-*katG-MAB_2299c*, the same overlap extension approach with outer and inner primers was first used to generate a single fused PCR amplicon containing 1-kb up- and downstream sequences of *MAB_2299c* so that it effectively carried a 560-bp deletion in the 666-bp *MAB_2299c* open reading frame. This PCR product was NheI digested and ligated to NheI-XmnI-linearized pUX1-*katG* to produce pUX1-*katG-MAB_2299c*. The pUX1-*katG-MAB_2300-MAB_2301* plasmid used to make a Δ*MAB_2299c* Δ*MAB_2300-MAB_2301* triple-knockout mutant was made using the same approach.

Unmarked deletions of *MAB_2299c* and *MAB_2300-MAB_2301* in *M. abscessus*. The generation of an unmarked *MAB_2299c* deletion in *M. abscessus* relied on two separate homologous recombination events. First, highly electrocompetent *M. abscessus* was transformed with pUX1-*katG-MAB_2299c*, as previously described (43). Kanamycin-resistant (growing at 200 μg/ml), red fluorescent colonies were selected, and the broth was cultured in the presence of kanamycin and subjected to PCR screening using either the primer set MAB_2299c_U_scrn_Fw and MAB_2299c_U_scrn_Rev or the primer set MAB_2299c_D_scrn_Fw and MAB_2299c_D_scrn_Rev (Table S2). Based on the PCR product sizes obtained using the two primer sets, clones that had undergone a single homologous recombination event in either the upstream or the downstream sequence flanking *MAB_2299c* were identified. Positive clones were washed to remove the antibiotics, cultured for 4 h in the absence of antibiotic, and then 10-fold serially diluted, and the dilutions were plated on 7H10 agar plates containing 50 μg/ml isoniazid (INH). INH-resistant, nonfluorescent colonies were restreaked on plates without selective antibiotics to obtain single colonies that were used to inoculate the broth cultures. These cultures were confirmed to be kanamycin sensitive and used to extract and purify genomic DNA, which was subsequently used to perform the same PCR screening described above to identify clones that had undergone a second homologous recombination event effectively deleting 85% of the *MAB_2299c* open reading frame from the *M. abscessus* genome. The PCR products were sequenced, and special attention was paid in the subsequent analyses of the sequencing data to verify the correct junctions between cloned sequences and chromosomal sequences to exclude the possibility of spurious PCR amplification products. The Δ*MAB_2299c* Δ*MAB_2300-MAB_2301* triple-knockout mutant was reared in a similar way, with the only difference being that the Δ*MAB_2299c* strain was the progenitor strain transformed with pUX1-*katG-MAB_2300-MAB_2301*.

SUPPLEMENTAL MATERIAL

Supplemental material for this article may be found at https://doi.org/10.1128/AAC.01316-18.

SUPPLEMENTAL FILE 1, PDF file, 1.3 MB.

ACKNOWLEDGMENTS

This work was supported by the Fondation pour la Recherche Médicale (FRM) (grant number DEQ20150331719 to L.K.; grant number ECO20160736031 to M.R.); the InfectioPôle Sud, which funded the Ph.D. fellowship of A.V.G.; the Wellcome Trust (098051, 107032AIA); and the Cystic Fibrosis Trust (to D.R.-R., I.E., J.P., and R.A.F.).

The funders had no role in study design, data collection and interpretation, or the decision to submit the work for publication.

We have no conflict of interest to declare.

REFERENCES

1. Singh M, Dugdale CM, Solomon IH, Huang A, Montgomery MW, Pomahac B, Yawetz S, Maguire JH, Talbot SG. 2016. Rapid-growing mycobacteria infections in medical tourists: our experience and literature review. Aesthet Surg J 36:NP246–NP253. https://doi.org/10.1093/asj/sjw047.
2. Roux A-L, Catherinot E, Ripoll F, Soismier N, Macheras E, Ravilly S, Bellis G, Vibet M-A, Le Roux E, Lemonnier L, Gutierrez C, Vincent V, Fauroux B, Rottman M, Guillemot D, Gaillard J-L, Herrmann J-L, for the OMA Group. 2009. Multicenter study of prevalence of nontuberculous mycobacteria in patients with cystic fibrosis in France. J Clin Microbiol 47:4124–4128. https://doi.org/10.1128/JCM.01257-09.
3. Medjahed H, Gaillard J-L, Reyrat J-M. 2010. *Mycobacterium abscessus*: a new player in the mycobacterial field. Trends Microbiol 18:117–123. https://doi.org/10.1016/j.tim.2009.12.007.
4. Griffith DE, Aksamit T, Brown-Elliott BA, Catanzaro A, Daley C, Gordin F, Holland SM, Horsburgh R, Huitt G, Iademarco MF, Iseman M, Olivier K, Ruoss S, von Reyn CF, Wallace RJ, Winthrop K, ATS Mycobacterial Diseases Subcommittee, American Thoracic Society, Infectious Diseases Society of America. 2007. An official ATS/IDSA statement: diagnosis, treatment, and prevention of nontuberculous mycobacterial diseases. Am J Respir Crit Care Med 175:367–416. https://doi.org/10.1164/rccm.200604-571ST.
5. Floto RA, Olivier KN, Saiman L, Daley CL, Herrmann J-L, Nick JA, Noone PG, Bilton D, Corris P, Gibson RL, Hempstead SE, Koetz K, Sabadosa KA, Sermet-Gaudelus I, Smyth AR, van Ingen J, Wallace RJ, Winthrop KL, Marshall BC, Haworth CS. 2016. US Cystic Fibrosis Foundation and European Cystic Fibrosis Society consensus recommendations for the management of non-tuberculous mycobacteria in individuals with cystic fibrosis: executive summary. Thorax 71:88–90. https://doi.org/10.1136/thoraxjnl-2015-207983.
6. Catherinot E, Roux A-L, Macheras E, Hubert D, Matmar M, Dannhoffer L, Chinet T, Morand P, Poyart C, Heym B, Rottman M, Gaillard J-L, Herrmann J-L. 2009. Acute respiratory failure involving an R variant of *Mycobacterium abscessus*. J Clin Microbiol 47:271–274. https://doi.org/10.1128/JCM.01478-08.
7. Esther CR, Esserman DA, Gilligan P, Kerr A, Noone PG. 2010. Chronic *Mycobacterium abscessus* infection and lung function decline in cystic fibrosis. J Cyst Fibros 9:117–123. https://doi.org/10.1016/j.jcf.2009.12.001.
8. Bryant JM, Grogono DM, Rodriguez-Rincon D, Everall I, Brown KP, Moreno P, Verma D, Hill E, Drijkoningen J, Gilligan P, Esther CR, Noone PG, Giddings O, Bell SC, Thomson R, Wainwright CE, Coulter C, Pandey S, Wood ME, Stockwell RE, Ramsay KA, Sherrard LJ, Kidd TJ, Jabbour N, Johnson GR, Knibbs LD, Morawska L, Sly PD, Jones A, Bilton D, Laurenson I, Ruddy M, Bourke S, Bowler IC, Chapman SJ, Clayton A, Cullen M, Daniels T, Dempsey O, Denton M, Desai M, Drew RJ, Edenborough F, Evans J, Folb J, Humphrey H, Isalska B, Jensen-Fangel S, Jönsson B, Jones AM, et al. 2016. Emergence and spread of a human-transmissible multidrug-resistant nontuberculous mycobacterium. Science 354:751–757. https://doi.org/10.1126/science.aaf8156.
9. Brown-Elliott BA, Nash KA, Wallace RJ. 2012. Antimicrobial susceptibility testing, drug resistance mechanisms, and therapy of infections with nontuberculous mycobacteria. Clin Microbiol Rev 25:545–582. https://doi.org/10.1128/CMR.05030-11.
10. Jarand J, Levin A, Zhang L, Huitt G, Mitchell JD, Daley CL. 2011. Clinical and microbiologic outcomes in patients receiving treatment for *Mycobacterium abscessus* pulmonary disease. Clin Infect Dis 52:565–571. https://doi.org/10.1093/cid/ciq237.
11. Nessar R, Cambau E, Reyrat JM, Murray A, Gicquel B. 2012. *Mycobacterium abscessus*: a new antibiotic nightmare. J Antimicrob Chemother 67:810–818. https://doi.org/10.1093/jac/dkr578.
12. Maurer FP, Bruderer VL, Ritter C, Castelberg C, Bloemberg GV, Böttger EC. 2014. Lack of antimicrobial bactericidal activity in *Mycobacterium abscessus*. Antimicrob Agents Chemother 58:3828–3836. https://doi.org/10.1128/AAC.02448-14.
13. Ferro BE, Srivastava S, Deshpande D, Pasipanodya JG, van Soolingen D, Mouton JW, van Ingen J, Gumbo T. 2016. Failure of the amikacin, cefoxitin, and clarithromycin combination regimen for treating pulmonary *Mycobacterium abscessus* infection. Antimicrob Agents Chemother 60:6374–6376. https://doi.org/10.1128/AAC.00990-16.
14. Griffith DE. 2014. *Mycobacterium abscessus* subsp *abscessus* lung disease: "trouble ahead, trouble behind. . . ." F1000Prime Rep 6:107. https://doi.org/10.12703/P6-107.
15. Wu M-L, Aziz DB, Dartois V, Dick T. 2018. NTM drug discovery: status, gaps and the way forward. Drug Discov Today 23:1502–1519. https://doi.org/10.1016/j.drudis.2018.04.001.
16. Reddy VM, O'Sullivan JF, Gangadharam PR. 1999. Antimycobacterial activities of riminophenazines. J Antimicrob Chemother 43:615–623. https://doi.org/10.1093/jac/43.5.615.
17. Yano T, Kassovska-Bratinova S, Teh JS, Winkler J, Sullivan K, Isaacs A, Schechter NM, Rubin H. 2011. Reduction of clofazimine by mycobacterial type 2 NADH:quinone oxidoreductase: a pathway for the generation of bactericidal levels of reactive oxygen species. J Biol Chem 286:10276–10287. https://doi.org/10.1074/jbc.M110.200501.
18. Shen G-H, Wu B-D, Hu S-T, Lin C-F, Wu K-M, Chen J-H. 2010. High efficacy of clofazimine and its synergistic effect with amikacin against rapidly growing mycobacteria. Int J Antimicrob Agents 35:400–404. https://doi.org/10.1016/j.ijantimicag.2009.12.008.
19. Singh S, Bouzinbi N, Chaturvedi V, Godreuil S, Kremer L. 2014. In vitro evaluation of a new drug combination against clinical isolates belonging to the *Mycobacterium abscessus* complex. Clin Microbiol Infect 20:O1124–O1127. https://doi.org/10.1111/1469-0691.12780.
20. Czaja CA, Levin AR, Cox CW, Vargas D, Daley CL, Cott GR. 2016. Improvement in quality of life after therapy for *Mycobacterium abscessus* group lung infection. A prospective cohort study. Ann Am Thorac Soc 13:40–48. https://doi.org/10.1513/AnnalsATS.201508-529OC.
21. Martiniano SL, Wagner BD, Levin A, Nick JA, Sagel SD, Daley CL. 2017. Safety and effectiveness of clofazimine for primary and refractory nontuberculous mycobacterial infection. Chest 152:800–809. https://doi.org/10.1016/j.chest.2017.04.175.
22. Yang B, Jhun BW, Moon SM, Lee H, Park HY, Jeon K, Kim DH, Kim S-Y, Shin SJ, Daley CL, Koh W-J. 2017. Clofazimine-containing regimen for the treatment of *Mycobacterium abscessus* lung disease. Antimicrob Agents Chemother 61:e02052-16. https://doi.org/10.1128/AAC.02052-16.
23. Matteelli A, Carvalho AC, Dooley KE, Kritski A. 2010. TMC207: the first compound of a new class of potent anti-tuberculosis drugs. Future Microbiol 5:849–858. https://doi.org/10.2217/fmb.10.50.
24. Andries K, Verhasselt P, Guillemont J, Göhlmann HWH, Neefs J-M, Winkler H, Van Gestel J, Timmerman P, Zhu M, Lee E, Williams P, de Chaffoy D, Huitric E, Hoffner S, Cambau E, Truffot PC, Lounis N, Jarlier V. 2005. A diarylquinoline drug active on the ATP synthase of *Mycobacterium tuberculosis*. Science 307:223–227. https://doi.org/10.1126/science.1106753.
25. Koul A, Dendouga N, Vergauwen K, Molenberghs B, Vranckx L, Willebrords R, Ristic Z, Lill H, Dorange I, Guillemont J, Bald D, Andries K. 2007. Diarylquinolines target subunit c of mycobacterial ATP synthase. Nat Chem Biol 3:323–324. https://doi.org/10.1038/nchembio884.
26. Haagsma AC, Podasca I, Koul A, Andries K, Guillemont J, Lill H, Bald D. 2011. Probing the interaction of the diarylquinoline TMC207 with its target mycobacterial ATP synthase. PLoS One 6:e23575. https://doi.org/10.1371/journal.pone.0023575.
27. Dupont C, Viljoen A, Thomas S, Roquet-Banères F, Herrmann J-L, Pethe K, Kremer L. 2017. Bedaquiline inhibits the ATP synthase in *Mycobacterium abscessus* and is effective in infected zebrafish. Antimicrob Agents Chemother 61:e01225-17. https://doi.org/10.1128/AAC.01225-17.
28. Biukovic G, Basak S, Manimekalai MSS, Rishikesan S, Roessle M, Dick T, Rao SPS, Hunke C, Grüber G. 2013. Variations of subunit {varepsilon} of the *Mycobacterium tuberculosis* F1Fo ATP synthase and a novel model for mechanism of action of the tuberculosis drug TMC207. Antimicrob Agents Chemother 57:168–176. https://doi.org/10.1128/AAC.01039-12.
29. Kundu S, Biukovic G, Grüber G, Dick T. 2016. Bedaquiline targets the ε subunit of mycobacterial F-ATP synthase. Antimicrob Agents Chemother 60:6977–6979. https://doi.org/10.1128/AAC.01291-16.
30. Pang Y, Zheng H, Tan Y, Song Y, Zhao Y. 2017. *In vitro* activity of bedaquiline against nontuberculous mycobacteria in China. Antimicrob Agents Chemother 61:e02627-16. https://doi.org/10.1128/AAC.02627-16.
31. Vesenbeckh S, Schönfeld N, Roth A, Bettermann G, Krieger D, Bauer TT, Rüssmann H, Mauch H. 2017. Bedaquiline as a potential agent in the treatment of *Mycobacterium abscessus* infections. Eur Respir J 49:1700083. https://doi.org/10.1183/13993003.00083-2017.
32. Obregón-Henao A, Arnett KA, Henao-Tamayo M, Massoudi L, Creissen E, Andries K, Lenaerts AJ, Ordway DJ. 2015. Susceptibility of *Mycobacterium*

abscessus to antimycobacterial drugs in preclinical models. Antimicrob Agents Chemother 59:6904–6912. https://doi.org/10.1128/AAC.00459-15.
33. Lerat I, Cambau E, Roth Dit Bettoni R, Gaillard J-L, Jarlier V, Truffot C, Veziris N. 2014. *In vivo* evaluation of antibiotic activity against *Mycobacterium abscessus*. J Infect Dis 209:905–912. https://doi.org/10.1093/infdis/jit614.
34. Philley JV, Wallace RJ, Benwill JL, Taskar V, Brown-Elliott BA, Thakkar F, Aksamit TR, Griffith DE. 2015. Preliminary results of bedaquiline as salvage therapy for patients with nontuberculous mycobacterial lung disease. Chest 148:499–506. https://doi.org/10.1378/chest.14-2764.
35. Cuthbertson L, Nodwell JR. 2013. The TetR family of regulators. Microbiol Mol Biol Rev 77:440–475. https://doi.org/10.1128/MMBR.00018-13.
36. Milano A, Pasca MR, Provvedi R, Lucarelli AP, Manina G, Ribeiro ALDJL, Manganelli R, Riccardi G. 2009. Azole resistance in *Mycobacterium tuberculosis* is mediated by the MmpS5-MmpL5 efflux system. Tuberculosis (Edinb) 89:84–90. https://doi.org/10.1016/j.tube.2008.08.003.
37. Hartkoorn RC, Uplekar S, Cole ST. 2014. Cross-resistance between clofazimine and bedaquiline through upregulation of MmpL5 in *Mycobacterium tuberculosis*. Antimicrob Agents Chemother 58:2979–2981. https://doi.org/10.1128/AAC.00037-14.
38. Halloum I, Viljoen A, Khanna V, Craig D, Bouchier C, Brosch R, Coxon G, Kremer L. 2017. Resistance to thiacetazone derivatives active against *Mycobacterium abscessus* involves mutations in the MmpL5 transcriptional repressor MAB_4384. Antimicrob Agents Chemother 61:e02509-16. https://doi.org/10.1128/AAC.02509-16.
39. Richard M, Gutiérrez AV, Viljoen AJ, Ghigo E, Blaise M, Kremer L. 2018. Mechanistic and structural insights into the unique TetR-dependent regulation of a drug efflux pump in *Mycobacterium abscessus*. Front Microbiol 9:649. https://doi.org/10.3389/fmicb.2018.00649.
40. Viljoen A, Blaise M, de Chastellier C, Kremer L. 2016. *MAB_3551c* encodes the primary triacylglycerol synthase involved in lipid accumulation in *Mycobacterium abscessus*. Mol Microbiol 102:611–627. https://doi.org/10.1111/mmi.13482.
41. Bailey TL, Boden M, Buske FA, Frith M, Grant CE, Clementi L, Ren J, Li WW, Noble WS. 2009. MEME Suite: tools for motif discovery and searching. Nucleic Acids Res 37:W202–W208. https://doi.org/10.1093/nar/gkp335.
42. Rominski A, Selchow P, Becker K, Brülle JK, Dal Molin M, Sander P. 2017. Elucidation of *Mycobacterium abscessus* aminoglycoside and capreomycin resistance by targeted deletion of three putative resistance genes. J Antimicrob Chemother 72:2191–2200. https://doi.org/10.1093/jac/dkx125.
43. Viljoen A, Gutiérrez AV, Dupont C, Ghigo E, Kremer L. 2018. A simple and rapid gene disruption strategy in *Mycobacterium abscessus*: on the design and application of glycopeptidolipid mutants. Front Cell Infect Microbiol 8:69. https://doi.org/10.3389/fcimb.2018.00069.
44. Griffith DE, Girard WM, Wallace RJ. 1993. Clinical features of pulmonary disease caused by rapidly growing mycobacteria. An analysis of 154 patients. Am Rev Respir Dis 147:1271–1278. https://doi.org/10.1164/ajrccm/147.5.1271.
45. Sermet-Gaudelus I, Le Bourgeois M, Pierre-Audigier C, Offredo C, Guillemot D, Halley S, Akoua-Koffi C, Vincent V, Sivadon-Tardy V, Ferroni A, Berche P, Scheinmann P, Lenoir G, Gaillard J-L. 2003. *Mycobacterium abscessus* and children with cystic fibrosis. Emerg Infect Dis 9:1587–1591. https://doi.org/10.3201/eid0912.020774.
46. Ripoll F, Pasek S, Schenowitz C, Dossat C, Barbe V, Rottman M, Macheras E, Heym B, Herrmann J-L, Daffé M, Brosch R, Risler J-L, Gaillard J-L. 2009. Non mycobacterial virulence genes in the genome of the emerging pathogen *Mycobacterium abscessus*. PLoS One 4:e5660. https://doi.org/10.1371/journal.pone.0005660.
47. Balhana RJC, Singla A, Sikder MH, Withers M, Kendall SL. 2015. Global analyses of TetR family transcriptional regulators in mycobacteria indicates conservation across species and diversity in regulated functions. BMC Genomics 16:479. https://doi.org/10.1186/s12864-015-1696-9.
48. Chen Y, Chen J, Zhang S, Shi W, Zhang W, Zhu M, Zhang Y. 2018. Novel mutations associated with clofazimine resistance in *Mycobacterium abscessus*. Antimicrob Agents Chemother 62:e00544-18. https://doi.org/10.1128/AAC.00544-18.
49. Alexander DC, Vasireddy R, Vasireddy S, Philley JV, Brown-Elliott BA, Perry BJ, Griffith DE, Benwill JL, Cameron ADS, Wallace RJ. 2017. Emergence of *mmpT5* variants during bedaquiline treatment of *Mycobacterium intracellulare* lung disease. J Clin Microbiol 55:574–584. https://doi.org/10.1128/JCM.02087-16.
50. Zhang S, Chen J, Cui P, Shi W, Zhang W, Zhang Y. 2015. Identification of novel mutations associated with clofazimine resistance in *Mycobacterium tuberculosis*. J Antimicrob Chemother 70:2507–2510. https://doi.org/10.1093/jac/dkv150.
51. Somoskovi A, Bruderer V, Hömke R, Bloemberg GV, Böttger EC. 2015. A mutation associated with clofazimine and bedaquiline cross-resistance in MDR-TB following bedaquiline treatment. Eur Respir J 45:554–557. https://doi.org/10.1183/09031936.00142914.
52. Andries K, Villellas C, Coeck N, Thys K, Gevers T, Vranckx L, Lounis N, de Jong BC, Koul A. 2014. Acquired resistance of *Mycobacterium tuberculosis* to bedaquiline. PLoS One 9:e102135. https://doi.org/10.1371/journal.pone.0102135.
53. Gupta S, Cohen KA, Winglee K, Maiga M, Diarra B, Bishai WR. 2014. Efflux inhibition with verapamil potentiates bedaquiline in *Mycobacterium tuberculosis*. Antimicrob Agents Chemother 58:574–576. https://doi.org/10.1128/AAC.01462-13.
54. Viljoen A, Dubois V, Girard-Misguich F, Blaise M, Herrmann J-L, Kremer L. 2017. The diverse family of MmpL transporters in mycobacteria: from regulation to antimicrobial developments. Mol Microbiol 104:889–904. https://doi.org/10.1111/mmi.13675.
55. Li H. 2013. Aligning sequence reads, clone sequences and assembly contigs with BWA-MEM. arXiv arXiv:1303-3997v2 [q-bio.GN].
56. Li H, Handsaker B, Wysoker A, Fennell T, Ruan J, Homer N, Marth G, Abecasis G, Durbin R, 1000 Genome Project Data Processing Subgroup. 2009. The sequence alignment/map format and SAMtools. Bioinformatics 25:2078–2079. https://doi.org/10.1093/bioinformatics/btp352.
57. Harris SR, Feil EJ, Holden MTG, Quail MA, Nickerson EK, Chantratita N, Gardete S, Tavares A, Day N, Lindsay JA, Edgeworth JD, de Lencastre H, Parkhill J, Peacock SJ, Bentley SD. 2010. Evolution of MRSA during hospital transmission and intercontinental spread. Science 327:469–474. https://doi.org/10.1126/science.1182395.
58. Aiyar A, Xiang Y, Leis J. 1996. Site-directed mutagenesis using overlap extension PCR. Methods Mol Biol 57:177–191. https://doi.org/10.1385/0-89603-332-5:177.

CHAPTER IV

Study of *Mycobacterium abscessus* resistance mechanism by the TetR-MmpL system

The TetR-family transcription factor MAB_2299c regulates the expression of two distinct MmpS-MmpL efflux pumps involved in cross-resistance to clofazimine and bedaquiline in *Mycobacterium abscessus*.

Gutiérrez, A.V., Richard, M., Roquet-Banères, F., Viljoen, A. and Kremer, L., 2019.

Antimicrobial agents and chemotherapy, pp.AAC-01000.

7. CHAPTER IV: Study of *Mycobacterium abscessus* resistance mechanism by the TetR-MmpL system

7.3. Article 3: The TetR-family transcription factor MAB_2299c regulates the expression of two distinct MmpS-MmpL efflux pumps involved in cross-resistance to clofazimine and bedaquiline in *Mycobacterium abscessus.*

In an elegant review Ghosh and O'Connor (2017) described different forms of redundancy in bacteria that act as contingency plans for enhancing bacterial survival and adaptation to extreme conditions in the environment and the host. Genetic redundancy can rely on two copies of the same gene encoding proteins that can compensate each other. This event can result from gene duplication and may involve the same regulatory network and the maintenance of each depends on individual selective pressures. Interestingly, considering gene duplication as the most likely event for molecular redundancy, other sources such as horizontal gene transfer and convergent evolution are usually underestimated.

MmpLs are membrane proteins that can mediate the export of multiple substrates, including lipids and drugs, positioning them as attractive targets, such as MmpL3, the mycolic acid transporter, inhibited by multiple small molecules (Dupont et al. 2016). Notably, *M. abscessus* contains a large repertoire of MmpL whose biological functions remain largely unknown (Viljoen et al. 2017).

We therefore we addressed whether resistance to clofazimine and/or bedaquiline is associated to a genetic redundancy of MmpL proteins. Homology analysis of the *M. abscessus* MmpS and MmpL repertoire unravelled MAB_1135c-MAB_1134c as the closest paralogous to MAB_2300-MAB_2301. Followed a strategy similar to the one used previously to identify the mechanism of cross-resistance to clofazimine and bedaquiline (Richard et al. 2019). We characterized *MAB_1135c-MAB_1134c* as an additional locus regulated by MAB_2299c.

These results reinforce our hypothesis about the redundancy of MmpL proteins in the multidrug resistance phenotype of *M. abscessus.*

zac-aac/zac01019/zac8327d19z | xppws | S=5 | 8/17/19 | 5:41 | 4/Color Fig: 1,4,6 | ArtID: 01000-19 | DOI:10.1128/AAC.01000-19 | CE: SSV

Editor: Kelly E. Dooley | Section: Mechanisms of Resistance | Designation: T

AMERICAN SOCIETY FOR MICROBIOLOGY | Antimicrobial Agents and Chemotherapy®

MECHANISMS OF RESISTANCE

The TetR Family Transcription Factor MAB_2299c Regulates the Expression of Two Distinct MmpS-MmpL Efflux Pumps Involved in Cross-Resistance to Clofazimine and Bedaquiline in *Mycobacterium abscessus*

AQ: au

Ana Victoria Gutiérrez,[a] Matthias Richard,[a] Françoise Roquet-Banères,[a] Albertus Viljoen,[a]* Laurent Kremer[a,b]

[a]Institut de Recherche en Infectiologie de Montpellier (IRIM), Université de Montpellier, CNRS UMR 9004, Montpellier, France
[b]INSERM, IRIM, Montpellier, France

ABSTRACT *Mycobacterium abscessus* is a human pathogen responsible for severe respiratory infections, particularly in patients with underlying lung disorders. Notorious for being highly resistant to most antimicrobials, new therapeutic approaches are needed to successfully treat *M. abscessus*-infected patients. Clofazimine (CFZ) and bedaquiline (BDQ) are two antibiotics used for the treatment of multidrug-resistant tuberculosis and are considered alternatives for the treatment of *M. abscessus* pulmonary disease. To get insights into their mechanisms of resistance in *M. abscessus*, we previously characterized the TetR transcriptional regulator MAB_2299c, which controls expression of the *MAB_2300-MAB_2301* genes, encoding an MmpS-MmpL efflux pump. Here, *in silico* studies identified a second *mmpS-mmpL* (*MAB_1135c-MAB_1134c*) target of MAB_2299c. A palindromic DNA sequence upstream of *MAB_1135c*, sharing strong homology with the one located upstream of *MAB_2300*, was found to form a complex with the MAB_2299c regulator in electrophoretic mobility shift assays. Deletion of *MAB_1135c-1134c* in a wild-type strain led to increased susceptibility to both CFZ and BDQ. In addition, deletion of these genes in a CFZ/BDQ-susceptible mutant lacking *MAB_2299c* as well as *MAB_2300-MAB_2301* further exacerbated the sensitivity of this strain to both drugs *in vitro* and inside macrophages. Overall, these results indicate that *MAB_1135c-1134c* encodes a new MmpS-MmpL efflux pump system involved in the intrinsic resistance to CFZ and BDQ. They also support the view that MAB_2299c controls the expression of two separate MmpS-MmpL efflux pumps, substantiating the importance of *MAB_2299c* as a marker of resistance to be considered when assessing drug susceptibility in clinical isolates.

KEYWORDS EMSA, MmpL, *Mycobacterium abscessus*, TetR regulator, bedaquiline, clofazimine, drug resistance mechanisms, efflux pumps

AQ: A

Mycobacterium abscessus is a rapidly growing nontuberculous mycobacterium (NTM) and an emerging pathogen that causes sporadic outbreaks worldwide (1). The *M. abscessus* complex comprises three subspecies, *M. abscessus sensu stricto*, *Mycobacterium bolletii*, and *Mycobacterium massiliense* (2, 3), differing in their drug susceptibility profile and evolution (4). Genomic analyses indicated that, in addition to specific genes linked to mycobacterial virulence, other virulence genes found in *Pseudomonas aeruginosa* and *Burkholderia cepacia*, pathogens commonly isolated from the lungs of cystic fibrosis (CF) patients and acquired by horizontal transfer, are also present in *M. abscessus* (5, 6). Likewise, the *M. abscessus* complex represents the most important cause of pulmonary infections by rapidly growing NTM in patients with chronic lung diseases, such as bronchiectasis and CF (7, 8), which can result in nodular and cavitary granulomas and persistent lung infection (7–10). Patients with chronic *M. abscessus*

Citation Gutiérrez AV, Richard M, Roquet-Banères F, Viljoen A, Kremer L. 2019. The TetR family transcription factor MAB_2299c regulates the expression of two distinct MmpS-MmpL efflux pumps involved in cross-resistance to clofazimine and bedaquiline in *Mycobacterium abscessus*. Antimicrob Agents Chemother 63:e01000-19. https://doi.org/10.1128/AAC.01000-19.

Address correspondence to Laurent Kremer, laurent.kremer@irim.cnrs.fr.

* Present address: Albertus Viljoen, Louvain Institute of Biomolecular Science and Technology, Université Catholique de Louvain, Louvain-la-Neuve, Belgium.

A.V.G. and M.R. contributed equally to this work.

Received 14 May 2019
Returned for modification 23 June 2019
Accepted 19 July 2019
Accepted manuscript posted online 22 July 2019
Published

zac-aac/zac01019/zac8327d19z | xppws | S=5 | 8/17/19 | 5:41 | 4/Color Fig: 1,4,6 | ArtID: 01000-19 | DOI:10.1128/AAC.01000-19 | CE: SSV

infections present higher rates of pulmonary function decline than those without NTM infections (11). Recent epidemiological studies also documented the transmission of dominant circulating *M. abscessus* clones that have spread globally between hospitals (12), highlighting *M. abscessus* as a major threat in many CF centers worldwide (8).

A recent meta-analysis reported that the treatment success rate across all patients with *M. abscessus* pulmonary disease was 45.6%, reaffirming that treatment outcomes are unsatisfactory (13). *M. abscessus* treatment remains very challenging. The American Thoracic Society (ATS)/Infectious Disease Society of America recommend multidrug therapy that includes a macrolide and one or more parenteral drugs (amikacin plus cefoxitin or imipenem) (7). *M. abscessus* has developed a large panel of drug resistance mechanisms that considerably restrict the available antimicrobials to treat these infections (14–16). They include the acquisition of mutations in the target genes, intrinsic resistance to drugs attributed to low permeability of the *M. abscessus* cell envelope, defective drug-activating systems that convert prodrugs into metabolically active compounds, induction of drug export systems, and the expression of numerous enzymes that can modify either the drug target or the drug itself (15, 17). Overall, this leads to the phenomenal resistance level of *M. abscessus* to most classes of antibiotics used for treatment of other infectious diseases, such as macrolides, aminoglycosides, rifamycins, β-lactams, quinolones, and tetracyclines.

Fueling a drug pipeline to discover and develop improved and safer treatments for *M. abscessus* infections relies on *de novo* drug discovery to identify new pharmacophores as well as repositioning of antimicrobials acting against validated targets for other infectious diseases (18). In this context, the repositioning of clofazimine (CFZ) and bedaquiline (BDQ) is gaining increasing interest for the treatment of *M. abscessus* pulmonary disease. CFZ is an orally administered drug, originally approved for the treatment of leprosy, that is reduced by the type 2 NADH:quinone oxidoreductase, a key component in the electron transport chain (19). *In vitro* studies highlighted its advantages in multidrug regimens against *M. abscessus*, acting in synergism with amikacin (AMK) (20) or tigecycline (TIG) (21) and in preventing bacterial regrowth observed with clarithromycin or AMK alone (22). BDQ, approved by the Food and Drug Administration and the European Medicines Agency for the treatment of multidrug-resistant tuberculosis, is a diarylquinoline that targets the ATP synthase in *M. tuberculosis* (23). We and others showed that BDQ exhibits very low MICs against NTM, including clinical *M. abscessus* strains from CF and non-CF patients (24–26). However, despite being a potent growth inhibitor at low concentrations, BDQ lacks bactericidal activity against *M. abscessus* (26, 27). In the *M. abscessus* zebrafish model of infection, BDQ acts very efficiently by reducing the number and size of abscesses, which represent a marker of disease severity and uncontrolled infection (28), protecting the infected larvae from killing by *M. abscessus* (26). The mode of action of BDQ in *M. abscessus* relies on the rapid depletion of ATP, and the transfer of single point mutations into the chromosomal *atpE* locus conferred high resistance levels to BDQ (26). In addition to *atpE*, mutations associated with cross-resistance to CFZ and BDQ were recently uncovered in *MAB_2299c*, encoding a TetR-family transcription factor that controls the expression level of the MmpS-MmpL (MAB_2300-2301) efflux pump (29).

Considering the extremely high number of TetR regulators and MmpL proteins in *M. abscessus* (30), it remains possible that additional TetR-dependent MmpS-MmpL efflux pump systems contribute to the drug resistance profile of *M. abscessus* to CFZ and BDQ. In this study, we identified a new *mmpS-mmpL* gene cluster (*MAB_1135c-MAB_1134c*; termed *MAB_1135c-1134c*) whose expression is also dependent on the MAB_2299c TetR repressor. Genetic approaches were used to demonstrate that this gene cluster participates in cross-resistance to both CFZ and BDQ. These findings expand our current understanding about transcriptional regulation of the MmpS-MmpL efflux pumps in mycobacteria and mechanisms of drug resistance in one of the most difficult-to-treat mycobacterial species.

zac-aac/zac01019/zac8327d19z | xppws | S=5 | 8/17/19 | 5:41 | 4/Color Fig: 1,4,6 | ArtID: 01000-19 | DOI:10.1128/AAC.01000-19 | CE: SSV

RESULTS

Identification of *MAB_1135c-1134c* as a close paralog of *MAB_2300-2301*. We recently demonstrated that mutations in the TetR regulator MAB_2299c lead to upregulation of the *MAB_2300-2301* gene cluster, encoding the MmpS-MmpL efflux pump membrane proteins accounting for cross-resistance to CFZ and BDQ in *M. abscessus* (29). With the objective to identify other potential MmpS-MmpL couples that are functionally homologous to MAB_2300-2301 and participate in CFZ/BDQ resistance, we performed a homology analysis of all *M. abscessus* MmpS and MmpL paralogs as well as all of the TetR family transcription factors present in close genomic vicinity to these MmpS-MmpL couples. This analysis identified MAB_1135c-1134c as the closest paralo- F1 gous MmpS-MmpL couple to MAB_2300-2301 (Fig. 1A). In addition, the TetR protein MAB_1136, whose gene is located upstream of *MAB_1135c*, was uncovered as the closest homologue of MAB_2299c. Indeed, a comparison of the two loci that contain the *mmpS-mmpL* genes as well as their adjacent upstream (containing the *tetR* genes and their nucleotide target sequences) and downstream nucleotide sequences suggests that one of the two *tetR-mmpS-mmpL* clusters arose as a duplication of the other (Fig. 1B), representing these genes as potential candidates in CFZ/BDQ cross-resistance.

Expression of *MAB_1135c-1134c* is not controlled by the TetR regulator MAB_1136. Careful inspection of the genomic organization around the *MAB_1135c-1134c* locus indicated that *MAB_1136* is an adjacent and divergently orientated gene AQ:B/F2 (Fig. 2A). To test the hypothesis that this potential regulator controls the expression of the *MAB_1135c-1134c* gene cluster, a *MAB_1136* deletion mutant was produced. This was achieved by using a recently developed strategy based on a new suicide vector, pUX1-*katG*, allowing easy and rapid generation of unmarked genetic deletions in the *M. abscessus* chromosome, facilitated by the presence of the brightly red fluorescent tdTomato positive selectable marker and the *katG* counterselectable marker (29, 31, 32). The selected INH-resistant, KAN-sensitive, and nonfluorescent clones were subsequently genotyped by PCR/sequencing analysis to confirm unmarked deletion of *MAB_1136* (Fig. 2A).

The drug susceptibility pattern of the Δ*MAB_1136* strain and its parental progenitor to imipenem (IPM; control drug), CFZ, and BDQ was next assessed by comparing growth on agar plates containing the corresponding drugs (Fig. 2B). The two strains displayed similar growth on agar supplemented with 16 μg/ml IPM, 0.125 μg/ml BDQ, or 1 μg/ml CFZ, indicating that the absence of *MAB_1136* does not influence the sensitivity of the strain to these compounds. These results were subsequently confirmed by T1 the failure of the Δ*MAB_1136* strain to show an upshift in the MIC levels (Table 1). Hypothesizing that MAB_1136 represses transcriptional expression of *MAB_1135c-1134c*, quantitative reverse transcription-PCR (qRT-PCR) analysis was performed, which failed to show increased expression of *MAB_1134c* or *MAB_1135c* in the Δ*MAB_1136* strain (data not shown). Together, these results suggest that expression of *MAB_1135c-1134c* is not controlled by MAB_1136.

The TetR regulator MAB_2299c represses expression of *MAB_1135c-1134c*. As mentioned above, our *in silico* study revealed a high level of primary protein sequence identity between MAB_1136 and MAB_2299c (Fig. 1A), which might point to a role for the latter in transcriptional repression of *MAB_1135c-1134c* in the absence of such a function of the former. Interestingly, we recently identified MAB_2299c as a TetR AQ: C transcriptional regulator that represses its *mmpS-mmpL* (*MAB_2300-2301*) target genes and found that different single-point mutations in MAB_2299c were associated with upregulation of the *MAB_2300-2301* efflux pump system, leading to cross-resistance to CFZ and BDQ (29). Therefore, to interrogate whether MAB_2299c regulates other target genes belonging to the MmpS-MmpL systems, qRT-PCR was performed on 30 *mmpL* genes identified in the *M. abscessus* chromosome (30) in a Δ*MAB_2299c* deletion mutant (29). This systematic analysis clearly indicated that, in addition to *MAB_2301*, identified previously (29), only one other *mmpL* gene (*MAB_1134c*) was upregulated in F3 the Δ*2299c* strain (Fig. 3A).

zac-aac/zac01019/zac8327d19z | xppws | S=5 | 8/17/19 | 5:41 | 4/Color Fig: 1,4,6 | ArtID: 01000-19 | DOI:10.1128/AAC.01000-19 | CE: SSV

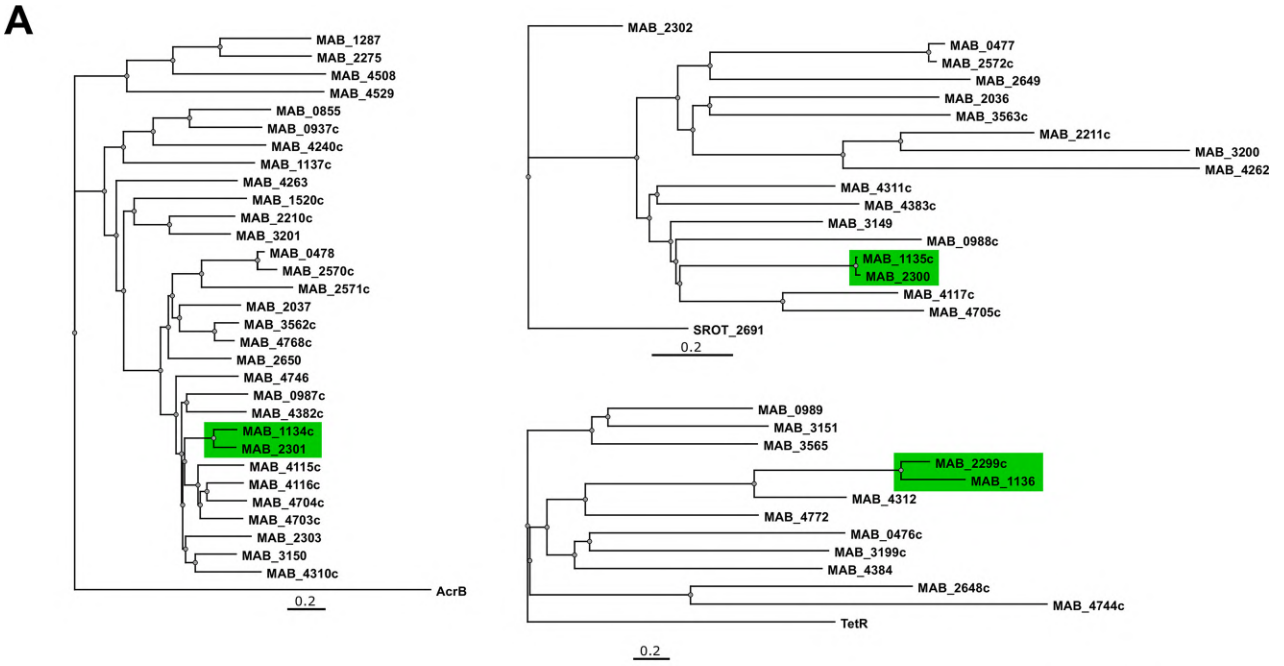

FIG 1 Closest paralogs of the MmpS-MmpL couple MAB_2300-2301, MAB_1135c-1134c, arose as a result of a gene duplication event. (A) Homology trees of all *M. abscessus* MmpL (left), all *M. abscessus* MmpS (top right), and several *M. abscessus* TetR/MarR family transcriptional regulators in close

(Continued on next page)

zac-aac/zac01019/zac8327d19z | xppws | S=5 | 8/17/19 | 5:41 | 4/Color Fig: 1,4,6 | ArtID: 01000-19 | DOI:10.1128/AAC.01000-19 | CE: SSV

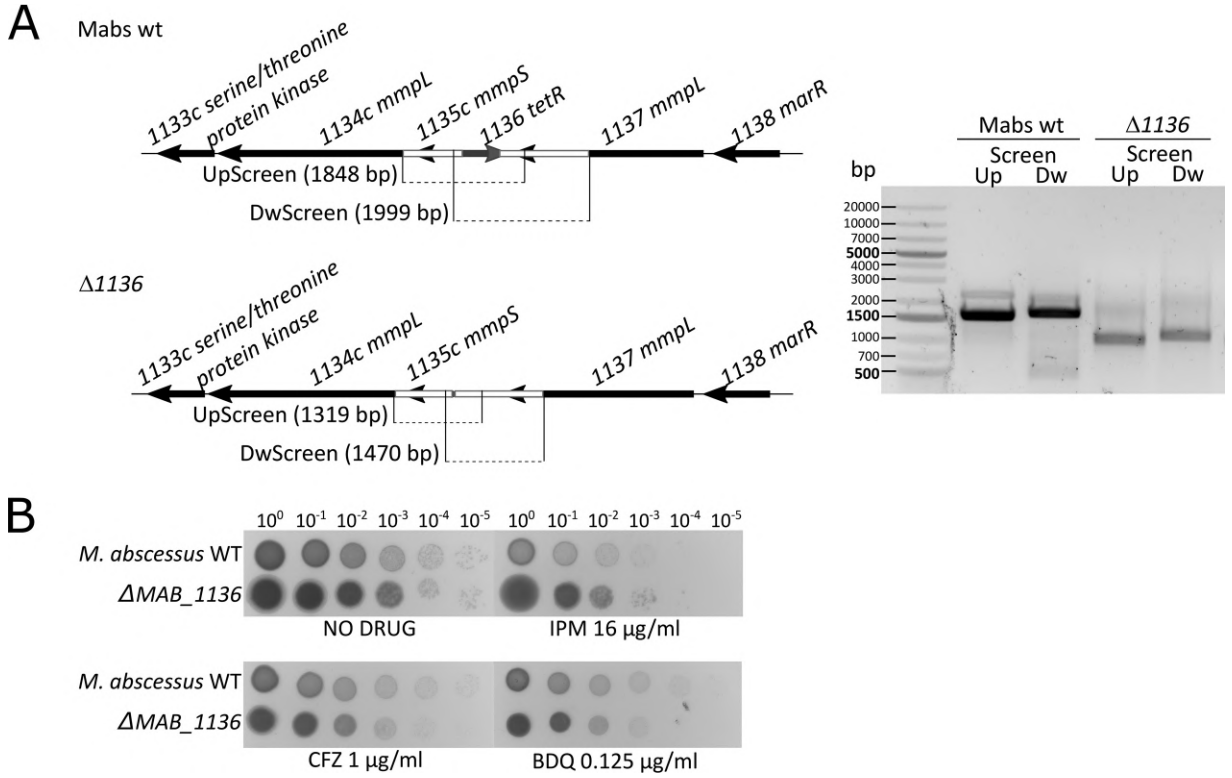

FIG 2 Deletion of *MAB_1136* does not confer resistance to CFZ or BDQ. (A) Genome organization of *MAB_1136* in *M. abscessus* and the screening approach used to confirm deletion of *MAB_1136*. White lines in the drawing represent the left and right arms flanking the region of *MAB_1136* targeted for deletion and exploited in the two-step homologous recombination procedure to generate the Δ*MAB_1136* strain. (Left) Dotted lines represent the size of the expected PCR products in *M. abscessus* WT and Δ*MAB_1136* strains. (Right) Gel migration profile of the amplicons in *M. abscessus* WT and Δ*MAB_1136* strains. All PCR products were purified and sequenced to confirm the *MAB_1136* deletion genotype. Up stands for upstream and Dw stands for downstream amplicons. (B) Susceptibility/resistance profiles of *M. abscessus* WT and Δ*MAB_1136* strains to various drugs. Five microliters of a 10-fold serially diluted bacterial suspension was spotted on 7H10^{OADC} alone or supplemented with 16 μg/ml imipenem (IPM), 1 μg/ml clofazimine (CFZ), or 0.125 μg/ml bedaquiline (BDQ). Growth was observed after 4 days of incubation at 37°C. All experiments were done on three independent occasions.

Increased transcription of both *mmpS-mmpL* gene clusters (*MAB_1135c-1134c* and *MAB_2300-2301*) was next confirmed by additional qRT-PCR analysis in both the parental *M. abscessus* smooth (S) strain and in the Δ*MAB_2299c* strain (Fig. 3B). Complementation of the Δ*MAB_2299c* strain by introducing the pMV261-*MAB_2299c* construct (Δ*MAB_2299c*.C) led to reduced transcriptional levels of both *mmpS-mmpL* pairs, as anticipated. The expression levels of the unrelated control gene *tgs1*, encoding the triacylglycerol synthase involved in the synthesis and accumulation of triglycerides in *M. abscessus* (33), remained unchanged in the various strains tested. As anticipated, the 6 CFZ-resistant mutants harboring mutations in MAB_2299c and associated with upregulation of the *MAB_2300-2301* efflux pump system (29) also expressed higher transcriptional levels of *MAB_1135c* and *MAB_1134c* (see Fig. S1 in the supplemental material). Together, these results indicate that expression of both *MAB_2300-2301* and *MAB_1135c-1134c* gene couples is repressed by MAB_2299c under normal growth conditions.

Unmarked deletion of the *MAB_1135c-1134c* efflux pump leads to increased susceptibility to CFZ and BDQ. Using the same strategy as that used to produce the

FIG 1 Legend (Continued)
proximity to MmpS-MmpL couples (bottom right). The scale bar below each tree indicates 0.2 amino acid substitutions per site. The trees were rooted to *Escherichia coli* AcrB (MmpL) and TetR (transcriptional regulator) and *Segniliparus rotundus* MmpS ortholog SROT_2691 (MmpS). (B) Dot plot generated using the YASS genomic similarity tool (http://bioinfo.lifl.fr/yass/yass.php), showing nucleotide similarity between the *MAB_2299c-2300-2301* and the *MAB_1136-1135c-1134c* loci (highlighted by a light blue inverted-L-shaped box). Green lines indicate forward matches, and red lines indicate reverse matches. The intergenic regions (IR) between the *tetR* genes (*MAB_2299c* and *MAB_1136*) and the *mmpS* genes (*MAB_2300* and *MAB_1135c*) are highlighted by light gray trapezoidal boxes.

zac-aac/zac01019/zac8327d19z | xppws | S=5 | 8/17/19 | 5:41 | 4/Color Fig: 1,4,6 | ArtID: 01000-19 | DOI:10.1128/AAC.01000-19 | CE: SSV

TABLE 1 Drug susceptibility/resistance profile of WT CIP104536, Δ*MAB_2299c*, Δ*MAB_1135c-1134c*, Δ*MAB_2299c-2300-2301*, Δ*MAB_2299c-2300-2301-1135c-1134c*, and Δ*MAB_1136* strains to various drugs

Strain	MIC_{99} (μg/ml)							
	IPM[a]	AMK	EMB	CFZ	TIG	LNZ	MOX	BDQ
CIP104536	8	16	16	2	16	64	32	0.25
Δ*MAB_2299c*	8	16	16	4	16	64	32	0.5
Δ*MAB_1135c-1134c*	8	16	16	0.5	16	64	32	0.125–0.06
Δ*MAB_2299c-2300-2301*	8	16	16	0.5	16	64	32	0.03–0.015
Δ*MAB_2299c-2300-2301-1135c-1134c*	8	16	16	0.25	16	64	32	0.015–0.0075
Δ*MAB_1136*	8	16	16	1	ND	ND	ND	0.125

[a]MIC_{99} values were visually determined on Middlebrook 7H10 agar after 4 days at 37°C. IPM, imipenem; AMK, amikacin; BDQ, bedaquiline; CFZ, clofazimine; EMB, ethambutol; TIG, tigecycline; LNZ, linezolid; MOX, moxifloxacin; ND, not determined.

Δ*MAB_1136* strain, a two-step homologous recombination procedure was first applied to generate a scarless deletion of *MAB_1135c-1134c* in the *M. abscessus* wild type (WT) (Fig. 3C, left). This unmarked deletion mutant, designated the Δ*MAB_1135c-1134c* strain, was subjected to PCR and sequencing analysis to confirm gene deletion (Fig. 3C, upper right). Although WT and Δ*MAB_1135c-1134c* strains displayed similar growth on agar without drugs or agar supplemented with 16 μg/ml IPM, AMK, or ethambutol (EMB), the mutant strain showed reduced growth in the presence of 1 μg/ml CFZ or 0.06 μg/ml BDQ (Fig. 3D). These results were confirmed by determination of the MIC values of CFZ and BDQ against the Δ*MAB_1135c-1134c* strain, which were almost 4 times lower than those of the parental strain (Table 1). Overall, this increased susceptibility to both drugs strongly suggests that MAB_1135c-1134c plays a role in intrinsic resistance to these compounds. That no differences in MIC values were observed with the unrelated drugs IPM, AMK, and EMB indicates that the drug efflux mechanism mediated by MAB_1135c-1134c is specific to CFZ and BDQ.

Since we previously demonstrated that a mutant lacking *MAB_2299c* and *MAB_2300-2301* was more sensitive to CFZ/BDQ, we next addressed whether the additional deletion of *MAB_1135c-1134c* in this mutant strain would further increase the susceptibility to these drugs. This was achieved by generating an unmarked deletion of *MAB_1135c-1134c* in the Δ*MAB_2299c-2300-2301* background (Fig. 3C). PCR analyses confirmed deletion of the genes, yielding a strain missing 5 genes: *MAB_2299c*, encoding the central transcriptional regulator, and its two pairs of *mmpS-mmpL* target genes. Whereas this quintuple mutant exhibited growth similar to that of the WT strain or the parental Δ*MAB_2299c-2300-MAB_2301* triple mutant in the absence of drugs (control plates) or in the presence of IPM, AMK, or EMB, it showed increased sensitivity to both CFZ and BDQ (Fig. 3D). The near absence of growth of the quintuple mutant in the presence of 0.06 μg/ml BDQ indicates that deletion of the second MmpS-MmpL couple further enhances the level of susceptibility of the strain. The MIC values of the quintuple mutant were 8-fold lower for CFZ and 16- to 32-fold lower for BDQ than those of the WT strain and 2-fold lower for both drugs compared to levels for the triple mutant lacking only one MmpS-MmpL pair (Table 1). The multiple deletion had no effect on the MIC of other drugs, including IPM, AMK, EMB, moxifloxacine (MOX), linezolid (LNZ), and tigecycline (TIG) (Table 1). As expected, the Δ*MAB_2299c* strain, in which both *MAB_2300-2301* and *MAB_1135c-1134c* are induced (Fig. 3B), failed to show growth inhibition in the presence of CFZ or BDQ (Fig. 3D) and displayed a 2-fold increased resistance to both drugs compared to that of the WT strain, as reported previously (29).

Collectively, these results indicate that both the *MAB_2300-2301* and the *MAB_1135c-1134c* efflux pump systems operate simultaneously in the resistance mechanism in *M. abscessus* against CFZ and BDQ.

MAB_2299c binds to a palindromic sequence upstream of *MAB_1135c*. We previously demonstrated that MAB_2299c binds to a palindromic sequence up-

zac-aac/zac01019/zac8327d19z | xppws | S=5 | 8/17/19 | 5:41 | 4/Color Fig: 1,4,6 | ArtID: 01000-19 | DOI:10.1128/AAC.01000-19 | CE: SSV

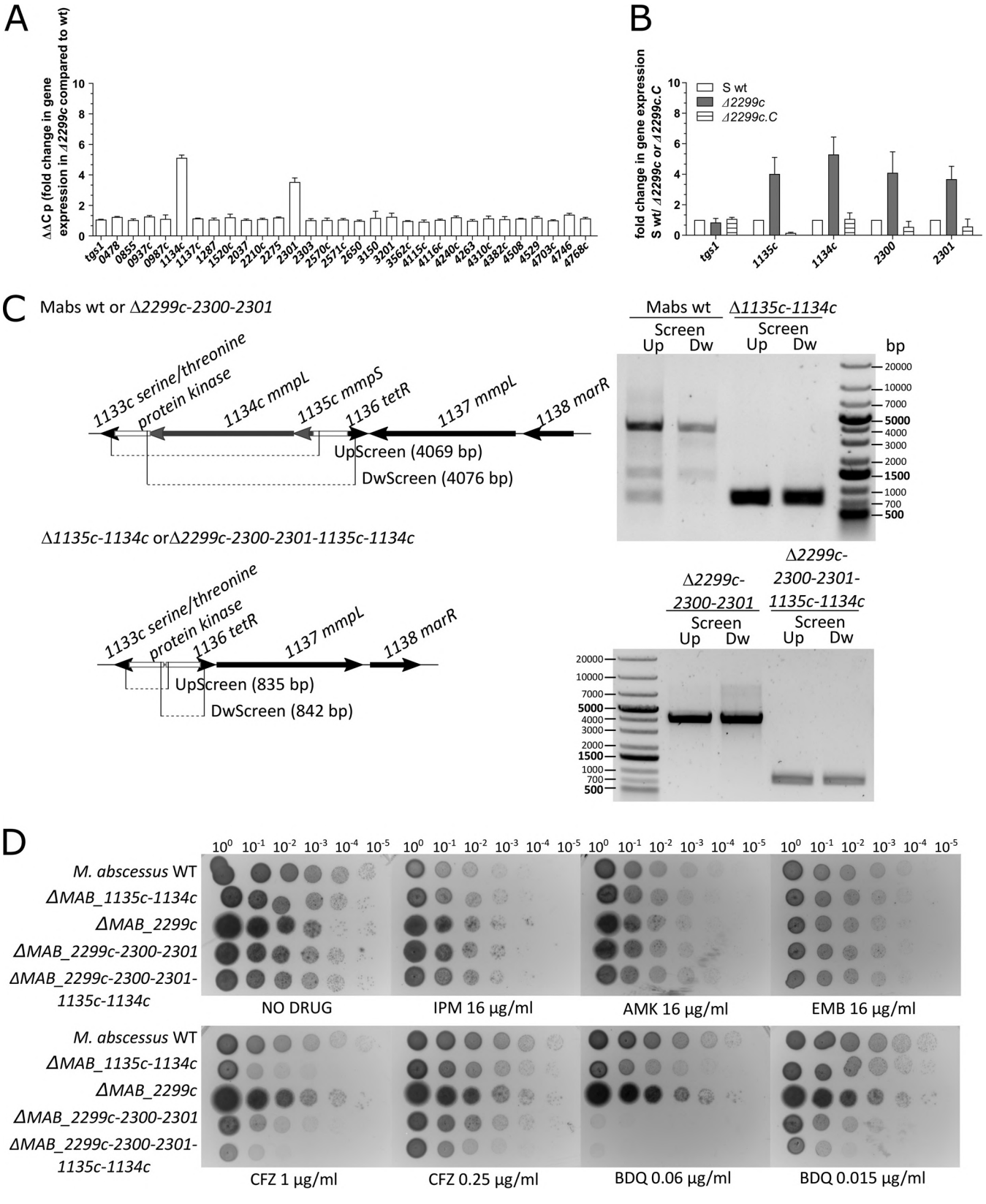

FIG 3 MAB_2299c represses expression of two distinct MmpS-MmpL efflux pump systems. (A) qRT-PCR analysis showing the transcriptional expression profile of 30 *mmpL* genes in the Δ*MAB_2299c* strain. (B) qRT-PCR analysis showing the transcriptional profiles of the *mmpS-mmpL* couples *MAB_1135c-1134c* and *MAB_2300-2301* in *M. abscessus* WT, the Δ*MAB_2299c* strain, and its Δ*MAB_2299c*.C complemented derivative. Results are expressed as fold induction levels in the mutant strains relative to levels of the parental strain. Error bars indicate standard deviations. Relative gene expression was calculated using the $2^{-\Delta\Delta CT}$ method with E correction. Data are representative of two independent experiments. (C) Genome organization of the *mmpS-mmpL* couple *MAB_1135c-1134c* in

(Continued on next page)

zac-aac/zac01019/zac8327d19z | xppws | S=5 | 8/17/19 | 5:41 | 4/Color Fig: 1,4,6 | ArtID: 01000-19 | DOI:10.1128/AAC.01000-19 | CE: SSV

stream of *MAB_2300*. That MAB_2299c also represses transcription of *MAB_1135c-1134c* suggested that it recognizes a conserved DNA-binding site located upstream of *MAB_1135c*. Using the MEME Suite software, we identified in the intergenic region upstream of *MAB_1135c* two palindromic sequences comprised of 7 nucleotides that are fully conserved with those found in the DNA-binding site upstream of *MAB_2300* (Fig. 4A). However, a major difference between the two sequences relies on a short spacer between the two palindromic sequences upstream of *MAB_1135c* and a longer spacer between the two palindromic sequences upstream of *MAB_2300*.

To confirm binding of the regulator to this palindromic sequence, electrophoretic mobility shift assays (EMSAs) were done by incubating increasing concentrations of purified MAB_2299c with a 64-bp DNA segment containing the two palindromes identified upstream of *MAB_1135c* and labeled at its 5′ end with fluorescein (probe A). Under these conditions, a DNA-protein complex was detected and specificity of binding was demonstrated in a competition assay by adding increasing concentrations of the corresponding unlabeled DNA fragment (cold probe), which led to a dose-dependent decrease in DNA-protein complex formation (Fig. 4B). In the presence of an excess of unlabeled probe B, corresponding to a 64-bp DNA fragment containing the palindromic sequence found upstream of *MAB_2300*, previously reported to bind to MAB_2299c (29), a dose-dependent decrease in DNA-protein complex formation, similar to the one found with probe A, was noticed (Fig. 4B). This indicates that binding to probe A can be outcompeted by probe B, emphasizing the fact that MAB_2299c has the capacity to bind to both probes. However, in the presence of an excess of a nonrelated probe the shift was maintained, further indicating that a specific protein-DNA complex was formed only when the TetR regulator was incubated with DNA containing its specific target (Fig. 4B). In addition, a pronounced shift impairment was observed when the regulator was incubated with fluorescent probe C, a variant of probe A harboring multiple DNA substitutions within the palindromic sequence (Fig. 4C). This indicates that the TAACGCA/TGCGTTA motif in the palindrome (conserved in probes A and B) is required for optimal binding of MAB_2299c to its operator region.

***M. abscessus* lacking both MmpS-MmpL pairs is highly susceptible to CFZ or BDQ treatment in macrophages.** In the absence of drug treatment, all *M. abscessus* strains (WT, Δ*MAB_2299c*, Δ*MAB_1135c-1134c*, Δ*MAB_2299c-2300-2301*, and Δ*MAB_2299c-2300-2301-1135c-1134c* strains) grew similarly in 7H9$^{T/OADC}$ (Middlebrook 7H9 broth supplemented with 0.05% Tween 80 and 10% oleic acid, albumin, dextrose, catalase [OADC enrichment]) at 30°C (Fig. 5A), indicating that the multiple-gene deletion of the TetR regulator and its target genes does not influence mycobacterial growth. Exposure of WT cultures to 0.25 μg/ml BDQ (corresponding to 2× MIC) showed an important growth inhibition over the 4-day period of treatment with CFU numbers remaining constant over time, confirming the bacteriostatic effect of BDQ reported earlier (26) (Fig. 5A). As anticipated, growth of the Δ*MAB_2299c* strain was only partially inhibited, confirming the BDQ-resistant phenotype of the strain. However, deletion of either one or both MmpS-MmpL pairs in Δ*MAB_2299c* fully abrogated the BDQ resistance phenotype. Moreover, after 4 days of treatment, the CFU numbers of the MmpS-MmpL mutants were approximately 1 to 2 logs lower than those of the WT strain and the original inoculum, indicating that these strains in effect became susceptible to killing by BDQ (Fig. 5A). Similar growth profiles were obtained when the different strains were exposed to a lower concentration of BDQ (0.06 μg/ml) (data not shown).

FIG 3 Legend (Continued)

M. abscessus and the screening approach for identification of Δ*MAB_1135c-1134c* in the *M. abscessus* WT and Δ*MAB_2299c-2300-2301* genetic backgrounds. White lines in the drawing represent the left and right arms of homology involved in two-step homologous recombination with the pUX1-*katG-MAB_1135c-1134c* suicide vector. Dotted lines represent the size of the expected PCR products in the WT and Δ*MAB_1135c-1134c* strains (left), along with the corresponding gel migration profile (right). All PCR products were purified and sequenced to confirm the *MAB_1135c-1134c* deletion genotype. (D) Susceptibility/resistance profiles of *M. abscessus* WT, Δ*MAB_2299c*, Δ*MAB_1135c-1134c*, Δ*MAB_2299c-2300-2301*, and Δ*MAB_2299c-2300-2301-1135c-1134c* strains to various drugs. Tenfold serially diluted bacterial suspensions were spotted (5 μl) on 7H10^{OADC} alone or supplemented with 16 μg/ml imipenem (IPM), 16 μg/ml amikacin (AMK), 16 μg/ml ethambutol (EMB), 0.25 μg/ml or 1 μg/ml clofazimine (CFZ), or 0.06 μg/ml or 0.015 μg/ml bedaquiline (BDQ). Growth was observed after 4 days of incubation at 37°C. All experiments were done on two separate occasions.

zac-aac/zac01019/zac8327d19z | xppws | S=5 | 8/17/19 | 5:41 | 4/Color Fig: 1,4,6 | ArtID: 01000-19 | DOI:10.1128/AAC.01000-19 | CE: SSV

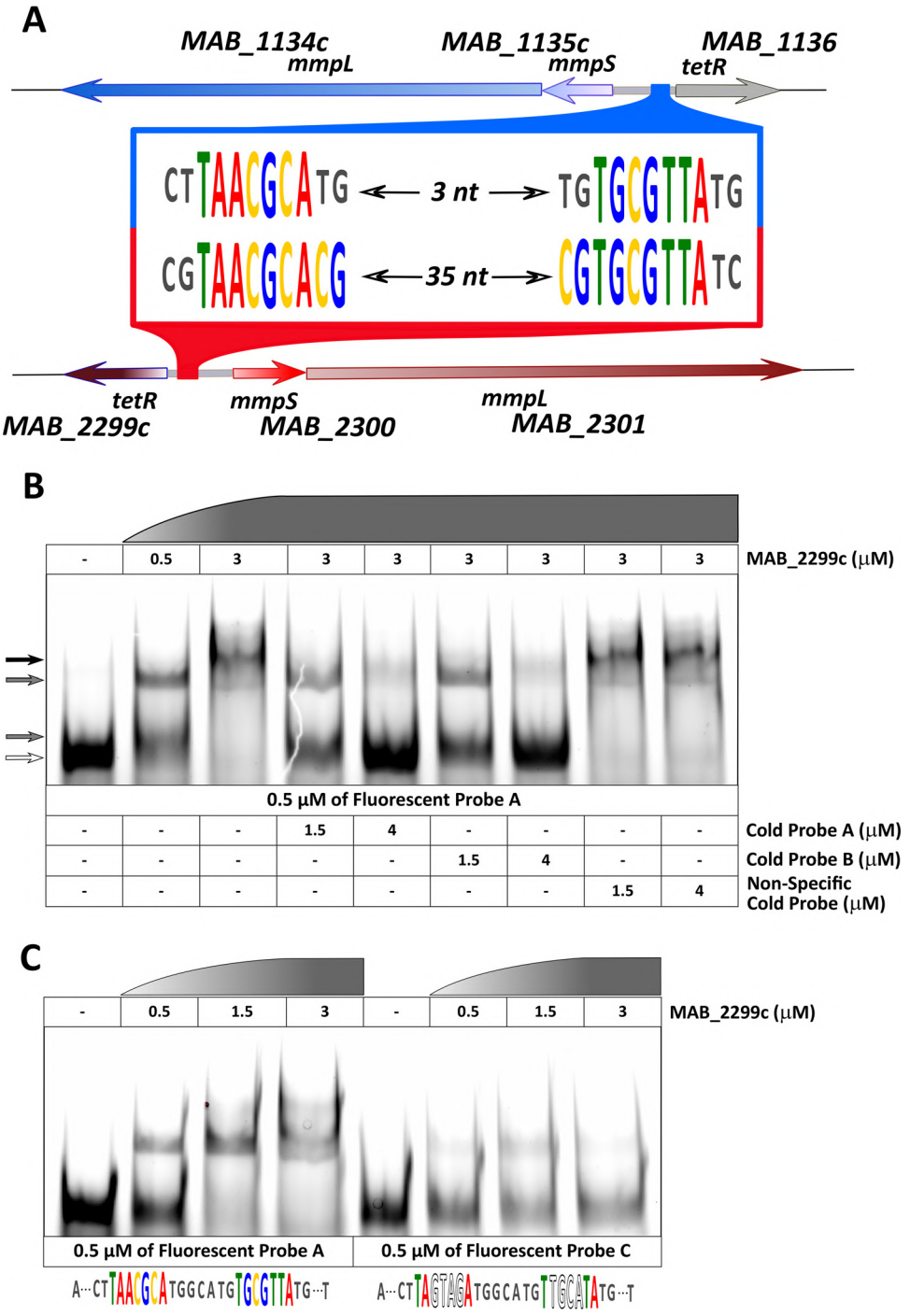

FIG 4 TetR regulator MAB_2299c binds to the intergenic region upstream of *MAB_1135c-1134c*. (A) Schematic representation of the DNA operators located upstream of *MAB_1135c-1134c* (comprising probe A) and *MAB_2300-2301* (comprising probe B). The palindromic sequences of 7 nucleotides in probe A are separated by a spacer and are identical to those found in probe B, in which they are separated by 35 nucleotides. (B) EMSA and competition assays using purified MAB_2299c and incubated with 5′ fluorescein-labeled probe A in the absence or presence of an excess of unlabeled probe A or probe B. A nonrelated probe was also included as a control of specificity of the TetR/DNA complex formed. Detection of the unbound or the complexed probe A was revealed by fluorescence emission. The white arrow indicates the DNA alone, gray arrows the formation of intermediate TetR/DNA complexes, and the black arrow the formation of a complete TetR/DNA complex. (C) Comparison of the EMSA pattern of MAB_2299c incubated with 5′ fluorescein-labeled probe A and probe C in which 4 of the central nucleotides forming the palindromic sequences of probe A were replaced by a random sequence, resulting in a clear defect in the formation of the TetR/DNA complex. The corresponding unbound and complexed probes were revealed by fluorescence emission.

COLOR

zac-aac/zac01019/zac8327d19z | xppws | S=5 | 8/17/19 | 5:41 | 4/Color Fig: 1,4,6 | ArtID: 01000-19 | DOI:10.1128/AAC.01000-19 CE: SSV

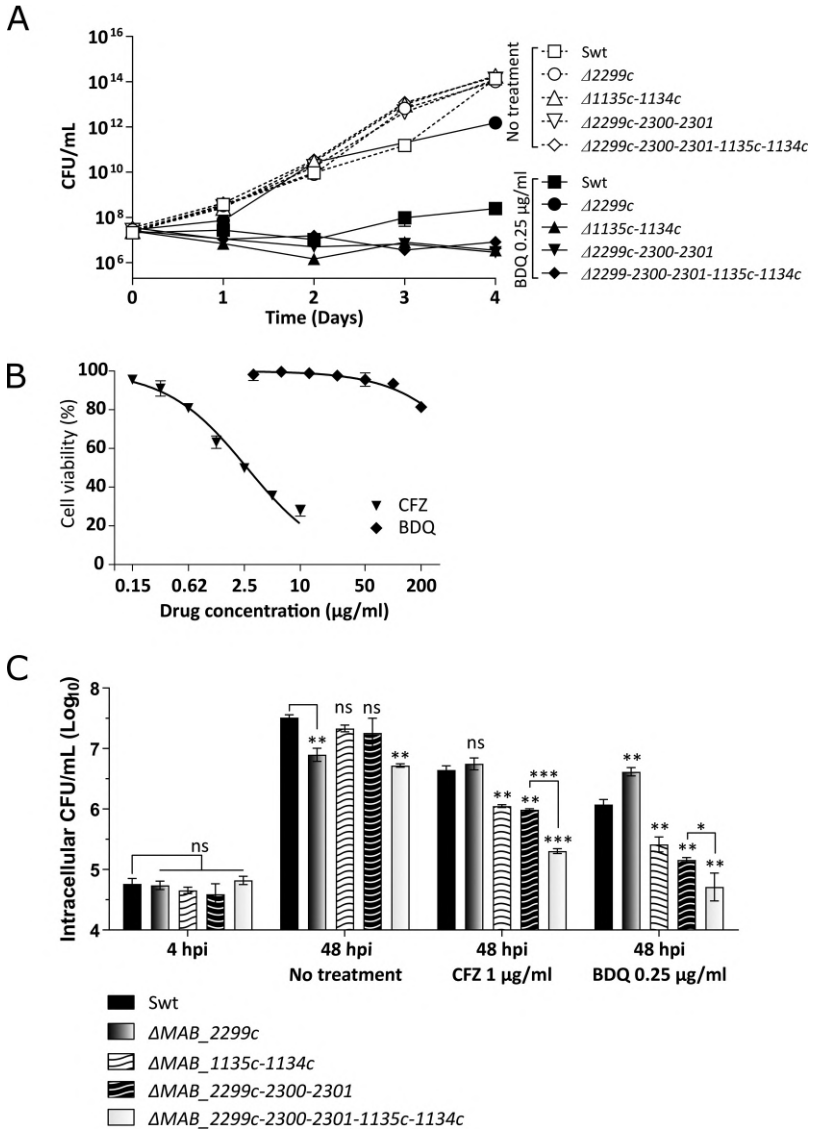

FIG 5 Activity of BDQ *in vitro* and in infected macrophages. (A) *M. abscessus* CIP104536^T WT and its mutant derivatives were either left untreated or exposed to 0.25 μg/ml BDQ in 7H9^{OADC} at 30°C. Bacterial suspensions were collected on a daily basis, diluted, plated on LB agar, and further incubated at 37°C for 4 days prior to CFU determination. Results are expressed as the means ± standard errors of the means from triplicates and are representative of two independent experiments. Ctrl, untreated cultures; Swt, smooth wild type. (B) Cytotoxicity assay of CFZ and BDQ toward THP-1 macrophages. Cells were treated for 48 h with increasing concentrations of CFZ or BDQ, and viability was determined using the CellTiter-Blue reagent. The percentage of cell survival was determined based on control cells incubated in DMSO-containing medium. (C) *M. abscessus*-infected THP-1 macrophages were exposed to either 1 μg/ml CFZ or 0.25 μg/ml BDQ for 2 days before they were lysed and plated for subsequent CFU enumeration. Histograms and error bars represent means and standard errors of the means calculated from three independent experiments. CFU numbers at 4 h postinfection reflect the sizes of the different inocula. For statistical analysis, Student's *t* test was applied. ns, *, **, and *** stand for nonsignificant, $P < 0.01$, $P < 0.001$, and $P < 0.0001$, respectively.

The hypersusceptibility of the quintuple mutant to CFZ and BDQ *in vitro* prompted us to investigate whether this phenotype was maintained when bacteria reside inside the macrophage. However, this required us to first examine the potential cytotoxicity induced by the two drugs over a 48-h period of treatment in THP-1 macrophages. The cytotoxicity profiles of CFZ and BDQ were very different, with BDQ showing extremely poor cytotoxicity (no macrophage killing at concentrations up to 50 μg/ml), while CFZ exhibited toxicity with a 50% inhibitory concentration of 2.6 μg/ml (Fig. 5B). Macro-

zac-aac/zac01019/zac8327d19z | xppws | S=5 | 8/17/19 | 5:41 | 4/Color Fig: 1,4,6 | ArtID: 01000-19 | DOI:10.1128/AAC.01000-19 | CE: SSV

phages next were infected with various *M. abscessus* strains at a multiplicity of infection (MOI) of 5. Following extensive washing and treatment with AMK to remove the extracellular bacilli, infected cells were either left untreated or were treated with low concentrations of drugs (1 μg/ml CFZ or 0.25 μg/ml BDQ) for 48 h. In the absence of drug treatment, all mycobacterial strains replicated in a comparable manner, with a 2-log increase in the intracellular CFU, except for Δ*MAB_2299c* and the quintuple mutant, both showing a slight reduction in the number of intracellular CFU (Fig. 5C). The Δ*MAB_2299c* mutant, however, exhibited slightly higher CFU numbers in macrophages after 48 h of treatment with BDQ than with untreated macrophages, in agreement with its increased resistance phenotype to BDQ *in vitro*. Importantly, the *in vitro* CFZ/BDQ-susceptible Δ*MAB_1135c-1134c* and Δ*MAB_2299c-2300-2301* mutants were also more susceptible to CFZ and BDQ inside macrophages than the wild-type strain. Moreover, the quintuple mutant (lacking both efflux pump systems) exhibited an even further increased sensitivity to CFZ and BDQ in macrophages compared to that of the triple mutant (lacking one efflux pump system only). Together, these results indicate that abrogating the functionality of multiple efflux pumps translates into additive effects, resulting in higher sensitivity to drugs *in vitro* and in infected host cells.

DISCUSSION

M. abscessus is intrinsically resistant to a wide range of antimicrobials, including most antitubercular drugs, posing a serious challenge for drug discovery. Hit rates in primary screens for *M. abscessus* are low, primarily because of the low level of susceptibility due to its expansive drug resistome (18). As environmental bacteria, NTM reside essentially in soil and water, and it is plausible that the selection pressure from antimicrobial-producing bacteria sharing the same biological niches have forced NTM to develop a wide diversity of resistance mechanisms, allowing them to survive in hostile environments. The antimicrobial resistome of *M. abscessus* results from mutations in antibiotic target genes or other related genes, mostly occurring during the prolonged course of treatment, as well as genes involved in intrinsic drug resistance mechanisms. Among the latter, efflux pump mechanisms, protecting bacteria against toxic compounds and promoting bacterial homeostasis by transporting toxins or metabolites to the extracellular environment (34), have drawn attention as important elements preventing the intracellular accumulation of drugs.

Resistance mechanisms associated with MmpL-derived efflux pump systems were recently identified in *M. abscessus*. In the case of thiacetazone analogs, mutations in the TetR repressor MAB_4384 led to upregulation of the adjacent genes encoding an MmpS-MmpL efflux pump system (35, 36). Increased expression of *MAB_4746*, encoding a member of the MmpL family, was also reported recently in LNZ-resistant isolates (37). In the case of CFZ, where CFZ-resistant strains demonstrated cross-resistance to BDQ (29), whole-genome sequencing analyses of the *in vitro*-selected resistors uncovered point mutations in MAB_2299c (29), a member of the TetR family of transcriptional regulators, representing the most abundant family of regulators in mycobacteria. These findings are supported by an independent study that also identified mutations in *MAB_2299c*, among other genes, in CFZ-resistant strain selected *in vitro* (38). It was originally shown that MAB_2299c regulates transcription of the *MAB_2300-2301* target genes, found in an orientation opposite that of *MAB_2299c* (29). Point mutations (L40W, L151P, and G215S) identified in the spontaneous resistant strains were correlated with a loss of DNA-binding activity of MAB_2299c, resulting in derepression of *MAB_2300-2301* (29) and *MAB_1135c-1134c* (this study) gene expression, leading to increased drug efflux and cross-resistance to CFZ and BDQ (29). In contrast to *MAB_2300-2301*, adjacent to *MAB_2299c*, *MAB_1135c-1134c* is located far from the regulator (Fig. 6). This indicates that MAB_2299c can act simultaneously on closely and distantly located target genes on the chromosome. That both efflux pump systems participate in CFZ and BDQ export strongly suggests that they are structurally and functionally related. This hypothesis was confirmed by the phylogenetic analysis that allowed us to identify *MAB_1135c-1134c*, along with *MAB_2300-2301*, products of a possible gene duplication event. That

zac-aac/zac01019/zac8327d19z | xppws | S=5 | 8/17/19 | 5:41 | 4/Color Fig: 1,4,6 | ArtID: 01000-19 | DOI:10.1128/AAC.01000-19 | CE: SSV

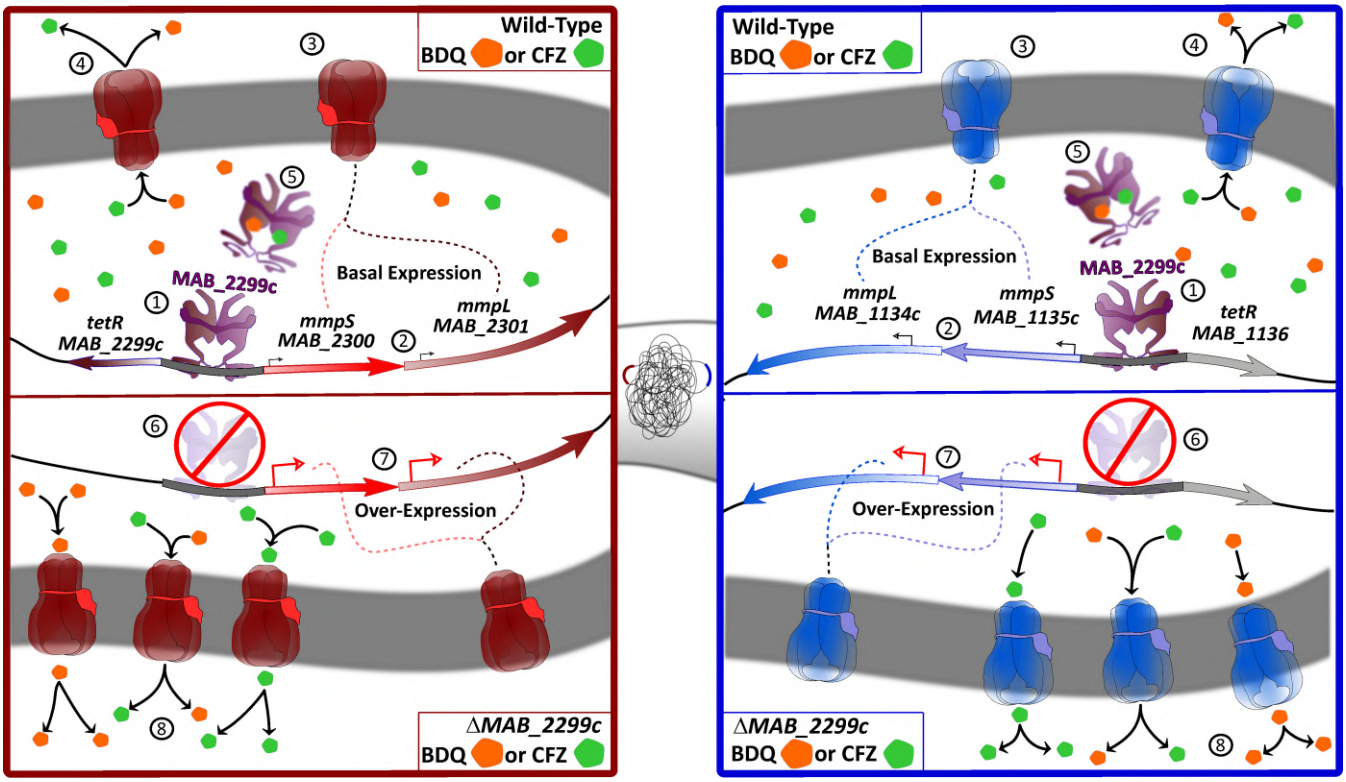

FIG 6 General schematic representing the mechanism of CFZ/BDQ resistance mediated by MAB_2299c-dependent MmpS-MmpL efflux pumps in *M. abscessus*. (1) Binding of MAB_2299c to the intergenic regions of *MAB_2300-2301* (left) and *MAB_1135c-1134c* (right). (2) Transcriptional repression of *MAB_2300-2301* (left) and *MAB_1135c-1134c* (right) allows only basal expression of the two efflux pumps. (3) Insertion of the two MmpS-MmpL efflux pumps into the plasma membrane. (4) Extrusion of CFZ and BDQ conferring intrinsic resistance to both drugs. (5) Possible interaction of the drugs with the TetR regulator, triggering its dissociation from the DNA operator and transcriptional derepression. (6) Lack of binding of the regulator to the intergenic regions either due to point mutations acquired in *MAB_2299c* under CFZ selective pressure *in vitro* or when *MAB_2299c* was inactivated through targeted deletion by homologous recombination. (7) Enhanced expression of the two drug efflux pumps and extrusion of CFZ and BDQ, leading to increased resistance levels to the drugs.

both MmpS-MmpL systems operate simultaneously was verified using multiple gene deletions thanks to the recent development of a suicide vector-based approach, which allows easy and rapid unmarked genetic alteration of the *M. abscessus* chromosome (29). While the triple mutant lacking the regulator and one efflux pump system (Δ*MAB_2299c-2300-2301*) was more sensitive to CFZ/BDQ than the WT progenitor, the quintuple mutant lacking the regulator and both efflux pump systems further gained in susceptibility to CFZ and BDQ treatment. To verify whether the two efflux pumps and MAB_2299c are widely distributed among *M. abscessus* clinical isolates or restricted to the CIP104536 type strain, a BLAST search for *MAB_2299c-2300-2301* and *MAB_1136-1135c-1134c* was performed (see Table S3 in the supplemental material). This revealed that both loci as well as their DNA operators are conserved in *M. bolletii*, *M. massiliense*, and *M. chelonae* and in all clinical isolates analyzed, suggesting that both efflux pump systems are present and presumably operating in all of these strains.

These results indicate that mutations in *MAB_2299c*, which can be easily selected on CFZ *in vitro* (29), affect the expression of two efflux pump systems, both contributing to the resistance mechanism. However, while our transcriptomic studies showed that only these two MmpS/MmpL pairs are regulated by MAB_2299c, one cannot exclude the possibility that additional MAB_2299c-independent MmpL proteins or unrelated efflux pump systems, such as members of the major facilitator superfamily or ATP-binding cassette (ABC) transporters, mediate cross-resistance to CFZ/BDQ. It also remains possible that MAB_2299c regulates other gene targets involved in various metabolic pathways and/or in intracellular survival of *M. abscessus* in macrophages. This hypothesis may be supported by a slightly reduced burden of the Δ*MAB_2299c*

zac-aac/zac01019/zac8327d19z | xppws | S=5 | 8/17/19 | 5:41 | 4/Color Fig: 1,4,6 | ArtID: 01000-19 | DOI:10.1128/AAC.01000-19 | CE: SSV

strain than the WT at 48 h postinfection in THP-1 cells in the absence of drug treatment (Fig. 5C).

We recently showed that verapamil improves the efficacy of BDQ activity against *M. abscessus* clinical isolates both *in vitro* and in macrophages (39). Interestingly, verapamil kept its capacity to potentiate the activity of BDQ even in *M. abscessus* mutants resistant to CFZ/BDQ (overexpressing both the MAB_2300-2301 and MAB_1135c-1134c efflux pumps), highlighting the value of the verapamil-BDQ combination in cases of low-level acquired resistance to BDQ in this mycobacterium. Importantly, the Δ*MAB_2299c-2300-2301* strain, in which this BDQ efflux pump was deleted, leading to increased BDQ sensitivity compared to that of WT *M. abscessus*, exhibited a further increase in sensitivity to BDQ in the presence of verapamil, suggesting that the mechanism whereby verapamil exerts its potentiating effect on BDQ activity is not dependent on this efflux pump, apparently excluding this efflux pump as the major target of verapamil. In fact, it was recently reported that verapamil targets membrane energetics in mycobacteria (40). The inhibition by BDQ of the ATP synthase in mycobacteria was also previously shown to impact membrane energetics, an effect which is probably compounded when verapamil is also present (41). Our genetics data suggest that if a specific inhibitor of the two highly related CFZ/BDQ efflux pumps (MAB_2300-2301 and MAB_1135c-1134c) could be developed, such a compound given in combination with BDQ/CFZ and a molecule targeting membrane potential would provide an extremely potent therapeutic cocktail against *M. abscessus*.

We previously speculated that, given the large *mmpL* repertoire (30) and high abundance of TetR transcriptional regulators (42) found in *M. abscessus*, efflux-based mechanisms represent a general mechanism to express its natural resistance pattern to antimicrobial agents. The present study confirms this to be true, at least regarding CFZ and BDQ resistance. In summary, we provide here additional mechanistic insights into the TetR-dependent regulation of MmpL efflux pumps responsible for cross-resistance to CFZ and BDQ in *M. abscessus*, which may have important clinical implications. Overall, this study underpins *MAB_2299c* as a marker of resistance to be considered when assessing the drug susceptibility profile of *M. abscessus* clinical isolates. However, future studies should also be dedicated to investigating whether mutations in *MAB_2299c* occur in clinical isolates from patients treated with CFZ or BDQ.

MATERIALS AND METHODS

Strains, growth conditions, and reagents. Bacterial strains used in this study are listed in Table S1 in the supplemental material. *M. abscessus* was grown in Middlebrook 7H9 broth (BD Difco) supplemented with 0.05% Tween 80 (Sigma-Aldrich) and 10% oleic acid, albumin, dextrose, catalase (OADC enrichment; BD Difco) ($7H9^{T/OADC}$) at 30°C (unless otherwise stated) in the presence of antibiotics, when required. On plates, colonies were selected either on Middlebrook 7H10 agar (BD Difco) supplemented with 10% OADC enrichment ($7H10^{OADC}$) or on LB agar. All drugs were purchased from Sigma-Aldrich.

Drug susceptibility testing. The MIC, defined as the minimal drug concentration required to inhibit 99% growth (MIC_{99}), was recorded on Middlebrook $7H10^{OADC}$ agar after 3 to 4 days of incubation at 30°C. All experiments were done on three independent occasions.

Quantitative real-time PCR. Isolation of RNA, reverse transcription, and qRT-PCR were done as reported earlier (35) using the primers listed in Table S2 in the supplemental material.

Expression and purification of MAB_2299c variants. The *E. coli* BL21(DE3) strain (New England Biolabs) possessing pRARE2 was transformed with a pET32a derivative containing the wild-type *MAB_2299c* gene. Expression in *E. coli* and purification of MAB_2299c was performed as described earlier (29).

Electrophoretic mobility shift assays (EMSAs). Thanks to the MEME Suite 4.20.0 online tool, we identified a perfect pair of palindromes comprised of 7 nucleotides each and separated by a 7-nucleotide spacer within the intergenic region upstream of *MAB_1135c*. These palindromes are identical to the ones located between *MAB_2299c* and *MAB_2300*. A double-stranded DNA fragment of 64 bp containing the pair of palindromes labeled at their 5′ ends with fluorescein (probe A) was purchased from Sigma-Aldrich. The 5′ fluorescein probes (500 nM) were coincubated for 1 h at room temperature in 1× Tris base–acetic acid–EDTA (TAE) buffer with increasing amounts of purified MAB_2299c protein with or without excess concentrations of cold probes (unlabeled DNA fragments). Electrophoresis was performed for 30 min at 100 V in 1× TAE buffer, and fluorescence was revealed using a ChemiDoc Imaging System (Bio-Rad). Sequences of the probes are listed in Table S2.

Generation of the *MAB_1136c* and *MAB_1135c-1134c* recombination plasmids. The suicide vector pUX1-*katG* (29) was used to generate pUX1-*katG-MAB_1136*. To produce pUX1-*katG-MAB_1136*, genomic DNA from *M. abscessus*, Q5 polymerase (New England Biolabs), and the primers

MAB_1136_LA_Fw and *MAB_1136_LA_Rev* were used to PCR amplify a left arm (LA). A similar PCR but with the primers *MAB_1136_RA_Fw* and *MAB_1136_RA_Rev* generated a right arm (RA). The purified LA and RA amplicons were added to a new PCR mix without any primers or genomic DNA. This reaction consisted of two cycles of 95°C for 30 s, 55°C for 2 min, and 72°C for 3 min prior to the addition of primers *MAB_1136_RA_Fw* and *MAB_1136_LA_Rev* and 25 additional cycles of 95°C for 10 s, 55°C for 30 s, and 72°C for 2 min. The 1.7-kb primer-overlap extension PCR product was restricted with NheI and MfeI and ligated to the NheI-MfeI-linearized pUX1-*katG*, yielding pUX1-*katG-MAB_1136*, designed to delete 530 bp (80%) of the *MAB_1136* open reading frame (Table S1).

The same approach was applied to generate pUX1-*katG-MAB_1135c-1134c*, using the primers *MAB_1135c-1134c_LA_Fw* and *MAB_1135c-1134c_LA_Rev* to produce the LA and the primers *MAB_1135c-1134c_RA_Fw* and *MAB_1135c-1134c_RA_Rev* to produce the RA. The ~1.4-kb primer overlap extension PCR product was restricted with NheI and MfeI and ligated to the NheI-MfeI-linearized pUX1-*katG*, yielding pUX1-*katG-MAB_1135c-1134c*, designed to delete 3,234 bp (96%) of the *MAB_1135c-1134c* gene cluster (Table S1).

Unmarked deletion in *M. abscessus*. Highly electrocompetent *M. abscessus* smooth (S) WT and S Δ*MAB_2299c-2300-2301* strains were prepared as reported earlier (31) and subsequently transformed with pUX1-*katG-MAB_1136* or pUX1-*katG-MAB_1135c-1134c*. Selection of bacteria having undergone the first homologous recombination was done by screening for red fluorescent colonies on 7H10^{OADC} supplemented with 200 μg/ml kanamycin. To promote the second homologous recombination event, the selected clones were subcultured overnight in 7H9^{OADC} in the absence of kanamycin. Cultures were 10-fold serially diluted and plated onto 7H10^{OADC} containing 50 μg/ml isoniazid (INH) to select for INH-resistant, KAN-sensitive, and nonfluorescent colonies. Following genomic DNA preparation from such colonies, PCR screening was set up using primer sets binding upstream of the LA and inside the RA or binding inside the LA and downstream of the RA. Amplicons were subsequently sequenced to confirm the junction between LA and RA and the correct unmarked deletion of *MAB_1136* and *MAB_1135c-1134c*.

Macrophage infections. THP-1 macrophages were grown at 37°C in a 5% CO_2 incubator in RPMI 1640 supplemented with 10% FBS (RPMI^{FBS}) and differentiated for 48 h prior to infection with 20 ng/ml phorbol myristate acetate (PMA). *M. abscessus* strains were cultured at 37°C in 7H9^{OADC} until they reach the exponential growth phase and were harvested by centrifugation and resuspended in phosphate-buffered saline (PBS). Single-cell preparations were prepared by passing the bacterial suspension through a 26.5-gauge needle (~20 times) and then through a 5.0-μm filter (Merck Millipore). THP-1 cells (5×10^5 cells/ml) were then infected at an MOI of 5 and incubated at 37°C in the presence of 5% CO_2. After 2 to 3 h of incubation, cells were washed three times with PBS and refed with RPMI^{FBS} supplemented with 250 μg/ml AMK for 1 h in order to kill extracellular bacilli. Cells were washed three times with PBS and incubated for an additional 48 h with either RPMI^{FBS} alone (no treatment; control of intracellular growth), RPMI^{FBS} containing 1 μg/ml CFZ, or RPMI^{FBS} containing 0.25 μg/ml BDQ. For intracellular CFU determination, cells were washed three times with PBS, and 100 μl of 1% PBS-Triton X-100 was added to lyse the cells at day 0 and day 2. Lysis was stopped by adding 900 μl of PBS. Tenfold dilutions were plated onto LB agar, and colonies were counted after 5 days of incubation at 37°C.

Cytotoxicity assay. THP-1 macrophages (5×10^5 cells/ml) in 96-well flat-bottom culture microtiter plates were differentiated for 48 h with PMA, after which RPMI^{FBS} was replaced with 180 μl of fresh medium containing increasing concentrations of either CFZ (ranging from 0.15 to 10 μg/ml) or BDQ (ranging from 3.1 to 200 μg/ml). After 48 h of incubation at 37°C with 5% CO_2, 20 μl of CellTiter-Blue reagent (Promega) was added and cells were incubated for an additional 2 h. The optical density at 560 nm (OD_{560}) was recorded using a microplate reader. The percentage of cell survival was determined considering the control wells (cells incubated in dimethyl sulfoxide-containing medium).

Multiple alignments and synteny analysis. Primary protein sequences were retrieved from the KEGG website (https://www.genome.jp/kegg/), and multiple alignments of the sequences were done with the MUSCLE algorithm using its default parameters in the UniProt UGENE suite (43). Phylogenetic trees were constructed from the multiple-alignment data using the PHYLIP neighbor-joining tree-building method with default parameters of the UGENE suite. Nucleotide sequences were also retrieved from the KEGG website, and syntenic comparisons of these sequences were done on the YASS genomic similarity tool web server (http://bioinfo.lifl.fr/yass/yass.php).

Statistical analysis. All statistical analyses were performed using GraphPad Prism 5 (version 5.03; GraphPad Software). Student's *t* test was used for all comparisons. A *P* value of less than 0.05 was considered significant (ns, nonsignificant; *, $P < 0.05$; **, $P < 0.01$; ***, $P < 0.001$).

SUPPLEMENTAL MATERIAL

Supplemental material for this article may be found at https://doi.org/10.1128/AAC.01000-19.

SUPPLEMENTAL FILE 1, PDF file, 0.8 MB.

ACKNOWLEDGMENTS

This work was supported by the Fondation pour la Recherche Médicale (FRM) (grant number DEQ20150331719 to L.K.; grant number ECO20160736031 to M.R.) and the InfectioPôle Sud for funding the Ph.D. fellowship of A.V.G.

We have no conflicts of interest to declare.

zac-aac/zac01019/zac8327d19z | xppws | S=5 | 8/17/19 | 5:41 | 4/Color Fig: 1,4,6 | ArtID: 01000-19 | DOI:10.1128/AAC.01000-19 | CE: SSV

REFERENCES

1. Davidson RM. 2018. A closer look at the genomic variation of geographically diverse *Mycobacterium abscessus* clones that cause human infection and disease. Front Microbiol 9:2988. https://doi.org/10.3389/fmicb.2018.02988.
2. Choo SW, Wee WY, Ngeow YF, Mitchell W, Tan JL, Wong GJ, Zhao Y, Xiao J. 2014. Genomic reconnaissance of clinical isolates of emerging human pathogen *Mycobacterium abscessus* reveals high evolutionary potential. Sci Rep 4:4061. https://doi.org/10.1038/srep04061.
3. Tan JL, Ngeow YF, Choo SW. 2015. Support from phylogenomic networks and subspecies signatures for separation of *Mycobacterium massiliense* from *Mycobacterium bolletii*. J Clin Microbiol 53:3042–3046. https://doi.org/10.1128/JCM.00541-15.
4. Tan JL, Ng KP, Ong CS, Ngeow YF. 2017. Genomic comparisons reveal microevolutionary differences in *Mycobacterium abscessus* subspecies. Front Microbiol 8:2042. https://doi.org/10.3389/fmicb.2017.02042.
5. Ripoll F, Pasek S, Schenowitz C, Dossat C, Barbe V, Rottman M, Macheras E, Heym B, Herrmann J-L, Daffé M, Brosch R, Risler J-L, Gaillard J-L. 2009. Nonmycobacterial virulence genes in the genome of the emerging pathogen *Mycobacterium abscessus*. PLoS One 4:e5660. https://doi.org/10.1371/journal.pone.0005660.
6. Le Moigne V, Belon C, Goulard C, Accard G, Bernut A, Pitard B, Gaillard J-L, Kremer L, Herrmann J-L, Blanc-Potard A-B. 2016. MgtC as a host-induced factor and vaccine candidate against *Mycobacterium abscessus* infection. Infect Immun 84:2895–2903. https://doi.org/10.1128/IAI.00359-16.
7. Griffith DE, Aksamit T, Brown-Elliott BA, Catanzaro A, Daley C, Gordin F, Holland SM, Horsburgh R, Huitt G, Iademarco MF, Iseman M, Olivier K, Ruoss S, von Reyn CF, Wallace RJ, Winthrop K, ATS Mycobacterial Diseases Subcommittee; American Thoracic Society, Infectious Disease Society of America. 2007. An official ATS/IDSA statement: diagnosis, treatment, and prevention of nontuberculous mycobacterial diseases. Am J Respir Crit Care Med 175:367–416. https://doi.org/10.1164/rccm.200604-571ST.
8. Floto RA, Olivier KN, Saiman L, Daley CL, Herrmann J-L, Nick JA, Noone PG, Bilton D, Corris P, Gibson RL, Hempstead SE, Koetz K, Sabadosa KA, Sermet-Gaudelus I, Smyth AR, van Ingen J, Wallace RJ, Winthrop KL, Marshall BC, Haworth CS. 2016. US Cystic Fibrosis Foundation and European Cystic Fibrosis Society consensus recommendations for the management of non-tuberculous mycobacteria in individuals with cystic fibrosis: executive summary. Thorax 71:88–90. https://doi.org/10.1136/thoraxjnl-2015-207983.
9. Medjahed H, Gaillard J-L, Reyrat J-M. 2010. *Mycobacterium abscessus*: a new player in the mycobacterial field. Trends Microbiol 18:117–123. https://doi.org/10.1016/j.tim.2009.12.007.
10. Catherinot E, Roux A-L, Macheras E, Hubert D, Matmar M, Dannhoffer L, Chinet T, Morand P, Poyart C, Heym B, Rottman M, Gaillard J-L, Herrmann J-L. 2009. Acute respiratory failure involving an R variant of *Mycobacterium abscessus*. J Clin Microbiol 47:271–274. https://doi.org/10.1128/JCM.01478-08.
11. Esther CR, Esserman DA, Gilligan P, Kerr A, Noone PG. 2010. Chronic *Mycobacterium abscessus* infection and lung function decline in cystic fibrosis. J Cyst Fibros 9:117–123. https://doi.org/10.1016/j.jcf.2009.12.001.
12. Bryant JM, Grogono DM, Rodriguez-Rincon D, Everall I, Brown KP, Moreno P, Verma D, Hill E, Drijkoningen J, Gilligan P, Esther CR, Noone PG, Giddings O, Bell SC, Thomson R, Wainwright CE, Coulter C, Pandey S, Wood ME, Stockwell RE, Ramsay KA, Sherrard LJ, Kidd TJ, Jabbour N, Johnson GR, Knibbs LD, Morawska L, Sly PD, Jones A, Bilton D, Laurenson I, Ruddy M, Bourke S, Bowler IC, Chapman SJ, Clayton A, Cullen M, Daniels T, Dempsey O, Denton M, Desai M, Drew RJ, Edenborough F, Evans J, Folb J, Humphrey H, Isalska B, Jensen-Fangel S, Jönsson B, Jones AM, Katzenstein TL, Lillebaek T, MacGregor G, Mayell S, Millar M, Modha D, Nash EF, O'Brien C, O'Brien D, Ohri C, Pao CS, Peckham D, Perrin F, Perry A, Pressler T, Prtak L, Qvist T, Robb A, Rodgers H, Schaffer K, Shafi N, van Ingen J, Walshaw M, Watson D, West N, Whitehouse J, Haworth CS, Harris SR, Ordway D, Parkhill J, Floto RA. 2016. Emergence and spread of a human-transmissible multidrug-resistant nontuberculous mycobacterium. Science 354:751–757. https://doi.org/10.1126/science.aaf8156.
13. Kwak N, Dalcolmo MP, Daley CL, Eather G, Gayoso R, Hasegawa N, Jhun BW, Koh W-J, Namkoong H, Park J, Thomson R, van Ingen J, Zweijpfenning SMH, Yim J-J. 2019. *Mycobacterium abscessus* pulmonary disease: individual patient data meta-analysis. Eur Respir J 54:1801991. https://doi.org/10.1183/13993003.01991-2018.
14. Brown-Elliott BA, Nash KA, Wallace RJ. 2012. Antimicrobial susceptibility testing, drug resistance mechanisms, and therapy of infections with nontuberculous mycobacteria. Clin Microbiol Rev 25:545–582. https://doi.org/10.1128/CMR.05030-11.
15. Nessar R, Cambau E, Reyrat JM, Murray A, Gicquel B. 2012. *Mycobacterium abscessus*: a new antibiotic nightmare. J Antimicrob Chemother 67:810–818. https://doi.org/10.1093/jac/dkr578.
16. van Ingen J, Boeree MJ, van Soolingen D, Mouton JW. 2012. Resistance mechanisms and drug susceptibility testing of nontuberculous mycobacteria. Drug Resist Updat 15:149–161. https://doi.org/10.1016/j.drup.2012.04.001.
17. Luthra S, Rominski A, Sander P. 2018. The role of antibiotic-target-modifying and antibiotic-modifying enzymes in *Mycobacterium abscessus* drug resistance. Front Microbiol 9:2179. https://doi.org/10.3389/fmicb.2018.02179.
18. Wu M-L, Aziz DB, Dartois V, Dick T. 2018. NTM drug discovery: status, gaps and the way forward. Drug Discov Today 23:1502–1519. https://doi.org/10.1016/j.drudis.2018.04.001.
19. Yano T, Kassovska-Bratinova S, Teh JS, Winkler J, Sullivan K, Isaacs A, Schechter NM, Rubin H. 2011. Reduction of clofazimine by mycobacterial type 2 NADH:quinone oxidoreductase: a pathway for the generation of bactericidal levels of reactive oxygen species. J Biol Chem 286:10276–10287. https://doi.org/10.1074/jbc.M110.200501.
20. van Ingen J, Totten SE, Helstrom NK, Heifets LB, Boeree MJ, Daley CL. 2012. *In vitro* synergy between clofazimine and amikacin in treatment of nontuberculous mycobacterial disease. Antimicrob Agents Chemother 56:6324–6327. https://doi.org/10.1128/AAC.01505-12.
21. Singh S, Bouzinbi N, Chaturvedi V, Godreuil S, Kremer L. 2014. *In vitro* evaluation of a new drug combination against clinical isolates belonging to the *Mycobacterium abscessus* complex. Clin Microbiol Infect 20:O1124–O1127. https://doi.org/10.1111/1469-0691.12780.
22. Ferro BE, Meletiadis J, Wattenberg M, de Jong A, van Soolingen D, Mouton JW, van Ingen J. 2016. Clofazimine prevents the regrowth of *Mycobacterium abscessus* and *Mycobacterium avium* type strains exposed to amikacin and clarithromycin. Antimicrob Agents Chemother 60:1097–1105. https://doi.org/10.1128/AAC.02615-15.
23. Matteelli A, Carvalho AC, Dooley KE, Kritski A. 2010. TMC207: the first compound of a new class of potent anti-tuberculosis drugs. Future Microbiol 5:849–858. https://doi.org/10.2217/fmb.10.50.
24. Pang Y, Zheng H, Tan Y, Song Y, Zhao Y. 2017. *In vitro* activity of bedaquiline against nontuberculous mycobacteria in China. Antimicrob Agents Chemother 61:e02627-16. https://doi.org/10.1128/AAC.02627-16.
25. Vesenbeckh S, Schönfeld N, Roth A, Bettermann G, Krieger D, Bauer TT, Rüssmann H, Mauch H. 2017. Bedaquiline as a potential agent in the treatment of *Mycobacterium abscessus* infections. Eur Respir J 49:1700083. https://doi.org/10.1183/13993003.00083-2017.
26. Dupont C, Viljoen A, Thomas S, Roquet-Banères F, Herrmann J-L, Pethe K, Kremer L. 2017. Bedaquiline inhibits the ATP synthase in *Mycobacterium abscessus* and is effective in infected zebrafish. Antimicrob Agents Chemother 61:e01225-17. https://doi.org/10.1128/AAC.01225-17.
27. Ruth MM, Sangen JJN, Remmers K, Pennings LJ, Svensson E, Aarnoutse RE, Zweijpfenning SMH, Hoefsloot W, Kuipers S, Magis-Escurra C, Wertheim HFL, van Ingen J. 2019. A bedaquiline/clofazimine combination regimen might add activity to the treatment of clinically relevant non-tuberculous mycobacteria. J Antimicrob Chemother 74:935–943. https://doi.org/10.1093/jac/dky526.
28. Bernut A, Herrmann J-L, Kissa K, Dubremetz J-F, Gaillard J-L, Lutfalla G, Kremer L. 2014. *Mycobacterium abscessus* cording prevents phagocytosis and promotes abscess formation. Proc Natl Acad Sci U S A 111:E943–E952. https://doi.org/10.1073/pnas.1321390111.
29. Richard M, Gutiérrez AV, Viljoen A, Rodriguez-Rincon D, Roquet-Baneres F, Blaise M, Everall I, Parkhill J, Floto RA, Kremer L. 2019. Mutations in the MAB_2299c TetR regulator confer cross-resistance to clofazimine and bedaquiline in *Mycobacterium abscessus*. Antimicrob Agents Chemother 63:e01316-18. https://doi.org/10.1128/AAC.01316-18.
30. Viljoen A, Dubois V, Girard-Misguich F, Blaise M, Herrmann J-L, Kremer L. 2017. The diverse family of MmpL transporters in mycobacteria: from regulation to antimicrobial developments. Mol Microbiol 104:889–904. https://doi.org/10.1111/mmi.13675.

zac-aac/zac01019/zac8327d19z | xppws | S=5 | 8/17/19 | 5:41 | 4/Color Fig: 1,4,6 | ArtID: 01000-19 | DOI:10.1128/AAC.01000-19 | CE: SSV

31. Viljoen A, Gutiérrez AV, Dupont C, Ghigo E, Kremer L. 2018. A simple and rapid gene disruption strategy in *Mycobacterium abscessus*: on the design and application of glycopeptidolipid mutants. Front Cell Infect Microbiol 8:69. https://doi.org/10.3389/fcimb.2018.00069.
32. Rominski A, Selchow P, Becker K, Brülle JK, Dal Molin M, Sander P. 2017. Elucidation of *Mycobacterium abscessus* aminoglycoside and capreomycin resistance by targeted deletion of three putative resistance genes. J Antimicrob Chemother 72:2191–2200. https://doi.org/10.1093/jac/dkx125.
33. Viljoen A, Blaise M, de Chastellier C, Kremer L. 2016. MAB_3551c encodes the primary triacylglycerol synthase involved in lipid accumulation in *Mycobacterium abscessus*. Mol Microbiol 102:611–627. https://doi.org/10.1111/mmi.13482.
34. Louw GE, Warren RM, Gey van Pittius NC, McEvoy CRE, Van Helden PD, Victor TC. 2009. A balancing act: efflux/influx in mycobacterial drug resistance. Antimicrob Agents Chemother 53:3181–3189. https://doi.org/10.1128/AAC.01577-08.
35. Halloum I, Viljoen A, Khanna V, Craig D, Bouchier C, Brosch R, Coxon G, Kremer L. 2017. Resistance to thiacetazone derivatives active against *Mycobacterium abscessus* involves mutations in the MmpL5 transcriptional repressor MAB_4384. Antimicrob Agents Chemother 61:e02509-16. https://doi.org/10.3389/fcimb.2018.00069.
36. Richard M, Gutiérrez AV, Viljoen AJ, Ghigo E, Blaise M, Kremer L. 2018. Mechanistic and structural insights into the unique TetR-dependent regulation of a drug efflux pump in *Mycobacterium abscessus*. Front Microbiol 9:649. https://doi.org/10.3389/fmicb.2018.00649.
37. Ye M, Xu L, Zou Y, Li B, Guo Q, Zhang Y, Zhan M, Xu B, Yu F, Zhang Z, Chu H. 2018. Molecular analysis of linezolid-resistant clinical isolates of *Mycobacterium abscessus*. Antimicrob Agents Chemother 63:e01842-18. https://doi.org/10.1128/AAC.01842-18.
38. Chen Y, Chen J, Zhang S, Shi W, Zhang W, Zhu M, Zhang Y. 2018. Novel mutations associated with clofazimine resistance in *Mycobacterium abscessus*. Antimicrob Agents Chemother 62:e00544-18. https://doi.org/10.1128/AAC.00544-18.
39. Viljoen A, Raynaud C, Johansen M, Roquet-Baneres F, Herrmann J-L, Daher W, Kremer L. 17 June 2019. Improved activity of bedaquiline by verapamil against *Mycobacterium abscessus in vitro* and in macrophages. Antimicrob Agents Chemother. https://doi.org/10.1128/AAC.00705-19.
40. Chen C, Gardete S, Jansen RS, Shetty A, Dick T, Rhee KY, Dartois V. 2018. Verapamil targets membrane energetics in *Mycobacterium tuberculosis*. Antimicrob Agents Chemother 62:e02107-17. https://doi.org/10.1128/AAC.02107-17.
41. Lamprecht DA, Finin PM, Rahman MA, Cumming BM, Russell SL, Jonnala SR, Adamson JH, Steyn AJC. 2018. Turning the respiratory flexibility of *Mycobacterium tuberculosis* against itself. Nat Comm 7:12393. https://doi.org/10.1038/ncomms12393.
42. Balhana RJC, Singla A, Sikder MH, Withers M, Kendall SL. 2015. Global analyses of TetR family transcriptional regulators in mycobacteria indicates conservation across species and diversity in regulated functions. BMC Genomics 16:479. https://doi.org/10.1186/s12864-015-1696-9.
43. Okonechnikov K, Golosova O, Fursov M, Withers M, Kendall SL, UGENE Team. 2012. Unipro UGENE: a unified bioinformatics toolkit. Bioinformatics 28:1166–1167. https://doi.org/10.1093/bioinformatics/bts091.

AUTHOR QUERIES

AUTHOR PLEASE ANSWER ALL QUERIES 1

AQau—Please confirm the given-names and surnames are identified properly by the colors. ■= Given-Name, ■= Surname

AQau—An ORCID ID was provided for at least one author during submission. Please click the name associated with the ORCID ID icon (🥝) in the byline to verify that the link is working and that it links to the correct author.

AQfund—The table below includes funding information that you provided on the submission form when you submitted the manuscript. This funding information will not appear in the article, but it will be provided to CrossRef and made publicly available. Please check it carefully for accuracy and mark any necessary corrections. If you would like statements acknowledging financial support to be published in the article itself, please make sure that they appear in the Acknowledgments section. Statements in Acknowledgments will have no bearing on funding data deposited with CrossRef and vice versa.

Funder	Grant(s)	Author(s)	Funder ID
Infectiopôle Sud		Ana Victoria Gutiérrez	
Fondation pour la Recherche Médicale (FRM)	DEQ20150331719	Laurent Kremer	https://doi.org/10.13039/501100002915
Fondation pour la Recherche Médicale (FRM)	ECO20160736031	Matthias Richard	https://doi.org/10.13039/501100002915

AQA—To ensure sequential order, references have been renumbered in the text and References. Please check and correct the renumbering if necessary. If any reference should be deleted from the References list, please mark "Reference deleted" in the margin next to that entry; do not renumber subsequent references.

AQB—In the legend to Fig. 2, please define Up and Dw, if they are abbreviations.

AQC—ASM style does not allow slashes between bacterial gene names. As a result, *mmpS/mmpL* has been changed to *mmpS-mmpL* throughout.

CONCLUSIONS & PERSPECTIVES

8. Conclusions and perspectives

Infections caused by *M. abscessus* are increasing worldwide, especially in patients suffering from CF. Multiple factors can converge to allow this environmental bacterium to become a successful human pathogen. Initial studies positioned an important element of the *M. abscessus* cell wall - the GPL- as a key element in the S/R morphotype. Putting together the available knowledge about *M. abscessus* GPL, a series of hypotheses have been combined to propose a chain of events associated with the pulmonary disease: 1) presence of GPL at the bacterial surface promotes interaction with host cells, 2) this can boost the anti-GPL humoral response due to immunogenic nature of GPL, 3) this subsequently leads to the selection of low-GPL-producing bacilli (characterized by a rough morphology); 4) this leads to the unmasking of underlaying pro-inflammatory elements, such as lipoproteins and phosphatidylinositol (Roux et al. 2011; Rhoades et al. 2009) that produce severe inflammation. In addition, the greater hydrophobicity in the R bacteria promotes the formation of aggregates rendering phagocytosis difficult. However, what are the environmental cues that lead to the morphology change of *M. abscessus* remains to be established in future studies.

A wide panoply of methods are available for genetic engineering in *M. tuberculosis* (Lamrabet and Drancourt 2012) but these methods are more limited in *M. abscessus* and the generation of knockout strains can still be challenging. Gene inactivation has largely contributed in elucidating important aspects in bacterial physiology, identifying drug targets and describing pathogenesis (Tang et al. 2015). Following our interest in understanding the molecular mechanisms responsible for the multidrug resistance and pathogenicity of *M. abscessus*, we developed a new set of tools to easily and efficiently generate knock-out mutants based on single and double homologous recombination. One of the main features of our initial suicide plasmid (pXU1) relies on the *tdTomato* red fluorescent marker that simplifies the selection of positive clones that have undergone gene disruption and which allows also to perform infection studies directly in zebrafish without any additional

fluorescent marker. The second plasmid (pXU3) developed to control gene expression showed leaky expression and therefore does not appear to be an optimal system for fine tuning regulation in *M. abscessus*. Introducing a counter-selectable marker (functional *katG* from *M. tuberculosis*) resulted in an improved construct particularly suited for the generation of unmarked deletion which allows to delete multiple genes in the same strain. These new tools could eventually be applied to other NTM species often neglected and refractory to gene manipulation. Thanks to this method, it becomes now possible to inactive large sets of genes/pathways to evaluate antibiotic resistance mechanisms and pathogenicity, ultimately contributing to the development of new chemotherapeutic strategies against *M. abscessus* and other NTM.

Several genetic determinants in *M. abscessus* are responsible for intrinsic resistance to toxic compounds, including drugs and detergents. MmpL proteins have been associated not only with drug resistance but also with lipid transport. In *M. tuberculosis*, the main focus of their functions has been devoted to lipid transport, such as the MmpL3 protein responsible for the transport of mycolates, which has been largely exploited as a valid drug target (Li et al. 2016). However, the export of siderophores in MmpL4 and MmpL5 and drug efflux activity of MmpL5 and MmpL7 are proofs of their multifaceted functions (Székely and Cole 2016). We have focused our research on the mechanisms of drug resistance involving MmpL efflux pumps and their regulation systems in *M. abscessus*. First, we describe the mechanistic regulation of *MAB_4382c-MAB_4383c*, the closest homologs to *mmpS5-mmpL5* in *M. tuberculosis*, by MAB_4384, a TetR transcriptional regulator. MAB_4384 binds to its unique operator sequence (ATAAGTGGATTGA/TCTATCCACTTTT) to repress the expression of *mmpS5/mmpL5* efflux pump. Furthermore, we showed the impact of the D14N and F57L amino acids substitutions in the formation of the MAB_4384/DNA complex, which explains the subsequent overexpression of *mmpS5/mmpL5* and the efflux of TAC analogues. However, we cannot discard the possibility that this efflux system participates in the extrusion of other

drugs and in important physiological processes.

We also described two additional efflux pumps (MAB_1135c-MAB_1134c and MAB_2300-MAB_2301) and their role in cross-resistance to clofazimine and bedaquiline. The TetR MAB_2299c appears as the main regulator of both efflux systems. The possible binding of clofazimine and bedaquiline to MAB_2299c may prevent formation of the protein/DNA complex, resulting in increased resistance levels. Importantly, we showed that mutations in this TetR leads to overexpression of both *MAB_1135c-MAB_1134*c and *MAB_2300-MAB_2301* and cross-resistance to clofazimine and bedaquiline. Therefore, sequencing *MAB_2299c* in isolates from patients under treatment with clofazimine and/or bedaquiline may help the clinician to anticipate drug resistance.

The genomic environment of *MAB_2299c* suggests that this locus is important for drug resistance mechanisms. This gene is surrounded not only with the *MAB_2300/MAB_2301* efflux pump involved in resistance to clofazimine and bedaquiline, but also with the *erm(41)* gene (*MAB_2297*), responsible for the intrinsic inducible resistance to macrolides. The presence of a second efflux pump encoded by *MAB_2302/MAB_2303* in this environment allows to speculate that it may also participate in antibiotic resistance, this hypothesis needs however to be investigated in future studies.

Alternative to clofazimine and bedaquiline as new therapeutic approaches for NTM, the recent approval of pretomanid ("FDA Approves Pretomanid for Highly Drug-Resistant Forms of Tuberculosis" n.d.) for the treatment of multidrug resistant TB opens the opportunity for new therapies against the difficult-to-treat NTM diseases. To date, there are no available studies dedicated to test the efficacy of this drug against *M. abscessus* infections.

In addition to the RND superfamily in which MmpLs belong to, four other different structural families of efflux pumps such as, the major facilitator superfamily (MFS), the small multidrug resistance (SMR) family, the adenosine triphosphate (ATP)-binding cassette (ABC) superfamily and the multidrug and toxic compound extrusion (MATE) family have been

related to drug cross-resistance in *M. tuberculosis* and *M. smegmatis* (Nasiri et al. 2017; Sander et al. 2000). It may thus be of particular interest to address in future studies whether these different classes of membrane proteins participate also in drug resistance mechanisms in *M. abscessus*.

Efflux pump inhibitors may improve the treatment against multidrug resistant *M. abscessus* by restricting drug extrusion and interfering with the transport of lipids that participate in cell wall assembly. Efflux pumps inhibitor tested *in vitro* in mycobacteria and other Gram-negative include verapamil, piperine, Phe-Arg-β-naphthylamine derivatives, P-glycoprotein inhibitors, thioxanthenes phenothiazines, reserpine, carbonyl cyanide m-chlorophenyl hydrazine, chlorpromazine and tetrahydropyridine derivative (Szumowski et al. 2013). In particular, a recent study reported the increased activity of bedaquiline against clinical isolates of *M. abscessus* when used in combination with verapamil (Viljoen et al. 2019). The introduction of efflux pumps inhibitors in clinical settings is difficult since some of them appear toxic. The development of specific inhibitors targeting efflux pumps but without affecting the host would be of a great clinical value.

In conclusion, this work allowed to describe new regulatory mechanisms of three MmpL efflux pumps in *M. abscessus,* opening the way to future therapeutic strategies. The genetic tools developed will undoubtedly contribute to the identification of new drug targets and, eventually, to the improvement of current strategies to fight against *M. abscessus* and other NTM. This research work was awarded with a Silver Medal on the Scientific Day of the Mediterranean Infection Foundation, in Marseille on July 7th, 2017.

REFERENCES

9. References

Alahari, Anuradha, Xavier Trivelli, Yann Guérardel, Lynn G. Dover, Gurdyal S. Besra, James C. Sacchettini, Robert C. Reynolds, Geoffrey D. Coxon, and Laurent Kremer. 2007. "Thiacetazone, an Antitubercular Drug That Inhibits Cyclopropanation of Cell Wall Mycolic Acids in Mycobacteria." *PloS One* 2 (12): e1343. https://doi.org/10.1371/journal.pone.0001343.

Alekshun, M. N., Y. S. Kim, and S. B. Levy. 2000. "Mutational Analysis of MarR, the Negative Regulator of MarRAB Expression in Escherichia Coli, Suggests the Presence of Two Regions Required for DNA Binding." *Molecular Microbiology* 35 (6): 1394–1404. https://doi.org/10.1046/j.1365-2958.2000.01802.x.

Andries, Koen, Peter Verhasselt, Jerome Guillemont, Hinrich W. H. Göhlmann, Jean-Marc Neefs, Hans Winkler, Jef Van Gestel, et al. 2005. "A Diarylquinoline Drug Active on the ATP Synthase of Mycobacterium Tuberculosis." *Science* 307 (5707): 223–27. https://doi.org/10.1126/science.1106753.

Asmar, Shady, Mohamed Sassi, Michael Phelippeau, and Michel Drancourt. 2016. "Inverse Correlation between Salt Tolerance and Host-Adaptation in Mycobacteria." *BMC Research Notes* 9 (April): 249. https://doi.org/10.1186/s13104-016-2054-y.

Barry, V. C., J. G. Belton, M. L. Conalty, J. M. Denneny, D. W. Edward, J. F. O'sullivan, D. Twomey, and F. Winder. 1957. "A New Series of Phenazines (Rimino-Compounds) with High Antituberculosis Activity." *Nature* 179 (4568): 1013–15. https://doi.org/10.1038/1791013a0.

Beck, C F, R Mutzel, J Barbé, and W Müller. 1982. "A Multifunctional Gene (TetR) Controls Tn10-Encoded Tetracycline Resistance." *Journal of Bacteriology* 150 (2): 633–42.

Belardinelli, Juan Manuel, Gérald Larrouy-Maumus, Victoria Jones, Luiz Pedro Sorio de Carvalho, Michael R. McNeil, and Mary Jackson. 2014. "Biosynthesis and Translocation of Unsulfated Acyltrehaloses in Mycobacterium Tuberculosis." *Journal of Biological Chemistry* 289 (40): 27952–65. https://doi.org/10.1074/jbc.M114.581199.

Bernut, Audrey, Jean-Louis Herrmann, Karima Kissa, Jean-François Dubremetz, Jean-Louis Gaillard, Georges Lutfalla, and Laurent Kremer. 2014. "Mycobacterium Abscessus Cording Prevents Phagocytosis and Promotes Abscess Formation." *Proceedings of the National Academy of Sciences of the United States of America* 111 (10): E943-952. https://doi.org/10.1073/pnas.1321390111.

Bernut, Audrey, Jean-Louis Herrmann, Diane Ordway, and Laurent Kremer. 2017. "The Diverse Cellular and Animal Models to Decipher the Physiopathological Traits of Mycobacterium Abscessus Infection." *Frontiers in Cellular and Infection Microbiology* 7: 100. https://doi.org/10.3389/fcimb.2017.00100.

Bernut, Audrey, Vincent Le Moigne, Tiffany Lesne, Georges Lutfalla, Jean-Louis Herrmann, and Laurent Kremer. 2014. "In Vivo Assessment of Drug Efficacy against Mycobacterium Abscessus Using the Embryonic Zebrafish Test System." *Antimicrobial Agents and Chemotherapy* 58 (7): 4054–63. https://doi.org/10.1128/AAC.00142-14.

Bernut, Audrey, Albertus Viljoen, Christian Dupont, Guillaume Sapriel, Mickaël Blaise, Christiane Bouchier, Roland Brosch, Chantal de Chastellier, Jean-Louis Herrmann, and Laurent Kremer. 2016. "Insights into the Smooth-to-Rough Transitioning in Mycobacterium Bolletii Unravels a Functional Tyr Residue Conserved in All Mycobacterial MmpL Family Members." *Molecular Microbiology* 99 (5): 866–83. https://doi.org/10.1111/mmi.13283.

Brambilla, Cecilia, Marta Llorens-Fons, Esther Julián, Estela Noguera-Ortega, Cristina Tomàs-Martínez, Miriam Pérez-Trujillo, Thomas F. Byrd, Fernando Alcaide, and Marina Luquin. 2016. "L." *Frontiers in Microbiology* 7: 1562. https://doi.org/10.3389/fmicb.2016.01562.

Burbaud, Sophie, Françoise Laval, Anne Lemassu, Mamadou Daffé, Christophe Guilhot, and Christian Chalut. 2016. "Trehalose Polyphleates Are Produced by a Glycolipid Biosynthetic Pathway Conserved across Phylogenetically Distant Mycobacteria." *Cell Chemical Biology* 23 (2): 278–89. https://doi.org/10.1016/j.chembiol.2015.11.013.

Busenlehner, Laura S., Mario A. Pennella, and David P. Giedroc. 2003. "The SmtB/ArsR Family of Metalloregulatory Transcriptional Repressors: Structural Insights into Prokaryotic Metal Resistance." *FEMS Microbiology Reviews* 27 (2–3): 131–43. https://doi.org/10.1016/S0168-6445(03)00054-8.

Camacho, Luis R., Patricia Constant, Catherine Raynaud, Marie-Antoinette Lanéelle, James A. Triccas, Brigitte Gicquel, Mamadou Daffé, and Christophe Guilhot. 2001. "Analysis of the Phthiocerol Dimycocerosate Locus OfMycobacterium Tuberculosis EVIDENCE THAT THIS LIPID IS INVOLVED IN THE CELL WALL PERMEABILITY BARRIER." *Journal of Biological Chemistry* 276 (23): 19845–54. https://doi.org/10.1074/jbc.M100662200.

Catherinot, E., J. Clarissou, G. Etienne, F. Ripoll, J.-F. Emile, M. Daffé, C. Perronne, C. Soudais, J.-L. Gaillard, and M. Rottman. 2007. "Hypervirulence of a Rough Variant of the Mycobacterium Abscessus Type Strain." *Infection and Immunity* 75 (2): 1055–58. https://doi.org/10.1128/IAI.00835-06.

Catherinot, Emilie, Anne-Laure Roux, Edouard Macheras, Dominique Hubert, Moussa Matmar, Luc Dannhoffer, Thierry Chinet, et al. 2009. "Acute Respiratory Failure Involving an R Variant of Mycobacterium Abscessus." *Journal of Clinical Microbiology* 47 (1): 271–74. https://doi.org/10.1128/JCM.01478-08.

Chalut, Christian. 2016. "MmpL Transporter-Mediated Export of Cell-Wall Associated Lipids and Siderophores in Mycobacteria." *Tuberculosis (Edinburgh, Scotland)* 100: 32–45. https://doi.org/10.1016/j.tube.2016.06.004.

Cholo, Moloko C., Maborwa T. Mothiba, Bernard Fourie, and Ronald Anderson. 2017. "Mechanisms of Action and Therapeutic Efficacies of the Lipophilic Antimycobacterial Agents Clofazimine and Bedaquiline." *The Journal of Antimicrobial Chemotherapy* 72 (2): 338–53. https://doi.org/10.1093/jac/dkw426.

Converse, Scott E., Joseph D. Mougous, Michael D. Leavell, Julie A. Leary, Carolyn R. Bertozzi, and Jeffery S. Cox. 2003. "MmpL8 Is Required for Sulfolipid-1 Biosynthesis and Mycobacterium Tuberculosis Virulence." *Proceedings of the National Academy of Sciences* 100 (10): 6121–26.

https://doi.org/10.1073/pnas.1030024100.

Cowman, Steven, Jakko van Ingen, David E. Griffith, and Michael R. Loebinger. 2019. "Non-Tuberculous Mycobacterial Pulmonary Disease." *The European Respiratory Journal* 54 (1). https://doi.org/10.1183/13993003.00250-2019.

Cox, Jeffery S., Bing Chen, Michael McNeil, and William R. Jacobs. 1999. "Complex Lipid Determines Tissue-Specific Replication of Mycobacterium Tuberculosis in Mice." *Nature* 402 (6757): 79–83. https://doi.org/10.1038/47042.

Cuthbertson, Leslie, and Justin R. Nodwell. 2013. "The TetR Family of Regulators." *Microbiology and Molecular Biology Reviews : MMBR* 77 (3): 440–75. https://doi.org/10.1128/MMBR.00018-13.

Dedrick, Rebekah M., Carlos A. Guerrero-Bustamante, Rebecca A. Garlena, Daniel A. Russell, Katrina Ford, Kathryn Harris, Kimberly C. Gilmour, et al. 2019. "Engineered Bacteriophages for Treatment of a Patient with a Disseminated Drug-Resistant Mycobacterium Abscessus." *Nature Medicine* 25 (5): 730–33. https://doi.org/10.1038/s41591-019-0437-z.

Delmar, Jared A., Chih-Chia Su, and Edward W. Yu. 2014. "Bacterial Multi-Drug Efflux Transporters." *Annual Review of Biophysics* 43: 93–117. https://doi.org/10.1146/annurev-biophys-051013-022855.

Domenech, Pilar, Michael B. Reed, Cynthia S. Dowd, Claudia Manca, Gilla Kaplan, and Clifton E. Barry. 2004. "The Role of MmpL8 in Sulfatide Biogenesis and Virulence of Mycobacterium Tuberculosis." *Journal of Biological Chemistry* 279 (20): 21257–65. https://doi.org/10.1074/jbc.M400324200.

Dover, Lynn G., Anuradha Alahari, Paul Gratraud, Jessica M. Gomes, Veemal Bhowruth, Robert C. Reynolds, Gurdyal S. Besra, and Laurent Kremer. 2007. "EthA, a Common Activator of Thiocarbamide-Containing Drugs Acting on Different Mycobacterial Targets." *Antimicrobial Agents and Chemotherapy* 51 (3): 1055–63. https://doi.org/10.1128/AAC.01063-06.

Drancourt, M. 2014. "Looking in Amoebae as a Source of Mycobacteria." *Microbial Pathogenesis* 77 (December): 119–24. https://doi.org/10.1016/j.micpath.2014.07.001.

Dubois, Violaine, Albertus Viljoen, Laura Laencina, Vincent Le Moigne, Audrey Bernut, Faustine Dubar, Mickaël Blaise, et al. 2018. "MmpL8MAB Controls Mycobacterium Abscessus Virulence and Production of a Previously Unknown Glycolipid Family." *Proceedings of the National Academy of Sciences of the United States of America* 115 (43): E10147–56. https://doi.org/10.1073/pnas.1812984115.

Dupont, Christian, Albertus Viljoen, Faustine Dubar, Mickaël Blaise, Audrey Bernut, Alexandre Pawlik, Christiane Bouchier, et al. 2016. "A New Piperidinol Derivative Targeting Mycolic Acid Transport in Mycobacterium Abscessus." *Molecular Microbiology* 101 (3): 515–29. https://doi.org/10.1111/mmi.13406.

Dupont, Christian, Albertus Viljoen, Sangeeta Thomas, Françoise Roquet-Banères, Jean-Louis Herrmann, Kevin Pethe, and Laurent Kremer. 2017. "Bedaquiline Inhibits the ATP Synthase in Mycobacterium Abscessus and Is Effective in Infected Zebrafish." *Antimicrobial Agents and Chemotherapy* 61 (11): e01225-17. https://doi.org/10.1128/AAC.01225-17.

Etienne, Gilles, Wladimir Malaga, Françoise Laval, Anne Lemassu, Christophe Guilhot, and Mamadou

Daffé. 2009. “Identification of the Polyketide Synthase Involved in the Biosynthesis of the Surface-Exposed Lipooligosaccharides in Mycobacteria.” *Journal of Bacteriology* 191 (8): 2613–21. https://doi.org/10.1128/JB.01235-08.

Falkinham, Joseph O. 2003. “Mycobacterial Aerosols and Respiratory Disease.” *Emerging Infectious Diseases* 9 (7): 763–67. https://doi.org/10.3201/eid0907.02-0415.

———. 2013. “Ecology of Nontuberculous Mycobacteria--Where Do Human Infections Come From?” *Seminars in Respiratory and Critical Care Medicine* 34 (1): 95–102. https://doi.org/10.1055/s-0033-1333568.

Falzon, Dennis, Geraldine Hill, Shanthi N Pal, Wimon Suwankesawong, and Ernesto Jaramillo. 2014. “Pharmacovigilance and Tuberculosis: Applying the Lessons of Thioacetazone.” *Bulletin of the World Health Organization* 92 (12): 918–19. https://doi.org/10.2471/BLT.14.142570.

“FDA Approves Pretomanid for Highly Drug-Resistant Forms of Tuberculosis.” n.d. Drugs.Com. Accessed August 21, 2019. https://www.drugs.com/newdrugs/fda-approves-pretomanid-highly-resistant-forms-tuberculosis-5029.html.

Franklin, T. J. 1967. “Resistance of Escherichia Coli to Tetracyclines. Changes in Permeability to Tetracyclines in Escherichia Coli Bearing Transferable Resistance Factors.” *Biochemical Journal* 105 (1): 371–78.

Fregnan, G. B., D. W. Smith, and H. M. Randall. 1962. “A MUTANT OF A SCOTOCHROMOGENIC MYCOBACTERIUM DETECTED BY COLONY MORPHOLOGY AND LIPID STUDIES.” *Journal of Bacteriology* 83 (4): 828–36.

Furuya, E. Yoko, Armando Paez, Arjun Srinivasan, Robert Cooksey, Michael Augenbraun, Miriam Baron, Karen Brudney, et al. 2008. “Outbreak of Mycobacterium Abscessus Wound Infections among ‘Lipotourists’ from the United States Who Underwent Abdominoplasty in the Dominican Republic.” *Clinical Infectious Diseases: An Official Publication of the Infectious Diseases Society of America* 46 (8): 1181–88. https://doi.org/10.1086/529191.

Garrelts, James C. 1991. “Clofazimine: A Review of Its Use in Leprosy and Mycobacterium Avium Complex Infection.” *DICP* 25 (5): 525–31. https://doi.org/10.1177/106002809102500513.

Ghosh, Soma, and Tamara J. O’Connor. 2017. “Beyond Paralogs: The Multiple Layers of Redundancy in Bacterial Pathogenesis.” *Frontiers in Cellular and Infection Microbiology* 7 (November). https://doi.org/10.3389/fcimb.2017.00467.

Gibson, Justine S., Rowland N. Cobbold, Myat T. Kyaw-Tanner, Peter Heisig, and Darren J. Trott. 2010. “Fluoroquinolone Resistance Mechanisms in Multidrug-Resistant Escherichia Coli Isolated from Extraintestinal Infections in Dogs.” *Veterinary Microbiology* 146 (1): 161–66. https://doi.org/10.1016/j.vetmic.2010.04.012.

Gong, Zhen, Hui Li, Yuhua Cai, Andrea Stojkoska, and Jianping Xie. 2019. “Biology of MarR Family Transcription Factors and Implications for Targets of Antibiotics against Tuberculosis.” *Journal of Cellular Physiology* 234 (11): 19237–48. https://doi.org/10.1002/jcp.28720.

Griffin, Isabel, Ann Schmitz, Christine Oliver, Scott Pritchard, Guoyan Zhang, Edhelene Rico, Emily Davenport, et al. 2018. "Outbreak of Tattoo-Associated Nontuberculous Mycobacterial Skin Infections." *Clinical Infectious Diseases: An Official Publication of the Infectious Diseases Society of America*, November. https://doi.org/10.1093/cid/ciy979.

Grzegorzewicz, Anna E., Jana Korduláková, Victoria Jones, Sarah E. M. Born, Juan M. Belardinelli, Adrien Vaquié, Vijay A. K. B. Gundi, et al. 2012. "A Common Mechanism of Inhibition of the Mycobacterium Tuberculosis Mycolic Acid Biosynthetic Pathway by Isoxyl and Thiacetazone." *The Journal of Biological Chemistry* 287 (46): 38434–41. https://doi.org/10.1074/jbc.M112.400994.

Grzegorzewicz, Anna E., Ha Pham, Vijay A. K. B. Gundi, Michael S. Scherman, Elton J. North, Tamara Hess, Victoria Jones, et al. 2012. "INHIBITION OF MYCOLIC ACID TRANSPORT ACROSS THE MYCOBACTERIUM TUBERCULOSIS PLASMA MEMBRANE." *Nature Chemical Biology* 8 (4): 334–41. https://doi.org/10.1038/nchembio.794.

Gupta, Sushim Kumar, Babu Roshan Padmanabhan, Seydina M. Diene, Rafael Lopez-Rojas, Marie Kempf, Luce Landraud, and Jean-Marc Rolain. 2014. "ARG-ANNOT, a New Bioinformatic Tool To Discover Antibiotic Resistance Genes in Bacterial Genomes." *Antimicrobial Agents and Chemotherapy* 58 (1): 212–20. https://doi.org/10.1128/AAC.01310-13.

Gutiérrez, Ana Victoria, Matthias Richard, Françoise Roquet-Banères, Albertus Viljoen, and Laurent Kremer. 2019. "The TetR-Family Transcription Factor MAB_2299c Regulates the Expression of Two Distinct MmpS-MmpL Efflux Pumps Involved in Cross-Resistance to Clofazimine and Bedaquiline in Mycobacterium Abscessus." *Antimicrobial Agents and Chemotherapy*, July, AAC.01000-19. https://doi.org/10.1128/AAC.01000-19.

Halloum, Iman, Séverine Carrère-Kremer, Mickael Blaise, Albertus Viljoen, Audrey Bernut, Vincent Le Moigne, Catherine Vilchèze, et al. 2016. "Deletion of a Dehydratase Important for Intracellular Growth and Cording Renders Rough Mycobacterium Abscessus Avirulent." *Proceedings of the National Academy of Sciences* 113 (29): E4228–37. https://doi.org/10.1073/pnas.1605477113.

Halloum, Iman, Albertus Viljoen, Varun Khanna, Derek Craig, Christiane Bouchier, Roland Brosch, Geoffrey Coxon, and Laurent Kremer. 2017. "Resistance to Thiacetazone Derivatives Active against Mycobacterium Abscessus Involves Mutations in the MmpL5 Transcriptional Repressor MAB_4384." *Antimicrobial Agents and Chemotherapy* 61 (4). https://doi.org/10.1128/AAC.02509-16.

Hartkoorn, Ruben C., Swapna Uplekar, and Stewart T. Cole. 2014. "Cross-Resistance between Clofazimine and Bedaquiline through Upregulation of MmpL5 in Mycobacterium Tuberculosis." *Antimicrobial Agents and Chemotherapy* 58 (5): 2979–81. https://doi.org/10.1128/AAC.00037-14.

Hillen, W., and C. Berens. 1994. "Mechanisms Underlying Expression of Tn10 Encoded Tetracycline Resistance." *Annual Review of Microbiology* 48: 345–69. https://doi.org/10.1146/annurev.mi.48.100194.002021.

Hillen, Wolfgang, Christiane Gatz, Lothar Altschmied, Klaus Schollmeier, and Iris Meier. 1983. "Control of Expression of the Tn10-Encoded Tetracycline Resistance Genes: Equilibrium and Kinetic

Investigation of the Regulatory Reactions." *Journal of Molecular Biology* 169 (3): 707–21. https://doi.org/10.1016/S0022-2836(83)80166-1.

Howard, Susan T., Elizabeth Rhoades, Judith Recht, Xiuhua Pang, Anny Alsup, Roberto Kolter, C. Rick Lyons, and Thomas F. Byrd. 2006. "Spontaneous Reversion of Mycobacterium Abscessus from a Smooth to a Rough Morphotype Is Associated with Reduced Expression of Glycopeptidolipid and Reacquisition of an Invasive Phenotype." *Microbiology (Reading, England)* 152 (Pt 6): 1581–90. https://doi.org/10.1099/mic.0.28625-0.

Hu, Yuli, Qian Hu, Rong Wei, Runcheng Li, Dun Zhao, Meng Ge, Qing Yao, and Xinglong Yu. 2019. "The XRE Family Transcriptional Regulator SrtR in Streptococcus Suis Is Involved in Oxidant Tolerance and Virulence." *Frontiers in Cellular and Infection Microbiology* 8. https://doi.org/10.3389/fcimb.2018.00452.

Hurst-Hess, Kelley, Paulami Rudra, and Pallavi Ghosh. 2017. "Mycobacterium Abscessus WhiB7 Regulates a Species-Specific Repertoire of Genes To Confer Extreme Antibiotic Resistance." *Antimicrobial Agents and Chemotherapy* 61 (11). https://doi.org/10.1128/AAC.01347-17.

Ingen, Jakko van, Beatriz E. Ferro, Wouter Hoefsloot, Martin J. Boeree, and Dick van Soolingen. 2013. "Drug Treatment of Pulmonary Nontuberculous Mycobacterial Disease in HIV-Negative Patients: The Evidence." *Expert Review of Anti-Infective Therapy* 11 (10): 1065–77. https://doi.org/10.1586/14787210.2013.830413.

Izaki, Kazuo, Kan Kiuchi, and Kei Arima. 1966. "Specificity and Mechanism of Tetracycline Resistance in a Multiple Drug Resistant Strain of Escherichia Coli." *Journal of Bacteriology* 91 (2): 628–33.

Jankute, Monika, Vijayashankar Nataraj, Oona Y.-C. Lee, Houdini H. T. Wu, Malin Ridell, Natalie J. Garton, Michael R. Barer, David E. Minnikin, Apoorva Bhatt, and Gurdyal S. Besra. 2017. "The Role of Hydrophobicity in Tuberculosis Evolution and Pathogenicity." *Scientific Reports* 7 (1): 1–10. https://doi.org/10.1038/s41598-017-01501-0.

Jia, Baofeng, Amogelang R. Raphenya, Brian Alcock, Nicholas Waglechner, Peiyao Guo, Kara K. Tsang, Briony A. Lago, et al. 2017. "CARD 2017: Expansion and Model-Centric Curation of the Comprehensive Antibiotic Resistance Database." *Nucleic Acids Research* 45 (Database issue): D566–73. https://doi.org/10.1093/nar/gkw1004.

Jönsson, Bodil E., Marita Gilljam, Anders Lindblad, Malin Ridell, Agnes E. Wold, and Christina Welinder-Olsson. 2007. "Molecular Epidemiology of Mycobacterium Abscessus, with Focus on Cystic Fibrosis." *Journal of Clinical Microbiology* 45 (5): 1497–1504. https://doi.org/10.1128/JCM.02592-06.

Kim, Hee-Youn, Byoung Jun Kim, Yoonwon Kook, Yeo-Jun Yun, Jeong Hwan Shin, Bum-Joon Kim, and Yoon-Hoh Kook. 2010. "Mycobacterium Massiliense Is Differentiated from Mycobacterium Abscessus and Mycobacterium Bolletii by Erythromycin Ribosome Methyltransferase Gene (Erm) and Clarithromycin Susceptibility Patterns." *Microbiology and Immunology* 54 (6): 347–53. https://doi.org/10.1111/j.1348-0421.2010.00221.x.

Kim, Hee-Youn, Yoonwon Kook, Yeo-Jun Yun, Chan Geun Park, Nam Yong Lee, Tae Sun Shim,

Bum-Joon Kim, and Yoon-Hoh Kook. 2008. “Proportions of Mycobacterium Massiliense and Mycobacterium Bolletii Strains among Korean Mycobacterium Chelonae-Mycobacterium Abscessus Group Isolates.” *Journal of Clinical Microbiology* 46 (10): 3384–90. https://doi.org/10.1128/JCM.00319-08.

Kisker, Caroline, Winfried Hinrichs, Karlheinz Tovar, Wolfganf Hillen, and Wolfram Saenger. 1995. “The Complex Formed Between Tet Repressor and Tetracycline-Mg2|ihsbop|+Reveals Mechanism of Antibiotic Resistance.” *Journal of Molecular Biology* 247 (2): 260–80. https://doi.org/10.1006/jmbi.1994.0138.

Kreutzfeldt, Kaj M., Paul R. McAdam, Pauline Claxton, Anne Holmes, A. Louise Seagar, Ian F. Laurenson, and J. Ross Fitzgerald. 2013. “Molecular Longitudinal Tracking of Mycobacterium Abscessus Spp. during Chronic Infection of the Human Lung.” *PLOS ONE* 8 (5): e63237. https://doi.org/10.1371/journal.pone.0063237.

Lamrabet, Otmane, and Michel Drancourt. 2012. “Genetic Engineering of Mycobacterium Tuberculosis: A Review.” *Tuberculosis* 92 (5): 365–76. https://doi.org/10.1016/j.tube.2012.06.002.

Lerat, Isabelle, Emmanuelle Cambau, Romain Roth dit Bettoni, Jean-Louis Gaillard, Vincent Jarlier, Chantal Truffot, and Nicolas Veziris. 2014. “In Vivo Evaluation of Antibiotic Activity Against Mycobacterium Abscessus.” *The Journal of Infectious Diseases* 209 (6): 905–12. https://doi.org/10.1093/infdis/jit614.

Levy, Stuart B., and Laura McMurry. 1974. “Detection of an Inducible Membrane Protein Associated with R-Factor-Mediated Tetracycline Resistance.” *Biochemical and Biophysical Research Communications* 56 (4): 1060–68. https://doi.org/10.1016/S0006-291X(74)80296-2.

Li, Wei, Andrés Obregón-Henao, Joshua B. Wallach, E. Jeffrey North, Richard E. Lee, Mercedes Gonzalez-Juarrero, Dirk Schnappinger, and Mary Jackson. 2016. “Therapeutic Potential of the Mycobacterium Tuberculosis Mycolic Acid Transporter, MmpL3.” *Antimicrobial Agents and Chemotherapy* 60 (9): 5198–5207. https://doi.org/10.1128/AAC.00826-16.

Lounis, Nacer, Tom Gevers, Joke Van Den Berg, Luc Vranckx, and Koen Andries. 2009. “ATP Synthase Inhibition of Mycobacterium Avium Is Not Bactericidal.” *Antimicrobial Agents and Chemotherapy* 53 (11): 4927–29. https://doi.org/10.1128/AAC.00689-09.

Luthra, Sakshi, Anna Rominski, and Peter Sander. 2018. “The Role of Antibiotic-Target-Modifying and Antibiotic-Modifying Enzymes in Mycobacterium Abscessus Drug Resistance.” *Frontiers in Microbiology* 9. https://doi.org/10.3389/fmicb.2018.02179.

Maddocks, Sarah E., and Petra C. F. Oyston. 2008. “Structure and Function of the LysR-Type Transcriptional Regulator (LTTR) Family Proteins.” *Microbiology (Reading, England)* 154 (Pt 12): 3609–23. https://doi.org/10.1099/mic.0.2008/022772-0.

McDOUGALL, A. C., W. R. Horsfall, J. E. Hede, and A. J. Chaplin. 1980. “Splenic Infarction and Tissue Accumulation of Crystals Associated with the Use of Clofazimine (Lamprene; B663) in the Treatment of Pyoderma Gangrenosum.” British Journal of Dermatology. February 1, 1980. https://doi.org/10.1111/j.1365-2133.1980.tb05697.x.

Medjahed, Halima, and Jean-Marc Reyrat. 2009. “Construction of Mycobacterium Abscessus Defined Glycopeptidolipid Mutants: Comparison of Genetic Tools.” *Applied and Environmental Microbiology* 75 (5): 1331–38. https://doi.org/10.1128/AEM.01914-08.

Meir, Michal, Tatyana Grosfeld, and Daniel Barkan. 2018. “Establishment and Validation of Galleria Mellonella as a Novel Model Organism To Study Mycobacterium Abscessus Infection, Pathogenesis, and Treatment.” *Antimicrobial Agents and Chemotherapy* 62 (4). https://doi.org/10.1128/AAC.02539-17.

Milano, Anna, Maria Rosalia Pasca, Roberta Provvedi, Anna Paola Lucarelli, Giulia Manina, Ana Luisa de Jesus Lopes Ribeiro, Riccardo Manganelli, and Giovanna Riccardi. 2009. “Azole Resistance in Mycobacterium Tuberculosis Is Mediated by the MmpS5–MmpL5 Efflux System.” *Tuberculosis* 89 (1): 84–90. https://doi.org/10.1016/j.tube.2008.08.003.

Moore, M., and J. B. Frerichs. 1953. “An Unusual Acid-Fast Infection of the Knee with Subcutaneous, Abscess-like Lesions of the Gluteal Region; Report of a Case with a Study of the Organism, Mycobacterium Abscessus, n. Sp.” *The Journal of Investigative Dermatology* 20 (2): 133–69. https://doi.org/10.1038/jid.1953.18.

Nasiri, Mohammad J., Mehri Haeili, Mona Ghazi, Hossein Goudarzi, Ali Pormohammad, Abbas A. Imani Fooladi, and Mohammad M. Feizabadi. 2017. “New Insights in to the Intrinsic and Acquired Drug Resistance Mechanisms in Mycobacteria.” *Frontiers in Microbiology* 8 (April). https://doi.org/10.3389/fmicb.2017.00681.

Nathavitharana, Ruvandhi R, Luke Strnad, Philip A Lederer, Maunank Shah, and Rocio M Hurtado. 2019. “Top Questions in the Diagnosis and Treatment of Pulmonary M. Abscessus Disease.” *Open Forum Infectious Diseases* 6 (7). https://doi.org/10.1093/ofid/ofz221.

Nessar, Rachid, Emmanuelle Cambau, Jean Marc Reyrat, Alan Murray, and Brigitte Gicquel. 2012. “Mycobacterium Abscessus: A New Antibiotic Nightmare.” *The Journal of Antimicrobial Chemotherapy* 67 (4): 810–18. https://doi.org/10.1093/jac/dkr578.

Neves, Marcelo S., Marlei Gomes da Silva, Grasiella M. Ventura, Patrícia Barbur Côrtes, Rafael Silva Duarte, and Heitor S. de Souza. 2016. “Effectiveness of Current Disinfection Procedures against Biofilm on Contaminated GI Endoscopes.” *Gastrointestinal Endoscopy* 83 (5): 944–53. https://doi.org/10.1016/j.gie.2015.09.016.

Nguyen, Liem, and Charles J. Thompson. 2006. “Foundations of Antibiotic Resistance in Bacterial Physiology: The Mycobacterial Paradigm.” *Trends in Microbiology* 14 (7): 304–12. https://doi.org/10.1016/j.tim.2006.05.005.

Nguyen, Thi Van Anh, Richard M. Anthony, Anne-Laure Bañuls, Thi Van Anh Nguyen, Dinh Hoa Vu, and Jan-Willem C. Alffenaar. 2018. “Bedaquiline Resistance: Its Emergence, Mechanism, and Prevention.” *Clinical Infectious Diseases* 66 (10): 1625–30. https://doi.org/10.1093/cid/cix992.

Obregón-Henao, Andrés, Kimberly A. Arnett, Marcela Henao-Tamayo, Lisa Massoudi, Elizabeth Creissen, Koen Andries, Anne J. Lenaerts, and Diane J. Ordway. 2015. “Susceptibility of Mycobacterium Abscessus to Antimycobacterial Drugs in Preclinical Models.” *Antimicrobial Agents and Chemotherapy* 59

(11): 6904–12. https://doi.org/10.1128/AAC.00459-15.

Oh, Chun-Taek, Cheol Moon, Myeong Seon Jeong, Seung-Hae Kwon, and Jichan Jang. 2013. "Drosophila Melanogaster Model for Mycobacterium Abscessus Infection." *Microbes and Infection* 15 (12): 788–95. https://doi.org/10.1016/j.micinf.2013.06.011.

Orth, P., D. Schnappinger, W. Hillen, W. Saenger, and W. Hinrichs. 2000. "Structural Basis of Gene Regulation by the Tetracycline Inducible Tet Repressor-Operator System." *Nature Structural Biology* 7 (3): 215–19. https://doi.org/10.1038/73324.

Pacheco, Sophia A., Fong-Fu Hsu, Katelyn M. Powers, and Georgiana E. Purdy. 2013. "MmpL11 Protein Transports Mycolic Acid-Containing Lipids to the Mycobacterial Cell Wall and Contributes to Biofilm Formation in Mycobacterium Smegmatis." *Journal of Biological Chemistry* 288 (33): 24213–22. https://doi.org/10.1074/jbc.M113.473371.

Pang, Hui, Guilian Li, Xiuqin Zhao, Haican Liu, Kanglin Wan, and Ping Yu. 2015. "Drug Susceptibility Testing of 31 Antimicrobial Agents on Rapidly Growing Mycobacteria Isolates from China." *BioMed Research International* 2015. https://doi.org/10.1155/2015/419392.

Park, In Kwon, Amy P. Hsu, Hervé Tettelin, Shamira J. Shallom, Steven K. Drake, Li Ding, Un-In Wu, et al. 2015. "Clonal Diversification and Changes in Lipid Traits and Colony Morphology in Mycobacterium Abscessus Clinical Isolates." *Journal of Clinical Microbiology* 53 (11): 3438–47. https://doi.org/10.1128/JCM.02015-15.

Pawlik, Alexandre, Guillaume Garnier, Mickael Orgeur, Pin Tong, Amanda Lohan, Fabien Le Chevalier, Guillaume Sapriel, et al. 2013. "Identification and Characterization of the Genetic Changes Responsible for the Characteristic Smooth-to-Rough Morphotype Alterations of Clinically Persistent Mycobacterium Abscessus." *Molecular Microbiology* 90 (3): 612–29. https://doi.org/10.1111/mmi.12387.

Pryjma, Mark, Ján Burian, Kevin Kuchinski, and Charles J. Thompson. 2017. "Antagonism between Front-Line Antibiotics Clarithromycin and Amikacin in the Treatment of Mycobacterium Abscessus Infections Is Mediated by the WhiB7 Gene." *Antimicrobial Agents and Chemotherapy* 61 (11). https://doi.org/10.1128/AAC.01353-17.

Rhoades, Elizabeth R., Angela S. Archambault, Rebecca Greendyke, Fong-Fu Hsu, Cassandra Streeter, and Thomas F. Byrd. 2009. "Mycobacterium Abscessus Glycopeptidolipids Mask Underlying Cell Wall Phosphatidyl-Myo-Inositol Mannosides Blocking Induction of Human Macrophage TNF-Alpha by Preventing Interaction with TLR2." *Journal of Immunology (Baltimore, Md.: 1950)* 183 (3): 1997–2007. https://doi.org/10.4049/jimmunol.0802181.

Richard, Matthias, Ana Victoria Gutiérrez, Albertus Viljoen, Daniela Rodriguez-Rincon, Françoise Roquet-Baneres, Mickael Blaise, Isobel Everall, Julian Parkhill, R. Andres Floto, and Laurent Kremer. 2019. "Mutations in the MAB_2299c TetR Regulator Confer Cross-Resistance to Clofazimine and Bedaquiline in Mycobacterium Abscessus." *Antimicrobial Agents and Chemotherapy* 63 (1): e01316-18. https://doi.org/10.1128/AAC.01316-18.

Ripoll, Fabienne, Caroline Deshayes, Sophie Pasek, Françoise Laval, Jean-Luc Beretti, Franck Biet,

Jean-Loup Risler, et al. 2007. “Genomics of Glycopeptidolipid Biosynthesis in Mycobacterium Abscessus and M. Chelonae.” *BMC Genomics* 8 (May): 114. https://doi.org/10.1186/1471-2164-8-114.

Rodrigues, Liliana, Diana Machado, Isabel Couto, Leonard Amaral, and Miguel Viveiros. 2012. “Contribution of Efflux Activity to Isoniazid Resistance in the Mycobacterium Tuberculosis Complex.” *Infection, Genetics and Evolution: Journal of Molecular Epidemiology and Evolutionary Genetics in Infectious Diseases* 12 (4): 695–700. https://doi.org/10.1016/j.meegid.2011.08.009.

Rodriguez-Coste, Michelle A., Ioana Chirca, Lisa L. Steed, and Cassandra D. Salgado. 2016. “Epidemiology of Rapidly Growing Mycobacteria Bloodstream Infections.” *The American Journal of the Medical Sciences* 351 (3): 253–58. https://doi.org/10.1016/j.amjms.2015.12.012.

Rottman, Martin, Emilie Catherinot, Patrick Hochedez, Jean-François Emile, Jean-Laurent Casanova, Jean-Louis Gaillard, and Claire Soudais. 2007. “Importance of T Cells, Gamma Interferon, and Tumor Necrosis Factor in Immune Control of the Rapid Grower Mycobacterium Abscessus in C57BL/6 Mice.” *Infection and Immunity* 75 (12): 5898–5907. https://doi.org/10.1128/IAI.00014-07.

Roux, Anne-Laure, Aurélie Ray, Alexandre Pawlik, Halima Medjahed, Gilles Etienne, Martin Rottman, Emilie Catherinot, et al. 2011. “Overexpression of Proinflammatory TLR-2-Signalling Lipoproteins in Hypervirulent Mycobacterial Variants.” *Cellular Microbiology* 13 (5): 692–704. https://doi.org/10.1111/j.1462-5822.2010.01565.x.

Roux, Anne-Laure, Albertus Viljoen, Aïcha Bah, Roxane Simeone, Audrey Bernut, Laura Laencina, Therese Deramaudt, et al. 2016. “The Distinct Fate of Smooth and Rough Mycobacterium Abscessus Variants inside Macrophages.” *Open Biology* 6 (11). https://doi.org/10.1098/rsob.160185.

Ruggerone, Paolo, Satoshi Murakami, and Klaas M. Pos and Attilio V. Vargiu. 2013. “RND Efflux Pumps: Structural Information Translated into Function and Inhibition Mechanisms.” Current Topics in Medicinal Chemistry. November 30, 2013. http://www.eurekaselect.com/117588/article.

Ruth, Mike Marvin, Jasper J. N. Sangen, Karlijn Remmers, Lian J. Pennings, Elin Svensson, Rob E. Aarnoutse, Sanne M. H. Zweijpfenning, et al. 2019. “A Bedaquiline/Clofazimine Combination Regimen Might Add Activity to the Treatment of Clinically Relevant Non-Tuberculous Mycobacteria.” *The Journal of Antimicrobial Chemotherapy* 74 (4): 935–43. https://doi.org/10.1093/jac/dky526.

Sander, Peter, Edda De Rossi, Boris Böddinghaus, Rita Cantoni, Manuela Branzoni, Erik C. Böttger, Howard Takiff, Rosalva Rodriquez, Gustav Lopez, and Giovanna Riccardi. 2000. “Contribution of the Multidrug Efflux Pump LfrA to Innate Mycobacterial Drug Resistance.” *FEMS Microbiology Letters* 193 (1): 19–23. https://doi.org/10.1111/j.1574-6968.2000.tb09396.x.

Sanguinetti, Maurizio, Fausta Ardito, Ersilia Fiscarelli, Marilena La Sorda, Patrizia D’Argenio, Gabriella Ricciotti, and Giovanni Fadda. 2001. “Fatal Pulmonary Infection Due to Multidrug-Resistant Mycobacterium Abscessus in a Patient with Cystic Fibrosis.” *Journal of Clinical Microbiology* 39 (2): 816–19. https://doi.org/10.1128/JCM.39.2.816-819.2001.

Santos, Catarina Lopes, Margarida Correia-Neves, Pedro Moradas-Ferreira, and Marta Vaz Mendes. 2012. “A Walk into the LuxR Regulators of Actinobacteria: Phylogenomic Distribution and Functional

Diversity." *PLoS ONE* 7 (10). https://doi.org/10.1371/journal.pone.0046758.

Schmalstieg, Aurelia M., Shashikant Srivastava, Serkan Belkaya, Devyani Deshpande, Claudia Meek, Richard Leff, Nicolai S. C. van Oers, and Tawanda Gumbo. 2012. "The Antibiotic Resistance Arrow of Time: Efflux Pump Induction Is a General First Step in the Evolution of Mycobacterial Drug Resistance." *Antimicrobial Agents and Chemotherapy* 56 (9): 4806–15. https://doi.org/10.1128/AAC.05546-11.

Segala, Elena, Wladimir Sougakoff, Aurelie Nevejans-Chauffour, Vincent Jarlier, and Stephanie Petrella. 2012. "New Mutations in the Mycobacterial ATP Synthase: New Insights into the Binding of the Diarylquinoline TMC207 to the ATP Synthase C-Ring Structure." *Antimicrobial Agents and Chemotherapy* 56 (5): 2326–34. https://doi.org/10.1128/AAC.06154-11.

Seoane, A S, and S B Levy. 1995. "Characterization of MarR, the Repressor of the Multiple Antibiotic Resistance (Mar) Operon in Escherichia Coli." *Journal of Bacteriology* 177 (12): 3414–19.

Sharma, Kirti, Meetu Gupta, Ananth Krupa, Narayanaswamy Srinivasan, and Yogendra Singh. 2006. "EmbR, a Regulatory Protein with ATPase Activity, Is a Substrate of Multiple Serine/Threonine Kinases and Phosphatase in Mycobacterium Tuberculosis." *The FEBS Journal* 273 (12): 2711–21. https://doi.org/10.1111/j.1742-4658.2006.05289.x.

Silva, Denise Rossato, Margareth Dalcolmo, Simon Tiberi, Marcos Abdo Arbex, Marcela Munoz-Torrico, Raquel Duarte, Lia D'Ambrosio, et al. 2018. "New and Repurposed Drugs to Treat Multidrug- and Extensively Drug-Resistant Tuberculosis." *Jornal Brasileiro de Pneumologia* 44 (2): 153–60. https://doi.org/10.1590/S1806-37562017000000436.

Szczepanowski, Rafael, Irene Krahn, Burkhard Linke, Alexander Goesmann, Alfred Pühler, and Andreas Schlüter. 2004. "Antibiotic Multiresistance Plasmid PRSB101 Isolated from a Wastewater Treatment Plant Is Related to Plasmids Residing in Phytopathogenic Bacteria and Carries Eight Different Resistance Determinants Including a Multidrug Transport System." *Microbiology (Reading, England)* 150 (Pt 11): 3613–30. https://doi.org/10.1099/mic.0.27317-0.

Székely, R., and S. T. Cole. 2016. "Mechanistic Insight into Mycobacterial MmpL Protein Function." *Molecular Microbiology* 99 (5): 831–34. https://doi.org/10.1111/mmi.13306.

Szumowski, John D., Kristin N. Adams, Paul H. Edelstein, and Lalita Ramakrishnan. 2013. "Antimicrobial Efflux Pumps and Mycobacterium Tuberculosis Drug Tolerance: Evolutionary Considerations." *Current Topics in Microbiology and Immunology* 374. https://doi.org/10.1007/82_2012_300.

Talati, Naasha J., Nadine Rouphael, Krutika Kuppalli, and Carlos Franco-Paredes. 2008. "Spectrum of CNS Disease Caused by Rapidly Growing Mycobacteria." *The Lancet. Infectious Diseases* 8 (6): 390–98. https://doi.org/10.1016/S1473-3099(08)70127-0.

Tang, Phooi Wah, Pooi San Chua, Shiue Kee Chong, Mohd Saberi Mohamad, Yee Wen Choon, Safaai Deris, Sigeru Omatu, Juan Manuel Corchado, and Weng Howe Chan and Raha Abdul Rahim. 2015. "A Review of Gene Knockout Strategies for Microbial Cells." Recent Patents on Biotechnology. November 30, 2015. http://www.eurekaselect.com/142199/article.

Tobes, Raquel, and Juan L. Ramos. 2002. “AraC-XylS Database: A Family of Positive Transcriptional Regulators in Bacteria.” *Nucleic Acids Research* 30 (1): 318–21.

Tortoli, Enrico, Thomas A. Kohl, Barbara A. Brown-Elliott, Alberto Trovato, Sylvia Cardoso Leão, Maria Jesus Garcia, Sruthi Vasireddy, et al. 2016. “Emended Description of Mycobacterium Abscessus, Mycobacterium Abscessus Subsp. Abscessus and Mycobacteriumabscessus Subsp. Bolletii and Designation of Mycobacteriumabscessus Subsp. Massiliense Comb. Nov.” *International Journal of Systematic and Evolutionary Microbiology* 66 (11): 4471–79. https://doi.org/10.1099/ijsem.0.001376.

Viljoen, Albertus, Violaine Dubois, Fabienne Girard-Misguich, Mickaël Blaise, Jean-Louis Herrmann, and Laurent Kremer. 2017. “The Diverse Family of MmpL Transporters in Mycobacteria: From Regulation to Antimicrobial Developments.” *Molecular Microbiology* 104 (6): 889–904. https://doi.org/10.1111/mmi.13675.

Viljoen, Albertus, Ana Victoria Gutiérrez, Christian Dupont, Eric Ghigo, and Laurent Kremer. 2018. “A Simple and Rapid Gene Disruption Strategy in Mycobacterium Abscessus: On the Design and Application of Glycopeptidolipid Mutants.” *Frontiers in Cellular and Infection Microbiology* 8. https://doi.org/10.3389/fcimb.2018.00069.

Viljoen, Albertus, Clément Raynaud, Matt D. Johansen, Françoise Roquet-Banères, Jean-Louis Herrmann, Wassim Daher, and Laurent Kremer. 2019. “Verapamil Improves the Activity of Bedaquiline against Mycobacterium Abscessus In Vitro and in Macrophages.” *Antimicrobial Agents and Chemotherapy* 63 (9): e00705-19. https://doi.org/10.1128/AAC.00705-19.

Wallace, R J, A Meier, B A Brown, Y Zhang, P Sander, G O Onyi, and E C Böttger. 1996. “Genetic Basis for Clarithromycin Resistance among Isolates of Mycobacterium Chelonae and Mycobacterium Abscessus.” *Antimicrobial Agents and Chemotherapy* 40 (7): 1676–81.

Wells, Ryan M., Christopher M. Jones, Zhaoyong Xi, Alexander Speer, Olga Danilchanka, Kathryn S. Doornbos, Peibei Sun, Fangming Wu, Changlin Tian, and Michael Niederweis. 2013. “Discovery of a Siderophore Export System Essential for Virulence of Mycobacterium Tuberculosis.” *PLOS Pathogens* 9 (1): e1003120. https://doi.org/10.1371/journal.ppat.1003120.

Whang, Jake, Yong Woo Back, Kang-In Lee, Nagatoshi Fujiwara, Seungwha Paik, Chul Hee Choi, Jeong-Kyu Park, and Hwa-Jung Kim. 2017. “*Mycobacterium Abscessus* Glycopeptidolipids Inhibit Macrophage Apoptosis and Bacterial Spreading by Targeting Mitochondrial Cyclophilin D.” *Cell Death & Disease* 8 (8): e3012. https://doi.org/10.1038/cddis.2017.420.

Wolff, Kerstin A., Hoa T. Nguyen, Richard H. Cartabuke, Ajay Singh, Sam Ogwang, and Liem Nguyen. 2009. “Protein Kinase G Is Required for Intrinsic Antibiotic Resistance in Mycobacteria.” *Antimicrobial Agents and Chemotherapy* 53 (8): 3515–19. https://doi.org/10.1128/AAC.00012-09.

Wolfson, Lara J., Anna Walker, Robert Hettle, Xiaoyan Lu, Chrispin Kambili, Andrew Murungi, and Gerhart Knerer. 2015. “Cost-Effectiveness of Adding Bedaquiline to Drug Regimens for the Treatment of Multidrug-Resistant Tuberculosis in the UK.” *PLoS ONE* 10 (3). https://doi.org/10.1371/journal.pone.0120763.

Wu, Mu-Lu, Dinah B. Aziz, Véronique Dartois, and Thomas Dick. 2018. "NTM Drug Discovery: Status, Gaps and the Way Forward." *Drug Discovery Today* 23 (8): 1502–19. https://doi.org/10.1016/j.drudis.2018.04.001.

Xavier, Basil Britto, Anupam J. Das, Guy Cochrane, Sandra De Ganck, Samir Kumar-Singh, Frank Møller Aarestrup, Herman Goossens, and Surbhi Malhotra-Kumar. 2016. "Consolidating and Exploring Antibiotic Resistance Gene Data Resources." *Journal of Clinical Microbiology* 54 (4): 851–59. https://doi.org/10.1128/JCM.02717-15.

Yang, H L, G Zubay, and S B Levy. 1976. "Synthesis of an R Plasmid Protein Associated with Tetracycline Resistance Is Negatively Regulated." *Proceedings of the National Academy of Sciences of the United States of America* 73 (5): 1509–12.

Yano, Takahiro, Sacha Kassovska-Bratinova, J. Shin Teh, Jeffrey Winkler, Kevin Sullivan, Andre Isaacs, Norman M. Schechter, and Harvey Rubin. 2011. "Reduction of Clofazimine by Mycobacterial Type 2 NADH:Quinone Oxidoreductase." *The Journal of Biological Chemistry* 286 (12): 10276–87. https://doi.org/10.1074/jbc.M110.200501.

Ye, Meiping, Liyun Xu, Yuzhen Zou, Bing Li, Qi Guo, Yongjie Zhang, Mengling Zhan, et al. 2019. "Molecular Analysis of Linezolid-Resistant Clinical Isolates of Mycobacterium Abscessus." *Antimicrobial Agents and Chemotherapy* 63 (2): e01842-18. https://doi.org/10.1128/AAC.01842-18.

Young, Kevin D. 2006. "The Selective Value of Bacterial Shape." *Microbiology and Molecular Biology Reviews* 70 (3): 660–703. https://doi.org/10.1128/MMBR.00001-06.

———. 2007. "Bacterial Morphology: Why Have Different Shapes?" *Current Opinion in Microbiology* 10 (6): 596–600. https://doi.org/10.1016/j.mib.2007.09.009.

Yu, Edward W., Julio R. Aires, and Hiroshi Nikaido. 2003. "AcrB Multidrug Efflux Pump of Escherichia Coli: Composite Substrate-Binding Cavity of Exceptional Flexibility Generates Its Extremely Wide Substrate Specificity." *Journal of Bacteriology* 185 (19): 5657–64. https://doi.org/10.1128/JB.185.19.5657-5664.2003.

Zhang, Shuo, Jiazhen Chen, Peng Cui, Wanliang Shi, Wenhong Zhang, and Ying Zhang. 2015. "Identification of Novel Mutations Associated with Clofazimine Resistance in Mycobacterium Tuberculosis." *Journal of Antimicrobial Chemotherapy* 70 (9): 2507–10. https://doi.org/10.1093/jac/dkv150.

Zweijpfenning, Sanne M. H., Jakko van Ingen, and Wouter Hoefsloot. 2018. "Geographic Distribution of Nontuberculous Mycobacteria Isolated from Clinical Specimens: A Systematic Review." *Seminars in Respiratory and Critical Care Medicine* 39 (3): 336–42. https://doi.org/10.1055/s-0038-1660864.